A novel chimeric brain slice culture model to study human microglia in homeostasis and disease

Dissertation

zur Erlangung des Grades eines
Doktors der Naturwissenschaften

der Mathematisch-Naturwissenschaftlichen Fakultät
und
der Medizinischen Fakultät
der Eberhard-Karls-Universität Tübingen

vorgelegt
von

Lena Erlebach
aus Hamburg, Deutschland

2026

Tag der mündlichen Prüfung: 20.01.2026

Dekan der Math.-Nat. Fakultät:	Prof. Dr. Thilo Stehle
Dekan der Medizinischen Fakultät:	Prof. Dr. Sara Y. Brucker
1. Berichterstatter:	Prof. Dr. Mathias Jucker
2. Berichterstatter:	Prof. Dr. Katja Schenke-Layland
Prüfungskommission:	Prof. Dr. Mathias Jucker
	Prof. Dr. Katja Schenke-Layland
	Prof. Dr. Jonas Neher
	Prof. Dr. Stefan Liebau

Erklärung / Declaration:

Ich erkläre, dass ich die zur Promotion eingereichte Arbeit mit dem Titel
„A novel chimeric brain slice culture model to study human microglia in homeostasis and disease“
selbständig verfasst, nur die angegebenen Quellen und Hilfsmittel benutzt und wörtlich oder inhaltlich übernommene Stellen als solche gekennzeichnet habe. Ich versichere an Eides statt, dass diese Angaben wahr sind und dass ich nichts verschwiegen habe. Mir ist bekannt, dass die falsche Abgabe einer Versicherung an Eides statt mit Freiheitsstrafe bis zu drei Jahren oder mit Geldstrafe bestraft wird.

I hereby declare that I have produced the work entitled
„A novel chimeric brain slice culture model to study human microglia in homeostasis and disease“
submitted for the award of a doctorate, on my own (without external help), have used only the sources and aids indicated and have marked passages included from other works, whether verbatim or in content, as such. I swear upon oath that these statements are true and that I have not concealed anything. I am aware that making a false declaration under oath is punishable by a term of imprisonment of up to three years or by a fine.

Tübingen, den ....

Datum / Date Unterschrift /Signature

What I love about science is that as you learn, you don't really get answers.

You just get better questions.

– John Green

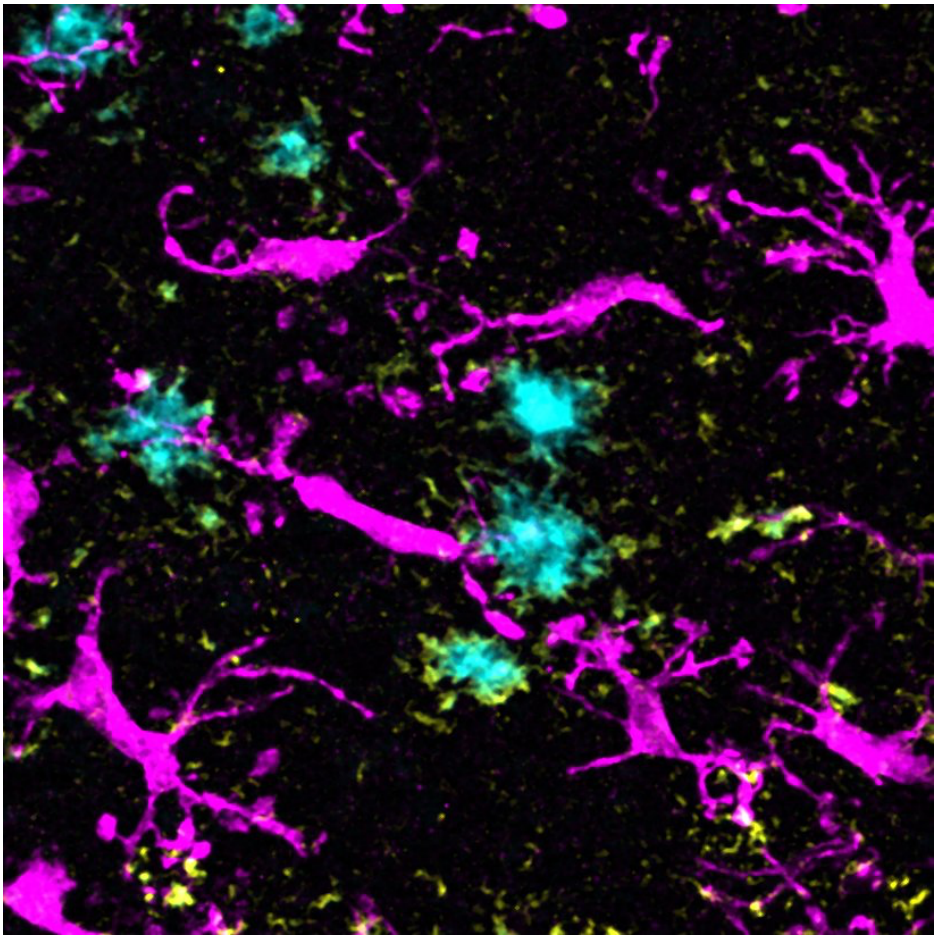

Table of Contents

1 Abstract

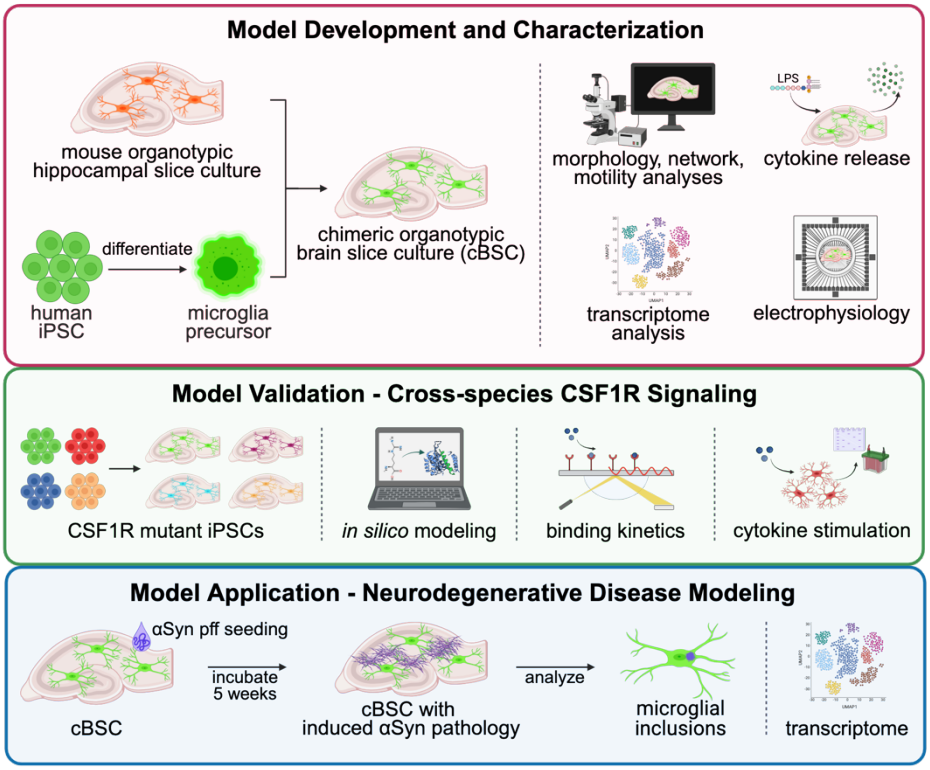

Figure 1 Graphical Abstract
Murine organotypic hippocampal slice cultures and human induced-pluripotent stem cell derived microglia (iMic) were combined to generate chimeric brain slice cultures (cBSC) – a novel model to study human microglia in a complex tissue environment *ex vivo*. The maturation and functionality of iMics in cBSCs was assessed using imaging techniques, analysis of cytokine release upon inflammatory stimulation, transcriptome and electrophysiological analyses. To understand the mechanisms of iMic integration and survival, colony stimulating factor 1 receptor (CSF1R) activation upon binding of human and murine ligands was investigated. The model depends on CSF1R signaling as CSF1R-deficient iMics did not sustain in cBSCs. Using *in silico* modeling, binding kinetic analyses and cytokine stimulation assays, murine interleukin-34 has been found to be the ligand responsible for iMic survival in cBSCs. The model was then adopted to study microglial contribution to aspects of neurodegenerative diseases by inducing protein aggregates associated with Parkinson's disease (alpha-synuclein, αSyn). iMics in αSyn-seeded cBSCs were analyzed for intra-microglial inclusions and transcriptomic changes. This figure was created in Biorender.com

Microglia are the resident immune cells in the central nervous system (CNS) and as such of high importance for brain homeostasis. Microglial contribution to neurodegenerative diseases has only been fully recognized in the last decade, and our understanding of their role in disease pathogenesis remains incomplete. Recent studies revealed significant differences between murine and human microglia in terms of their gene expression profiles, morphology and responses to pathology. Furthermore, it has become evident that the brain environment is crucial for understanding microglial homeostasis.

In this thesis, I describe the establishment of a novel model system to study human induced pluripotent stem cell-derived microglia cells (iMic) in *ex vivo* brain tissue. To generate chimeric

brain slice cultures (cBSC), microglia in murine organotypic hippocampal slice cultures were depleted and replaced by human iMic precursor cells. iMics in cBSCs differentiated and matured to closely resemble human *ex vivo* microglia in their morphology, network parameters and transcriptome. Furthermore, iMics responded to focal laser lesions and global immunogenic stimulation with shielding of the lesion site and release of cytokines, respectively, and supported neuronal activity for several months. Interestingly, cBSCs sustained human microglia without the supplementation of human colony stimulating factor 1 (CSF1) and interleukin-34 (IL34), contrasting *in vivo* xenotransplantation models. Using *in vitro*, cell-free and *in silico* approaches, I could demonstrate a cross-species interaction between human CSF1-receptor and its cognate murine ligands CSF1 and IL34. The transplantation of CSF1R loss-of-function iMics verified that CSF1R signaling was required for survival and differentiation, whereas *in silico* modeling of receptor:ligand interactions and the analysis of binding kinetics pointed to murine IL34 as the primary interaction partner. The latter was confirmed by blocking murine IL34 in cBSCs and by cytokine stimulation assays. Finally, cBSCs were adopted to model disease conditions. The induction of α-synuclein (αSyn) pathology in cBSCs resulted in wide-spread neuronal αSyn lesions and intra-microglial inclusions of aggregated proteins, as observed in murine microglia. Additionally, αSyn-treated iMics presented transcriptional phenotypes described in human Alzheimer's and Parkinson's disease patients, such as the upregulation of disease-associated microglia genes including *APOE* and *TREM2*. These observations emphasize the opportunities cBSCs offer for studying microglia in disease conditions.

In conclusion, cBSCs are a promising new tool to study human iPSC-derived microglia in a biologically relevant environment under both homeostatic and disease conditions. This model can be easily adapted for screening of potential therapeutics or for delineating the cell type-specific effect of disease-associated mutations by utilizing brain slice cultures from genetically engineered mouse models and by using mutant iPSC lines.

2 Introduction

2.1 Microglia

Microglia are the resident immune cells in the central nervous system (CNS) and play a crucial role throughout life to sustain a healthy brain environment (Paolicelli et al. 2022). Although Pio del Río-Hortega described microglia for the first time in 1919 (Del Río-Hortega 1932; Sierra et al. 2016; Sierra, Paolicelli, and Kettenmann 2019), and they make up 5-20 % of the glial population (Lawson et al. 1990; Hugh Perry 1998), neuroscientific research has mostly ignored and overlooked these cells until the early 2000s. Since then, microglia research has gained popularity and has grown exponentially (Sierra, Paolicelli, and Kettenmann 2019; Paolicelli et al. 2022).

2.1.1 Microglial origin and development

The origin of microglial cells has been debated for a long time (Ginhoux et al. 2013) as they share many characteristics with monocyte-derived macrophages (V. H. Perry, Hume, and Gordon 1985; Akiyama and McGeer 1990) like the expression of specific markers (F4/80, cluster of differentiation (CD) 11b, Fc receptor) and their phagocytic capacity (V. H. Perry, Hume, and Gordon 1985; C. S. Morris and Esiri 1991; Alliot et al. 1991). On the other hand, microglia are unique due to the expression of distinct marker proteins including transmembrane protein 119 (TMEM119), Runt-related transcription factor 1 (RUNX1) or CD39 not found in peripheral macrophage populations (Ginhoux et al. 2010; Schulz et al. 2012; Butovsky et al. 2012; M. L. Bennett et al. 2016).

By now, consensus has been reached that microglia are yolk sac (YS)-derived tissue resident macrophages that are self-sustained throughout life (Ginhoux et al. 2013). The YS is an extra-embryonic mesodermal tissue, highly conserved across evolution (Palis et al. 1999; Bessis et al. 2007; Chan, Kohsaka, and Rezaie 2007; Verney et al. 2010; Swinnen et al. 2013), that gives rise to primitive hematopoietic progenitor cells of the erythro-myeloid lineages in early embryonic development (M. A. S. Moore and Metcalf 1970; Palis et al. 1999; Bertrand et al. 2005). Shortly after gastrulation, at embryonic day (E) 7.0 in mice, primitive hematopoiesis is initiated in the YS blood islands and in a unique process without monocyte intermediates (K. Takahashi, Yamamura, and Naito 1989; Lichanska and Hume 2000). Once the circulatory system has fully developed around E8.5, these primitive macrophage progenitor cells migrate into the embryo proper (McGrath et al. 2003) and colonize the neuroepithelium around E9.5 (K. Ashwell 1990; K. W. Ashwell and Waite 1991; Alliot et al. 1991; Chan, Kohsaka, and Rezaie 2007; Ginhoux et al. 2010;

Mizutani et al. 2012). By E16, macrophage-like cells localize in “hot spots” within the brain parenchyma (V. H. Perry, Hume, and Gordon 1985) until a homogenous distribution is achieved around post-natal day (p)14 (Alliot et al. 1991; Sierra, Paolicelli, and Kettenmann 2019; Paolicelli et al. 2022).

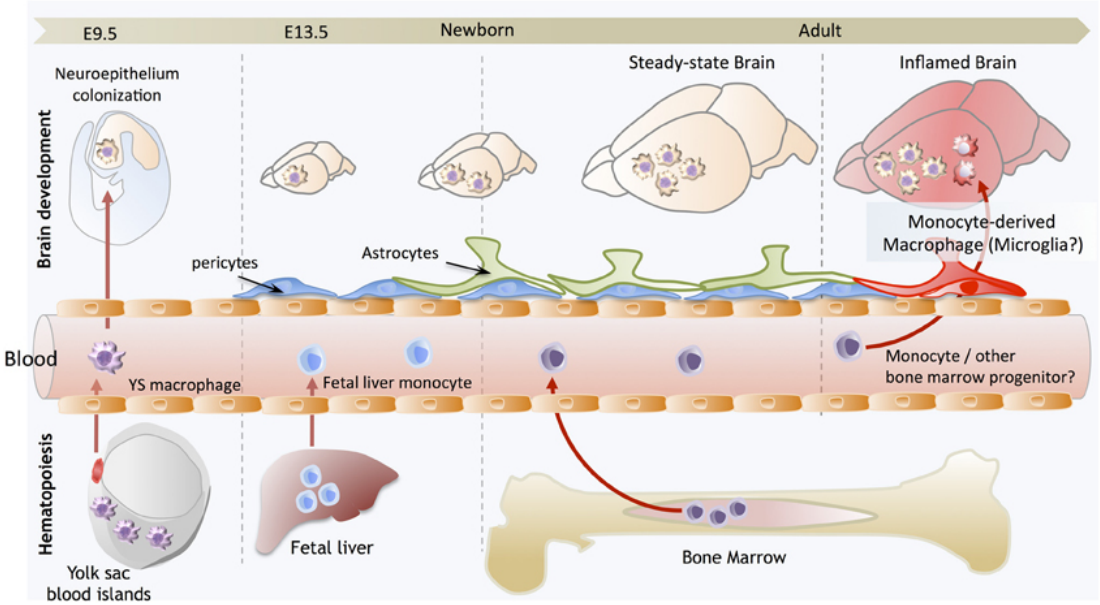

Figure 2 Microglia origin and homeostasis
Primitive macrophages are released from blood islands in the yolk sac at the onset of circulation and colonize the brain rudiment from E9.5. These cells will give rise to microglia. The blood brain barrier forms at E13.5 and prevents definitive hematopoietic progenitor cells released from the fetal liver to contribute to the microglial population. Embryonic microglia proliferate and colonize the entire CNS until adulthood. This population is self-sustained via local proliferation during development and upon injury and inflammation in the adult brain. Under exceptional conditions after inflammation or bone marrow transplantation, peripheral monocyte-derived macrophages can invade the brain. However, the persistence of these cells and their contribution to microglial networks is not yet resolved. Figure taken from Ginhoux et al. 2013, published in Frontiers in Cellular Neurology under a Creative Commons CC-BY license (CC-BY 4.0).

Contrastingly, the intra-embryonic mesoderm has undergone determination toward the hematopoietic lineage on E8.5 to generate a second wave of hematopoietic progenitors in the aorta, gonads and mesonephros (AGM) region (Godin et al. 1993; Medvinsky et al. 1993), which will give rise to definitive hematopoietic cells (Orkin and Zon 2008). Subsequently, around E10.5 primitive YS- and definitive AMG-macrophages migrate to the fetal liver, which becomes the central site for monocyte production from E11.5 onwards (Naito, Takahashi, and Nishikawa 1990; Kumaravelu et al. 2002). Fetal liver-derived macrophages replace the so-called “embryonic macrophages” in most tissues including skin, liver and spleen (Hoeffel et al. 2012; Guilliams et al. 2013; Hoeffel et al. 2015). The formation of the blood-brain-barrier (BBB) coincides with the release of fetal liver-derived macrophages to the circulatory system around E13.5 (Daneman et

al. 2010). Thus, microglia are exempt from this replacement. While definitive hematopoiesis depends on the transcription factor Myb, primitive YS-macrophages are Myb-independent (Schulz et al. 2012) emphasizing the distinct ontogeny of the different lineages.

Due to the limited accessibility of human fetal/embryonic tissue, most studies about microglial origin and development have been performed in rodents. Still, it is known that the ontogeny and differentiation in humans follow the same trajectory, albeit at a slower pace. The first microglia-like cells can be found in the brain rudiment at 3 weeks of estimated gestational age (Hutchins et al. 1990), with continued maturation throughout gestation until well-differentiated microglia are detected at 35 weeks of gestation (Esiri, al Izzi, and Reading 1991).

Although the embryonic origin of microglia has been well established by now, the contribution of blood-derived monocytes to the microglial population later in life is still under debate. For example, in mice lacking endogenous microglia due to the knockout of the myeloid transcription factor *PU.1*, monocytes establish the entire microglia compartment upon bone marrow (BM) transplantation (Beers et al. 2006). Similarly, irradiation of mice and early post-natal BM transplantations allow monocytes to penetrate the brain (Ling 1976; 1979; Ling, Penney, and Leblond 1980; Imamoto and Leblond 1978; Leong and Ling 1992), albeit at low numbers and the long-term persistence of infiltrated monocytes is barely known (Ling, Penney, and Leblond 1980; Priller et al. 2001; Ginhoux et al. 2013). Contrastingly, monocyte contribution to reactive microgliosis, the increase of microglial numbers upon inflammation, is still under investigation. Shielding the brain from irradiation and thus decreasing the opening of the BBB, prevents the infiltration of monocyte-derived macrophages and underlines that a conditioning of the CNS is required for monocyte contribution (Ajami et al. 2007; Mildner et al. 2007). On the other hand, the long-standing assumption of the brain being an '*immune-privileged*' site without peripheral immunity contributions is being called into question (Louveau, Harris, and Kipnis 2015; Castellani et al. 2023) and monocyte-derived macrophage contribution to perivascular and meningeal macrophage populations after irradiation, injury or during disease is by now well-established (Unger et al. 1993; Lassmann et al. 1993; Vallières and Sawchenko 2003; D. Han, Liu, and Gao 2020; Yan et al. 2022). So, even though monocytes have been shown to invade and locally proliferate in brain tissue under extraordinary circumstances and upon conditioning of the CNS (Hickey and Kimura 1988; Capotondo et al. 2012), the microglial population is generally self-sustained and independent of peripheral progenitors during steady state and inflammation (Lawson, Perry, and Gordon 1992; Davalos et al. 2005; Nimmerjahn, Kirchhoff, and Helmchen 2005; Ginhoux et al. 2010; Kierdorf et al. 2013; Füger et al. 2017).

2.1.2 Microglial functions in health – from development to aging

From earliest development onwards, microglia play a crucial role in the establishment of neuronal circuits and sustenance of a healthy CNS environment. During pre-natal development, microglia act as guideposts for axons and neurons to integrate into establishing neuronal circuits (Squarzoni, Thion, and Garel 2015) and actively shape those circuits by phagocytosing axons and excess synaptic connections (Paolicelli et al. 2011; D. P. Schafer and Stevens 2013; Vainchtein et al. 2014). While microglial processes are in constant contact with neuronal synapses at the pre- (D. P. Schafer and Stevens 2010; D. P. Schafer et al. 2012; D. P. Schafer and Stevens 2013) and post-synaptic site for pruning (Wake et al. 2009; Tremblay, Lowery, and Majewska 2010), the cells are also able to phagocytose entire neuronal progenitor cells during phases of enhanced neurogenesis and actively induce neuronal apoptosis (Brown and Neher 2014; Brown and Vilalta 2015; Luo, Koyama, and Ikegaya 2016).

Post-natal microglia actively shape neuronal circuits in an activity-dependent manner. They sense synaptic activity based on spine size (Alvarez and Sabatini 2007; Tremblay, Lowery, and Majewska 2010), but also express various neurotransmitter receptors, including different classes of glutamate and γ-aminobutyric acid (GABA) receptors which allow for specific modifications of neuronal activity and synapse strength by microglial release of cytokines and growth factors (D. L. Taylor et al. 2005; Pocock and Kettenmann 2007; M. Lee, Schwab, and McGeer 2011; J. Zhang et al. 2014). For instance, active synapses are strengthened by microglial release of trophic factors like brain-/ glia-derived neurotrophic factors (BDNF, GDNF, respectively) (Elkabes, DiCicco-Bloom, and Black 1996; Parkhurst et al. 2013; Kettenmann, Kirchhoff, and Verkhratsky 2013), whereas inactive and surplus synapses are eliminated in coordination with astrocytes via the activation of the complement system (Stevens et al. 2007; D. P. Schafer et al. 2012). Furthermore, the release of IL1β disrupts the formation of dendritic spines by suppressing the release of BDNF (Tong et al. 2012; Lynch 2015). As in the developing brain, microglia phagocytose apoptotic cells without the induction of inflammation (Sierra et al. 2010; Fourgeaud et al. 2016). Conversely, the release of cytokines including IL1β, IL6 and tumor necrosis factor alpha (TNFα) from microglia can also induce adult neurogenesis in the hippocampus, underlining the tight regulation of neuronal circuits by microglia (Bachstetter et al. 2011; Shigemoto-Mogami et al. 2014).

In the healthy brain, microglia are constantly surveilling their surrounding for changes in the environment caused by neuronal or astrocytic activity (Davalos et al. 2005; Nimmerjahn,

Kirchhoff, and Helmchen 2005), or induced by disease-causing agents like pathogens or protein aggregations which they sense with a variety of surface receptors known as 'sensome' (S. E. Hickman et al. 2013; Heneka et al. 2015). To achieve this, microglial constantly extend and retract their processes within their non-overlapping territories (Nimmerjahn, Kirchhoff, and Helmchen 2005; Davalos et al. 2005). Surveillance is influenced by neuronal activity and process motility increases upon decreased neuronal input and vice-versa (i.e. during sleep or under anesthesia) (Y. U. Liu et al. 2019; Cserép et al. 2020; Haruwaka et al. 2024). Furthermore, microglial activity and the release of cytokines regulate the permeability of the BBB. While the release of IL1β and IL6 opens the BBB and makes it more leaky, vascular endothelial growth factor (VEGF) or transforming growth factor beta 1 (TGFβ1) decrease BBB permeability (Ronaldson and Davis 2020; Mayer and Fischer 2024) and promote angiogenesis required for tissue repair processes (Fantin et al. 2010; Arnold and Betsholtz 2013, 2).

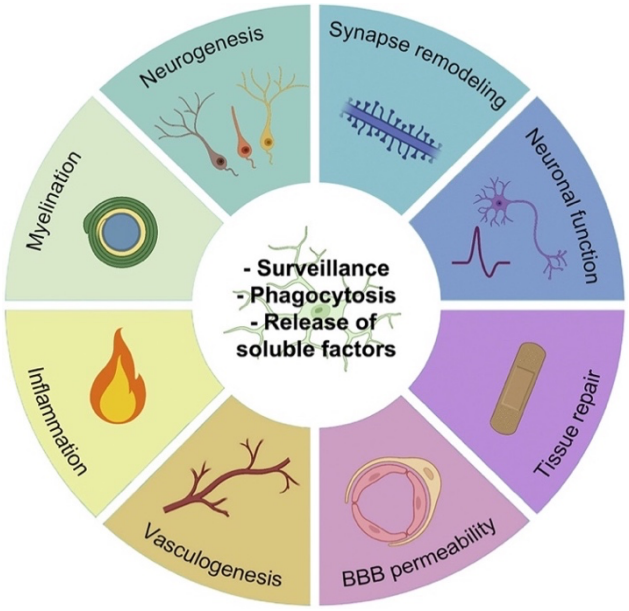

Figure 3 Microglial core functions
Microglial core properties of surveillance, phagocytosis and release of soluble factors (inner circle) are needed for microglial contribution to key biological functions (outer circle) during development, homeostasis and disease. Image taken from Paolicelli et al. 2022, published in Neuron with permission by Elsevier under the License Number 6005260996224.

Upon immunological stimulation, microglia respond by clearing the detected harmful material via phagocytosis and with the release of cytokines to mediate inflammatory reactions in the surrounding tissue (Colonna and Butovsky 2017; Liddelow et al. 2017). Additionally, microglia present antigens to peripheral immune cells like T-cells invading the brain during inflammation and respond to peripheral inflammatory processes (Hayes, Woodroofe, and Cuzner 1987; Sala

Frigerio et al. 2019; Olah et al. 2020; Goddery et al. 2021; X. Chen et al. 2023). Even though microglia are historically considered to be innate immune cells, recent publications have shown that microglia form an immune memory in response to peripheral immune stimulation (Wendeln et al. 2018), which is a hallmark of the adaptive immune system and highlights the complexity of these cells and their functions.

With age, microglial morphology changes towards a dystrophic phenotype characterized by an increased soma size and less ramified processes with more swellings (Streit et al. 2004; Streit 2006; Flanary et al. 2007; Sierra et al. 2007; Damani et al. 2011). Furthermore, microglial surveillance in an aged brain decreases and laser lesion responses are delayed (Damani et al. 2011; Hefendehl et al. 2014). Depending on their immediate environment, dysfunctional microglia with decreased phagocytic activity and lysosomal impairment are observed (Safaiyan et al. 2021) as well as hypersensitive microglia that mediate chronic inflammation-mediating responses (Naj et al. 2014; Butovsky et al. 2015; Holtman et al. 2015; C. S. Moore et al. 2015). Their impaired homeostatic functionality finally leads to a loss of homogenous network parameters, resulting in microglia clustering in specific brain areas while others become unoccupied (Hefendehl et al. 2014). Thus, in older age microglia can switch from being beneficial for brain homeostasis to being deleterious by exacerbating inflammatory and disease processes.

2.1.3 Microglial transcriptional phenotypes

Phenotypic distinction of microglia subtypes has mostly relied on morphological descriptions and only three states were considered to exist: homeostatic ‘resting’ microglia, activated ‘pro-inflammatory M1’ and ‘anti-inflammatory M2’ microglia (Ransohoff 2016; Paolicelli et al. 2022). However, morphology and function do not always go hand in hand and the three categories were unable to explain microglial heterogeneity. With the advent of single-cell RNA sequencing (scRNAseq), the plethora of microglial functions became apparent in highly distinct transcriptomic states that differ in development, health, age and disease (Galatro et al. 2017; Olah et al. 2018; Hammond et al. 2019; X. Li et al. 2023; Sun et al. 2023; Guvenek et al. 2024). The expression of key genes in each subcluster provide information about the cells’ functions. Against previous assumption, the relative frequency of these subclusters is not fixed but rather changes consistently in response to developmental stages and environmental factors (Tay et al. 2017; Hammond et al. 2019). Furthermore, microglia readily transition between these states: microglia isolated from the brain rapidly lose their homeostatic profile and transition into an ‘activated’ state characterized by the downregulation of homeostatic markers including purinergic receptor

P2RY12 and the concurrent upregulation of *TNFα*. Re-transplantation of these isolated cells into the brain environment, however, results in the adaptation of the previous homeostatic state (Gosselin et al. 2017; F. C. Bennett et al. 2018).

During aging, key homeostatic markers like *P2RY12* become downregulated and microglia express more 'activation'-associated genes, leading to more responsive substates (Galatro et al. 2017; Olah et al. 2018; X. Li et al. 2023). The downregulation of genes associated with microglial homeostatic functions like axon guidance, cell adhesion and surface receptors reflect the decreased functionality observed in aged microglia (Galatro et al. 2017) and might be mediated by reduced TGFβ expression (Olah et al. 2018). On the other hand, genes involved in pathogen-response are upregulated in aging. This includes antigen presentation (major histocompatibility complex class II (*MHC-II*)), innate immune functions (interferon responses), phagocytosis and reactive oxygen species (ROS) production (Olah et al. 2018; 2020; X. Li et al. 2023). Furthermore, protein-degradation, iron and lipid metabolism are altered, resulting in microglia that accumulate lipids and have decreased phagocytic ability (Marschallinger et al. 2020). In the aging mouse brain, two major microglial subclasses emerge: The first, named '*interferon-response microglia*' (IRM), is characterized by the upregulation of genes involved in innate immune responses and interferon type I response pathways (interferon-induced proteins *IFIT2, IFIT3, IFITM3; IRF7* and *OASL2*) which are usually associated with viral infection responses (Fensterl and Sen 2014; Olah et al. 2018; Sala Frigerio et al. 2019). These IRMs have also been detected in aged human brains. The second, called '*activated response microglia*' (ARM), presents with upregulation of genes involved in inflammatory processes (*CST7, CLEC7A, ITGAX*), antigen presentation via MHC-II (*CD74, CTSB, CTSD*) and tissue regeneration (*SPP1*). Interestingly, many of these differentially expressed genes are known risk factors for neurodegenerative diseases like Alzheimer's disease and are usually highly expressed during disease, indicating a correlation between subcluster regulation and disease development (Olah et al. 2018; Sala Frigerio et al. 2019). Future studies will be needed to further dissect the connections between transcriptome, proteome, microglial function and disease development.

2.2 Colony Stimulating Factor 1 Receptor

As immune cells, microglia express a plethora of surface receptors to detect and respond to changes in their environment. Furthermore, receptor proteins are required to sense cytokines and growth factors that induce signaling cascades in microglia. These cascades ultimately lead to the expression of genes required for microglial differentiation, maturation and survival. One of those

receptors essential for macrophage and microglia development and survival is colony stimulating factor 1 receptor (CSF1R), which is highly conserved throughout evolution in fish, birds and mammals (Gow et al. 2012; David A. Hume et al. 2020; Hason et al. 2022).

2.2.1 CSF1R and its ligands

CSF1R is a tyrosine kinase transmembrane receptor of the CSF1/PDGF receptor family expressed by cells of the hematopoietic system and required for microglia cell survival and maturation (Stanley and Chitu 2014). In humans, the *CSF1R* gene is located on chromosome 5 and its expression is regulated by several transcription factors including PU.1 (Rocio Rojo et al. 2017). Human CSF1R has 972 amino acids and a predicted molecular weight of 107.984 kilodaltons (https://www.uniprot.org/uniprotkb/P07333/entry). The protein consists of a single-pass transmembrane helix, one intra- and one extracellular domain. The extracellular domain has three N-terminal immunoglobulin (Ig) domains (D_1-D_3), which bind the ligand, two Ig domains to stabilize ligand binding (D_4-D_5) and a linker region. The intracellular domain consists of a juxtamembrane domain, and a tyrosine kinase domain interrupted by a kinase insert domain (Coussens et al. 1986; Rothwell and Rohrschneider 1987; Yeung et al. 1987; Hampe et al. 1989; Mun, Park, and Park-Min 2020). Without ligand binding, the juxtamembrane domain prevents signaling of the cytosolic domain by entering an autoinhibitory position (H. Liu et al. 2012). Ligand binding to the extracellular D_1-D_3 domains induces noncovalent dimerization of two CSF1R molecules and autophosphorylation of several tyrosine residues in the intracellular domains (H. Liu et al. 2012; Mun, Park, and Park-Min 2020). Phosphorylated CSF1R activates various downstream signaling pathways including PI3K/AKT and MAPK/ERK which convey the signal to the nucleus and activate genes required for microglial survival, proliferation and maturation (Xiong et al. 2011; Yu et al. 2012). Phosphorylation also induces the covalent binding of the two CSF1R molecules via disulfide bonds which eventually leads to receptor endocytosis, trafficking of receptor:ligand complexes to lysosomes and thus the termination of signaling (P. S. Lee et al. 1999; Mun, Park, and Park-Min 2020).

CSF1R has two known ligands: colony stimulating factor 1 (CSF1) and interleukin-34 (H. Lin et al. 2008; Elmore et al. 2014; Chitu et al. 2016; Paolicelli et al. 2022). While the primary amino acid sequences of the two ligands show little homology, the tertiary structures are overlapping (Felix et al. 2013; 2015). Although both ligands bind the receptor in the same binding pocket, the current understanding is that each ligand has a distinct binding region and thus exerts differential effects (Chihara et al. 2010; Garceau et al. 2010). CSF1 is critical for microglial development, whereas

IL34 seems to be essential for the maintenance of microglia postnatally but dispensable for microglial development. Interestingly, the expression of CSF1 and IL34 additionally has specific regional patterns: While CSF1 is predominantly found in astrocytes, oligodendrocytes and microglia in the cerebellum and white matter, IL34 is expressed by neurons in the grey matter (Easley-Neal et al. 2019; Badimon et al. 2020; Devlin et al. 2024). These differential expression patterns may influence microglial heterogeneity across brain regions and affect their functionality.

Human and murine CSF1 share about 80 % homology in the N-terminal region, which is required for conveying the biological activity (Stanley et al. 1997). Even though homology is high, so far it has been shown that human CSF1 can activate murine receptors (Guilbert and Stanley 1986; Stanley et al. 1997; D. A. Hume et al. 1988) whereas no activation of human CSF1R has been reported upon murine ligand binding (Sieff 1987; Roussel et al. 1988; Rathinam et al. 2011). Murine and human IL34 share 71 % sequence identity (H. Lin et al. 2008; Otsuka, Wada, and Seino 2021). While human IL34 has been reported to not activate murine CSF1R, mIL34 can activate human CSF1R signaling (Chihara et al. 2010; Gow et al. 2013). However, it has not been investigated yet whether cross-species activation of human CSF1R by murine IL34 can sustain human microglia *in situ*.

2.2.2 Microglia depend on CSF1R signaling

Early microglia development is CSF1R-dependent (Ginhoux et al. 2010) and mutations in the gene cause Hereditary Diffuse Leukoencephalopathy with Spheroids (HDLS, also known as Adult-onset Leukodystrophy with Neuroaxonal Spheroids and Pigmented Glia (ALSP)) (Marotti et al. 2004; Rademakers et al. 2011). HDLS is a very rare autosomal-dominant disease characterized by reduced microglia numbers (Tada et al. 2016), wide-spread white matter degeneration, axon and myelin loss, the formation of neuroaxonal spheroids and lipid-laden, pigmented macrophages/microglia. Patients present in their 40s to 50s with frontotemporal lobar degeneration (FTLD)-like symptoms including psychological changes and motor impairments (Axelsson et al. 1984; Marotti et al. 2004; Rademakers et al. 2011).

By now, more than 70 mutations in *CSF1R* have been identified to be causative for HDLS (Konno et al. 2018). The mutations impair tyrosine kinase function by point mutations within the tyrosine kinase domain-encoding exons (Rademakers et al. 2011; Konno et al. 2018) or by splice-site mutations in the surrounding introns (Oosterhof et al. 2019). Mutant CSF1R is unable to autophosphorylate upon ligand binding (Rademakers et al. 2011), while influences on surface

expression and dominant-negative effects exerted by mutant receptors are under debate (Konno et al. 2018). Homozygous carriers of *CSF1R* mutations are rare and present without detectable microglia and severe brain abnormalities (Oosterhof et al. 2019; L. Guo et al. 2019). This underlines the assumption that CSF1R signaling and microglia are required for proper brain development and that phenotype severity depends on the level of functional CSF1R (Konno et al. 2018).

2.2.3 Targeted microglia depletion

Due to microglial dependency on CSF1R, several approaches have been developed to selectively target and deplete microglia for experimental and potential therapeutic purposes by inhibiting the receptor (J. Han et al. 2022). Targeted microglia depletion offers the opportunity to selectively eliminate microglia from a living organism to study their role in health and disease by observing the consequences of microglia depletion on neuronal function, brain homeostasis, repair and/or behavior (Green, Crapser, and Hohsfield 2020). On the other hand, targeted depletion could facilitate the exchange of microglia harboring disease-associated mutations to healthy microglia to halt or prevent disease progression. This, however, will require a lot of future research on both depletion as well as transplantation conditions. A prime example would be the correction of mutations in triggering receptor expressed on myeloid cells-2 (TREM2) or its adapter protein TYRO protein tyrosine kinase-binding protein (TYROBP), that have been associated with Nasu-Hakola disease. Nasu-Hakola is a very rare autosomal-recessive disease characterized by psychotic symptoms, early-onset neurodegeneration, encephalopathy and bone cysts that results in premature death at the age of 40-50 (Paloneva et al. 2002). A replacement of dysfunctional microglia is potentially able to rescue the neurological symptoms of the disease, as it is considered a primary microgliopathy (Bianchin and Snow 2022).

Small molecule inhibitors of CSF1R that are able to pass the BBB including PLX3397, PLX5622, GW2580 and BLZ946 are highly effective in mice, resulting in near complete loss of microglia (80-99 % reduction) within a matter of days (Conway et al. 2005; Coniglio et al. 2012; Krauser et al. 2015; J. Han, Harris, and Zhang 2017; J. Han et al. 2022; Green, Crapser, and Hohsfield 2020). These CSF1R-inhibitors stabilize CSF1R molecules in their auto-inhibited confirmation, thus preventing the binding of substrates and adenosine triphosphate (ATP) to the kinase domain and subsequent microglial demise (Benner et al. 2020). While depletion is rapid and extensive, withdrawal of inhibitors leads to microglial proliferation and repopulation of the brain tissue from the cells that withstood depletion. Within a few weeks, microglial repopulation exceeds the basal

microglia density but subsequently stabilizes itself to previous levels (Elmore et al. 2014; Huang et al. 2018). At present, little is known about the processes and microglial cells involved in repopulation, but Zhan et al. have identified a small progenitor-like microglial subpopulation highly expressing galectin-3 (encoded by *MAC2*) that appears to be resistant to CSF1R inhibition (L. Zhan et al. 2020; Huang et al. 2018). Since depletion using small molecule CSF1R inhibitors and subsequent repopulation is also observed in slice culture models (Coleman Jr, Zou, and Crews 2020; Barth 2023), peripheral monocyte/macrophage contribution to repopulation plays only a minor role. Although microglia are the only cells in the CNS expressing CSF1R, small molecule-mediated depletion can have direct and/or indirect effects on other neural cell types including oligodendrocytes and astrocytes, which have to compensate for microglial phagocytosis and might be affected by microglial debris (Hagemeyer et al. 2017; Coleman Jr, Zou, and Crews 2020).

Alternatively, clodronate liposomes are commonly applied to deplete microglia independently of CSF1R. The liposomes are selectively taken up by phagocytic cells and processed within the lysosomes. There, the toxin is released to induce apoptosis (Van Rooijen and Sanders 1994; X. Han et al. 2019; Green, Crapser, and Hohsfield 2020). This more unspecific approach, however, can also affect astrocytes and induces increased pro-inflammatory cytokine levels as they possess phagocytic function, albeit to a lower extent than microglia (X. Han et al. 2019; Konishi, Koizumi, and Kiyama 2022).

Pharmacological depletion of microglia using small molecules or clodronate liposomes does not discriminate between different animal species, which makes them universal tools to be applied in rodent and human models (Chadarevian et al. 2022). However, this low specificity renders the generation of chimeric models difficult, as grafted microglia respond to the inhibitor in a similar way as host cells and consequently do not engraft the tissue. Thus, other approaches are needed to deplete microglia for this kind of research:

Constitutive *CSF1R* knock-out (KO) animal models (Chitu et al. 2015) lack microglia but present with postnatal brain development impairment and decreased survival because peripheral monocytes and osteoclasts are also ablated (Erblich et al. 2011). On the other hand, mice with constitutive mutations in the *fms* intronic regulatory element (FIRE), a highly conserved super-enhancer of *CSF1R*, lack tissue-resident macrophages (including microglia) from early embryonic development while monocytes are not affected (Rocío Rojo et al. 2019). These $CSF1R^{\Delta FIRE/\Delta FIRE}$ mice are healthy, without the neurological and developmental abnormalities or decreased fertility and survival observed in *CSF1R* KO animals (Rocío Rojo et al. 2019) and are commonly utilized

(Baligács et al. 2024; Munro et al. 2024; Chadarevian et al. 2024). Alternatively, conditional KO and drug-based approaches have been established to selectively deplete microglia in adult mice upon the administration of the ligand for the genetically introduced death receptor (Frank L. Heppner et al. 2005; Varvel et al. 2012; Bruttger et al. 2015) or activator of recombinases (see **2.3.7 below**).

Antibodies directed against CSF1R offer a more precise inhibition of the receptor and its downstream signaling that can be species-specific and thus support xenotransplantation of microglia. Antibodies are not commonly used to deplete microglia, as they are unable to penetrate the BBB *in vivo* but could be of great value in *in vitro* studies (David A. Hume and MacDonald 2012).

Lastly, the Bennett lab has genetically engineered human induced pluripotent stem cells (iPSC, see **2.3.5 below**) to express mutant CSF1R that renders iPSC-microglia insensitive to PLX3397 which allows combining small molecule microglia depletion with engraftment (Chadarevian et al. 2022) and highlights the plethora of possibilities the receptor offers for experimental manipulation and how microglia replacement therapies could be established in humans.

2.3 Model systems to study microglia

The inaccessibility of human brain tissue results in the inability to study human microglia *in vivo*. Consequently, several methods and model systems have been developed to study human microglia biology. While none is the perfect surrogate, each model comes with its own advantages and disadvantages. Depending on the scientific question at hand, different model systems might be chosen after carefully considering the complexity and reproducibility each system offers.

2.3.1 Primary cell culture

Primary microglia are derived from fetal, perioperative or post-mortem human brains, sacrificed rodents or non-human primates. Upon homogenization of the brain tissue, microglia are usually isolated via density-gradient centrifugation and cultivated *in vitro* (Bohlen et al. 2017; Galatro et al. 2017; Grabert and McColl 2018; Agalave et al. 2020). While primary microglia remain ramified and motile in culture, retain their phagocytic capacity and respond to inflammatory stimuli (Takata et al. 2010; Grabert and McColl 2018; Agalave et al. 2020), they change their gene expression profiles within hours resulting in the decreased expression of homeostatic genes like *P2RY12* or *TMEM119* and upregulated immune activation genes (Gosselin et al. 2017; Bohlen et al. 2017; F. C. Bennett et al. 2018; Popova et al. 2021; Cadiz et al. 2022). However, many key

functions of microglia including the characterization of soluble factors released from microglia after immunogenic stimulation, known as their secretome, have been established using primary microglia cultures (J. Shi et al. 2010; He et al. 2021). The largest drawback is the limited cell yield, which cannot be increased over cultivation period as isolated microglia do not proliferate and variable culture quality that can lead to inconsistent findings and conclusions (Horvath et al. 2008).

2.3.2 Immortalized cell lines

To increase cell numbers and decrease variability, primary microglia can be immortalized by the transduction of oncogenes or SV40 large T antigen (Janabi et al. 1995; Nagai et al. 2001). Immortalized cell lines like human HMC3 (Janabi et al. 1995) or HM06 (Nagai et al. 2001) or murine BV2 (Blasi et al. 1990) come with the advantages of easy maintenance and high availability due to cell proliferation. They are capable of basic microglial functions like secretion of IL8 and TNFα upon lipopolysaccharide (LPS) stimulation (Nagai et al. 2001; Ahn et al. 2008; Dello Russo et al. 2018; Timmerman, Burm, and Bajramovic 2018). However, their validity is highly debated as the cells present a decreased expression of microglia-specific genes, the absence of important immune-response genes like MHC-II (Melief et al. 2016) and the inability to release key inflammation-mediating cytokines like IL1β and IL6 (Nagai et al. 2001; Ahn et al. 2008; Timmerman, Burm, and Bajramovic 2018). Furthermore, the process of immortalizing might alter microglial cell biology. Immortalized microglia do not depend on trophic support of a complex environment anymore (Horvath et al. 2008; Henn et al. 2009; Stansley, Post, and Hensley 2012). However, the environment is known to have substantial effects on microglial phenotypes (F. C. Bennett et al. 2018; Gosselin et al. 2017) and the loss of depending on environmental cues indicates altered cellular processes. Immortalized lines in general are only capable of reproducing the most basic cellular functions and thus are not suitable to model complex microglial interactions in the brain.

2.3.3 Peripheral monocyte-induced microglia

Several attempts to reprogram peripheral monocytes into microglia have been undertaken, to overcome complications induced by immortalization of primary microglia (Ohgidani, Kato, and Kanba 2015; C. M. Sellgren et al. 2017; Carl M. Sellgren et al. 2019; Scheiblich et al. 2021). To this end, patient-derived peripheral blood mononuclear cells or monocytes are supplemented with microglia-inducing factors including IL34 and CSF1 for transformation. These monocyte-derived microglia-like cells become ramified and are capable of synapse engulfment and cytokine release

(Ohgidani, Kato, and Kanba 2015; C. M. Sellgren et al. 2017; Carl M. Sellgren et al. 2019; Scheiblich et al. 2021). While the expression of microglia markers has been described, the expression of fractalkine receptor (CX3CR1) and PU.1 is not specific for microglia and could be remnants from their monocyte origin whereas the described expression of key microglial markers TMEM119 and P2RY12 (C. M. Sellgren et al. 2017; Carl M. Sellgren et al. 2019) appears to be highly variable and generally low. In the same line, the transcriptomes of monocyte-derived microglia-like cells show highly variable overlap with *ex vivo* human microglia (between 27 % and 75 %) due to inconsistent protocols (Muffat et al. 2016; Ryan et al. 2017; Rai et al. 2020), ontogenic differences between monocytes and microglia as well as lacking environmental clues (van Wilgenburg et al. 2013; Takata et al. 2017; C. Z. W. Lee, Kozaki, and Ginhoux 2018; Sargeant and Fourrier 2023). Therefore, results from monocyte-derived microglia must be carefully considered with regards to protocol validations and their translatability.

2.3.4 Primary tissue culture

To increase biological relevance, organotypic brain slice cultures (BSC) offer the opportunity to study primary microglia *in situ*. The brain tissue is sliced into thin sections (250-350 µm) and cultivated on semi-permeable membranes at the air-liquid interface for several weeks (Stoppini, Buchs, and Muller 1991; Novotny et al. 2016; Barth et al. 2021). BSCs are usually generated from newborn rodents (Stoppini, Buchs, and Muller 1991; Humpel 2015) but can also be prepared from perioperative adult human brain tissue or fetal tissue obtained during elective abortion (Schwarz et al. 2017; 2019; Wickham et al. 2020; McLeod et al. 2023; Marshall et al. 2024; L. W. Taylor et al. 2024). The major advantage of BSCs over other *in vitro* models is the conservation of tissue cytoarchitecture and sustained cell-cell contacts between microglia and all other neural cell types (Gähwiler et al. 1997; Berki et al. 2024). However, most BSCs are prepared from neonate rodents and thus allow studying microglia during development while BSCs prepared later in life do not sustain for prolonged cultivation time (Humpel 2015) and therefore render *in vitro* studies of aged microglia difficult. The major disadvantage of BSCs comes from preparation as the sectioning causes axonal damage and consequently microglial activation and tissue inflammation in form of astro- and microgliosis referred to as “glial scar” (Grabiec et al. 2017). Upon migration towards the lesion sites at BSC surfaces, microglia gradually re-adapt a more homeostatic phenotype within the first two weeks in culture (Hailer, Jarhult, and Nitsch 1996; F. L. Heppner et al. 1998) with a ramified morphology reminiscent of *in vivo* microglia (Czapiga and Colton 1999; Hailer, Jarhult, and Nitsch 1996) and transcriptomes more closely resembling *in vivo*

rather than primary *in vitro* microglia (Delbridge et al. 2020). Brain slice cultures have successfully been used to investigate microglial function upon ischemia (Steiner and Humpel 2022) and in the context of neurodegeneration (Novotny et al. 2016; Tanriöver et al. 2020; Barth et al. 2021). For example, using microglia specific knockouts of neurodegenerative disease-associated genes like TREM2 allows to understand the protein's role in microglia function with results obtained in BSCs closely resembling *in vivo* observations (Mazaheri et al. 2017). On the other hand, the induction of alpha-synuclein protein aggregates in BSCs has been shown to cause microglial inclusions of misfolded αSyn (Tanriöver et al. 2020; Barth et al. 2021). This allows studying cellular and molecular responses to neurodegenerative stimuli and highlights that microglial function can be investigated from several angels in BSCs. In addition to the sustained *in vivo*-like environment for extended culture periods (Czapiga and Colton 1999), BSCs are highly accessible for manipulations like microglia depletion or administration of pharmacological compounds and for direct observation using live-cell microscopy or electrophysiological approaches (Croft et al. 2019; Schwarz et al. 2019; Coleman Jr, Zou, and Crews 2020; Barth et al. 2021; Berki et al. 2024). Thus, BSCs are a versatile model to study more complex microglial functions and in comparison to *in vivo* studies reduce the number of experimental animals needed as multiple slices are obtained from each animal, allowing the assessment of several experimental conditions (Croft et al. 2019; Barth et al. 2021).

2.3.5 Induced pluripotent stem cell-derived microglia

In vitro studies of microglia have advanced in the past 10-15 years due to the advent of induced pluripotent stem cell research. Developed by Kazutoshi Takahashi and Shin'ya Yamanaka in 2006, iPSCs have quickly progressed to become a key tool in cellular and molecular biology and were awarded with a Nobel Prize for Medicine and Physiology in 2012. Terminally differentiated somatic cells like adult human fibroblasts or monocytes are transformed into a pluripotent state by the introduction of four transcription factors: *OCT3/4*, *SOX2*, *C*-MYC and *KLF4* (Kazutoshi Takahashi and Yamanaka 2006; Kazutoshi Takahashi et al. 2007). The overexpression of these four transcription factors reverts differentiation and iPSCs closely resemble embryonic stem cells (ESC) in their gene expression profile, their ability to proliferate indefinitely and the potential to differentiate into any cell type of the three germ layers (Freude et al. 2014). To date, iPSCs enable studying human cells in health and disease and opened the door to examine the effects of disease-associated mutations in unprecedented detail by generating patient-derived cell lines or genome-editing (Dolmetsch and Geschwind 2011; Freude et al. 2014; Y. Shi et al. 2017).

By now, several protocols have been established to differentiate microglia from iPSCs taking their yolk sac-derived ontogeny into account (Muffat et al. 2016; Takata et al. 2017; Haenseler et al. 2017; Abud et al. 2017; Pandya et al. 2017; C. Z. W. Lee, Kozaki, and Ginhoux 2018; McQuade et al. 2018). The protocols share the induction of mesodermal fate and subsequent hemogenic endothelial/myeloid differentiation via varying compositions and concentrations of growth factors including bone morphogenetic protein 4 (BMP4), stem cell factor (SCF), VEGF and IL3. The obtained embryonic macrophage precursor cells are then expanded and sustained via CSF1 and IL3 and finally matured to microglia using CSF1 and IL34 (Speicher et al. 2019; Warden et al. 2023). The protocols differ in their media compositions and duration, varying between three and ten weeks (C. Z. W. Lee, Kozaki, and Ginhoux 2018; Speicher et al. 2019). In principle, two major types of protocols exist: 1) Embryoid body (EB)-based approaches simulate cell-cell signaling crucial for meso-endodermal induction whereas 2) monolayer-based approaches have a more stringent external control of cell fate by cytokine supplementation and the induction of hypoxic conditions (C. Z. W. Lee, Kozaki, and Ginhoux 2018). Recently, Dräger at al. published a new approach that generates high numbers of iPSC-derived microglia upon the overexpression of six transcription factors within 8 days (Dräger et al. 2022).

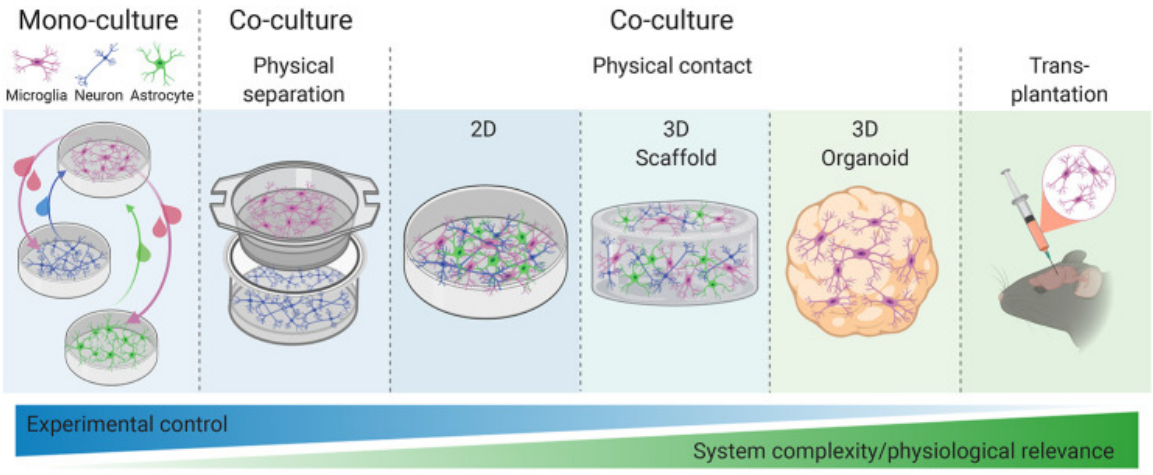

Figure 4 iPSC-based model systems to study microglia
Model systems for the study of microglia range from easy 2D cell culture models to complex 3D *in vitro* models and xenotransplantation of iPSC-derived microglia for *in vivo* investigation of human microglia. Increasing complexity of the model increases the physiological relevance of the experiments but at the same the experimental control is reduced. From Hedegaard et al. 2020, published in Frontiers in Immunology under a Creative Commons CC-BY license (CC-BY 4.0).

iPSC-derived microglia-like cells (iMicros) in monoculture express microglial markers like P2RY12, TMEM119 and IBA1 (Muffat et al. 2016; Douvaras et al. 2017) which distinguishes them from other tissue-resident macrophages or peripheral monocytes (M. L. Bennett et al. 2016).

However, the lack of the CNS environment results in an immature transcriptional phenotype, including the lack of the key microglial transcription factor Sal-like 1 (SALL1) (Gosselin et al. 2017; Park et al. 2023) as well as the upregulation of immune-response and disease-associated genes in comparison to adult human microglia (Gosselin et al. 2017; F. C. Bennett et al. 2018; Timmerman, Burm, and Bajramovic 2018; Dubbelaar et al. 2018; Dolan et al. 2023; Sun et al. 2023). Still, monocultured iMicros offer the opportunity to study basic microglial functions and the effect of disease-associated mutations as the cells are ramified, phagocytically active and respond to immune stimulation with the release of adequate cytokines (Muffat et al. 2016; Abud et al. 2017; Haenseler et al. 2017; McQuade et al. 2018). Combining iMicros with other iPSC-derived neural cell types like neurons and/or astrocytes in co-culture models results in more mature microglial phenotypes characterized by increased ramification, less pro-inflammatory and more homeostatic gene expression profiles including the expression of *SALL1* (Abud et al. 2017; Haenseler et al. 2017; Vahsen et al. 2022; Park et al. 2023), underlining the importance of the environment on microglial identity.

Even though iMicros more closely reflect the transcriptomic signature of acutely isolated microglia compared to cultivated primary or immortalized microglia (Gosselin et al. 2017; Abud et al. 2017; F. C. Bennett et al. 2018; Speicher et al. 2019; Dolan et al. 2023; Stöberl et al. 2023), findings obtained from iMicro studies should always be validated with more complex models due to their reflection of early developmental stages (Takata et al. 2017) and lack of adult homeostatic signatures when cultivated in monoculture.

2.3.6 Cerebral organoids

While the 2D models described above have the advantage of dissecting basic cell-autonomous effects, 3D models more realistically reflect cell-cell interactions occurring in the brain needed to answer complex biological questions (W. Zhang et al. 2023). Cerebral organoids, first described in 2013 by Lancaster et al., are iPSC-derived, self-organizing structures that contain various brain cell types including neurons and radial glia, as well as astrocytes and oligodendrocyte precursor cells (Lancaster et al. 2013; Lancaster and Knoblich 2014; Quadrato et al. 2017; Velasco et al. 2019; Tanaka et al. 2020). Cerebral organoids are unable to model the entire brain at once, but by now several protocols have been published to differentiate specific brain regions including cortex, hippocampus and midbrain (Paşca et al. 2015; Sakaguchi et al. 2015; Jo et al. 2016). Generation of cerebral organoids can be achieved in a patterned way by dual SMAD inhibition or in an unpatterned approach without dual SMAD inhibition (Lancaster et al. 2013; Paşca et al. 2015;

Quadrato et al. 2017). Since dual SMAD inhibition blocks mesodermal lineage differentiation (Chambers et al. 2009), microglia are not naturally arising in patterned organoids, whereas spontaneous iPSC differentiation towards mesodermal fate is possible in unpatterned ones (Ormel et al. 2018; Qian, Song, and Ming 2019; W. Zhang et al. 2023). Due to the low degree of spontaneous microglial induction, which varies between iPSC lines and protocols, organoids are nevertheless considered to be devoid of microglia and microglia have to be introduced to organoids experimentally (Quadrato et al. 2017; Melief et al. 2016; Bodnar et al. 2021; Pérez et al. 2021; W. Zhang et al. 2023). To this end, organoids and microglia are differentiated separately and microglial precursor cells are grafted into the organoids where they mature into microglia-like cells (Abud et al. 2017; Song et al. 2019; Jin et al. 2022; Park et al. 2023). Engraftment rates and microglial densities vary between protocols and no consensus on methodology has been reached yet (Abud et al. 2017; Jin et al. 2022; Park et al. 2023; W. Zhang et al. 2023; Warden et al. 2023; Sabogal-Guaqueta et al. 2024).

Microglia in cerebral organoids migrate towards lesion sites (Abud et al. 2017), release cytokines and ROS in response to immune stimuli like LPS and phagocytose a range of pathogens, cellular debris and neurodegeneration-associated stimuli like amyloid-beta peptides (Abud et al. 2017; Muffat et al. 2018; Ormel et al. 2018; Eme-Scolan and Dando 2020; Cakir et al. 2022). Furthermore, microglia interact with synapses and seem to enhance neuronal maturation (Fagerlund et al. 2021; Sabate-Soler et al. 2022; Park et al. 2023), whereas extended organoid maturation can induce cellular senescence (Shaker et al. 2021). Still, microglia in organoids more closely resemble human fetal rather than adult microglia (Hasselmann and Blurton-Jones 2020) and retain artifacts of their *in vitro* environment as observed for primary microglia cultures (Ormel et al. 2018; Popova et al. 2021).

2.3.7 In vivo mouse models and biological differences between human and mouse

Although *in vitro* models have advanced in their complexity, they are still unable to fully recapitulate microglial *in vivo* phenotypes. To study microglia *in vivo*, model organisms including rodents, non-human primates and zebrafish are commonly utilized (Sharma, Bisht, and Eyo 2021). I will only discuss the use of mice, to not exceed the scope of this thesis.

One of the most widely utilized tools for visualizing and manipulating microglia are genetically modified mice. These models exploit the Cre/loxP recombination system (Sauer 1998; Sauer and Henderson 1989) under the control of microglial promoters for the targeted expression or deletion

of genes of interest (McLellan, Rosenthal, and Pinto 2017; Stifter and Greter 2020). While the CX3CR1^{CreER} line is the most widely used, several other promoters are utilized by now including TMEM119, P2RY12 and HEXB (Eme-Scolan and Dando 2020; Faust et al. 2023). Each model comes with its own advantages, including high recombination, and drawbacks, like recombination in other myeloid cells, that must be considered when planning an experiment (Eme-Scolan and Dando 2020). Similarly, reporter mice expressing fluorescent proteins under microglia-specific promoters, like CX3CR1^{EGFP} or IBA1^{EGFP} mice have been developed (Jung et al. 2000; Hirasawa et al. 2005) and refined for higher cell type-specificity utilizing TMEM119, SALL1 and HEXB promoters (Eme-Scolan and Dando 2020; Masuda et al. 2020). Alternatively, microglia can be targeted using viral approaches, which generally cause microglial cell activation and thus render studying microglia in homeostasis difficult. Optimization of the adeno-associated virus (AAV) 9 capsid has achieved maximized microglial transduction without immune activation (R. Lin et al. 2022) and might become an important tool in the future. The tools described above can be used for fate mapping studies (Ginhoux et al. 2010; Tay et al. 2017; Barry-Carroll et al. 2023; Schulz et al. 2012) and are commonly used for 2-Photon *in vivo* live cell imaging to assess microglial motility, network dynamics, injury responses and Calcium imaging (Davalos et al. 2005; Nimmerjahn, Kirchhoff, and Helmchen 2005; Hefendehl et al. 2014; Füger et al. 2017; Cserép et al. 2020; Eme-Scolan and Dando 2020). These seminal studies, together with tools for microglia depletion (see **2.2.3 above**) have drastically advanced our knowledge about microglia biology and their role in neurodevelopment and disease. But recent studies have highlighted that mice are not the perfect model for human microglia, which must be considered when findings from mouse studies should be translated to humans:

As described before, microglia development is highly conserved between human and mice, and microglia of both species share a high overlap in 'core signature' gene expression (Galatro et al. 2017). However, many human genes enriched in microglia share little homology with their murine orthologs, if an ortholog exists at all (Mancuso et al. 2019; Hasselmann and Blurton-Jones 2020). For example, of 44 Alzheimer's disease risk genes found in human microglia only 29 have a murine ortholog with sequence similarity larger than 60 %, while nine, including CD33, have no ortholog (Mancuso et al. 2019). Additionally, the cell type-specific expression of neurodegeneration-associated risk genes is not conserved between rodents and humans (Y. Zhang et al. 2014; 2016; de Soysa et al. 2022). Together, these genetic differences render disease modelling and dissection of microglial contribution to neurodegeneration difficult.

Furthermore, human and murine microglia have been found to age differently, and discrete functional states have been described (Keren-Shaul et al. 2017; Hammond et al. 2019; Q. Li et al. 2019; Masuda et al. 2019; Geirsdottir et al. 2020). While some studies found that functional states are mostly overlapping (Mukherjee et al. 2020), others found that significant disparities in gene expression modules exist during aging (Srinivasan et al. 2020) and only few differentially expressed genes (DEG) are shared (Galatro et al. 2017). For example, adult human microglia present with a higher expression of genes involved in immune functions including sialic acid-binding immunoglobulin-type lectin (*SIGLEC*) and *MHC* genes (Galatro et al. 2017). This 'pre-activated' state is not seen in mice (Zrzavy et al. 2017), which might be explained by the limited exposure of lab mice to immune stimuli (Smith and Dragunow 2014; Geirsdottir et al. 2020). On the other hand, some microglial states, including white matter-associated microglia, have so far only been described in mice (Safaiyan et al. 2021). Distinct functional states might be biologically relevant but could also be the result of differences in processing and analysis for human and murine samples (Y. Chen and Colonna 2021; de Soysa et al. 2022; Marsh et al. 2022) and require further investigation.

2.3.8 Xenotransplantation models

To overcome the limitations of iPSC-derived microglia and mouse models, xenotransplantation models combining both approaches have been established in the past years. Pluripotent stem cell-derived microglia precursor cells are transplanted into the brains of immunodeficient mice and subsequently engraft the brain parenchyma forming a human microglia network within the mouse brain (Abud et al. 2017; Mancuso et al. 2019; Hasselmann et al. 2019; Svoboda et al. 2019; McQuade et al. 2020; Xu et al. 2020; Fattorelli et al. 2021; Claes et al. 2021). These xenotransplanted human microglia express key homeostatic markers like P2RY12 and TMEM119, are highly ramified and their transcriptome closely resembles that of adult human microglia *ex vivo* while the *in vitro* phenotype observed in monoculture or organoids is overcome (Hasselmann et al. 2019; Mancuso et al. 2019; Xu et al. 2020). Furthermore, the cells retain their microglia-specific functions and have been shown to migrate towards lesion sites, phagocytose neuronal debris (Hasselmann et al. 2019), synaptic structures and myelin (Xu et al. 2020). Similarly, peripheral immune stimulation with LPS results in morphological changes and an upregulation of phagocytosis and activation marker CD68, as observed for murine microglia (Svoboda et al. 2019).

These models offer great opportunities to cross-validate findings from mouse models while allowing the study of human microglia-specific functions and effects in health and disease. For instance, transplanting precursors into animal models of Alzheimer's disease (AD) has shown that human microglia cluster around amyloid-beta (Aβ) plaques, phagocytose Aβ, show a downregulation of homeostatic genes and an upregulation of disease-associated microglia (DAM) genes, similar to those observed in mice (Abud et al. 2017; Keren-Shaul et al. 2017; Hasselmann et al. 2019; Claes et al. 2021; Baligács et al. 2024). More in depth analysis, however, revealed that human and mouse microglia share only about one third of DAM genes and that human cells have several hundred more differentially expressed genes (Keren-Shaul et al. 2017; Hasselmann et al. 2019), underlining how important the study of human cells is. On the other hand, xenotransplanted microglia bearing disease-associated mutations can be studied in a physiological environment to delineate cell type-specific disease risk (McQuade et al. 2020; Claes et al. 2021; Baligács et al. 2024).

The major disadvantage of these models is the need for immunodeficient mice that additionally express human CSF1R ligands CSF1 or IL34 to enable and sustain human microglia engraftment (Abud et al. 2017; Hasselmann et al. 2019; Mancuso et al. 2019; Mathews et al. 2019; Hasselmann and Blurton-Jones 2020; Fattorelli et al. 2021). The effect of a missing peripheral immune system on microglia function, however, has not been studied and more research is needed. Nevertheless, xenotransplantation models are a very good model to study complex biological questions and are constantly adapted and advanced to obtain even more *in vivo*-like human microglia in a more human environment, i.e. by transplanting human cerebral organoids with microglia into mice (S. T. Schafer et al. 2023).

2.4 Neurodegenerative diseases

Neurodegenerative diseases are diseases of the central nervous system characterized by the progressive and irreversible loss of neurons that lead to severe disability and premature death (Wilson et al. 2023; Heneka et al. 2024). While each neurodegenerative disease has its own, distinct pathological cascade and manifestation, these disorders often share atypical protein aggregations, induced cell death and neuroinflammation as key hallmarks and aging as the major risk factor (Wilson et al. 2023). Neurodegenerative diseases include Alzheimer's disease (with accumulations of amyloid-beta and tau), Parkinson's disease (alpha-synuclein), Huntington's disease (huntingtin), Amyotrophic lateral sclerosis (ALS; SOD1, TDP-43, FUS, C9ORF72 and tau), frontotemporal lobar degeneration (TDP-43, FUS, C9ORF72) and Creutzfeldt-Jacob disease (CJD;

Prion protein) (Jucker and Walker 2013; Prusiner 2013; Jucker and Walker 2018; Wilson et al. 2023). Despite more than a century of research on neurodegenerative diseases, disease processes remain poorly understood and therapeutic interventions are currently limited to symptomatic treatment while causative treatment approaches remain scarce (Wilson et al. 2023). Due to increased life expectancy and aging populations, neurodegenerative diseases are a major challenge for health care systems world-wide with cases expected to double within the next 25 years (Prusiner 2013; Alzheimer's Association 2024; Alzheimer's Disease International 2024). Currently AD and other dementias account for 360 billion dollars of socio-economic burden in the United States alone, with costs expected to triple until 2050 (Alzheimer's Association 2024; Alzheimer's Disease International 2024), underlining the need to further the understanding of disease processes and development of disease-halting treatments.

2.4.1 Alzheimer's disease

Alzheimer's disease is the most common and best studied neurodegenerative disease. AD affects approximately 55 million people worldwide, accounting for 60-70 % of all dementia cases (Alzheimer's Association 2024; Alzheimer's Disease International 2024). Patients experience memory deficits, problems with language, disorientation, mood swings and changes in behavior before bodily functions are lost, ultimately leading to death (Alzheimer's Association 2024). Molecularly, the disease is characterized by the extracellular aggregation of amyloid-beta peptide into plaques, intracellular aggregation of hyperphosphorylated tau into neurofibrillary tangles, chronic neuroinflammation and progressive neuron loss (O'Brien and Wong 2011). Aβ is the cleavage product of two subsequent cleavage events of the amyloid precursor protein (APP) by β- and ɣ-secretases (Haass and Selkoe 1993; Hampel et al. 2021). Released Aβ molecules can aggregate to form soluble oligomers which can grow to form insoluble fibrils that deposit in the extracellular space forming plaques (Glenner and Wong 1984; O'Brien and Wong 2011; Jucker and Walker 2013). This aggregation occurs in a templated manner, where certain misfolded oligomers serve as "seeds" that will corrupt the folding of subsequent monomers leading to a chain reaction of protein misfolding as observed for prions (Prusiner 1991; Jucker and Walker 2013). Aggregated Aβ is neurotoxic (O'Brien and Wong 2011) and according to the '*Amyloid cascade hypothesis*' induces the misfolding of the second proteopathic protein in AD, namely tau (D. J. Selkoe 1991; Hardy and Higgins 1992; Dennis J. Selkoe and Hardy 2016). Tau is a protein that stabilizes microtubules in axons and aggregates due to pathological hyperphosphorylation, leading to neurofibrillary tangles and neuronal demise (O'Brien and Wong 2011). The mechanisms by which

Aβ induces tau aggregation and how aggregated tau spreads within the brain are still under debate (Dennis J. Selkoe and Hardy 2016).

AD is commonly considered a disease of the old, with more than 95 % of cases being diagnosed in people over the age of 65 (Alzheimer's Association 2024). However, very few people (1-2 % of AD patients) with inheritable, autosomal-dominant AD are known who develop symptoms as early as in their thirties (Long and Holtzman 2019). These patients carry mutations in the APP gene or in one of the two presenilin genes (*PSEN1* and *PSEN2*) comprising the ɣ-secretase and enable the investigation of disease progression and the development of treatments (Bekris et al. 2010; J. C. Morris et al. 2012). On the other hand, late-onset AD has many genetic and environmental risk factors, and the exact cause remains to be elucidated (Karch and Goate 2015; Andrews et al. 2023). First described by Alois Alzheimer in 1906, AD was considered a neuron-autonomous disease for about 100 years even though the very first descriptions of the disease highlighted morphological changes in (micro-) glial cells (Alois Alzheimer 1907; A. Alzheimer et al. 1995). By now, glial and neuroinflammatory contribution to disease progression are well-established due to large genome-wide association studies (GWAS) that linked most AD risks to microglia, astrocytes and neuroinflammation (Karch and Goate 2015; Bellenguez et al. 2022; Andrews et al. 2023; Reitz et al. 2023)(see **2.4.3 below**).

2.4.2 Parkinson's disease

Parkinson's Disease (PD) is a neurodegenerative disease primarily affecting the dopamine-producing neurons in the substantia nigra pars compacta which results in motor symptoms including tremors, bradykinesia, rigidity and difficulties in balance (Kalia and Lang 2015; Poewe et al. 2017). In PD, alpha-synuclein, a protein involved in vesicle trafficking and intracellular transport, becomes phosphorylated and forms intracellular aggregates coined Lewy bodies (Spillantini et al. 1997). As for Aβ and tau, misfolding follows a prion-like amplification and stereotypic spreading of aggregates across the brain (Braak et al. 2003; Jucker and Walker 2013). Similarly, the underlying cause for PD is unknown, but many risk factors have been identified (H. R. Morris et al. 2024). Age is the leading risk factor for sporadic PD, as prevalence increases from ca. 1 % in people over 65 to approximately 4.3 % in those above 85 years of age (Coleman and Martin 2022). Environmental risk factors include exposure to pesticides and heavy metals (De Miranda et al. 2022; H. R. Morris et al. 2024, 202). Genetically, mutations in the *SNCA* gene encoding αSyn, in *LRRK2*, *PINK1*, *PRKN*, *DJ1* and *GBA1* are known to be disease-causing but are found in only 5-10 % of patients (Polymeropoulos et al. 1997; Singleton and Gasser 2020; Salles,

Tirapegui, and Chaná-Cuevas 2024; H. R. Morris et al. 2024). In sporadic patients, more than 90 gene variants have been identified in GWAS analyses that indicate immune functions, lipid metabolism, lysosomal and autophagosomal pathways and vesicle transport as key drivers of disease (Bandres-Ciga et al. 2020; Kim et al. 2024).

2.4.3 Microglial functions in disease

As mentioned above, microglial function declines with age whereas neurodegenerative diseases manifest in older age, which raises the question about microglial contribution to neurodegeneration. GWAS of Alzheimer's disease patients have by now identified more than 80 genetic loci that modulate disease risk (de Rojas et al. 2021; Holstege et al. 2022), with almost 25 % being highly or exclusively expressed by microglia. At the same time, microglial contribution is well documented in all stages of disease progression (McQuade and Blurton-Jones 2019). Concomitantly, transcriptomic analyses of microglia in human AD brains and murine models of the disease have revealed an upregulation of GWAS hits in disease condition (Keren-Shaul et al. 2017; Krasemann et al. 2017; Olah et al. 2020; Sala Frigerio et al. 2019).

In early stages of the disease, microglia are recruited to Aβ plaques to phagocytose and clear the aggregates (S. E. Hickman, Allison, and El Khoury 2008; S. Hickman et al. 2018; Streit et al. 2014). With age, however, microglial phagocytosis of Aβ decreases and plaques grow larger (S. E. Hickman et al. 2013; Streit et al. 2014). Nevertheless, microglia in AD brains interact with plaques and are found to compact them by the secretion of apolipoprotein E (APOE) (Namba et al. 1991; Burns et al. 2003; Kaji et al. 2024). The formation of a tight barrier around plaques by microglia is considered to protect the surrounding neurons from neurotoxic effects exerted by Aβ (Yuan et al. 2016; Parhizkar et al. 2019). Plaque-associated microglia have a unique transcriptomic signature, coined disease associated microglia (DAM), that is defined by the upregulation of two major sporadic AD risk genes, APOE and TREM2 (Karch and Goate 2015; Krasemann et al. 2017; Keren-Shaul et al. 2017). These DAM show an upregulation of genes involved in phagocytosis, lipid metabolism, inflammation and proliferation and a downregulation of homeostatic markers like P2RY12 not observed in microglia further away from plaques and in line with previously described functional changes (Kamphuis et al. 2016; Krasemann et al. 2017; Keren-Shaul et al. 2017; Sala Frigerio et al. 2019). DAM-like transcriptomes have by now been described for mouse models of several other neurodegenerative diseases including PD, ALS and FTLD (Holtman et al. 2015; Srinivasan et al. 2016; Mathys et al. 2017), whereas human transcriptome analyses have revealed not one distinct 'DAM' cluster but rather gene expression changes across several different clusters

(Srinivasan et al. 2020; Sun et al. 2023). This highlights the differences between human and murine microglia in AD, underlining the caution needed when interpreting results from animal models (Sun et al. 2023).

Although shielding the neurons from Aβ seems beneficial, plaque-associated microglia also convey deleterious effects due to the prolonged stimulation by Aβ. Chronically activated microglia induce inflammation by the release TNFα and IL1β leading to microglia-induced neurotoxicity (Streit et al. 2004; Streit 2006; V. Hugh Perry, Cunningham, and Holmes 2007; L. E. Rojo et al. 2008; S. E. Hickman, Allison, and El Khoury 2008) and increased aggregation of Aβ (Heneka et al. 2015). Furthermore, microglia have been shown to become overwhelmed with the breakdown of Aβ due to lysosomal dysfunction. Instead, they start to accumulate intracellular Aβ aggregates which is exocytosed and thus might facilitate seeding of new plaques and spreading of the disease within the brain (Joshi et al. 2014; Venegas et al. 2017). On the other hand, models of microglia depletion have shown that the number of plaques remained unchanged while the neuronal loss and intra-neuronal accumulation of Aβ were decreased in the absence of microglia (E. E. Spangenberg et al. 2016; Sosna et al. 2018), highlighting the ambiguous role microglia play in the development and progression of AD.

Intriguingly, microglia have been shown to drive tau pathology via NLRP3 inflammasome activation (Ising et al. 2019). The loss of the NLRP3 inflammasome results in decreased tau hyperphosphorylation and subsequently reduced tau accumulation downstream of Aβ deposition in mouse models (Ising et al. 2019), supporting microglia as a mediator of Aβ toxicity in the amyloid cascade hypothesis of AD. In the white matter of murine AD models, microglia filled with lipid droplets become dysfunctional, resulting in reduced phagocytic ability and increased production of ROS and pro-inflammatory cytokines (Marschallinger et al. 2020; Hou et al. 2022). Conversely, AD pathology also induces the upregulation of MHC-II-mediated antigen presentation by microglia and the recruitment of T-cells into the brain (Sala Frigerio et al. 2019; Olah et al. 2020; X. Chen et al. 2023) which is mostly considered beneficial.

In PD, microglial involvement is underlined by the high expression of risk genes leucine-rich repeat kinase 2 (*LRRK2*) and β-glucocerebrosidase (*GBA1*) in those cells (J.-Q. Li, Tan, and Yu 2014; Brunialti et al. 2021; L. Feng et al. 2023), but the role of microglia has not been studied as extensively yet. Microglia have been shown to phagocytose extracellular αSyn in monomeric, oligomeric and fibrillar form and neuronal debris in models of synucleinopathies including PD, most likely mediated by Toll-like receptors (Fellner et al. 2013). Recognition of monomeric αSyn reportedly induces the release of anti-inflammatory cytokines whereas oligomeric and fibrillar

αSyn species elicit the detrimental release of IL1β, TNFα and ROS (Fellner et al. 2013; Joers et al. 2017; Hughes et al. 2019; Y. Feng et al. 2019; N. Li et al. 2020). Chronic microglial stimulation by αSyn leads to sustained microgliosis (Joers et al. 2017), and a vicious cycle of inflammatory cytokine release and enhanced αSyn aggregation ensues (Gordon et al. 2018). Upon phagocytosis, αSyn is subjected to autophagolysosomal degradation, a pathway enriched with PD risk genes including *LRRK2* and *GBA1* (L. Feng et al. 2023; J.-Q. Li, Tan, and Yu 2014). Microglia-specific knockout of autophagy results in an increased loss of dopaminergic neurons in a mouse model of PD (Choi et al. 2020), underlining the beneficial role of microglia in PD. Furthermore, my laboratory was able to show, that microglia in mouse models of PD contain αSyn inclusions that stain positive for amyloid-binding luminescent conjugated oligothiophene (LCO) dyes (Tanriöver et al. 2020). Although the origin of these inclusions remains unknown, intra-microglial amplification of phagocytosed material is a likely explanation that remains to be validated in models without αSyn overexpression. Moreover, the release of αSyn-containing exosomes from microglia is implicated in the spreading of αSyn to seed new lesions and as a possible mechanism of αSyn neuron-to-neuron spreading (Danzer et al. 2012; Grozdanov and Danzer 2018; Xia et al. 2019; M. Guo et al. 2020). Another proposed mechanism of cell-to-cell transfer has been described by Scheiblich et al., who observed the transfer of αSyn from microglial cells with a high burden to those with a lower burden via tunneling nanotubes for joint degradation (Scheiblich et al. 2021), but the translational relevance for disease progression remains to be elucidated.

While this thesis focusses on microglial contribution in AD and PD, several studies have investigated them in other neurodegenerative diseases including ALS and multiple sclerosis (MS) and found a common downregulation of homeostatic markers and increased expression of APOE in a phenotype named ‘microglial neurodegenerative phenotype’ (MGnD) (Krasemann et al. 2017). Furthermore, microglia are highly implicated in neurodevelopmental and psychiatric disorders including autism spectrum disorder and schizophrenia due to dysregulated synaptic pruning and neuronal circuit modulation (Y. Zhan et al. 2014; Petrelli, Pucci, and Bezzi 2016; Filipello et al. 2018) as well as in stroke (Patel et al. 2013; Brown and Neher 2014). In all diseases, microglia exert both beneficial and detrimental effects which have to be delineated further to eventually utilize microglia as a therapeutic target.

2.5 Aim of the study

Microglia are the yolk sac-derived resident immune cells of the CNS. Under homeostatic conditions microglia are long-lived and self-sustained. Due to limited access to live human brain tissue, most of the current knowledge has been derived from murine models. At the same time, microglia have emerged as key players in neurodegenerative diseases as they highly express many risk genes and directly interact with pathological protein aggregates. Many of these human risk genes, however, have limited amino acid homology or orthologs in mice, which complicates the study of microglial contributions to pathological processes.

To overcome the confounding effects of current model systems, the main goal of this study was to establish a novel *in vitro* model system to study human microglia in a complex, yet easily manipulatable environment. For this purpose, I generated a chimeric organotypic brain slice culture model (cBSC), by transplanting human iPSC-derived microglia into microglia-depleted murine brain slice cultures. I characterized the model and analyzed the human microglia phenotype from single cell level to network organization and basic functionality. Furthermore, I investigated the molecular basis for human cell differentiation in murine tissue exemplified by human CSF1R interaction with murine ligands. Lastly, I established cBSCs as a novel tool for studying human microglia in the context of neurodegenerative disease pathology. As proof-of-principle, I investigated human microglia responses in cBSCs to seeded αSyn and showcase how the chimeric model can be adapted to study the cell type-specific effects of disease-associated variants.

3 Material and Methods

3.1 Material

3.1.1 Cell and tissue culture media

Table 1 EB Induction Medium

Component	Manufacturer and Article No.	Final Concentration
mTeSR Plus	Stemcell Technologies 100-0276	1x
hBMP4	Miltenyi Biotec 130-111-167	50 ng/ml
hVEGF	Miltenyi Biotec 130-109-396	50 ng/ml
hSCF	R&D Systems 255-SC-050	20 ng/ml
+Y-27632 on Day1	Stemcell Technologies 72304	10 µM

Table 2 EB Differentiation Medium

Component	Manufacturer and Article No.	Final Concentration
X-Vivo15	Lonza BE02-053Q	1x
hCSF1	Miltenyi Biotec 130-096-493	100 ng/ml
hIL3	Miltenyi Biotec 130-095-069	25 ng/ml
Penicillin/Streptomycin	Gibco 15140122	100 U/ml/ 100 µg/ml
Glutamax	Gibco 35050-038	2 mM
Beta-mercaptoethanol	Gibco 31350010	0.055 mM

Table 3 Supplemented Stempro34 Medium

Component	Manufacturer and Article No.	Final Concentration
Stempro 34 SFM	Gibco 10639011	1x
Penicillin/Streptomycin	Gibco	100 U/ml/ 100 µg/ml

	15140122	
Glutamax	Gibco 35050-038	2 mM
Ascorbic acid	Sigma-Aldrich A4403-100mg	0.5 mM
Transferrin from human serum	Roche 10652202001	150 µg/ml
Monothioglycerol	Sigma-Aldrich M6145	0.45 mM

Table 4 SF Diff Medium

Component	Manufacturer and Article No.	Final Concentration
Iscove's Modified Dulbecco's Medium (IMDM) plus Glutamax	Gibco 31980030	0.75x
F12 Medium	Gibco 11765054	0.25x
N2 Supplement	Gibco 17502048	0.5x
B27 Supplement with vitamin A	Gibco 17504001	1x
Bovine Serum Albumin Fraction V	Gibco 15260037	0.5 mg/ml
Penicillin/Streptomycin	Gibco 15140122	100 U/ml/ 100 µg/ml

Table 5 iMic Monoculture Medium

Component	Manufacturer and Article No.	Final Concentration
Advanced Dulbecco's Modified Essential Medium (DMEM)-F12	Gibco 12634010	0.5x
Advanced Neurobasal Medium	Gibco 10888-022	0.5x
beta-mercaptoethanol	Gibco 31350010	50 µM
Gluatamax	Gibco 35050-038	2 mM
B27 Supplement with vitamin A	Gibco 17504001	1x
hCSF1	Miltenyi Biotec 130-096-493	20 ng/ml
hIL34	Peprotec 200-34	100 ng/ml

Table 6 BSC Preparation Medium

Component	Manufacturer and Article No.	Final Concentration
Minimum Essential Medium (MEM, without Phenolred), 2x	Gibco 21935028	1x
UltraPure Distilled Water	Invitrogen 10977035	-

Table 7 BSC Culture Medium

Component	Manufacturer and Article No.	Final Concentration
Minimum Essential Media (MEM)	Gibco 32360034	1x
Horse serum (Heat-Inactivated)	Gibco 26050088	20 %
Glutamax	Gibco 35050-038	1 mM
Ascorbic acid	Sigma-Aldrich A4403-100mg	0.00125 %
Insulin	Gibco 12585014	0.001 mg/ml
Calcium chloride ($CaCl_2$)	Sigma-Aldirch 21115-100ml	1 mM
Magnesium sulfate ($MgSO_4$)	Sigma-Aldrich 83266-100ml-F	2 mM
D-Glucose (water-free)	Roth X997.1	13 mM
Penicillin/Streptomycin	Gibco 15140122	100 U/ml/100 µg/ml
pH = 7.28 sterile filtered		

3.1.2 Buffers

Table 8 RIPA Buffer

Component	Manufacturer and Article No.	Concentration
Triton X-100	Sigma-Aldrich T9284	1 %
Sodium deoxycholate	Sigma-Aldrich 30970	0.5 %
Sodium dodecyl sulfate (SDS)	Sigma-Aldrich 71725-100g	0.1 %
Tris-HCl	Thermo Fisher Scientific	25 mM

	15568025	
Sodium chloride NaCl	Sigma-Aldrich S7653	100 mM

Table 9 10x Hank's Buffered Salt Solution (HBSS)

Component	Manufacturer and Article No.	Concentration
Sodium chloride (NaCl)	Sigma-Aldrich S7653	1.38 M
Potassium chloride (KCl)	Applichem A1164,0500	53.3 mM
Potassium dihydrogen phosphate (KH_2PO_4)	VWR International 1.04873.1000	4.4 mM
Disodium hydrogen phosphate (Na_2HPO_4)	VWR International 1.06580.1000	3 mM
Sodium hydrogencarbonate ($NaHCO_3$)	Sigma-Aldrich S6297-250G	40 mM
D-Glucose	Roth X997.1	56 mM
HEPES	Roth 9105.2	25 mM
ddH_2O		Fill up to 1 L

Table 10 Homogenization Buffer

Component	Manufacturer and Article No.	Amount
1x HBSS	Self-made from 10x stock	10 ml
45 % D-Glucose Self-made stock in ddH_20	Roth X997.1	120 µl
DNAse I	Sigma-Aldrich D5025	1 mg

Table 11 Western Blot Transfer Buffer

Component	Manufacturer Article No.	Final Concentration
Glycine	Bio-Rad Laboratories 161-0718	192 mM
Tris-HCl	Applichem A1086,1000	25 mM
Methanol	Sigma-Aldrich 494437	20 %

Table 12 Tris-Buffered Saline Solution with Tween-20 (TBS-T)

Component	Manufacturer Article No.	Final Concentration
Sodium chloride (NaCl)	Sigma-Aldrich S7653	150 mM
Tris-HCl	Applichem A1086,1000	15.22 mM
Trizma Base	Sigma-Aldrich RDD008	4.62 mM
Tween-20	Roth 9127.1	0.1 %

Table 13 Extracellular Recording Solution

Component	Manufacturer Article No.	Final Concentration
Sodium chloride (NaCl)	Sigma-Aldrich S7653	124 mM
Sodium hydrogencarbonate ($NaHCO_3$)	Sigma-Aldrich S6297-250G	26 mM
Potassium chloride (KCl)	Applichem A1164,0500	3.5 mM
Magnesium chloride $MgCl_2$	Sigma-Aldrich 208337	1 mM
Calcium chloride ($CaCl_2$)	Sigma-Aldirch 21115-100ml	2 mM
Disodium hydrogen phosphate (Na_2HPO_4)	VWR International 1.06580.1000	1.2 mM
D-Glucose	Roth X997.1	20 mM
pH 7.4, osmolarity 305 mOsm/kg, equilibrated with 95 % O_2/5 % CO_2		

3.1.3 Cytokines and antibodies

Table 14 Cytokines in iPSC culture

Cytokine	Manufacturer	Article No.
Human BMP4	Miltenyi Biotec	130-111-167
Human SCF	R&D Systems	255-SC-050
Human VEGF	Miltenyi Biotec	130-109-396
Human IL3	Miltenyi Biotec	130-095-069
Human IL34	PeproTech	200-34
Human CSF1	Miltenyi Biotec	130-096-493
Human IL6	Miltenyi Biotec	130-095-0352

Human DKK1	Miltenyi Biotec	130-103-444
CHIR99021	Miltenyi Biotec	130-103-926
Human bFGF	Miltenyi Biotec	130-093-564
Mouse CSF1	Miltenyi Biotec	130-101-706
Mouse IL34	Biolegend	577604

Table 15 Receptors for SPR

Component	Manufacturer	Article Number
Mouse CSF1R Fc Chimera Protein	R&D Systems	3818-MR-050
Human CSF1R Fc Chimera Protein	R&D Systems	329-MR-100/CF
Human PDGDRb Fc Chimera Protein	R&D Systems	385-PR-100/CF

Table 16 Antibodies for Western Blot

Antigen (+ Tag)	Host Species	Dilution, Incubation	Manufacturer Article No.	Use
CSF1R	Rabbit	1:1000 4 °C, o/n	Cell Signaling Technology 3152S	Primary AB
Phospho-CSF1R (Tyr723)	Rabbit	1:1000 4 °C, o/n	Cell Signaling Technology 3155S	Primary AB
ERK1/2	Rabbit	1:1000 4 °C, o/n	Cell Signaling Technology 9102S	Primary AB
Phospho-ERK1/2 (Thr202/Tyr204)	Rabbit	1:1000 4 °C, o/n	Cell Signaling Technology 9101S	Primary AB
GAPDH (6C5)	Mouse	1:100,000 rt, 1 h	HyTest Ltd 5G4-6C5	Primary AB
β-III-tubulin	Rabbit	1:2000 rt, 1 h	Sigma-Aldrich T2200-200µl	Primary AB
Rabbit-HRP	Goat	1:20,000 rt, 1h	Jackson ImmunoResearch 111-035-003	Secondary AB
Mouse-HRP	Goat	1:20,000 rt 1h	Jackson ImmunoResearch 115-035-068	Secondary AB

Table 17 Primary antibodies for immunofluorescence

Antigen	Host Species	Dilution	Manufacturer Article No.	Antigen Retrieval Incubation Time
Aβ (CN6)	Rabbit Polyclonal	1:1000	ImmunoK A006915-RB5935	4 °C, o/n
Iba1	Goat polyclonal	1:250	Novus Biologicals NB100-1028	4 °C, o/n
Iba1	Rabbit polyclonal	1:250	Thermo Fisher Scientific PA521274	4 °C, o/n

KU80 (STEM101)	Mouse monoclonal	1:250	Takara Bio Y40400	4 °C, o/n
PU.1	Rabbit monoclonal	1:250	Thermo Fisher Scientific MA5-15064	4 °C, o/n
pS129	Rabbit monoclonal	1:1000	AbCam ab51253	4 °C, o/n
tdTomato	Roat polyclonal	1:250	SICGEN AB8181-200	4 °C, o/n
Human TMEM119	Rabbit polyclonal	1:100	AbCam ab185333	Antigen retrieval: Citrate Buffer + 0.05 % Tween, 10 min, 97 °C 4 °C, 3 days
Human TREM2	Goat monoclonal	1:50	R & D Systems AF1828-SP	4 °C, o/n

Table 18 Secondary antibodies for immunofluorescence

Antigen + Tag	Host Species	Dilution	Manufacturer Article No.	Incubation Time
Goat-Alexa 488	Donkey	1:250	Jackson ImmunoResearch 705-545-147	rt, 2 h
Goat-Alexa 568	Donkey	1:250	Invitrogen A-11057	rt, 2 h
Goat-Alexa 647	Donkey	1:250	Jackson ImmunoResearch 705-605-147	rt, 2 h
Mouse-Alexa 488	Donkey	1:250	Jackson ImmunoResearch 715-545-150	rt, 2 h
Mouse-Alexa 647	Donkey	1:250	Jackson ImmunoResearch 715-605-151	rt, 2 h
Rabbit-Alexa 488	Donkey	1:250	Jackson ImmunoResearch 711-545-152	rt, 2 h
Rabbit-Alexa 568	Donkey	1:250	Invitrogen A10042	rt, 2 h
Rabbit-Alexa 647	Donkey	1:100	Jackson ImmunoResearch 711-605-152	rt, 2 h

Table 19 Amyloid-binding dyes

Component	Manufacturer	Concentration used	Incubation Time
Methoxy-X04	Biomol Cay20476-10	0.04 mg/ml	rt, 30 min
pFTAA	Peter R. Nilsson Linköping, Sweden	3 µM	rt, 30 min

Table 20 Other antibodies

Antigen	Host Species	Concentration	Manufacturer Article No.	Use
Mouse CSF1R	Rat monoclonal	5 µg/ml	BioLegend 135539	Depletion of mouse microglia in BSC
Mouse IL34	Rat monoclonal	1 µg/slice	Bio-Techne MAB5195	Block of mIL34 signaling in BSC

3.1.4 Other chemicals, kits and consumables

Table 21 Kits

Kit	Manufacturer	Article Number
Chromium Next GEM Chip G Single Cell Kit	10X Genomics	1000120
Chromium Next GEM Single Cell 3' Kit v3.1	10X Genomics	1000268
DNeasy Blood & Tissue Isolation Kit	Qiagen	69504
Dual Index Plate TT Set A	10X Genomics	1000215
High Sensitivity D5000 Buffer and Ladder	Agilent Technologies	5067-5592
High Sensitivity D5000 ScreenTape Device	Agilent Technologies	5067-5593
Mouse Cell Depletion Kit	Miltenyi	130-104-694
QIAquick PCR Purification Kit	Qiagen	28104
QIAxcel DNA screening kit	Qiagen	929004
REDextract-N-Amp™ Tissue PCR Kit	Sigma-Aldrich	XNAT-1000RXN
SPRIselect Reagent Kit	Beckmann Coulter	B23317
V-PLEX Human Proinflammatory Panel II (4-Plex, IL-1b, IL-6, IL-8, TNF-a) kit	Meso Scale Discovery	K15053D-2

Table 22 Other chemicals and reagents

Chemical	Manufacturer	Article Number
4',6-diamidino-2-phenylindole (DAPI)	Sigma-Aldrich	D9542-1mg
AAVS1-Pur-CAG-EGFP Plasmid	Addgene	#80945
Amyloid-beta 1-40	Bachem Holding	4014442
Beta-mercaptoethanol (Western Blot)	Applichem	A1108.0025
Boric Acid	Sigma-Aldrich	B6768-500G
Bovine Serum Albumin (Cell Culture)	Gibco	15260037
Bovine Serum Albumin (Western Blot)	Biomol	1400.100
Cremophore EL	Sigma-Aldrich	C51335-500G
Dako Fluorescence Mounting Medium	Agilent Technologies	S302380-2

Ethylenediaminetetraacetic acid (EDTA)	Sigma-Aldrich	E7889
Geltrex	Gibco	A1413302
Halt™ Protease and Phosphatase Inhibitor Cocktail	Thermo Fisher Scientific	78443
HEPES (for SPR)	Thermo Fisher Scientific	15630-080
Lipopolysaccharide (LPS)	Sigma-Aldrich	L6511-100mg
Normal Donkey Serum	Biozol Diagnostika	LIN-END9000
NuPage™ LDS Sample Buffer	Thermo Fisher Scientific	NP0007
NuPage™ MOPS SDS Running Buffer	Thermo Fisher Scientific	NP0001
Pierce™ BCA Protein Assay	Thermo Fisher Scientific	23227
Poly-D-Lysine	Thermo Fisher Scientific	A3890401
Pre-formed fibrils of alpha-synuclein	Ronald Melki Institut François Jacob, Fontenay-aux-Roses, France	n/a
Puromycin	Sigma-Aldrich	P8833-10mg
ReLeSR	StemCell Technologies	100-0483
Skim Milk Powder	Merck	70166-500G
Sodium Azide	Sigma-Aldrich	S2002-5G
Stempro™ Accutase	Gibco	A1110501
SuperSignal™ West Dura Extended Duration Substrate	Thermo Fisher Scientific	34076
SuperSignal™ West Substrate Pico Plus Chemiluminescent Substrate	Thermo Fisher Scientific	34080
Tween-20	Sigma-Aldrich	P2287

Table 23 Plasticware and consumables

Article	Manufacturer	Article Number
12-well plate, Costar TC-treated	Corning	CLS3513-50EA
256-MEA chip	Multi-Channel Systems	256MEA100/30iR-ITO-pr
6-well plate, Costar TC-treated	Corning	CLS3516-50EA
8-Tube Strip, PCR Consumables	Brand	BR781320
AggreWell800, 24-well	StemCell Technologies	34811
Amersham Protan Nitrocellulose Membranes, 0.2 µm	VWR International	10600001
Amersham™ Hyperfilm™ films	VWR International	28-9068-36
Neubauer Zählkammer Improved	Sigma-Aldrich	BR717820-1E
Cell Lifter	VWR International	734-2979

Cell Strainer, 40 µm EASYSTRAINER	Greiner Bio-One	542040
Conical tubes, 15 and 50 ml	Greiner Bio-One	188261-N and 210261
Coverslips 24 x 50 mm	Menzel	MZ-0029
Coverslips, 19 mm	VWR International	631-0155
DNA Lobind tubes, safelock 0.5, 1.5, 2 ml	Eppendorf	00301080-35/-51/78
Dounce Homogenizer, 5 ml	Thermo Fisher Scientific	10127661
Filcon Cell Strainer	BD Biosciences	340607
harp slice grid	Multi-Channel Systems	ALA HSG-MEA-5B
Micro reaction tubes, safe-lock, 0.5, 1.5, 2 ml	Eppendorf	00301233-01/-28/-44
Micropipettes, Research Plus 2 – 1000 µl	Eppendorf	3123000942
Millicell® Standing Cell Culture Inserts	Millipore	PICM0RG50
Nunc Petri dish, 35 mm	Thermo Fisher Scientific	153066
NuPAGE Bis-Tris 4-12% Gels, 20 well	Thermo Fisher Scientific	WG1402BOX
Potter-Elvehjem Tissue Grinders, 5 ml	Thermo Fisher Scientific	10127661
Sensor Chip Protein A	Cytiva	29127557
TOMO Adhesive Slides	VWR International	631-1109E
Wheaton Dounce Homogenizer, 7 ml	Thermo Fisher Scientific	06-435A

3.1.5 Devices

Table 24 Devices

Device	Manufacturer	Article Number
Amaxa Nucleofactor II Device	Lonza	
Biacore™ X100 system	Cytiva	BR110073
Cell Culture Microscope	Leica	
CellXpert® C170i Incubator	Eppendorf	6731000051
Chromium Controller	10X Genomics	120270
Eppendorf Centrifuge 5810R	Eppendorf	5811000015
Eppendorf Microcentrifuge 5424R	Eppendorf	5404900023
Heracell™ VIOS 160i CO2 Incubator	Thermo Fisher Scientific	15363212
Heraeus Megafuge 1.0R	Kendro	75003060
HM 650 V Vibrating-Blade Microtome	Thermo Fisher Scientific	12082999
KONICA SRX-101A developer	Konica Minolta	
LS MACS Separation Columns	Miltenyi	130-042-401
LSM 880 NLO microscope	Carl Zeiss	
McIllwain Tissue Chopper	Stoelting Europe	51350V

MEA Headstage	Multi Channel Systems	MEA2100-256-headstage
MEA Interface Board	Multi Channel Systems	MCS-IFB 3.0 Multiboot
MEA Internal Heating Element and Temperature Controller	Multi Channel Systems	TC02
MEA Perfusion cannula with a heating element	Multi Channel Systems	PH01
MEA Peristaltic Perfusion System	Multi Channel Systems	PPS2
MEA Workstation Sensapex uM	Sensapex, Oulu, Finland	
Mesoscale Sector Imager 6000	Meso Scale Discovery	
Microcentrifuge 5424R	Eppendorf	
MS MACS Separation Columns	Miltenyi	130-042-201
Nanodrop2000	Thermo Fisher Scientific	ND-2000
OctoMACS	Miltenyi	130-042-108
ProFlex™ PCR System	Thermo Fisher Scientific	4484073
QIAxcel Advanced	Qiagen	
Stereomicroscope Stemi 508	Zeiss	435064-9020
Trans-Blot Turbo Blot System	Bio-Rad Laboratories	170-4150
W Plan-Apochromat x20/1.0 objective	Carl Zeiss	421452-9700-000

3.1.6 Software

Table 25 Software

Software	Manufacturer
Affinity Designer v. 1.10.8	Serif Europe, West Bridgford, United Kingdom
Biacore Analysis Software	Cytiva, Marlborough, Massachusetts, USA
FIJI 2.1.0/1.53c	Schindelin et al. 2012
GraphPad Prism 10	GraphPad Software Inc., San Diego, California, USA
Huygens Essential 20.04	Scientific Volume Imaging B.V., Hilversum, The Netherlands
Imaris 9.7.2	Bitplane, Belfast, United Kingdom
MARS Data Analysis-Software	BMG Labtech, Ortenberg, Germany
MSD discovery workbench software 3.0	Meso Scale Discovery, Rockville, Maryland, USA
Multi Channel Experimenter	Multi Channel Systems MCS GmbH, Reutlingen, Germany
Python	https://www.python.org/
QIAxcel ScreenGel 1.5.0	Qiagen, Hilden, Germany
Snapgene	https://www.snapgene.com
Time Series Analyzer v3 for FIJI	https://imagej.nih.gov/ij/plugins/timeseries.html
Zen Black	Zeiss, Oberkochen, Germany

3.2 Methods

3.2.1 Cell and tissue culture

3.2.1.1 Induced pluripotent stem cell culture

Human induced pluripotent stem cells (iPSC, for details about lines see **Table 26**) were maintained in mTeSR Plus medium (mTeSR$^+$, Stemcell Technologies) on Geltrex-coated (Thermo Fisher Scientific) 6-well plates (Corning) until reaching ~ 80 % confluency. iPSCs were routinely split using ReLeSR (Stemcell Technologies). After a wash with PBS (Gibco), iPSCs were incubated with ReLSR for 5-6 minutes (min) at 37 °C and collected using Wash Buffer (Advanced DMEM-F12 + 0.1 % BSA Fraction V, both Gibco). Cells were maintained in small clumps during rinsing and resuspension. Detached iPSCs were collected in a conical tube (Greiner) and centrifuged at 300 g for 5 min (Heraeus Multifuge 3-SR) at room temperature (rt) prior to seeding them on a freshly coated plate, splitting ratios varied between 1:6 to 1:15. For the first 24 hours after splitting, 10 µM Rock-Inhibitor Y27632 (Stemcell Technologies) was added to the medium to enhance cell survival. iPSCs were cultured at 37 °C, 5 % CO_2 and 100 % humidity with media changes 24 h after splitting and subsequently every other day.

Table 26 iPSC lines

iPSC Line	Other Name / Identification Number	Genotype	Donor	Source
BIONi010-C	K3P53	Control WT	Male, African-American (Black), 15-19 years old	European Bank for induced pluripotent Stem Cells (EBiSC)
KOLF2.1J	JIPSC1000	Control WT	Male, Caucasian (White), 55-59 years old	Jackson Laboratories, (Jax)
KOLF2.1J_ CSF1R het	JIPSC1046	$CFS1R^{+/E633K}$	Derived from KOLF2.1J	Jax
KOLF2.1J_ CSF1R hom	JIPSC1044	$CFS1R^{E633K/E633K}$	Derived from KOLF2.1J	Jax
KOLF2.1J_ CSF1R KO	330_CSF1R_KO	$CSF1R^{-/-}$	Derived from KOLF2.1J	Jax
INDB-5-1	K5	Control WT	Male, Caucasian (White), 24 years old	Institute of Anatomy, University of Tübingen, Liebau Lab

3.2.1.2 Transfection of iPSCs

To generate iPSCs that uniformly express green fluorescent protein (GFP), cells were transfected using in Human Stem Cell Nucleofector© Kit 2 (Lonza) following manufacturer's instructions. In brief, iPSCs were cultured as described above. Upon reaching 80 % confluency, cells were given new medium containing 10 µM Y27632 one hour before they were detached to single cells using Accutase (Gibco, 6-minute incubation). 1 million cells were resuspended in Nucleofector© Solution 2 (Lonza), mixed with 2 µg plasmid DNA (AAVS1-Pur-CAG-EGFP, Addgene), electroporated using Nucleofector© program B-016 and immediately plated into pre-warmed mTeSR⁺ supplemented with 10 µM Y27632 onto Geltrex-coated plates. After 24 hours, fresh medium was added to the cells, the first full medium change was performed 48 hours post-transfection. Three to four days post-transfection, puromycin selection (0.5 µg/ml, Sigma-Aldrich) was started and the supplemented medium was refreshed every day for 5 days. After fluorescence was confirmed at an epifluorescence microscope (Leica), iPSCs were expanded without further selection.

3.2.1.3 Embryoid body-based differentiation of iMics

Unless otherwise noted, iPSCs were differentiated to microglial cells (iMic) following the embryoid body (EB)-based protocol established by (Haenseler et al. 2017) with slight modifications. For this, iPSCs were washed with PBS and treated with Accutase for 6-7 min to detach them as single cells. Cells were collected in Wash Buffer before they were centrifuged at 300 g at rt for 5 min (Heraeus Multifuge 3-SR). The supernatant was aspirated, the cells were resuspended in Wash Buffer and the cell number was determined using a hemocytometer (Neubauer Zählkammer Improved, Brand). The appropriate volume containing 2.5 million cells was centrifuged again, before iPSCs were resuspended in 2 ml EB Induction Medium (mTeSR⁺ + 20 ng/ml SCF (R & D Systems) + 50 ng/ml BMP4 (Miltenyi Biotec) + 50 ng/ml VEGF (Miltenyi Biotec), supplemented with 10 µM Y27632 for the first 24 hours) and seeded into one 24-well in an AggreWell800 plate (pre-treated with anti-adherence rinsing solution, both Stemcell Technologies). The cells were centrifuged at 800 g for 3 min without break to achieve a homogenous distribution within the microwells that allows the formation of similarly sized EBs. The cells were cultivated in the microwell plate at 37 °C and 5 % CO_2 for 5 days with daily 75 % medium changes.

After 5 days, EBs were carefully dislodged from the AggreWell and transferred to 2 6-well plates with an equal number of EBs per well in 2 ml EB Differentiation Medium (X-Vivo 15 (Lonza), 2 mM Glutamax (Gibco), 0.55 mM β-mercaptoethanol (Gibco), 100 U/ml/ 100 µg/ml

Penicillin/Streptomycin (ThermoFisher Scientific), 25 ng/ml IL-3 (Miltenyi Biotec), 100 ng/ml CSF1 (Miltenyi Biotec) per well. The EBs were kept in EB Differentiation Media at 37 °C and 5 % CO_2 with media changes every 7 days.

3.2.1.4 Monolayer-based differentiation of iMics

Additionally, iPSCs were differentiated to iMics following the monolayer-based protocol by (Takata et al. 2017). For this, iPSCs were cultivated as usual and plated at roughly 10,000 cells/cm^2 (in clumps) onto Geltrex-coated plates in mTeSR$^+$ supplemented with 10 µM Y27632. After 24 hours denoted as Day 0, the medium was changed to Stempro34 SFM (Gibco) supplemented with 2 mM Glutamax (Gibco), 0.5 mM Ascorbic Acid (Sigma-Aldrich), 150 µg/ml Transferrin (Roche), 0.45 mM Monothioglycerol (Sigma-Aldrich), 100 U/ml/ 100 µg/ml Penicillin/Streptomycin (Gibco) for the remainder of cultivation period, with medium changes every 2 days. On Day 0, the Supplemented Stempro34 medium was supplemented with 5 ng/ml BMP4 (Miltenyi), 50 ng/ml VEGF and 2 µM CHIR99021 (Miltenyi) and cells were transferred to hypoxia conditions for the next 8 days (37 °C, 5 % CO_2, 5 % O_2, Eppendorf CellXpert® C170i). On Day 2, the medium was supplemented with 5 ng/ml BMP4, 50 ng/ml VEGF and 20 ng/ml bFGF (Miltenyi). On Day 4, the medium contained 15 ng/ml VEGF, 55 ng/ml bFGF. From Day 6 onwards, free-floating precursor cells started to emerge. During all subsequent media changes, the supernatant medium was collected, centrifuged (300 g, 5 min, rt) and the cells were resuspended in the respective medium of the day and returned to the culture wells. On Day 8 the cells were transferred to normoxic incubator conditions (37 °C, 5 % CO_2, atmospheric O_2). Media composition for Day 6-10: Supplemented Stempro-34 + 10 ng/ml VEGF, 10 ng/ml IL6 (Miltenyi), 20 ng/ml IL3, 30 ng/ml DKK1 (Miltenyi), 50 ng/ml SCF. For Day 12 and 14, the medium was supplemented with 10 ng/ml bFGF, 10 ng/ml IL6, 20 ng/ml IL3 and 50 ng/ml SCF. For the final differentiation, SF Medium (0.75x IMDM-Glutamax (Gibco), 0.25x F12 (Gibco), 0.5x N2 Supplement (Gibco), 1x B27 Supplement with Vitamin A (Gibco), 0.5 mg/ml BSA (Gibco), 100 U/ml/ 100 µg/ml Penicillin/Streptomycin (Gibco)) was supplemented with 50 ng/ml CSF1 (Miltenyi) on Days 16-22, before pre-iMics were harvested once on Day 25 and grafted to HSCs as described below.

3.2.1.5 iMic precursor harvesting and engrafting

After 2-3 weeks of EB cultivation, non-adherent microglial precursor cells (pre-iMic) started to be released into the culture medium. Pre-iMics were harvested from EB cultures once per week during media changes. For this, the supernatant medium was strained through a 40 µm filter (Greiner) and collected in 50 ml conical tubes (Greiner). The EBs and cells remaining in the well were provided with 2 ml fresh EB Differentiation Medium. The collected medium containing non-

adhesive cells was centrifuged at 300 g for 5 min, the supernatant was aspirated, the cells were resuspended in Wash Buffer and counted using a hemocytometer. Subsequently, the appropriate volume was taken from the suspension and centrifuged again. Pre-iMics were resuspended at 10,000 cells/µl in EB Differentiation Medium (unless otherwise noted) and 1 µl of the cell suspension was added onto each BSC for engraftment.

3.2.1.6 iMic monoculture

For experiments utilizing iMic monocultures (mono iMic), pre-iMics were harvested as described above. The appropriate number of pre-iMics was resuspended in iMic Monoculture Medium (50 % Advanced Neurobasal Medium (Gibco), 50 % Advanced DMEM-F12 (Gibco), 1 x B27 Supplement with Vitamin A (Gibco), 2 mM Glutamax (Gibco), 0.1 mM β-mercaptoethanol (Gibco), 100 ng/ml IL-34 (Miltenyi Biotec), 20 ng/ml M-CSF (Miltenyi Biotec)) and seeded at a density of 15,000-20,000 cells/cm^2 into multiplate wells. Pre-iMics differentiated to mono iMics over the course of at least two weeks prior to any experiments. Mono iMics were cultivated at 37 °C and 5 % CO_2 with 3 media changes per week.

For experiments with subsequent immunofluorescence staining, mono iMics were cultivated on Poly-D-Lysine-coated ((Gibco) 50 µg/ml in Borate Buffer (100 mM, pH 7.4)) glass coverslips (VWR) in 12-well plates. At the end of the cultivation period, cells were briefly washed with PBS and fixed with 4 % paraformaldehyde (PFA) in PBS for 10 minutes at room temperature. After three washes with PBS (10 min each), fixed cells were stored at 4 °C until immunofluorescence staining was performed.

3.2.1.7 Cytokine stimulation assay

KOLF2.1J iMics were harvested and plated as monocultures in 6-well plates as described above and differentiated in iMic Monoculture Medium for 14 days with 3 medium changes per week. The last medium change was carried out 48 hours before the cytokine stimulation. On the day of stimulation, the culture medium was replenished with 100 ng/ml hCSF1, hIL34, both human cytokines, mCSF1 or mIL34, respectively, for 5 min at 37 °C. Subsequently, the cells were washed once with cold PBS and lysed with RIPA Buffer (1 % Triton X-100, 0.5 % sodium deoxycholate, 0.1 % sodium dodecyl sulfate, 25 mM Tris-HCl, 100 mM NaCl) on ice for 5 min. The cells were scraped off the well, the cell lysates were collected and vortexed twice for 30 seconds followed by centrifugation at 10,000 g (microcentrifuge 5424R, Eppendorf SE) at 4 °C for 10 min. The supernatant was transferred to a new tube and either used for downstream analysis or frozen at - 80 °C until further processing.

3.2.2 Organotypic slice cultures

3.2.2.1 Mice and genotyping

For the preparation of organotypic hippocampal brain slice cultures (BSC), C57BL/6J (Jackson) and heterozygous B6.Cg-Tg(Aif1-EGFP)1Kohs/J- (short: Iba1-EGFP) (Hirasawa et al. 2005) were used. All animal experiments were performed in accordance with German Animal Protection Laws and were registered as N04/19M and N03/24M with the Regierungspräsidium Tübingen. To determine the genotype of Iba1-EGFP mice, prepared HSC were observed under an epifluorescence microscope (Leica) immediately after preparation and checked for fluorescence in the green channel. Adult animals used for breeding Iba1-EGFP mice were marked with ear tags and the tissue obtained during that process was used for subsequent genotyping. The tissue was lysed, and the DNA was extracted using the REDextract-N-Amp™ Tissue PCR Kit (Sigma-Aldirch) according to the manufacturer's instructions. Presence of the transgene was determined via polymerase chain reaction (PCR) and analysis using a QIAxcel Advanced with a QIAxcel DNA screening kit and the QIAxcel ScreenGel 1.5.0 software (all Qiagen).

3.2.2.2 Generation of hippocampal brain slice cultures

Murine organotypic hippocampal brain slice cultures (BSC) were prepared following the protocol initially described by (Stoppini, Buchs, and Muller 1991). In brief, p4 to p6 mouse pups (C57BL/6J or Iba1-EGFP) were decapitated using scissors before the brain was exposed and removed by incisions of skin and skull. The brain was transferred to a 35-mm Petri Dish (ThermoFisher Scientific) containing cold Preparation Medium (minimum essential medium (MEM; no phenol red; Gibco) supplemented with 2 mM Glutamax (Gibco) at pH 7.35) for further dissection. The hippocampi were isolated under a preparation microscope (Zeiss) and cut into 350 µm thick sections using a tissue chopper (McIlwain). All slices from both hippocampi were transferred into a new Petri dish with fresh preparation medium. Intact BSCs were subsequently randomly distributed onto sterile Millicell Cell Culture Inserts (Merck) (3-4 slices/insert) in 6-well plates with 1.2 ml pre-warmed culture medium (SCM; MEM (Gibco) + 20 % Horse Serum (Gibco), 1 mM Glutamax (Gibco), 0.00125 % Ascorbic Acid (Sigma-Aldrich), 0.001 mg/ml Insulin (Gibco), 1 mM $CaCl_2$ (Sigma-Aldrich), 2 mM $MgSO_4$ (Sigma-Aldrich), 13 mM D-Glucose (Roth), 100 U/ml/100 µg/ml Penicillin/Streptomycin; pH 7.28). The cultures were kept at 37 °C and 5 % CO_2 and the medium was replaced three times per week.

3.2.2.3 Murine microglia depletion and iMic engraftment

To allow engraftment of iMics into BSCs, endogenous mouse microglia were depleted using a mouse-specific anti-CSF1R (CD115) antibody (Biolegend, 5 µg/ml). Unless otherwise noted, the depletion antibody was chronically supplemented to the culture medium from the day of preparation until the end of the experiment. iMic precursors were harvested as described above (see **3.2.1.5**). Unless otherwise noted, they drop-grafted onto BSCs by adding 1 µl of cell suspension onto each BSC 2-4 days post-slice culture preparation. Subsequently, iMics were allowed to integrate for at least 14 days before any treatments were started.

3.2.2.4 LPS stimulation of BSCs

Brain slice cultures were stimulated with lipopolysaccharide (LPS) to elicit pro-inflammatory microglial responses. cBSCs were generated as described above, before LPS was supplemented to the medium for 24 hours (‘*acute’*) or 7 days (‘*chronic’*). ‘Chronic’ treatment was started on 14 DIV by adding 25 ng/ml LPS to the medium and replenishing it with every medium change whereas ‘acute’ treatment (200 ng/ml LPS) was started on 20 DIV. For both conditions, culture medium was collected on 21 DIV and analyzed for pro-inflammatory cytokine release via MSD (see **3.2.3.2**). Untreated cBSCs and BSCs without human microglia served as controls.

3.2.2.5 Induction of alpha-synuclein pathology in BSCs

Alpha-synuclein lesions in cBSCs were induced as previously described (Barth et al. 2021). In brief, cBSCs were prepared as described above. At 28 DIV 0.5 µg/µl pre-formed fibrils (pff, kindly gifted by Ronald Melki, Institut François Jacob) of synthetic alpha-synuclein (αSyn) were added on top of each cBSC once. Pathology subsequently developed over 5 weeks.

3.2.2.6 Induction of amyloid-beta pathology in BSCs

Following the protocol established by Novotny et al**.**, amyloid-beta (Aβ) deposits were seeded in cBSCs by once adding 1 µl of brain homogenate (3000 g supernatant of 10 % homogenate, kindly provided by Natalie Beschorner, Tübingen) of plaque-bearing APP23 mice (Sturchler-Pierrat et al. 1997) onto each slice and supplementing the SCM with 1.5 µM synthetic $A\beta_{1-40}$ (American Peptide/Bachem Holding) at each subsequent medium change for up to 6 weeks (Novotny et al. 2016).

3.2.2.7 Fixation of BSCs

Slice cultures were fixed for 2 hours at room temperature by adding 1.2 ml 4 % PFA in PBS below and above the inserts after the culture medium had been aspirated and inserts had been washed

with PBS once. Upon fixation, the PFA was removed and fixed slices were washed 3 three times with PBS for 15 min. Slices were stored in PBS at 4 °C for up to 4 weeks.

3.2.2.8 Human brain tissue and slice cultures

Healthy human brain tissue was obtained from the access tissue of resective brain tumor surgeries in cooperation with the University Hospital Aachen (RWTH Aachen). The tissue was sliced at 250 µm per slice using a vibratome (Thermo Fisher Scientific) and fixed in 4 % PFA immediately after slicing, as described in (Schwarz et al. 2017; 2019). Tissue from two tumor patients (both male, 50 and 66 years-old, respectively) was used to assess microglial network parameters in homeostasis *ex vivo*. To investigate iMic maturation in human tissue, human organotypic brain slice cultures were generated as described by (Schwarz et al. 2017; 2019). Human brain slice cultures were prepared from a 57-year old, male tumor-patient and a cultivated at the air-liquid interphase at 37 °C, 5 % CO_2 with human cerebrospinal fluid as medium for up to 7 days with 3 medium changes per week. Pre-iMics were grafted as described above. All Patients gave their informed written consent for tissue donation for scientific use prior to surgery. All procedures were approved by the institutional ethics board before the study onset (E064/20).

3.2.2.9 Ethics and approval of animal and human tissue work

All mouse experiments were registered with the Regierungspräsidium Tübingen as N04/19M and N03/24M and were performed in accordance with German Animal Protection Laws. All procedures including primary human brain tissue were approved by the institutional ethics board before the study onset (E064/20) and patients gave their informed written consent for tissue donation for scientific use prior to surgery. Data about patients was processed in accordance with the EU *General Data Protection Regulation* and sample labeling does not enable the identification of patients.

3.2.3 Biochemistry and molecular biology

3.2.3.1 DNA isolation and Sanger sequencing

To confirm the genotype of iPSCs and iMics, cells were collected as described above, washed 1x with PBS (centrifugation at 300 g for 5 min), pelleted in 1.5 ml micro-reaction tubes and pellets were frozen to -80 °C until further processing. DNA was isolated from cells using the DNeasy Blood & Tissue Mini Kit (Qiagen) according to manufacturer's instructions. Isolated DNA was stored at -20 °C until further processing or used immediately for PCR amplification. PCR was performed using REDextract-N-Amp™ Tissue PCR Kit as described above.

PCR products were purified using the QIAquick PCR Purification Kit (Qiagen) according to the manufacturer's instruction and eluted in 30 µl water. Upon determining the DNA concentration, samples were sent to LGC Genomics for Sanger sequencing utilizing the same primers as for amplification. Resulting chromatograms and sequences were analyzed using SnapGene (snapgene.com).

3.2.3.2 Mesoscale measurements

Levels of secreted cytokines from iMics in cBSCs was analyzed in the supernatant medium at timepoints described in the respective sections. The medium was frozen to -80 °C until all samples had been collected. Cytokine levels were measured in undiluted samples using a V-PLEX Human Proinflammatory Panel II kit (4-Plex, IL-1b, IL-6, IL-8, TNF-a) (Meso Scale Discovery, MSD) according to manufacturer's instructions with a Mesoscale Sector Imager 6000. An internal reference sample was run for every measurement and the data was analyzed using the MSD discovery workbench software 3.0.

3.2.3.3 Surface Plasmon Resonance

Binding kinetics of CSF1-receptor and its cognate human and murine ligands were assessed using the Biacore™ X100 system (Cytiva) for surface plasmon resonance (SPR). Both, human CSF1R (hCSF1R, R&D Systems) and mouse CSF1R (mCSF1R, AcroBiosystems) were bound to Protein A-coated Sensor Chips (Cytiva) via a human Fc-tag. The receptors were diluted to 2.5 µg/ml in Running Buffer (10 mM HEPES, 150 mM NaCl, 3 mM EDTA, 0.5 % Tween-20, pH 7.4, supplemented with 0.1 % BSA) and washed over the chip with a flow rate of 5 µl/min. Human PDGFRβ (R&D Systems) was used as negative control. Subsequently, increasing concentrations of human or mouse CSF1 (both Miltenyi) and human (Miltenyi) or mouse (BioLegend) IL34, respectively, were washed over the bound receptors at 25 °C to analyze binding kinetics. Association and dissociation times differed for different receptor-cytokine combinations and are listed in

Table 27. After each cycle, the receptor was dissociated from the chip surface using 10 mM Glycine, pH 1.5 for 30 sec using a flow rate of 30 µl/min.

Kinetics data was analyzed using the Biacore Analysis Software (Cytiva). Utilizing the *Monovalent Binding Model for Kinetic Curve Fitting,* binding curves were fitted to obtain association (k_a), dissociation (k_d) and equilibrium (K_D) constants. The combination of hCSF1R and mCSF1 showed kinetic parameters outside the analysis program's scope, hence an equilibrium-based fitting was performed.

Table 27 SPR analyte details

Ligand analyte combination	Association time	Dissociation time	Flow rate	Concentration cytokine
hCSF1R + hCSF1	180 s	3600 s	30 µl/min	8 nM -0.48 pM
hCSF1R + mCSF1	180 s	3600 s	30 µl/min	250 nM - 0.12 nM
hCSF1R + hIL34	180 s	4200 s	30 µl/min	40 nM - 0.04 nM
hCSF1R + mIL34	180 s	4200 s	30 µl/min	40 nM - 0.04 nM
mCSF1R + mCSF1	300 s	3600 s	10 µl/min	20 nM - 0.01 nM
mCSF1R + hCSF1	180 s	3600 s	10 µl/min	40 nM - 0.02 nM
mCSF1R + mIL34	180 s	3600 s	30 µl/min	10 nM - 0.01 nM
mCSF1R + hIL34	120 s	4200 s	20 µl/min	80 nM - 0.04 nM
hPDGFRβ + hCSF1	180 s	3600 s	30 µl/min	8 nM - 0.48 pM
hPDGFRβ + hIL34	180 s	1800 s	30 µl/min	250 nM - 0.12 nM
hPDGFRβ + mCSF1	180 s	4200 s	30 µl/min	80 nM - 0.04 nM
hPDGFRβ + mIL34	180 s	4200 s	30 µl/min	80 nM - 0.04 nM

3.2.3.4 Determination of protein concentration

The protein concentration in cell lysates was determined with the Pierce™ BCA Protein Assay Kit (Thermo Fisher Scientific) according to the manufacturer's instruction. In brief, samples were diluted 1:10 in double-distilled water and incubated with the working reagent at 37 °C for 30 min. Absorption was assessed with FLUOstar Omega (BMG Labtech) at 562 nm. A standard curve with bovine serum albumin (BSA) concentrations ranging from 25-2000 µg/ml was generated using the MARS Data Analysis Software (BMG Labtech) and protein concentrations in samples was calculated.

3.2.3.5 Gel electrophoresis and Western Blot

For gel electrophoretic separation of proteins, cell lysates containing 10 µg total protein were mixed with 1x NuPAGE™ LDS sample buffer (Thermo Fisher Scientific) containing 5 % β-mercaptoethanol and denatured at 70 °C for 10 min. Gel electrophoresis was performed on NuPAGE™ Bis-Tris 4-12 % gels (Thermo Fisher Scientific) using 1x NuPAGE™ MOPS SDS running buffer (Thermo Fisher Scientific) at 200 V and 20 mA per gel. Subsequently, separated proteins were transferred to Amersham™ Protan® 0.2 µm nitrocellulose membranes (Cytiva, pre-activated in transfer buffer (192 mM glycine, 25 mM Tris, 20 % methanol) for 5 min) using the Trans-Blot®

Turbo™ Transfer System (Bio-Rad Laboratories) at 200 mA and 25 V for 60 min. Uniform transfer of proteins was confirmed by Ponceau S staining (0.2 % Ponceau S, 10 % acetic acid) at rt for 5 min.

All following washing steps were repeated 3 times with TBS-T (150 mM NaCl, 15.22 mM Tris HCl, 4.62 mM Trizma Base, 0.1 % Tween-20) at rt for 10 min. Membranes were blocked in 5 % skim milk (Merck) or 5 % BSA (Biomol) in TBS-T at rt for 1 hour before washing and subsequent primary antibody incubation (anti-CSF1R, anti-phospho CSF1R, anti-ERK1/2, anti-phospho ERK1/2; for details see **Table 16**; diluted in 5% BSA in TBS-T with 0.2% sodium azide) at 4 °C over night. After washing, membranes were incubated with secondary antibodies (goat-anti-rabbit-HRP and donkey-anti-mouse-HRP; for details see **Table 16**; diluted in 5 % BSA in TBS-T with 0.2 % sodium azide) at rt for 1 h and incubated with SuperSignal™ West Pico PLUS or Dura Chemiluminescent Substrate (Thermo Fisher Scientific) for 5 min after another wash. Western Blot development onto Amersham™ Hyperfilm™ films (Cytiva) was performed with a KONICA SRX-101A developer (Konica Minolta, Marunouchi, Japan). House-keeping genes (anti-GAPDH, anti-β-III-tubulin; diluted in TBS-T with 0.2% sodium azide) were assessed as described above to control for cellular protein levels. Quantitative analysis of Western Blots was performed with FIJI. To obtain the change of protein levels upon stimulation, total signal of bands of interest was normalized to the respective house-keeping gene and subsequently to the mean value of technical repeats of the respective control.

3.2.4 Single-cell RNA-sequencing

3.2.4.1 Re-isolation of iMics from cBSCs

For single-cell RNA-sequencing (scRNAseq), iMics were re-isolated from cBSCs after 4, 8, 12 weeks. cBSCs were carefully removed from the insert using the small end of a cell lifter (VWR) and transferred to 7-ml Dounce Homogenizers (Wheaton, tight-fit piston) in 2 ml cold Dissection Medium (1x HBSS (140 mM NaCl, 5 mM KCl, 0.2 mM KH_2PO_4, 3 mM D-Glucose, 25 mM HEPES), 0.5 % Glucose, 0.1 mg/ml DNAse I (Sigma). After 5 slow homogenization strokes, the cell suspension was transferred to 5-ml Potter-Elvehjem Tissue Grinders (Thermo Fisher) and homogenized 3 more times. Subsequently, the cell suspension was filtered through a 70-µm cell strainer (Filcon Filter, BD Bioscience) into a 15-ml conical tube and centrifuged at 400 g for 15 min without break (Eppendorf 5810R). The supernatant was discarded, and cells were resuspended in 80 µl cold MACS Buffer (PBS + 0.5 % BSA Fraction V). Human cells were separated from mouse cells using the Mouse Cell Depletion Kit (Miltenyi) with MS columns (Miltenyi) according to manufacturer's instructions. In brief, 20 µl of kit solution was added to the cells and they were

incubated on a rotor at 4 °C for 15 min. The volume was adjusted to 500 µl and the cell suspension was applied to the prepared columns. The columns were subsequently washed twice with 500 µl MACS Buffer and the flow-through containing unbound, human cells was collected and pooled. Afterwards, cells were centrifuged for 10 min (400 g, 4 °C, no break). The pellet was resuspended in 100 µl PBS + 0.04 % BSA and the cell number was determined. The cell concentration was adjusted to 1,000 cells/µl prior downstream processing for scRNAseq.

For each biological replicate, slices from 3-4 plates of cBSCs were pooled, while 3 biological replicates were processed for each timepoint and pooled for downstream analysis. Different replicates were defined by different, independent differentiations of iMics.

3.2.4.2 Collection of pre-iMics for scRNAseq

Pre-iMics harvested on the day of cBSC engraftment were immediately processed for scRNAseq to investigate maturation changes over time. Pre-iMics were harvested as described above and the cell number was determined. Subsequently, an appropriate volume was transferred to a microcentrifugation tube, cells were collected by centrifugation (5 min, 300 g, rt) and resuspended at 1,000 cells/µl in PBS + 0.04 % BSA. Cell suspension was kept at 4 °C until loading the scRNAseq chip (see **3.2.4.4**).

3.2.4.3 Collection of monoculture iMics for scRNAseq

As comparison, iMics were cultured in monoculture for 21 DIV as described above (see **3.2.1.6**). Cells had been plated at 15,000 cells/cm^2 on 50-mm-dishes with three full medium changes per week. On the day of sample preparation, the medium was aspirated, cells were briefly washed with PBS and detached as single cells using Accutase (Gibco). After a 6-minute incubation at 37 °C, cells were washed off the plate using Wash Buffer and collected in conical tubes. Cells were centrifuged at 300 g for 5 min, and the pellet was resuspended in PBS + 0.04 % BSA. The cell number was determined using a hemocytometer and cells were centrifuged again. The cell density was adjusted to 1,000 cells/µl in PBS + 0.04 % BSA and cells were stored at 4 °C until sample processing was performed as described below.

3.2.4.4 scRNAseq sample processing

Obtained pre-iMics, mono iMics or recovered cBSC-iMics were immediately processed for scRNAseq using Chromium Next GEM Single Cell 3’ Kit v3.1 (10X Genomics) according to manufacturer’s instructions (User Guide Rev C, August 2021). All samples were loaded at 1,000 cells/µl onto Chromium Next GEM Chip (Chip G, 10X Genomics) for GEM generation using Chromium Controller (10X Genomics). cDNA amplification, fragmentation, A-tailing, and indexing

were performed according to the protocol using SPRIselect (Beckman Coulter) as cleanup reagent. Quality control and determination of cDNA concentrations were performed using TapeStation4200 and D5000 High Sensitivity ScreenTapes (both Agilent), as recommended. For each sample, one separate library was generated using the 3' Gene Expression Dual Index Library Construction kit with Dual Index Plate TT Set A (both 10X Genomics). Libraries were stored at - 20 °C until samples were prepared for sequencing.

3.2.4.5 scRNAseq sample sequencing

Final sample preparation and sequencing were performed at the NGS Competence Center Tübingen (NCCT). scRNAseq was performed with the Illumina NovaSeq 6000 system and the NovaSeq 6000 SP Reagent Kit v1.5 (Illumina) using a NovaSeq 6000 S2 flow cell (Illumina) with a sequencing mode of: Read 1: 28 + Index i7: 10 + Index i5: 10 + Read 2: 90.

3.2.4.6 scRNAseq analysis

Processing and analysis of scRNAseq data was performed at the Zentrum für Quantitative Biologie (QBiC) Tübingen by Dr. Jun-Hoe Lee using the CellRanger analysis pipeline (v7.10). Quality control was performed to exclude empty droplets, doublets and dying cells. For this, cells with >10 % mitochondrial counts were excluded from downstream analysis as well as cells that had more than 4,500 or less than 200 unique feature counts. Reads were aligned to the reference and a gene expression matrix (containing UMI counts per gene per cell) was generated. Dimensionality reduction analysis was performed using the R package Seurat (v5.0.1). For cell clustering, the k-nearest neighbors of each cell were determined based on Euclidean distance in PCA space. The edge weights between any two cells were refined based on shared overlap in their local neighborhoods (PCs:30, resolution: 0.8). Cell clusters were plotted using the uniform manifold approximation and projection (UMAP) technique.

Finally, gene-expression levels for a selected set of genes were compared for pre-iMics, monocultures iMics at 21 DIV, and grafted iMics at 28, 56 and 84 DIV. A similar set of genes was compared for grafted iMics at 28 and 56 DIV from cBSCs with and without induced synucleinopathy. Graphs were produced in RStudio with R version 4.3.2 (2022-10-31) mainly using the R package ggplot2 v3.5.0. Final reports were produced using the R package rmarkdown v2.25, with knitr v1.45.

3.2.5 Immunohistochemistry and imaging

3.2.5.1 Immunofluorescence staining of brain slice cultures

Fixed but unsectioned brain slice cultures were used for immunofluorescent staining. BSCs remained attached to the membrane to maintain the top-bottom orientation for later imaging and analysis and were thus carefully excised from the insert using a scalpel and transferred to a 48-well plate (Corning; one well per condition). Antigen retrieval was only performed for hTMEM119 staining. Slices were washed for 10 min in PBS on a shaker prior to 2 h of blocking unspecific bindings (5 % Normal Donkey Serum (NDS; Biozol Diagnostica), 0.3 % Triton X-100 (Sigma-Aldrich) in PBS) at rt. Primary antibody incubation was performed in 2 % NDS and 0.3 % Triton X-100 in PBS at 4 °C (for dilution and incubation duration see **Table 17**). Subsequently, slices were washed three times with PBS at rt for 15 min before they were incubated with secondary antibodies (in 1 % NDS, 0.3 % Triton X-100 in PBS, for details see **Table 18**) at rt for 2 . After another 3 washes in PBS slices were either stained with amyloid-binding dyes (see **below**) or carefully mounted onto adhesive glass slides (TOMO) by carefully detaching them from the membrane with a brush. To attach slices to slides, they were dried at 37 °C for 15 min and then coverslipped with Dako Fluorescent Mounting Medium (Dako). Slides were dried at room temperature in the dark over night and subsequently stored at 4 °C.

3.2.5.2 Immunofluorescence staining of mono iMics

Coverslips with mono iMics were permeabilized with 0.3 % Triton-X 100 in PBS at room temperature for 10 minutes. Subsequently, cells were washed 3x 5 min with PBS and blocked 1 hour at rt with 0.1 % Tween-20 (Sigma-Aldrich) + 10 % NDS to prevent unspecific antibody binding. Primary antibody incubation was performed overnight at 4 °C in 10 % NDS in 0.1 % PBS-Tween-20 (for antibodies used, see **Table 17**). Cells were again washed 3x 5 min with PBS-Tween-20 before the fluorescently labeled secondary antibodies (see **Table 18**) were incubated for 1 hour at rt. After 2 washes with PBS, counterstaining using DAPI (1:1,000 in PBS; Sigma-Aldrich) was performed for 5 min at rt. Finally, slices were washed two more times with PBS and mounted onto TOMO IHC adhesive glass slides using Dako Fluorescent Mounting Medium. Slides were dried at room temperature in the dark over night and subsequently stored at 4 °C.

3.2.5.3 LCO staining

To stain amyloid aggregates in tissue and cells, BSCs were stained with Luminescent Conjugated Oligothiophenes (LCO) which specifically bind to distinct amyloid structures. This staining was performed subsequently to the incubation with fluorescently labelled secondary antibodies (see

above). The LCO dye pentamerformyl thiophene acetic acid (pFTAA; 3 µM) was incubated with BSCs for 30 min at rt before slices were washed three times with PBS and mounted as described above.

3.2.5.4 Methoxy-XO4 staining

Alternatively, aggregated amyloid-beta in BSCs was visualized using Methoxy-X04 (Biomol). As for LCOs, the immunofluorescent protocol was performed as usual before 0.04 mg/ml Methoxy-X04 in PBS was added to slice cultures for 30 min at room temperature.

3.2.5.5 Confocal imaging

Confocal images were obtained using an upright Zeiss LSM 880 NLO microscope with ZEN Black Software (Zeiss). All images were acquired using a water-immersion x20 objective (W Plan-Apochromat x20/1.0; Carl Zeiss). To depict microglial morphology, z-stack images were acquired, and maximum intensity projections were generated.

3.2.5.6 2-Photon live cell imaging

Timelapse movies of live cell movement of GFP-positive microglia (BSCs of Iba1-EGFP mice or cBSCs with CAG-GFP transgenic iMics) were acquired using an upright Zeiss LSM 880 NLO microscope with an IR-optimized water-immersion x20 objective (W Plan-Apochromat x20/1.0, Carl Zeiss). During acquisition the slice cultures were placed in a custom-made slice culture holder, which securely keeps the inserts at the same position. BSCs were sub-merged in pre-warmed SCM, that was constantly supplemented with carbogen (5 % CO_2: 95 % O_2). The medium was steadily pumped to the imaging chamber via the customized slice culture holder and stage-top incubator to guarantee stable imaging conditions.

Two-photon excitation was obtained with a MaiTai eHP (Spectra Physics) laser, tuned at 920 nm for excitation of GFP. The emitted light was collected using Non-Descanned GaAsP detectors with a 520/50 emission filter. Images were acquired every two min at a resolution of 0.208 x 0.208 x 0.830 µm per voxel. To induce focal laser lesions, the MaiTai eHP laser was tuned to 810 nm, set to '*point scan*' mode on lowest scanning speed with maximum power for 8 seconds.

3.2.6 Image processing

All movies acquired with 2-Photon live-cell imaging were deconvolved using Huygens Essential (Scientific Volume Imaging B.V., Hilversum) prior further processing and analysis.

All images for figures were generated using "*Maximum Intensity Projections*" of z-stacks in FIJI.

3.2.6.1 Analysis of microglia morphology

Confocal images were imported into the *Imaris* Software version 9.7.2 (Bitplane) to analyze microglial morphology parameters. First, nuclear signals obtained from KU80 (human nuclei) and PU.1 (microglia nuclei) were semi-automatically reconstructed using the '*Spots*' function. The '*Surfaces*' tool was utilized to reconstruct the entire slice culture volume by applying a very low absolute intensity threshold (between 1 and 5 for 8-bit images). The number of nuclei per channel was subsequently normalized to the total culture volume to quantify graft numbers and efficiencies. Additionally, nuclear signals were used for nearest-neighbor distance analyses using the implemented statistics for '*Distance to Nearest Neighbor*' in Imaris.

To reconstruct microglial morphology, the signal of Iba1 staining was used. Based on the absolute intensity of the Iba1 signal, cells were semi-automatically reconstructed with the '*Surfaces*' tool. Microglia that touched the borders of images were excluded from the analyses. The obtained 3D-reconstruction of cells was used to create a new channel in the image which removed all signal outside of the reconstructed microglia to improve downstream analysis using the '*Filaments*' tool. In the '*Statistics*' tab of the '*Filaments*' tool, '*Filament Length (sum)*' (Length of all microglial processes per cell) and '*Filament No. Dendrite Branch Pts*' (Number of microglial branchpoints per cell) were analyzed as measures for ramification and cellular complexity.

Finally, the volume occupied by each microglia (the volume of the convex hull) was calculated using *MATLAB 2021b* and the MATLAB plug-in '*Convex hull*' for Imaris, available on the Imaris customer portal.

3.2.6.2 Analysis of microglia dynamics

Microglia dynamics obtained from 2-Photon live-cell imaging were analyzed using *Imaris*. Using the 'Surfaces' and '*Filaments*' tools, the microglial morphology was reconstructed as descried above (see **3.2.6.1**) for each timepoint of the timelapse movie and process movement was tracked by the '*Filaments*' tool up to a distance of 10 µm between two subsequent frames.

In order to quantify microglial responses to a focal laser lesion, the injury site was reconstructed at the first frame after lesion-induction using the '*Spots*' function when no microglial processes were present at the site yet. The obtained reconstruction was duplicated onto all subsequent timepoints and pixel values for this area were set to zero in all frames. Next, a vantage plot was generated in Imaris (Spatial View) to calculate the average pixel intensity in dependence of the distance to the lesion site at each timepoint. Lastly, the intensity values for each movie were

normalized to the highest value of the respective movie and averaged over all movies per group using MATLAB (see **11 Scripts and Macros**).

3.2.6.3 Microglial inclusions

LCO-positive inclusions within iMics were analyzed using Imaris. 3D-reconstruction of iMics in tilescans of entire cBSCs were performed as described above (see **3.2.6.1**). Afterwards, all voxels of the LCO (pFTAA) channel outside of the reconstructed microglial surfaces were set to 'zero' to exclude them from analysis. LCO-positive signal within iMics in this created channel were subsequently reconstructed with the '*Spots*' tool in order to quantify the number of "LCO-positive inclusion"-positive microglia. This number was divided by the total number of iMics to obtain the relative amount of iMics with LCO-positive inclusions. Furthermore, the relative volume of LCO-positive inclusions within iMics was determined by reconstructing the LCO-positive signal using the '*Surfaces*' function in an intensity-based manner as described above for microglia and normalizing it to the total cBSC volume.

3.2.7 Electrophysiology

3.2.7.1 Multi-electrode array measurements

To assess neuronal network activity in BSCs and cBSCs, slices were recorded after 6 and 12 weeks *in vitro* using multi-electrode arrays (MEA). For each timepoint, 3 slices of each condition were recorded. All recordings were performed using a standard extracellular solution (124 mM NaCl, 26 mM $NaHCO_3$, 3.5 mM KCl, 1 mM $MgCl_2$, 2 mM $CaCl_2$, 1.2 mM NaH2PO4, 20 mM Glucose (pH 7.4, osmolarity: 305 mOsm/kg, equilibrated with 95 % O_2/5 % CO_2).

The slice cultures were carefully removed from the insert using a fine brush and transferred to the submerged recording chamber of a 256MEA chip (Multi Channel Systems) attached to a MEA2100-256 headstage (Multi Channel Systems) and fixed with a harp slice grid (Multi Channel Systems). Due to the small size of BSCs, only a fraction of the electrodes was covered by the tissue, which was documented by microscopy images together with the exact position (using an Olympus UPlanFLN 4x objective).

To reduce confounding effects of handling the BSC and mounting of the chip, recordings were initiated after 5 min using the '*Multi Channel Experimenter*' software. The recording chamber was perfused with extracellular recording solution at a rate of 6.5 ml/min using a Peristaltic Perfusion System (Multi Channel Systems) and the temperature was set to 34 °C. Baseline activity was recorded for 10 min at a sampling rate of 25 Hz. Subsequently, slices were perfused with a

modified recording solution containing 8 mM KCl (“high potassium”) to provoke accelerated activity. Upon 5 min of incubation in the “high potassium” solution, neuronal activity was again recorded for 10 min.

3.2.7.2 MEA analysis

The average spike count per slice was analyzed using a custom-made Python script based on SpyKING CIRCUS (https://github.com/spyking-circus/spyking-circus; Yger et al. 2018). Channels not covered by tissue were registered as ‘*dead channels*’ and were not analyzed. For each recording, default steps filtering, whitening, clustering, fitting, and merging were performed. To analyze spike counts, a 300 Hz butterworth filter and the recommended threshold for spike detection were used.

3.2.8 Structure prediction by ColabFold

The tertiary structures of hCSF1R$_{D1\text{-}D3}$ with hCSF1, hIL34, mCSF1 and mIL34 were predicted using ColabFold: Alphafold2 using Mmseqs2 (Mirdita et al. 2022). The receptor and ligand sequences were added twice, separated by colon symbol to ensure the prediction of quadromers. All models were run for 5 recycles with version v3. The structures with highest pLDDT values were selected for further analysis. Representations of all structural models were prepared with ChimeraX (Pettersen et al. 2021). The PAW Viewer (Elfmann and Stülke 2023) was used to visualize Predicted Aligned Error plots. Interaction interfaces for each complex were computed using the PDB Proteins, Interfaces, Structures, and Assemblies (PISA) interface (Krissinel and Henrick 2007)

3.2.9 Data analysis

All statistical analysis including the creation of figures were performed in GraphPad Prism 9 (GraphPad Software, San Diego, California). Unless otherwise noted, individual datapoints represent biological replicates with one to three technical replicates each. Error bars represent the standard error of the mean (SEM). P-values smaller than 0.05 were considered statistically significant. All graphical schematics were created in Biorender.com, graphs were generated with GraphPad Prism (version 10.1.1) and figures were designed with Affinity Designer (version 1.10.8).

4 Results

4.1 Establishment and characterization of chimeric brain slice cultures

4.1.1 Generation of iPSC-derived microglia

Studying human microglia has advanced in the past 15 years due to the generation of several protocols deriving microglia-like cells from induced pluripotent stem cells (Speicher et al. 2019). These protocols take into account the distinct microglial ontogeny but vary in their timing and methodology applied. I differentiated iPSCs to microglia-like cells using two previously published protocols to compare their feasibility. Following the protocol established by Haenseler et al. 2017, iPSCs were pushed towards mesodermal lineage differentiation during embryoid body (EB) formation followed by induction of primitive hematopoiesis in medium containing IL3 and CSF1. During that time, EBs formed cysts (**Figure 5 A**: EB body: blue asterisk, cyst: green arrow head) from which microglial precursor cells (pre-iMic, pink asterisk) were released into the medium after two to three weeks. EBs attached to the cell culture well via endothelium-like cells (pink arrowhead). Pre-iMics were collected and differentiated towards iMics in 2D cultures with medium containing CSF1 and IL34 (**Figure 5 A+C**). On the other hand, using the protocol established by Takata et al. 2017, microglia-like cells were derived using a monolayer-based approach. iPSCs were subjected to hypoxic (5 % O_2) conditions for the first 8 days with a more vigorous external control of growth factors to induce mesodermal fate (**Figure 5 B**). This was followed by the induction of the primitive hematopoietic lineage by the additional supplementation of IL6, IL3, dickkopf-1 (DKK1) and SCF. From Day 16 onwards, precursor cultures were subjected to CSF1 to induce final precursor maturation, before pre-iMics were collected and plated in 2D as EB-based iMics.

iMics derived from those two protocols were indiscernible by eye and behaved very similarly in their subsequent maturation and differentiation. Adhesion and extension of first processes was observed after 24 hours. iMics first presented as spindle-shaped cells that became more complex over cultivation time (**Figure 5 A**). At 14 days in culture, iMics from both protocols were ramified and expressed key microglial markers IBA1, TMEM119 and TREM2 (**Figure 5 C**). Independent of the protocol, however, iMics cultured in 2D monocultures never reach the maturity observed in *ex vivo* adult human microglia (Park et al. 2023). Thus, to study human iPSC-derived microglia in a

more relevant setting, I aimed to establish a novel *in vitro* model system that combines the high accessibility of 2D culture systems with the tissue complexity found *in vivo*.

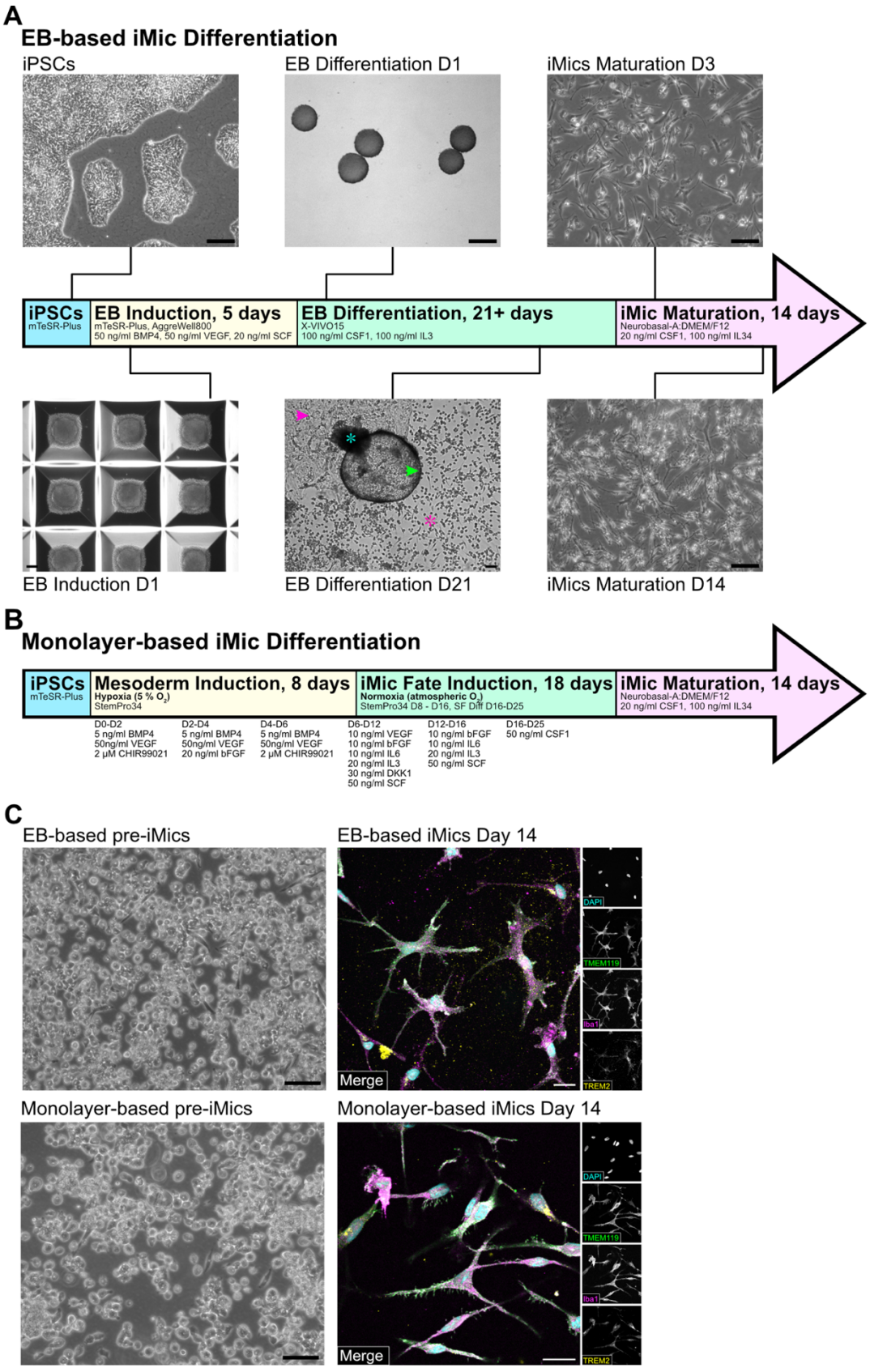

Figure 5 Generation of iPSC-derived microglia
A) Timeline and representative images of cell states during differentiation of human induced pluripotent stem cells (iPSC) towards iPSC-derived microglia (iMics) following the embryoid body (EB)-based protocol by Haenseler et al. 2017. After 5 days in AggreWell200 plates, uniform EBs were plated to differentiate for at least 21 days in medium containing 100 ng/ml CSF1 and 100 ng/ml IL3. During differentiation, EBs grew and formed cystic structures (EB body: blue asterisk, cyst: green arrow head) and attached to the cell culture well via endothelium-like cells (pink arrow head). iMic precursor cells (pre-iMics, pink asterisk) were released from EBs and could be collected from the medium. Scale bars: 100 µm. **B)** Timeline to differentiate iPSCs to iMics using the monolayer-based protocol by Takata et al. 2017. Monolayer differentiation was subjected to hypoxic conditions (5 % O_2) for the first eight days of differentiation and relied on external supplementation of more mesoderm-inducing cytokines. While the individual stages of the protocols vary in length, the overall length for both protocols was the same. Independent of the protocol, final iMic differentiation lasts 14 days in medium containing 20 ng/ml CSF1 and 100 ng/ml IL34. **C)** Representative images of pre-iMics obtained from both protocols (left) and immunofluorescent images for key microglial markers TMEM119 (green), Iba1 (magenta) and TREM2 (yellow) after 14 days in culture show no obvious difference between protocols. Scale bars: brightfield images: 100 µm; immunofluorescent images: 20 µm.

4.1.2 Murine microglia depletion in brain slice cultures using a mouse-specific anti-CSF1R antibody

Previous studies engrafting human iPSC-derived microglia into the brains of mice have shown that engraftment is more efficient if murine microglia are absent from the brain, indicating that a niche has to be generated (Hasselmann et al. 2019; Mancuso et al. 2019). I aimed to investigate whether these xenotransplantation models could be adopted *in vitro*, by utilizing organotypic hippocampal brain slice cultures (BSC) and engrafting them with human iPSC-derived microglial precursor cells. Before I could establish grafting paradigms, I evaluated microglia depletion approaches. Mouse models with genetic ablation of microglia could present with decreased fertility and neurodevelopmental defects (Erblich et al. 2011; Rocío Rojo et al. 2019) and were not considered due to legal restrictions. Small molecule inhibitors of CSF1R like PLX are not species-specific, which negatively affects engraftment rates of iMics (Chadarevian et al. 2022; Ogaki, Ikegaya, and Koyama 2022). To overcome the negative effect of depletion on potential grafting efficiency, I established a depletion protocol for murine microglia using a mouse-specific anti-CSF1R antibody (CD115, Biolegend). By applying the antibody directly to the slice culture medium, the limitation of BBB penetration by antibodies *in vivo* is overcome.

BSCs were generated from four- to six-day-old C57BL6/J (B6) mice and cultivated with slice culture medium (SCM) for 10 days until culture conditions stabilized. Medium was then supplemented with the mouse-specific α-CSF1R-antibody (5 µg/ml) for 7 days before cultures were either fixed or switched back to regular SCM. For the time of depletion, the depletion antibody was re-administered with every medium change (**Figure 6 A**). During depletion, microglial numbers rapidly decreased by 85.6 ± 3.01 % within one week (**Figure 6 B+C**;

p = 0.0077). However, withdrawal of the antibody resulted in a repopulation to 67.85 ± 15.48 % of control levels after seven days (**Figure 6 B+D**; p = 0.025). This indicates that depletion is highly efficient, but that some cells withstood the treatment for at least seven days. These non-depleted microglia also retained the ability to divide and replenish the microglial niche once the inhibition of CSF1R was ceased. The findings are in line with previously published data for microglia depletion using small molecules *in vitro* and *in vivo* (J. Han, Harris, and Zhang 2017; Coleman Jr, Zou, and Crews 2020; L. Zhan et al. 2020; Barth 2023) and demonstrated that microglia depletion, in principle, can be achieved using the mouse-specific α-CSF1R-antibody.

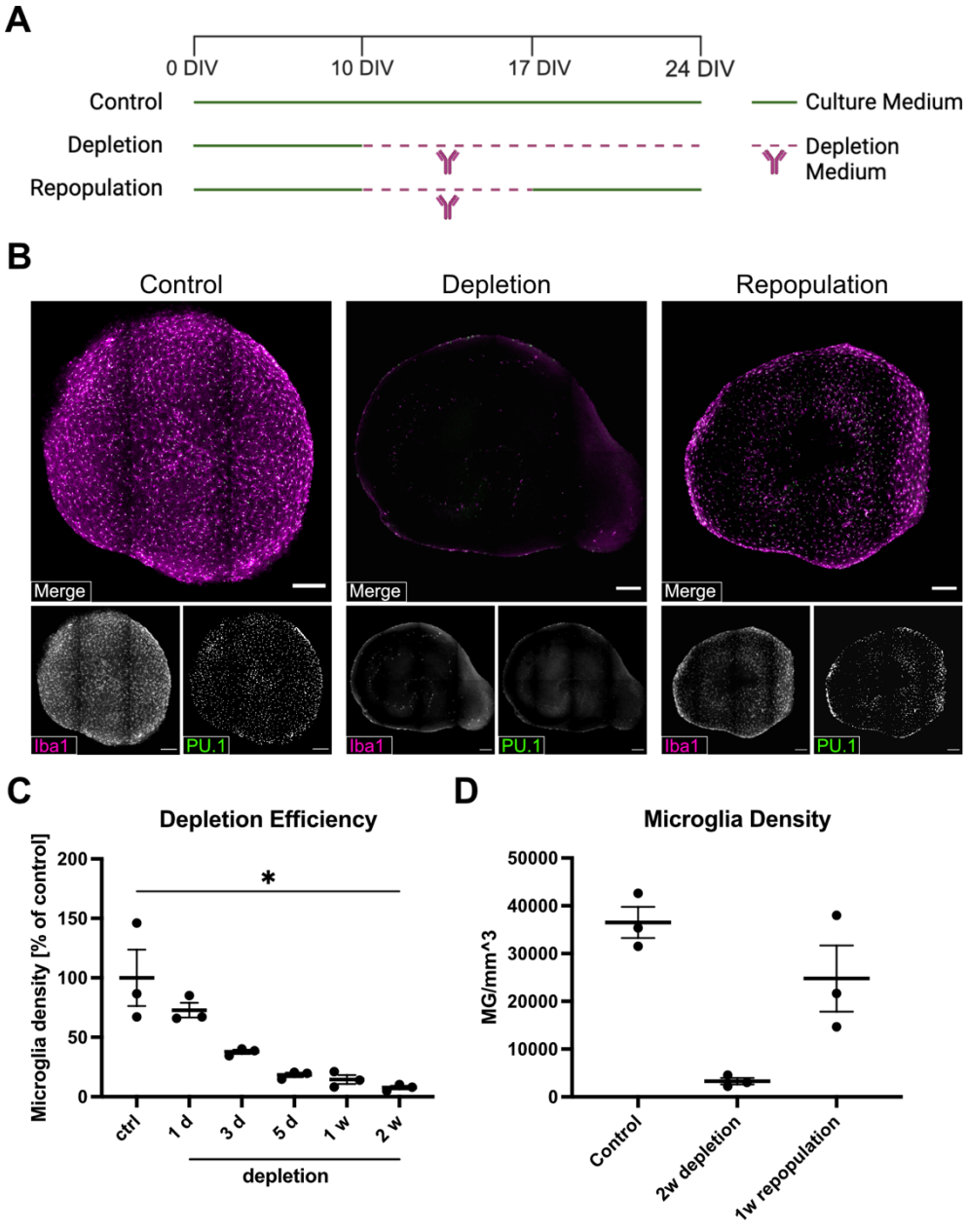

Figure 6 Depletion of murine microglia in brain slice cultures using a mouse-specific anti-CSF1R antibody
A) Experimental timeline: All mouse BSCs were cultured for 10 days *in vitro* (DIV) in regular slice culture medium (SCM) before treatment onset. The 'control' group was cultured in SCM for the entire experiment. For treatment, the 'repopulation' and 'depletion' groups were switched to culture medium supplemented with 5 µg/ml anti-CSF1R depletion antibody for 7 and 14 days, respectively. The 'repopulation' group was cultured with regular SCM after 7 days of depletion. Generated with Biorender.com. **B)** Representative images of entire BSCs for the three experimental groups. Microglia were stained against Iba1 (magenta; microglial cytoplasm) and PU.1 (green; microglial nuclei). Scale bars: 200 µm. **C)** Microglia depletion efficiency measured as microglial density (number of $PU.1^+$ cells per volume) compared to control. Treatment with anti-CSF1R antibody decreased microglial cell numbers to 8 % of control cultures after 2 weeks. N (groups) = 6; number of independent experiments per group = 3; Kruskal-Wallis test with Dunn's multiple comparison test p = 0.0077. **D)** Microglia density in the three experimental groups in A) measured as microglia ($PU.1^+$) per volume. After withdrawal of the anti-CSF1R antibody, microglia repopulated the BSC, to 68 % of the original density within one week. n (groups) = 3; number of independent experiments per group = 3; Kruskal-Wallis test with Dunn's multiple comparison test p = 0.025. All plots show mean ± SEM.

4.1.3 Optimization of iMic grafting conditions

Next, I generated chimeric brain slice cultures (cBSC) by grafting BINOi010C pre-iMics to BSCs. I wondered if iMics required a microglia-free niche or could co-exist with murine microglia in BSC. To this end, pre-iMics were introduced to BSCs with intact microglial networks or those depleted of endogenous microglia for one or two weeks, respectively (**Figure 7 A**). In contrast to the previous experiments, the depletion antibody was supplemented from the day of BSC preparation, as depletion efficiency reportedly decreases upon microglial reactivity (Le, O'Banion, and Majewska 2024). Pre-iMics were added on the day depletion was initiated and fixed after 14 days *in vitro* (DIV). Human cells in cBSCs were identified by staining for the human-specific nuclear marker KU80 (STEM101, Takata Bio) in all experiments to distinguish them from murine cells. $KU80^+$ cells that additionally expressed the microglial transcription factor PU.1 were defined as iMics, whereas $PU.1^+$ but $KU80^-$ cells were defined as endogenous murine microglia.

Only a continuous depletion with α-ms-CSF1R-antibody for 2 weeks resulted in high counts of human-derived cells and grafting efficiencies (percentage of iMics per total microglia). Non-depleted BSCs were barely engrafted. When murine microglia were suppressed throughout the experiment, human-derived cells ($KU80^+$ and $PU.1^+$) accounted for 92.9 ± 0.53 % of all microglia (total $PU.1^+$). In contrast, only 7.64 ± 2.61 % of all microglia were of human origin in non-depleted cBSCs which was only slightly increased to 21.8 ± 4.13 % in 1-week depleted slices (**Figure 7 B-D**; Panel C: p = 0.0107, Panel D: p = 0.0036). This shows, that iMics depend on a microglia-free niche to engraft BSCs and that this niche needs to be sustained throughout the experiment by a continuous suppression of murine microglia. Additionally, α-ms-CSF1R-antibody treatment does not affect human cells, as they would not engraft otherwise.

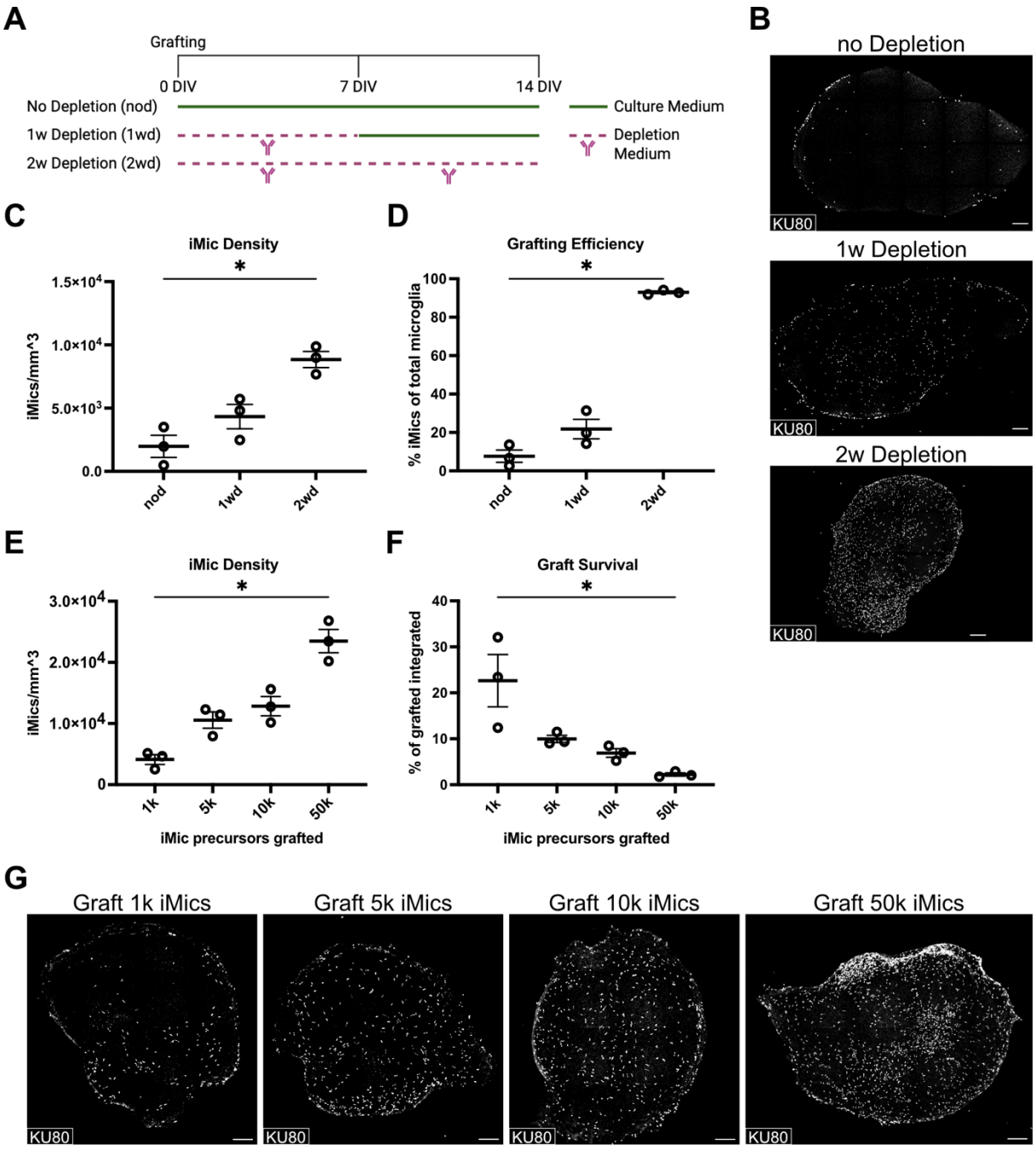

Figure 7 Optimization of iMic grafting conditions to generate chimeric brain slice cultures

A) Schematic of experimental timeline. iMics were grafted on the day of preparation for all conditions. 'No Depletion' BSCs (nod) were cultivated in regular SCM for the entire experiment. The '1 w Depletion' (1wd) and '2 w Depletion' (2wd) groups were cultivated in depletion medium (SCM + 5 µg/ml anti-CSF1R antibody) from the day of preparation. After 1 week, the '1wd' group was switched back to regular SCM whereas the '2wd' group remained in depletion medium. Created in Biorender.com. **B)** Representative images of the three culture conditions. Human-derived cells stained positive for KU80 (white, human-specific nuclear marker) and were evenly distributed in 2wd but not 'nod' and '1wd' conditions. Scale bars: 200 µm. **C)** iMic density in cBSCs measured as iMics ($KU80^+$) per volume. Continuous depletion of murine microglia resulted in higher numbers of iMics integrating into cBSCs. n (groups)=3; number of independent experiments per group = 3; Kruskal-Wallis test with Dunn's multiple comparison test p = 0.0107. **D)** Grafting efficiency of iMics in cBSCs calculated by dividing number of iMics ($KU80^+$ cells, human) by the total number of microglial cells ($PU.1^+$ cells, human and murine). Only continuous depletion over 2 weeks resulted in a high grafting efficiency. n (groups) = 3; number of independent experiments per group = 3; Kruskal-Wallis test with Dunn's multiple comparison

test p = 0.0036. **E)** iMic density at 28 DIV depending on the number of pre-iMics initially grafted. Only grafts of initially 50k cells resulted in significantly higher densities. n (groups) = 4, number of independent experiments per group = 3, Kruskal-Wallis test with Dunn's multiple comparison test p = 0.0006 **F)** Survival of grafted iMics calculated by dividing the number of iMics at 28 DIV by the size of the graft. n (groups) = 4, number of independent experiments per group = 3, Kruskal-Wallis test with Dunn's multiple comparison test p < 0.0001. **G)** Representative images of iMics integrated at 28 DIV for the different graft sizes in F) and G). Grafting of 1k cells led to a lower number of KU80^{+} cells (white), while 50k grafts showed clustering of iMics at cBSC edges. Scale bars: 200 µm. All plots show mean ± SEM. iPSC: induced pluripotent stem cell; iMic: iPSC-derived microglia; DIV: days *in vitro*; BSC: brain slice culture; cBSC: chimeric brain slice culture; SCM: slice culture medium.

After determining the conditions needed to ensure high grafting efficiencies, I wondered whether the number of pre-iMics added to each culture affected the final number of human microglia in cBSCs. I, thus, titrated the number of pre-iMics added to each culture by grafting 1,000; 5,000; 10,000 and 50,000 pre-iMics in 1 µl to each BSC, respectively. After 4 weeks, the number of iMics in cBSCs was determined (**Figure 7 E-G**). While 22.64 ± 4.65 % of all pre-iMics initially grafted survived in the 1k graft condition, only 9.96 ± 0.64 %, 6.91 ± 0.77% or 2.23 ± 0.29 % were present for 5k, 10k, and 50k grafts, respectively (**Figure 7 F+G**). When looking at total numbers, the final density was only significantly different between 1k and 50k grafts (4117.5 ± 654.88 vs. 23490.18 ± 1555.50 iMics/mm^3), whereas no significant difference was observed for 5k (10563.45 ± 1087.05 iMic/mm^3) or 10k (12842.4 ± 1283.13 iMics/mm^3). Consequently, iMic density in cBSCs does not correlate with graft size in a linear manner but appears to be controlled by the tissue environment within a certain range to prevent overpopulation. However, when 50k were grafted, iMics appeared to be less mature as indicated by many observed human nuclei (KU80^{+}) that were PU.1^{low} and IBA1^{low}.

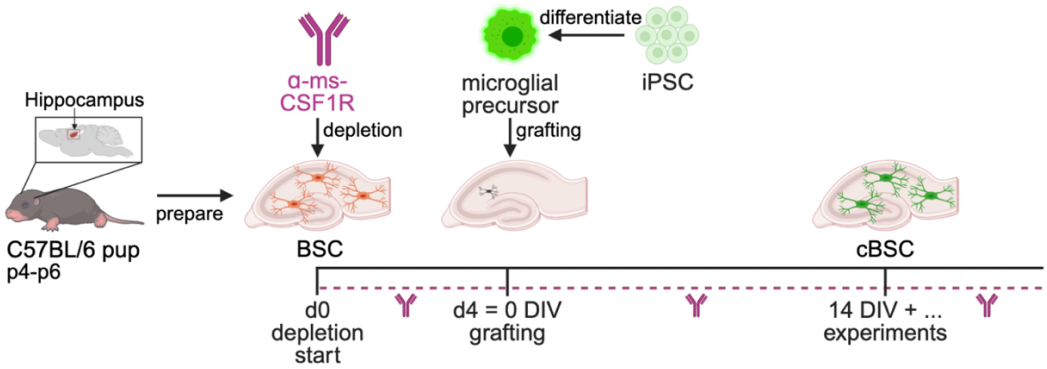

Figure 8 Generation of chimeric brain slice cultures
Experimental set-up established after consideration of previous experiments. Hippocampal brain slice cultures were prepared from 4–6-day-old B57BL6/J mice according to Stoppini et al. 1991. Endogenous murine microglia were depleted by the continuous administration of an anti-mouse-CSF1R antibody supplemented to the medium from the day of preparation. 10,000 pre-iMics derived from iPSCs according to Haenseler et al. 2017 were drop-grafted in 1 µl medium on top of each BSC on day 4 post-preparation, this is denoted as 0 DIV. After at least 14 days of differentiation, cBSCs were used for experiments. iPSC: induced pluripotent stem cell, DIV: day *in vitro*; BSC: brain slice culture, cBSC: chimeric brain slice culture; SCM: Slice culture medium. CSF1R: colony stimulating factor 1 receptor.

All these observations led to the establishment of a protocol for the generation of chimeric brain slice cultures. This was subsequently used throughout the study: On the day of BSC preparation, endogenous microglia depletion was initiated by the addition of α-ms-CSF1R-antibody to the culture medium. On Day 2-4 post-preparation 10,000 pre-iMics that had been differentiated in parallel following the EB-based protocol were drop-grafted in 1 µl of EB Differentiation Medium on top of each microglia-depleted BSC. This day is denoted as "0 days *in vitro*". Unless otherwise noted, iMics then differentiated in cBSCs for at least 14 DIV before downstream experiments were performed (**Figure 8**).

4.1.4 iMic engraftment in cBSCs is independent of iPSC line and differentiation protocol

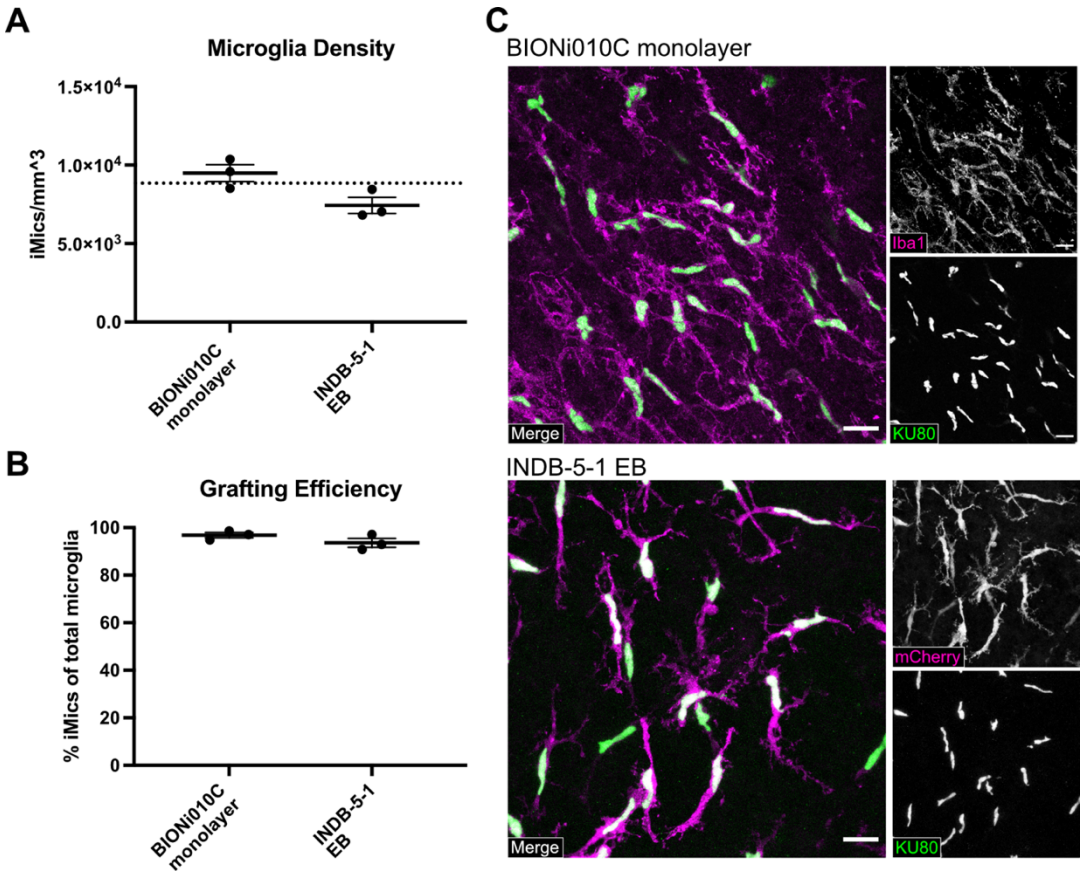

Figure 9 iMic engraftment in cBSCs is independent of iPSC line and differentiation protocol
A) Microglia density in cBSCs measured as iMics (identified by KU80) per volume. BIONi010C pre-iMics derived using the monolayer-based approach (Takata et al. 2017) and from another iPSC-line (INDB-5-1) integrated in similar numbers like EB-based BIONi010C iMics (dotted line) after 2 weeks. n (groups) = 2, number of independent experiments per group = 3; two-tailed Mann Whitney test p = 0.1000. **B)** Grafting efficiency of iMics in cBSCs calculated by dividing the number of iMics ($KU80^+$) by the total number of microglia ($PU.1^+$, human and mouse). No difference in grafting efficiency was observed between lines and protocols, as iMics made up 94-97 % of all microglia in cBSCs. n (groups) = 2, number of independent experiments per group = 3; two-tailed Mann Whitney test p = 0.2000. Plots show mean ± SEM. **C)** Representative images of iMics in cBSCs at 14 DIV derived using the monolayer-based protocol and INDB-5-1 as second iPSC line. iMics (identified by KU80, green) were highly ramified (Iba1, magenta) independent of line and protocol.

After establishing the protocol, I validated it by utilizing two additional iPSC lines (KOLF2.1J and INDB-5-1) and the monolayer-based iMic differentiation protocol established by (Takata et al. 2017). As for BIONi010C iMics derived by the EB-protocol, monolayer-derived BIONi010C precursors and EB-based INDB-5-1 precursors integrated well. At 14 DIV, iMic density was 9489.96 ± 440.56 iMics/mm^3 for monolayer-BIONI010C and 7433.03 ± 219.06 iMics/mm^3 for INDB-5-1-EB (**Figure 9 A**; BIONi010C-EB represented as dotted line) with a respective grafting efficiency of 96.82 ± 0.91 % and 93.62 ± 1.49 % (**Figure 9 B**). iMics grafted into cBSCs showed high grafting efficiencies and highly ramified morphologies (**Figure 9 C**) independently of their genetic background and derivation protocol, demonstrating the ease by which cBSCs can be adopted by other researchers. Unless otherwise noted, BIONi010C iMics derived from the EB-based protocol were used for all further experiments.

4.1.5 iMics integrate into cBSCs and adapt human ex vivo microglia-like phenotypes

To further validate cBSCs as a model to study human microglia in a complex environment *in vitro*, I analyzed iMics in cBSCs in regards of their morphological and network parameters. First, I confirmed that iMics express key microglial markers Iba1, PU.1 and TMEM119 by immunofluorescent staining. PU.1 and Iba1 were present from 7 DIV onwards and TMEM119 was highly expressed at 28 DIV (**Figure 10 A+H**). Next, iMic maturation was assessed by immunofluorescent staining over the course of six weeks post-grafting. Expression of Iba1 steadily increased from 7 DIV to 42 DIV while iMics (identified by human-specific nuclear marker KU80) continued to be evenly distributed throughout cBSCs without a preference for specific areas or the absence of human-derived cells in others (**Figure 10 A**). Morphologically, iMics developed from spindle-shaped, elongated cells at 7 DIV to highly ramified, complex cells with defined, non-overlapping territories at 42 DIV (**Figure 10 A**, upper panel). Quantification of the number of iMics in chimeric slice cultures revealed a decrease from around 27,000 ± 4100 iMics/mm^3 at 7 DIV to around 8,800 ± 266 iMics/mm^3 at 28 DIV with a stabilization of total iMic numbers thereafter (**Figure 10 B**, n (groups) = 6; p = 0.9547). This stabilization of iMics per culture is close to the reported number of murine microglia in the hippocampus (5990 microglia/mm^3; dotted line) (Keller, Erö, and Markram 2018). iMic also accounted for 96-97 % of all microglia in cBSCs from 21 DIV onwards (**Figure 10 C**, n (groups) = 6; p = 0.1417), underlining that cBSCs can be utilized to study human microglia *in vitro* for at least six weeks.

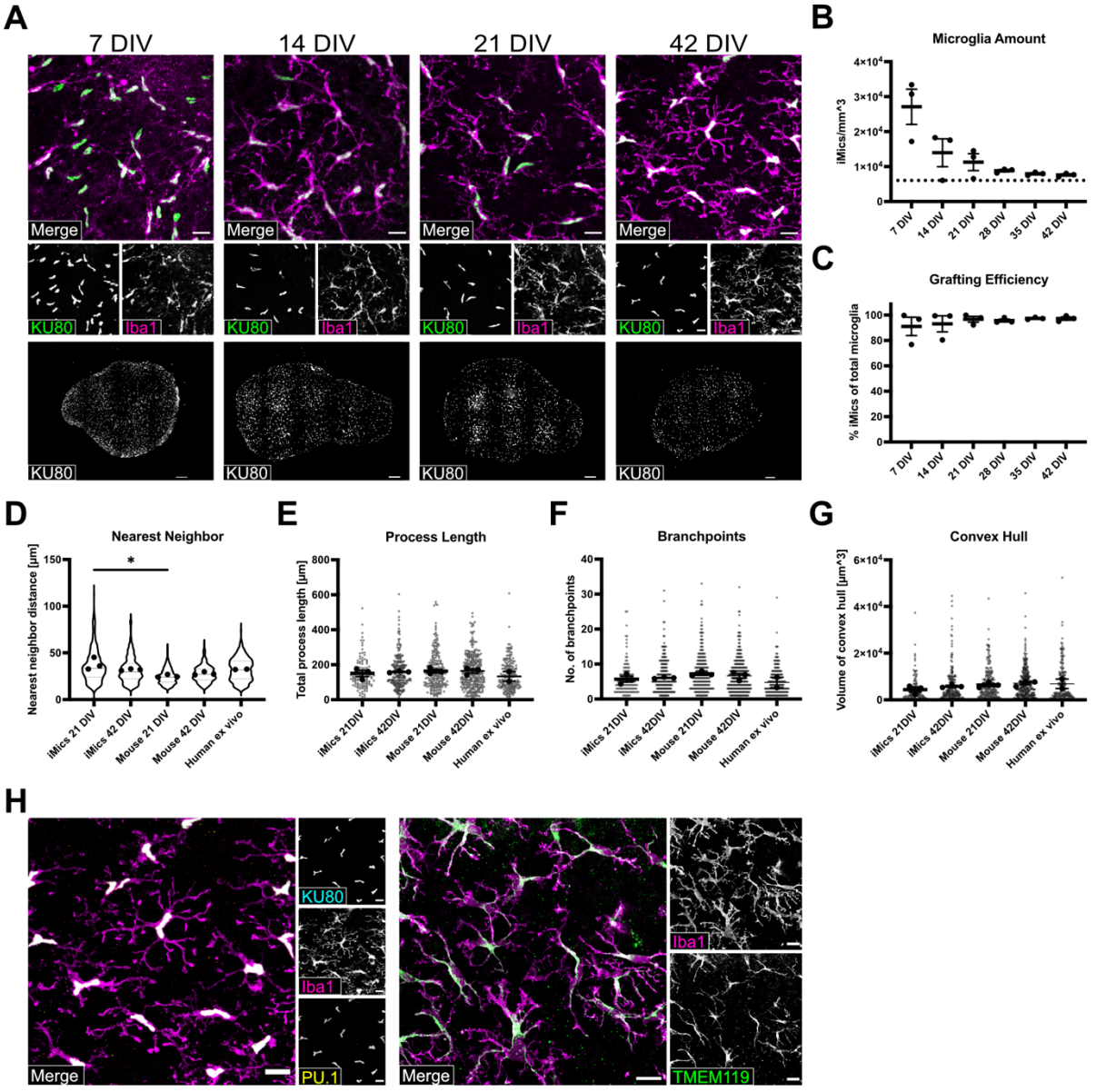

Figure 10 iMics present stable integration into cBSCs and adapt human *ex vivo* microglia-like morphologies
A) Representative images of cBSCs at different timepoints of differentiation. iMics were identified as human by KU80 (green) and stained positive for Iba1 (microglia marker, magenta). Uniform distribution (overview images, bottom row) remained stable, while increased ramification was observed over extended cultivation period (close-up images, top row). Scale bars: 20 µm (close-ups) and 200 µm (overview images). **B)** iMic density in cBSCs measured as KU80$^+$ cells per volume. Microglial numbers decreased drastically within the first 2 weeks post-grafting but stabilized from 21 DIV onwards. The dotted line represents endogenous microglial density in the murine hippocampus (5990 cells/mm^3) (Keller, Erö, and Markram 2018). n (groups) = 6; number of independent experiments per group = 3; Kruskal-Wallis test p = 0.9547. **C)** Grafting efficiency calculated by dividing the number of iMics (KU80$^+$, human nuclei) by the total number of microglia (PU.1$^+$, human and mouse). After 21 DIV the grafting efficiency stabilized above 96 %. n (groups) = 6; number of independent experiments per group = 3; Kruskal-Wallis test p = 0.1417. **D-G)** Network and morphological parameters of iMics in cBSCs. Nearest-neighbor-distance [µm] (**D**), total process length [µm] (**E**), number of branchpoints (**F**) and surveilled volume (volume of convex hull, [µm^3]) (**G**) of iMics were compared to endogenous mouse microglia and *ex vivo* human microglia. The mean of all microglia from cBSCs obtained from one animal (3 cBSCs) are indicated as black dots, the individual values are indicated as grey dots. n (groups) = 5; number of independent experiments per group = 2-3; Kruskal-Wallis test with Dunn's multiple comparison test: **D:** p = 0.0006: **E:** p = 0.3844, **F:** p = 0.8680, **G:** p = 0.4667. **H)** Representative immunofluorescent images of microglial markers. KU80$^+$

iMics (cyan) expressed key microglial markers Iba1 (cytoplasm, magenta) and PU.1 (nucleus, yellow) (left panel) from 7 DIV onwards, shown are cells at 42 DIV. The right panel shows the expression of human TMEM119 (green) in Iba1$^+$ (magenta) cells at 28 DIV, a marker for homeostatic microglia. Scalebars: 20 µm. All plots show mean ± SEM. DIV: days *in vitro*.

Microglial morphology and network parameter were assessed at 21 DIV and 42 DIV. iMics in cBSCs were compared to their respective murine counterparts and to *ex vivo* human microglia in tissue obtained during resective brain surgery. The tissue from the five sources was immunohistochemically stained for PU.1 and Iba1 and microglial cells were reconstructed using the 'Spots' and 'Filaments' tools in *Imaris*. Based on the coordinates of each cell's nucleus (determined by PU.1) a nearest-neighbor-distance (NND) approach was used to determine the distribution of iMics throughout cBSCs. The mean NND for iMics at 42 DIV (31.96 ± 0.43 µm) was almost indiscernible from that of human microglia *ex vivo* (32.42 ± 0.12 µm) (**Figure 10 D**; p = 0.0006, Kruska-Wallis Analysis with Dunn's multiple comparison test) whereas mouse microglia in BSCs had a comparably shorter NND at 42 DIV (**Figure 10 D**; 27.84 ± 0.82 µm), indicative for a higher density of murine microglia in BSC.

Microglial processes were reconstructed using the 'Filaments' tool based on the Iba1 staining to assess total process length and number of branchpoints per cell. From 21 DIV to 42 DIV total process length increased slightly but not significantly from 150.50 ± 15.02 µm to 158.90 ± 2.50 µm for iMics and was comparable to human microglia *ex vivo* (132.94 ±19.70 µm; **Figure 10 E**; p = 0.3844). Similarly, the number of branchpoints increased only slightly from 5.68 ± 0.68 to 6.07 ± 0.10 branchpoints/cell and was not significantly different from human *ex vivo* (4.74 ± 1.04 per cell; **Figure 10 F**; p = 0.8680).

Lastly, the volume surveilled by microglia in each group was compared by reconstructing the cells based on the Iba1 staining and calculating the volume of the convex hull. iMics in cBSCs surveilled slightly lower volumes than human microglia *ex vivo*. On average, each iMic surveilled 4463.59 ± 870.48 µm^3 at 21 DIV and 5893.06 ± 317.71 µm^3 at 42 DIV, whereas human microglia *ex vivo* surveilled 6938.26 ± 1450.21 µm^3 per cell, however, no significant differences were found (**Figure 10 G**, p = 0.4667). Overall, these data suggest that iMics in cBSCs mature to reach the morphological complexity and a tissue distribution very similar to homeostatic human microglia *ex vivo* that allows studying mature human microglia networks *ex vivo*.

4.2 Functional characterization of iMics in cBSCs

4.2.1 iMic processes are highly motile during homeostasis and respond to focal tissue lesions

After confirming iMic identity as microglial, I assessed their functionality using 2-Photon live cell imaging. For live cell imaging approaches, BIONi010C-iPSCs were transfected with AAVS1-Pur-CAG-EGFP (Addgene) to constitutively express EGFP and subsequently differentiated to iMics. $EGFP^+$ iMics were observed during homeostatic process movement at 21 DIV and compared with their murine equivalents in Iba1-EGFP BSCs (Hirasawa et al. 2005). Z-stack images of one position were acquired every two minutes for 20 minutes and homeostatic process motility over time was tracked using the *Imaris* 'Filaments' tool (**Figure 11 A**). No significant differences were revealed between iMic (0.02902 µm/s) and murine microglia (0.02925 µm/s) terminal point movement velocities (**Figure 11 B**, p = 0.8203).

One microglial key function is to rapidly respond to tissue injuries in their vicinity. A common assay to test this function is by inducing a focal laser lesion injury in the tissue and measuring how quickly microglia shield the injury site (Davalos et al. 2005). For this purpose, a laser beam (λ = 810 nm, t = 8 sec) was directed to a position between microglial cells and z-stacks were acquired every two minutes for 30 minutes to observe the ensuing microglial reaction. Within minutes, both iMics and endogenous murine microglia responded to the lesion by extending their processes towards the injury site while the cell soma remained stationary (**Figure 11 C**). To quantify the microglial reaction to laser lesion injuries, the normalized fluorescent intensity of the iMic/microglia channel was plotted against the distance to the lesion site. Prior to the lesion, the normalized fluorescent intensity was distributed randomly across the field of view for both iMics and mouse microglia. Upon lesion induction, the fluorescent intensity quickly increased in proximity to the lesion site (< 10 µm), while more distant parts (> 50 µm) remained unaffected, confirming that cells moved proximal processes towards the injury site. Both reaction time and the type of movement did not differ between iMics in cBSCs and endogenous mouse microglia in BSCs, indicating functionality of iMics in cBSCs (**Figure 11 D**).

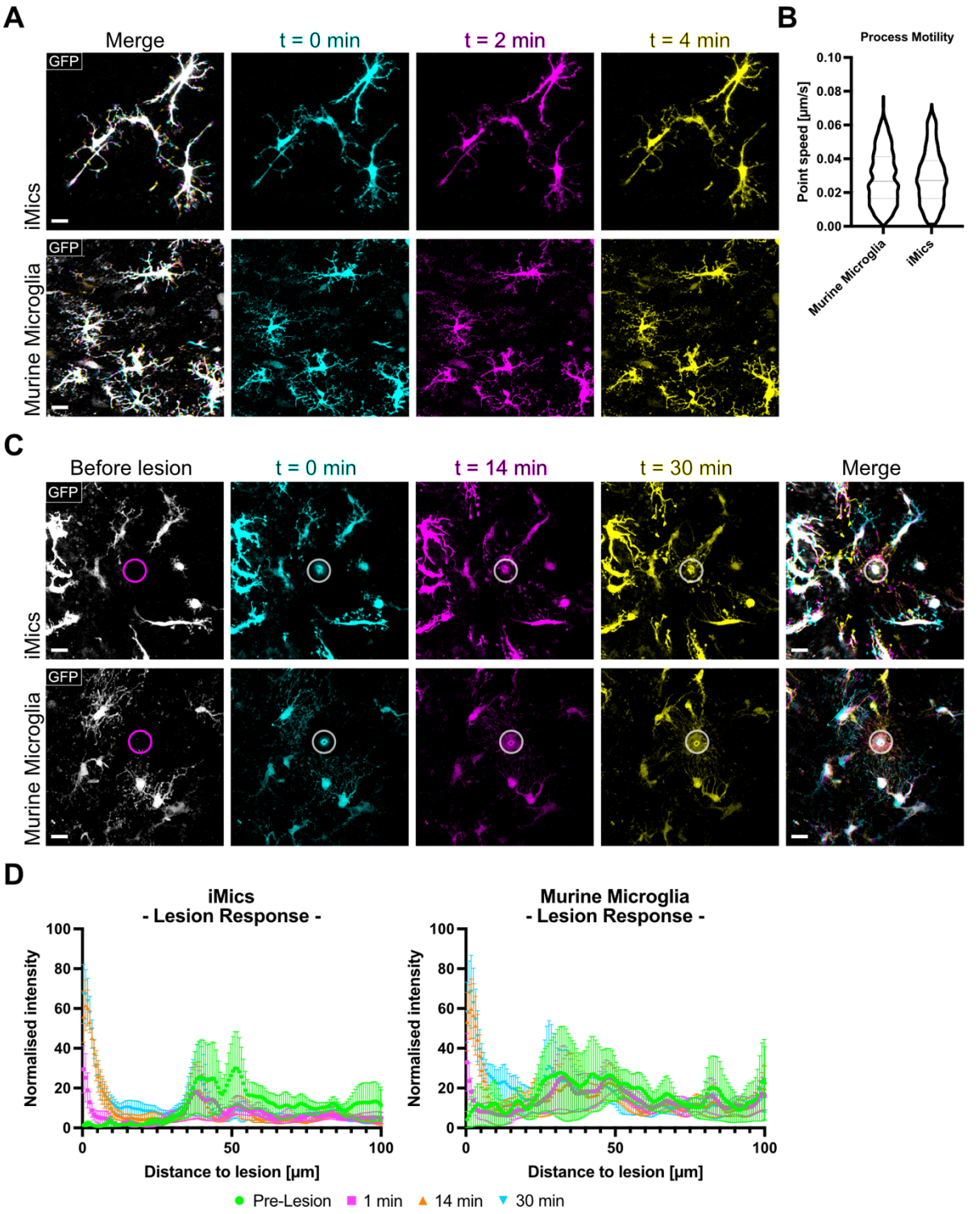

Figure 11 iMic processes are highly motile during homeostasis and respond to focal tissue lesions

A) Representative images of homeostatic movement of iMics in cBSCs (upper panel, BIONi010C-CAG-GFP) and endogenous mouse microglia (lower panel, Iba1-GFP mice) at 21 DIV. Z-stack images of GFP⁺ microglia were acquired every 2 minutes for 20 minutes using 2-Photon microscopy. Images for 0 min (cyan), 2 min (magenta) and 4 min (yellow) are depicted and merged to a white overlay. Colorful processes represent movement at a given timepoint. Scale bars: 20 µm. **B)** Quantification of process movement velocity in violin plots. Processes were semi-automatically tracked with *Imaris* in 30 min movies with 2 min intervals and the point speed of process endpoints was calculated. n (mouse) = 769 (tracked processes); n (iMics) = 390 (tracked processes); Mann-Whitney-Test: p = 0.8203. **C)** Representative images of

microglial responses to focal laser lesions (top panel: iMics in cBSCs, lower panel: murine microglia in BSCs). Images are shown for pre-injury (white, not included in merge), 0 min (right after lesion induction, cyan), 14 min (magenta) and 30 min (yellow) post-lesion induction. The lesion site is marked with a circle in all images. The colorful processes in the merge images depict process extension towards the injury site and the formation of a barrier. Scale bars: 20 µm. **D)** Quantification of normalized fluorescent intensity against distance to lesion site for 4 timepoints (pre, 1 min, 14 min and 30 min) represented in different colors. Left: human iMics, right: murine microglia. A sharp increase of intensity in proximity to lesion site (0-10 µm) was observed over time for both groups. n = 9 movies from independent cultures for each group; plotted are means ± SEM.

4.2.2 iMics respond to global pro-inflammatory stimulation

Another microglial key function is to respond to inflammatory stimuli with the release of cytokines. To test whether iMics in cBSCs possess the ability to secrete cytokines upon global immunogenic stimulation, cBSCs were subjected to lipopolysaccharide treatment to mimic a bacterial infection. A low-dose LPS stimulus (25 ng/ml) administered chronically for seven days was compared with an acute high-dose (200 ng/ml) treatment for 24 hours (**Figure 12 A**). Subsequently, the concentration of human pro-inflammatory cytokines in the medium was measured using a human-specific cytokine panel on the Mesoscale Discovery (MSD) platform.

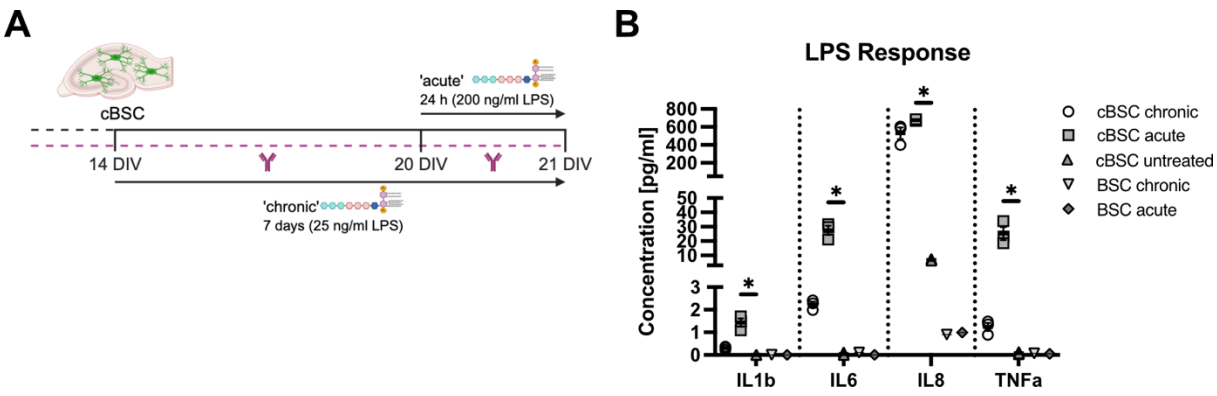

Figure 12 iMics in cBSCs respond to global pro-inflammatory stimulation
A) Schematic representing the experimental set-up. 14 days post-grafting a chronic low-dose (25 ng/ml) LPS stimulus was given with each medium change for 7 days, while acute high-dose (200 ng/ml) stimulation for 24 hours was started on 20 DIV. Medium from both conditions was collected on 21 DIV and analyzed for released pro-inflammatory cytokines using a human-specific mesoscale cytokine measurement. DIV: days *in vitro*, LPS: lipopolysaccharide. Created in Biorender.com. **B)** Secretion of the four inflammatory cytokines IL1β, IL6, IL8 and TNFα was increased upon both acute and chronic LPS stimulation but not in untreated cBSCs or in BSCs without human microglia (BSC acute and chronic). Data represented as mean values ± SEM (Kruskal Wallis test with Dunn's correction, $* p \leq 0.05$) with n (groups) = 5; number of independent experiments per group = 3.

While human cytokine levels were under the detection level (or found only in minute quantities) in untreated cBSCs or in LPS-treated BSCs without human iMics, both the acute and the chronic LPS stimulation evoked a distinct release of pro-inflammatory cytokines in cBSCs – an increase in IL1β, TNFα, IL6 and IL8 was measured. Interestingly, the acute stimulation elicited higher cytokine releases than the chronic stimulation for IL1β (acute: 1.43 pg/ml, chronic: 0.03 pg/ml),

TNFα (25.18 pg/ml vs. 1.24 pg/ml) and IL6 (27.50 pg/ml vs. 2.23 pg/ml) while IL8 levels were comparable between treatments (675 pg/ml vs. 529.75 pg/ml) (**Figure 12 B**). Nevertheless, both paradigms confirmed the functional response of iMics in cBSCs to global pro-inflammatory stimulation.

4.2.3 iMics support neuronal network activity in cBSCs for extended culture periods

Finally, I aimed to investigate whether iMics were able to support neuronal network activity in cBSCs for extended cultivation periods. Previous reports have demonstrated that microglia are required for neuronal network activity in mice both in early development and later in life (Szalay et al. 2016). To this regard, cBSCs with iMics and BSCs containing endogenous mouse microglia were cultivated as usual and the neuronal network activity was analyzed using multi-electrode array (MEA) recordings after 6 and 12 weeks, respectively. After transfer to the recording chamber, slices were allowed to adjust in the extracellular recording solution for 5 min before spontaneous baseline activity was recorded for 10 min, followed by a 10-min recording in a high potassium (8 mM KCl) solution to provoke increased activity.

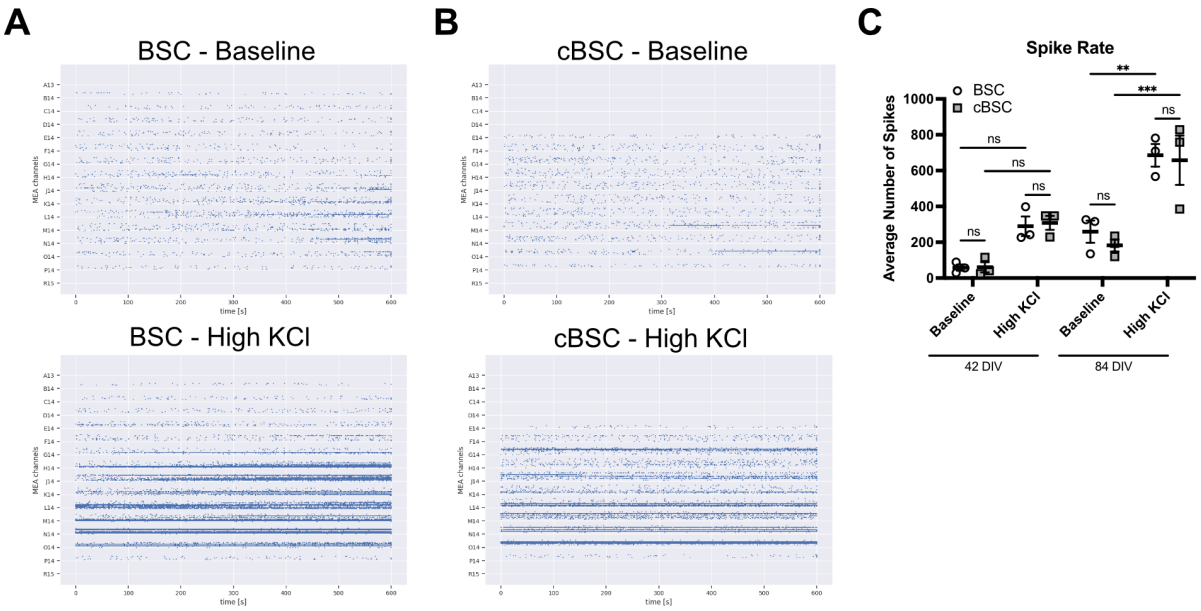

Figure 13 iMics support neuronal network activity for extended culture periods
A+B) Representative multielectrode array (MEA) spike trains for BSCs with endogenous microglia (**A**) and cBSCs grafted with iMics (**B**) after 6 weeks in culture at baseline levels and upon wash-in of 8 mM potassium-chloride (high KCl, bottom). Each vertical line represents one electrode on the MEA, synchronous activity (blue dot) on several electrodes was considered a spike. **C)** Quantification of average number of spikes per culture at 6 and 12 weeks at baseline and high potassium conditions. Depicted are means ± SEM. n = 3 independent cultures per group, two-way ANOVA with Tukey correction for multiple comparisons (∗ $p \leq 0.05$, ∗∗ $p \leq 0.01$, ∗∗∗ $p \leq 0.001$).

Surprisingly, overall network activity (measured in average spike number per slice) was increased for both BSCs and cBSCs at 12 weeks compared to 6 weeks even under baseline conditions. Independent of timepoint and microglia species within slice cultures, however, high potassium elicited increased spike counts in all slices (

Figure 13 **A-C**). This not only indicates that iMics support neuronal network connectivity in cBSCs but also underlines that slice cultures are still viable, and neurons remained active after 12 weeks in culture.

4.3 Transcriptional profile of iMics in cBSCs recapitulates *ex vivo* human microglia phenotypes

4.3.1 Maturation-dependent clustering of iMic transcriptomes

While morphological, network and functional properties give information about microglial identity, they do not convey detailed information about microglial maturation and the diversity of cells within cBSCs. Thus, I applied single-cell RNA sequencing (scRNAseq) on iMics re-isolated from cBSCs after 4, 8 and 12 weeks *in vitro* to investigate maturation dynamics and transcriptional profiles of iMics with single-cell resolution. iMics from cBSCs were compared to precursor cells (at the day of engraftment) and iMics cultured in monoculture for 3 weeks. cBSCs from 3 animals were pooled and mechanically homogenized using Dounce homogenizers (Wheaton). Human cells were extracted by negative selection using the *Mouse Cell Depletion* kit (Miltenyi Biotec) for magnetic advanced cell sorting (MACS). Murine cells were detected by magnetic bead-conjugated antibodies whereas human cells remained untagged and passed through the magnetic column during separation. The recovered human cells were subsequently subjected to *Chromium Next GEM Single Cell 3' GEM* (10x Genomics) single-cell RNA processing (**Figure 14 A**). Monocultured iMics (mono iMics) were detached from the culture vessel using Accutase (Gibco) treatment for 6 minutes whereas precursor cells were collected from the culture medium of EB cultures. Neither precursors nor monocultured iMics were subjected to homogenization or MACS. In total, this yielded 45,011 cells from three independent iMic differentiations after sequencing and quality control.

Next, principal component analysis (PCA) of normalized read counts was performed followed by dimensionality reduction using uniform manifold approximation and projection for dimension reduction (UMAP). I found that the cells grouped into three major clusters, which subclustered into 26 distinct populations (**Figure 14 B**). Using the expression of marker genes, cluster '8' was

identified as neurons (*GRIA2, DLG2*), clusters ‘13’ and ‘19’ were identified as neural precursor cells (SOX2*, CRYAB, SNAP25, SYN2*) and clusters ‘10’, ‘16’ and ‘25’ as oligodendrocytes (*PLP1, MBP, DLG2*). These clusters were excluded from further analysis. After contaminating murine cells had been excluded, the three microglial clusters clearly separated according to developmental stage: precursors and monocultured iMics separated from the iMics recovered from cBSCs after 4, 8 and 12 weeks, which clustered together (**Figure 14 C**). Subclustering revealed 20 molecularly distinct subpopulations which were analyzed in depth (**Figure 14 D**).

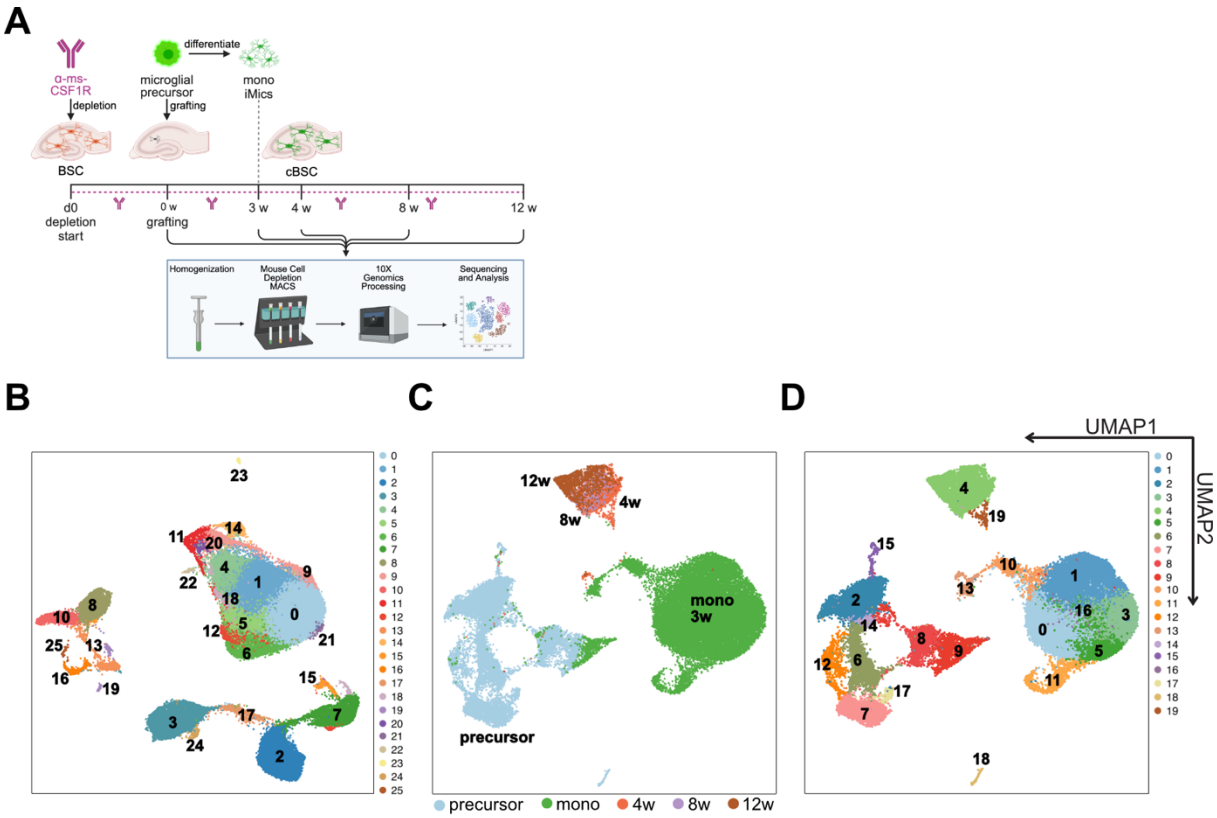

Figure 14 Maturation-dependent clustering of iMic transcriptomes

A) Experimental set-up. At 4-, 8- and 12-weeks post-grafting, respectively, iMics were re-isolated from cBSCs by mechanical tissue homogenization and magnetic cell sorting depleting the cell suspension of murine cells. Recovered iMics were processed for 10x Genomics single-cell RNA-sequencing. Transcriptomes of cBSC-iMics were compared to precursors processed on the day of grafting and iMics differentiated in monoculture for 3 weeks. w: weeks, MACS: magnetic advanced cell sorting. Created in Biorender.com. **B-D)** Scatterplots after principal component analysis and uniform manifold approximation and projection (UMAP) of microglial transcriptomes colored by cluster. **B)** 26 clusters were identified upon first analysis. Clusters ‘8’, ‘10’, ‘13’, ’16, ‘19’, ‘25’ were identified as murine neuronal cells or oligodendrocytes. These clusters were excluded from further analysis. **C)** iMics included into further analysis grouped into 3 distinct clusters depending on maturation state. **D)** 20 molecularly distinct subpopulations were identified within the three major clusters. n = 40,578 cells with n = 3 independent iMic differentiations per timepoint.

4.3.2 iMics in cBSCs recapitulate diverse human transcriptional states

Almost all 40,578 investigated cells expressed the human-specific gene *XRCC5* (KU80) as well as the canonical microglial markers *SPI1* (PU.1)*, AIF1* (IBA1), *ITGAM* (CD11b) (**Figure 15 A+B**), albeit with different expression levels and patterns. Precursor cells had higher expression levels of *ITGAM* (clusters '2', '6', '8', '12') compared to monoculture iMics (especially low expression in clusters '0' and '1'), but lower expression of *AIF1* (**Figure 15 A+B**). High levels of cell cycle progression genes *CENPF*, *MKI67*, and *TOP2A* were observed in clusters '2', '7', '12', '17' (precursor), cluster '11' (mono iMics), cluster '19' (cBSC-iMics). Both the number of cells in the clusters and the proportion of those expressing proliferation markers declined with time in culture (average percentage of proliferation markers per timepoint: 'precursor': 9.81 %; 'mono iMics': 4.49 %; '4w': 2.92 %; '8w': 0.43 %; '12w': 0.15 %) (**Figure 15 A+B**). This implies that the proliferative capacity declines with time in culture reflecting previous reports that microglia remain proliferative capacity to some extent throughout life (Nimmerjahn, Kirchhoff, and Helmchen 2005; Füger et al. 2017; Askew et al. 2017).

Cells in precursor clusters '2', '6', '7', '12', '17' presented high expression of early (yolk sac) microglial genes mannose receptor 1 (*MRC1),* disabled homolog 2 (*DAB2*)*,* and lymphatic vessel endothelial hyaluronic acid receptor 1 (*LYVE1*) as well as lysosome-related genes cathepsin D (*CTSD*), legumain (*LGMN*), and lipase A (*LIPA*) (**Figure 15 A+B**), reflecting enhanced lysosomal activity previously observed in embryonic microglia (Masuda et al. 2019; Y. Li et al. 2022). Contrastingly, microglial maturation- and homeostasis-related genes (*CX3CR1, P2RY12, SORL1, C3*) were highly expressed by iMics recovered from CBSCs (clusters '4' and '19') and to a lower extent in mono iMics (clusters '0', '1', '3', '5', '16') (**Figure 15 A+B**). In general, mono iMics often presented with intermediate expression levels between precursors and cBSC-iMics, indicating a less mature phenotype (**Figure 15 A+B**). For example, cBSC-iMics were enriched for differentially expressed genes (DEG) associated with mature microglia immunological function (Ximerakis et al. 2019; Sun et al. 2023) which was not found in mono iMics. This includes antigen presentation (*HLA-DRA, CD74, B2M*) in cluster '4' and ribosome biogenesis (*RPS27, RPL41*) in clusters '4' and '19' (**Figure 15 C**), highlighting functional and homeostatic microglia that reflect healthy aging. On the other hand, mono iMics enriched for DEGs associated with senescence (p16 (*CDKN2A*)) and changes in iron homeostasis marked by the upregulation ferritin-light chain (*FTL*) (clusters '0', '1', '3', '5', '16') (**Figure 15 C**). Furthermore, mono iMics expressed many disease-associated microglia genes (*PICALM, GPNMB, CCL2, LPL*) that were not observed in cBSC-iMics (**Figure 15 A-C**). While this can be interpreted as mature (Dolan et al. 2023), the concurrent lack of homeostatic and

functional markers indicates that mono iMics have an altered transcriptome compared to cBSC iMics that should be kept in mind when studying microglia in 2D.

In summary, the data indicates that iMics in cBSCs adopt a molecular profile that closely resembles homeostatic human microglia *ex vivo* whereas mono iMics show signs of stress and DAM phenotypes. Together with the morphological and functional analyses this implies that cBSCs allow studying mature human microglia in homeostasis to answer biologically relevant questions.

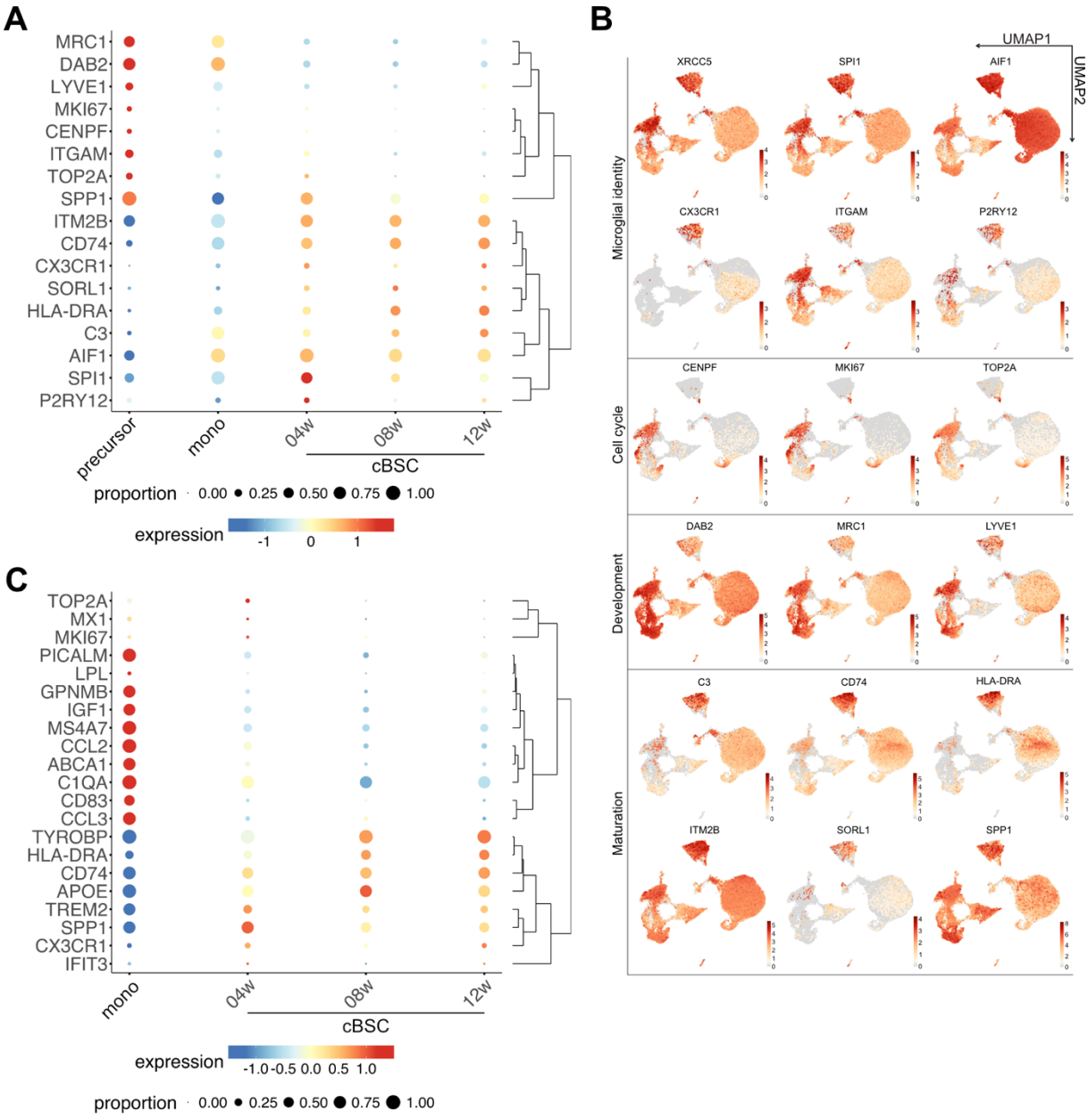

Figure 15 iMics in cBSCs recapitulate mature *ex vivo* human transcriptional phenotype
A) Bubbleplot of RNA expression levels and proportion of cells expressing the gene for key microglial genes across different maturation stages. The size of each circle depicts the percentage of cells per cluster in which the given

transcript was detected, while the color coding represents the normalized z-scores. **B)** Scatterplots after principal component analysis and UMAP overlayed with the z-scores of marker gene expression of genes depicted in (A). Genes are sorted to confirm microglial identity, cell cycle progression, microglial development and maturation stages. n = 40,578 cells with n = 3 independent iMic differentiations per timepoint. **C)** Bubbleplot comparing the expression of genes associated with microglial aging and maturation by Dolan et al. 2023 between monoculture iMics and cBSC-iMics. Mono iMics presented a more primed and activated phenotype, whereas cBSC iMics expressed maturation-associated and homeostatic markers. The size of each circle depicts the percentage of cells per cluster in which the given transcript was detected, while the color coding represents the normalized z-scores.

4.4 Cross-species CSF1R receptor:ligand interactions enable cBSCs

4.4.1 Human CSF1R signaling is required for iMic differentiation in 2D

After confirming microglial identity and functionality of iMics in cBSCs, I was interested in how integration and differentiation is mediated in slice cultures. Xenotransplantation models rely on the transgenic expression of human CSF1 for adequate engraftment of iPSC-microglia in murine brains (Rathinam et al. 2011; Hasselmann and Blurton-Jones 2020; Fattorelli et al. 2021) and it has been a long-standing presumption, that murine ligands are unable to bind and activate human CSF1-receptors (Sieff 1987) which are essential for microglial differentiation, maturation and survival. The cBSC model, however, is generated using wildtype (WT) B6 animals and no human cytokines are supplemented to the medium, implying that iMic differentiation is driven by murine cytokines.

To confirm, that the growth factors required for iMic integration in cBSCs are tissue-derived and that the differentiation is CSF1R-dependent, pre-iMics were cultivated as monocultures in 2D in Slice Culture Medium, iMic Medium with and without CSF1R ligands hCSF1 and hIL34, respectively. While iMics cultivated in complete iMic Medium (with hCSF1 and hIL34) attached to the tissue culture plate within 24 hours and extended processes immediately, differentiation was delayed for those cultivated without the cytokines (**Figure 16 A**, bottom row). Cells deprived of CSF1R-ligands remained more amoeboid, with less and shorter processes and showed comparably lower densities than cells in complete medium (**Figure 16 A**, middle row). On the other hand, iMics cultured in SCM did not attach to the culture plate at all and did not show any sign of differentiation (**Figure 16 A**, top row), indicating that the SCM per se does not induce microglial differentiation and rather inhibits iMic maturation.

Next, CSF1R-dependency was investigated by utilizing iPSCs with isogenic *CSF1R* variants. KOLF2.1J iPSCs (The Jackson Laboratories) carrying either one or two of the disease-associated E633K (Rademakers et al. 2011), two knockout or two wildtype *CSF1R* alleles (**Table 26**,

Supplementary Figure 1) were differentiated towards iMics using the EB-based protocol. While EB induction was successful for all genotypes, pre-iMics of the homozygous E633K ($CSF1R^{E633K/E633K}$) and KO ($CSF1R^{-/-}$) genotypes were produced in lower quantities (**Figure 16 B**, upper panel; small dark dots around EB are pre-iMics). The pre-iMics were smaller than those of WT ($CSF1R^{+/+}$) EBs while no difference in pre-iMic quantity and size was observed for heterozygous E633K ($CSF1R^{+/E633K}$) cells (**Figure 16 B**, middle panel). When pre-iMics were collected and plated as monocultures in complete iMic medium, differentiation of iMics in 2D monoculture resulted in a high density of ramified cells for $CSF1R^{+/+}$ after 7 DIV. Cell density was decreased for $CSF1R^{+/E633K}$, while the cellular complexity was comparable. Contrastingly, no attachment and differentiation were observed for $CSF1R^{E633K/E633K}$ and $CSF1R^{-/-}$ cells (**Figure 16 B**, lower panel).

Taken together, these findings implicate that CSF1R signaling is required for iMic maturation and that the lack of functional CSF1R signaling affects both the generation of proper precursor cells and the subsequent differentiation to microglia-like cells.

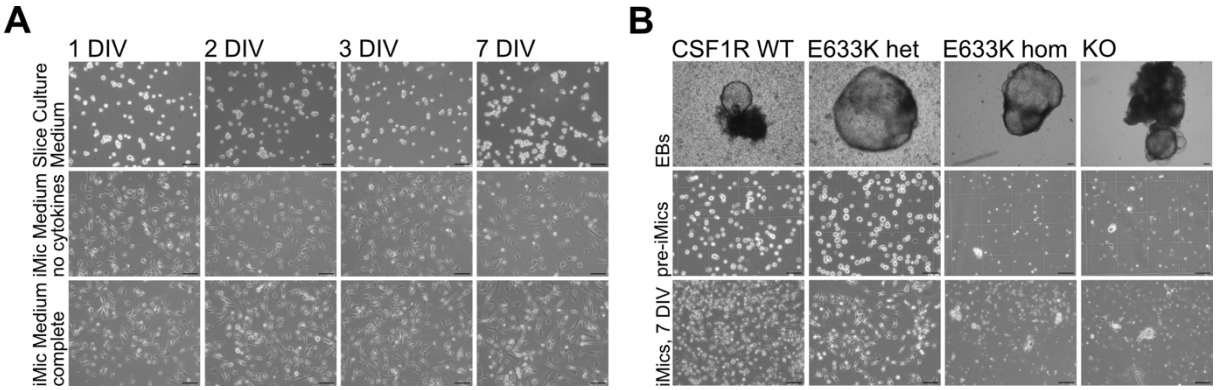

Figure 16 Human CSF1R signaling is required for iMic differentiation in 2D
A) iMic precursor cells were plated as monocultures in slice culture medium, cytokine-free iMic medium or complete iMic medium, respectively, for 7 days. iMics in SCM (top row) did not differentiate at all, while iMic medium without supplementation of hCSF1 (20 ng/ml) and hIL34 (100 ng/ml) differentiated, albeit to a lesser degree (middle row) than those in complete iMic medium (bottom row). Scale bars: 20 µm. **B)** KOLF2.1J iPSCs isogenic for genetic variants in CSF1R (WT, heterozygous E633K mutation, homozygous E633K mutation, KO) were differentiated to iMics following the EB-based protocol. Without functional CSF1R (E633K hom and KO) pre-iMic production and final iMic differentiation was impaired (3rd and 4th column, middle and bottom rows) to a degree that no iMics differentiated. Differentiation of E633K het pre-iMics was not impaired, but final iMic density was lower compared to WT (2nd column). Scale bars: 20 µm.

4.4.2 iMic integration, differentiation and survival in cBSCs is CSF1R-dependent

After confirming the necessity of CSF1R signaling for iMic maturation in 2D, I investigated how impaired receptor function affects iMic integration into cBSCs and if iMic differentiation in the tissue is CSF1R-dependent. To this regard, pre-iMics harboring the four different CSF1R

genotypes described above were grafted to microglia-depleted BSCs as usual and iMic numbers and distribution were assessed after 7, 14 and 28 DIV.

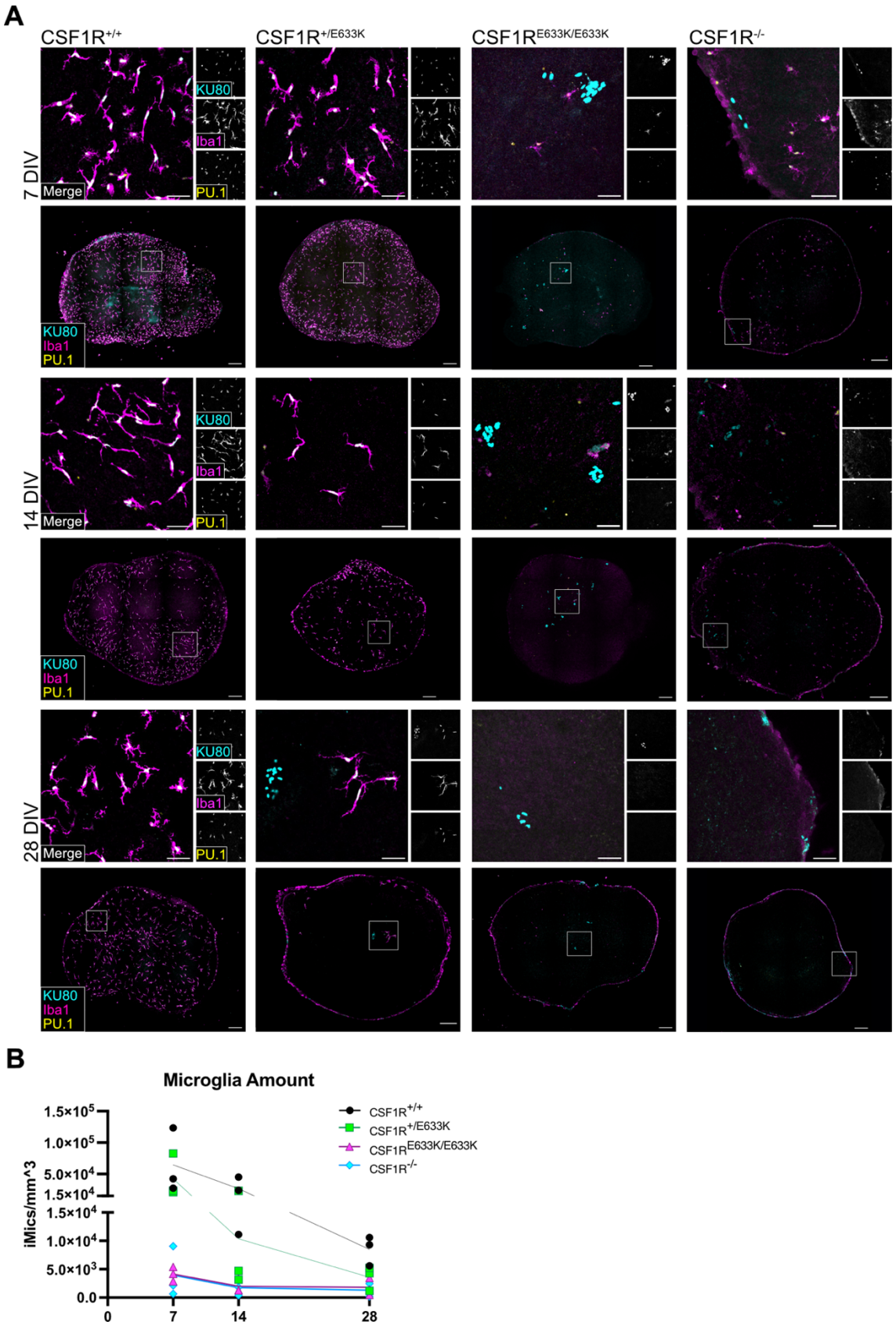

Figure 17 iMic integration, differentiation and survival in cBSCs is CSF1R-dependent
A) Representative immunofluorescent images for CSF1R-variant iMics grafted to cBSCs at 7, 14 and 28 DIV depicting the integration and survival of grafts. iMics were stained against KU80 (human nuclear marker, cyan), Iba1 (microglia surface, magenta) and PU.1 (microglia nucleus, yellow). WT (1st column) integration and distribution was stable (overview images) while iMics matured morphologically into highly ramified cells (close-up). CSF1R$^{+/E633K}$ iMics (2nd column) initially engrafted cBSCs at similar levels as CSF1R$^{+/+}$ cells at 7 DIV but presented decreased survival from 14 DIV onwards. iMics without functional CSF1R barely engrafted BSCs and surviving cells did not express Iba1 or PU.1 (CSF1R$^{E633K/E633K}$ and CSF1R$^{-/-}$: 3rd and 4th column, respectively). Scale bars: 50 µm (close-up), 200 µm (overview). **B)** Quantification of iMic density in cBSCs as measured by iMics (KU80^{+} cells) per volume for CSF1R-variant iMics. n (groups) = 4, number of independent experiments per group = 3; Kruskal-Wallis Test with Dunn's multiple comparisons p = 0.0382. Values depicted are means of each independent experiment.

While KOLF2.1J-CSF1R$^{+/+}$ iMics integrated and sustained as observed for BIONi010C in all experiments before (8485.36 iMics/mm^3 at 28 DIV), mutant variants showed impaired integration and maturation (**Figure 17 A+B**). CSF1R$^{+/E633K}$ engrafted with a similar density and iMic morphology at 7 DIV (WT: 64413.90 iMics/mm^3, Het: 42348.80 iMics/mm^3). CSF1R$^{+/E633K}$, however, did not sustain for longer as seen by the decreased iMic density at 14 DIV and the almost absence within the tissue sections at 28 DIV (WT: 8455.36 iMics/mm^3, Het: 3573.91 iMics/mm^3, **Figure 17 B**, p = 0.0382). iMics without functional CSF1R (CSF1R$^{E633K/E633K}$ and CSF1R$^{-/-}$) did not differentiate at all. While some human-derived nuclei (identified by KU80) were observed for both lines at all timepoints, these cells did not express microglial markers PU.1 nor Iba1 (**Figure 17 A**, 3rd and 4th column) and were predominantly found at the edges of BSCs or on top but not within the tissue.

These findings imply that iMic differentiation in cBSCs is dependent on CSF1R signaling and that no other pathways compensate for the absence of a functional receptor. Since no human cytokines were supplemented to cBSCs, this suggests that murine ligands are capable of binding and activating the human receptor and downstream signaling cascade.

4.4.3 Cross-species receptor:ligand interaction modelling predicts binding of mIL34 to hCSF1R

Experimental evidence showed a microglial dependency on CSF1R signaling *in vitro*. Next, potential cross-species receptor:ligand interactions were analyzed *in silico*. ColabFold (Mirdita et al. 2022) was deployed to predict the ternary complex of one hCSF1 or mCSF1 dimer with two extracellular hCSF1R$_{D1-D3}$ domains and hIL34 or mIL34 with two hCSF1R$_{D1-D3}$, respectively (**Supplementary Figure 2**). Inspection of binding interfaces between hCSF1 or mCSF1 with hCSF1R$_{D1-D3}$ revealed that the key residues within hCSF1R establishing salt bridges or hydrogen bonds with the respective ligand were R142, R144, R146 (**Figure 18 C**, site 1) and R150 and H151 (**Figure 18 C**, site 2), which is in accordance with previously published crystal structures (Ma et

al. 2012; Felix et al. 2015). Key residues for hCSF1R:hIL34 interaction were R142, R144, R146 (**Figure 18 D**, site 1) and N254 (**Figure 18 D**, site 2). Overall, fewer hydrogen bonds and salt bridges were observed in the mCSF1:hCSF1R ternary complexes than in hCSF1:hCSF1R (mCSF1:hCSF1R: 13 hydrogen bonds, 19 salt bridges; hCSF1:hCSF1R: 15 hydrogen bonds; 25 salt bridges), while total numbers of salt bridges and hydrogen bonds were similar between mIL34:hCSF1R and hIL34:hCSF1R (mIL34:hCSF1R: 17 hydrogen bonds; 12 salt bridges; hIL34:hCSF1R: 15 hydrogen bonds, 13 salt bridges) (**Supplementary Figure 2**).

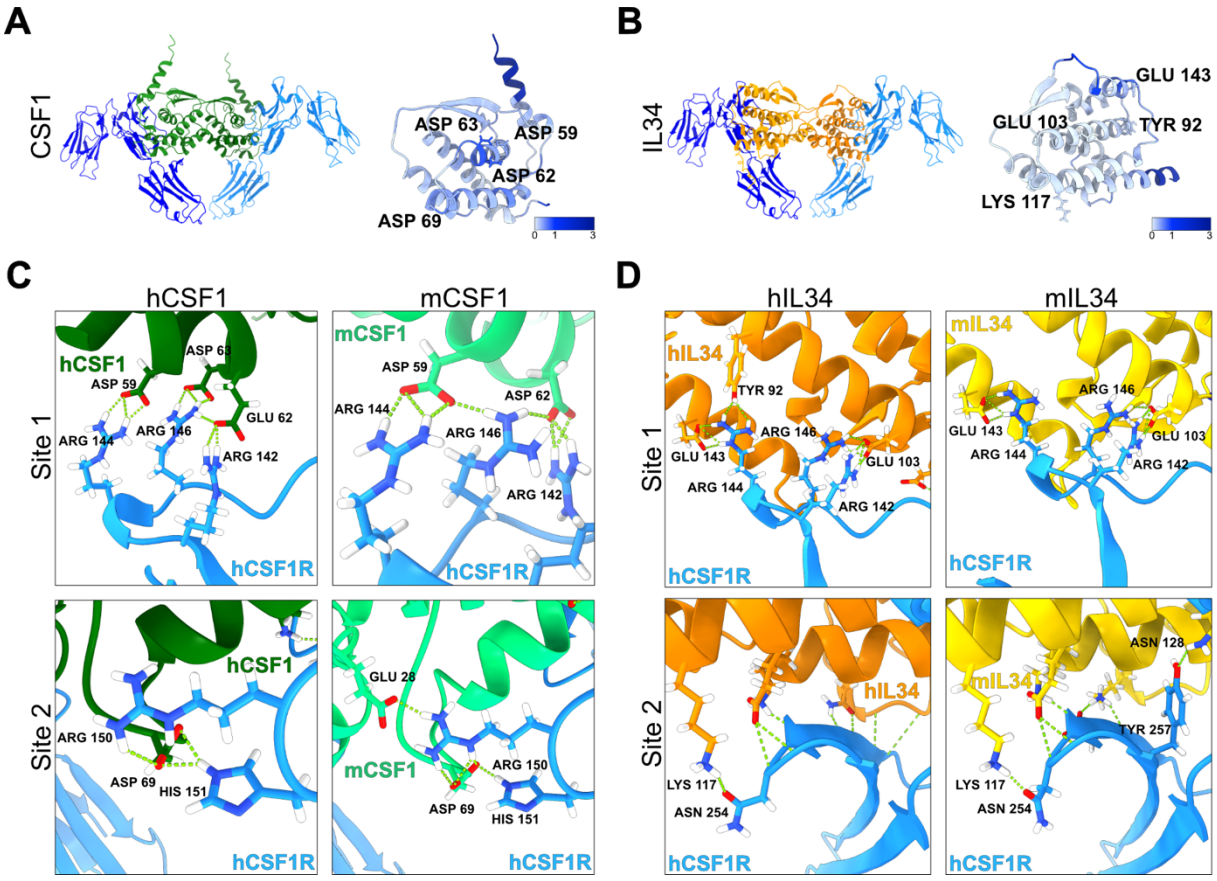

Figure 18 Cross-species receptor:ligand interaction modelling by ColabFold predicts binding of murine ligands to human CSF1R

A+B) ColabFold predicted models of the ternary complex of two hCSF1R$_{D1-D3}$ with its cognate dimerized ligands hCSF1 (A) and hIL34 (B) and superimposed structure of mCSF1 onto hCSF1 and mIL34 onto hIL34, respectively. Color key indicating the distance of the root-mean-square deviation (RMSD) between the Cα atomic coordinates of superimposed murine and human ligands when in the ternary complex. The darker the color, the larger the RMSD value. There was more deviation between hCSF1 and mCSF1 than between hIL34 and mIl34. **C+D)** Detailed view of the ligands with key residues that establish salt bridges and hydrogen bonds with hCSF1R. The receptor is depicted in blue, CSF1 in green colors (C) and IL34 in yellow/orange (D). Note that less interactions between mCSF1 and hCSF1R are formed at 'Site 1' than between hCSF1 and hCSF1R.

Next, the root-mean-square deviation (RMSD) between the Cα atomic coordinates of ternary hCSF1:hCSF1R and mCSF1:hCSF1R complexes was assessed to compare the binding interface

of the respective ligands with hCSF1R in the complexes (**Figure 18 A**). Two of the four key residues of hCSF1/mCSF1:hCSF1R complexes had Cα RMSD values that deviated by more than 1 Å. This is due to an exchange of amino acids at positions 62 and 63. While hCSF1 has an aspartic acid at position 62 (D62) and a glutamic acid at position 63 (E63), it is the other way around for mCSF1 (E62, D63). For the hIL34/mIL34:hCSF1R complexes neither interacting residues' Cα were 1 Å or more apart (**Figure 18 B**). The observed discrepancy of interacting residues' Cα between mCSF1 and hCSF1 indicates subtle structural differences that could lead to differential receptor:ligand kinetics and downstream signaling, whereas very similar binding kinetics could be expected for mIL34 and hIL34 based on the applied ColabFold models.

4.4.4 Murine ligands bind and activate human CSF1R signaling cascade

To confirm the predictions of the modeled receptor:ligand interactions, surface plasmon resonance (SPR) was utilized to examine binding kinetics and affinities of human and murine ligands to hCSF1R. Recombinant hCSF1R-Fc chimera proteins (Miltenyi) were coupled to SPR sensors via anti-Fc antibody binding. The analytes (human and murine growth factors) were washed over the bound receptors and dose-dependent titrations were performed to assess binding kinetics (**Figure 19 A**). hCSF1, hIL34 and mIL34 tightly bound to the receptors at very low concentrations (< 1 nM), resulting in high affinities (K_D hCSF1:hCSF1R: 0.25 pM, K_D hIL34:hCSF1R 0.82 pM; K_D mIL34:hCSF1R: 0.49 pM; **Figure 19 B-E**). In contrast, mCSF1 presented fast-on and fast-off kinetics which prevented fitting an appropriate binding model. Instead, equilibrium affinity measurements were assessed and demonstrated much lower affinities of mCSF1 for hCSF1R (K_D mCSF1:hCSF1R: 20 mM; **Figure 19 B+F**). To ascertain specificity of these findings, analytes' binding kinetics and affinities for human platelet-derived growth factor receptor beta (hPDGFRβ), another member of the receptor tyrosine kinase typ III subfamily, were examined. No biding between any of the ligands and hPDGFRβ was detected (**Supplementary Figure 3**). These findings are in line with the predicted models that suggested differential receptor:ligand kinetics for mCSF1 binding but similar ones for mIL34 and hIL34.

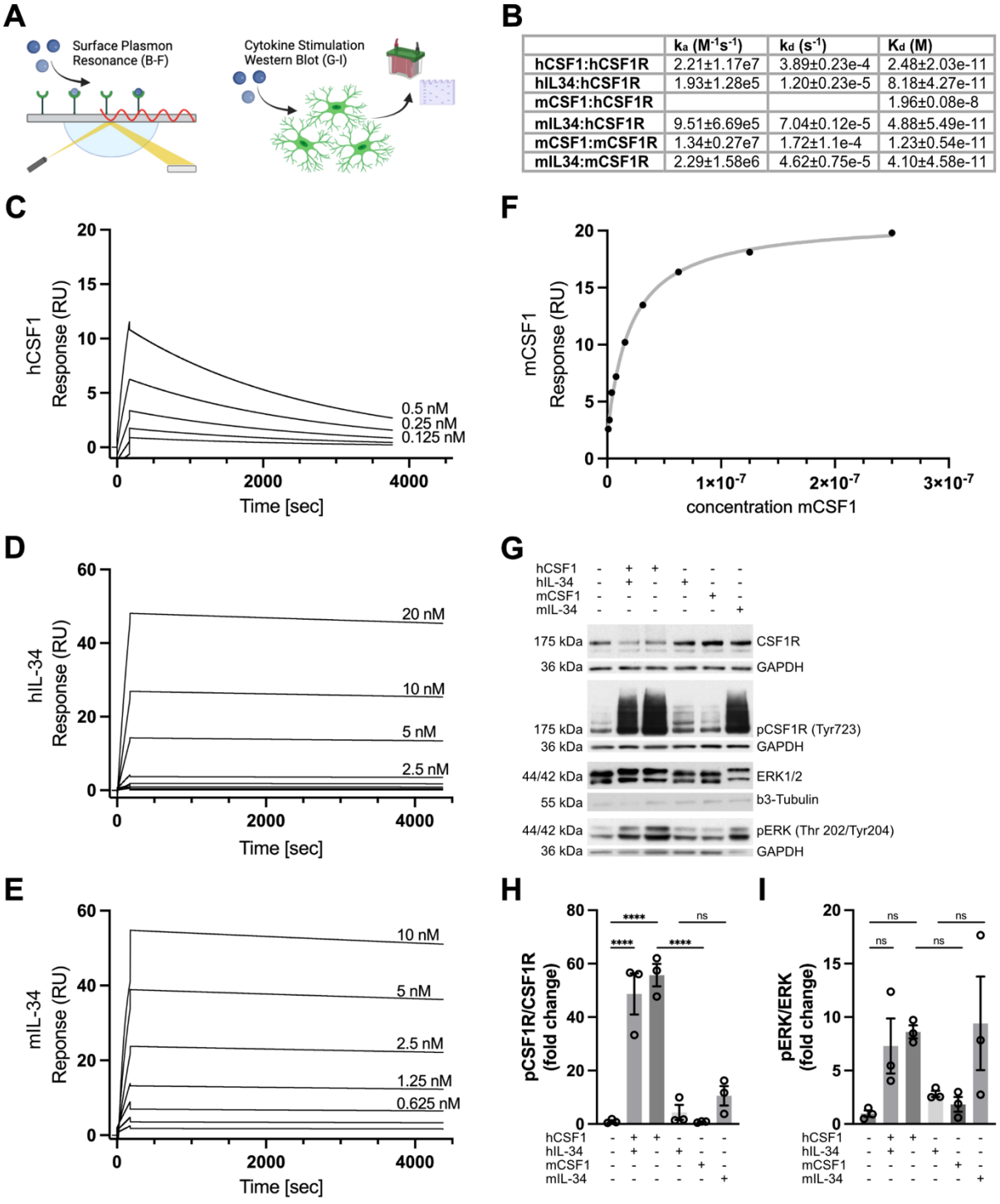

	k_a ($M^{-1}s^{-1}$)	k_d (s^{-1})	K_d (M)
hCSF1:hCSF1R	2.21±1.17e7	3.89±0.23e-4	2.48±2.03e-11
hIL34:hCSF1R	1.93±1.28e5	1.20±0.23e-5	8.18±4.27e-11
mCSF1:hCSF1R			1.96±0.08e-8
mIL34:hCSF1R	9.51±6.69e5	7.04±0.12e-5	4.88±5.49e-11
mCSF1:mCSF1R	1.34±0.27e7	1.72±1.1e-4	1.23±0.54e-11
mIL34:mCSF1R	2.29±1.58e6	4.62±0.75e-5	4.10±4.58e-11

Figure 19 Murine CSF1R-ligands bind and activate human CSF1R signaling cascade

A) Schematic depiction of methods used to investigate cross-species receptor:ligand interaction. Created in Biorender.com. **B)** Table summarizing binding affinities and kinetics analyzed in surface plasmon resonance (SPR). **C-F)** Sensogram plots generated by SPR demonstrating the association and dissociation characteristics between the immobilized ligand (hCSF1R) and the analytes (hCSF1, hIL34, mCSF1, mIL34). hCSF1, hIL34 and mIL34 bound the immobilized receptor with high affinity at concentrations < 1 nM, whereas mCSF1 showed fast-on and fast-off kinetics with much lower affinity for hCSF1R (20 mM). n = 3 independent replicates for each ligand. **G)** Representative images of immunoblots for CSF1R, phospho-CSF1R, ERK1/2 and phospho-ERK1/2 in iMic cell lysates upon cell stimulation with respective growth factors for 5 min. **H+I)** Quantification of immunoblot analysis measured as fold change of phospho-

CSF1R vs. total CSF1R and phospho-ERK1/2 vs. total ERK1/2 upon ligand binding, normalized to GAPDH/b3-tubulin and to untreated control. Combination of hCSF1 and hIL34 as well as hCSF1 or mIL34 stimulation elicited strong activation of CSF1R and ERK1/2 whereas hIL34 and mCSF1 alone did not induce CSF1R nor downstream ERK1/2 activation. Values depicted are mean ± SEM, n = 3 independent stimulations per group and n = 3 technical replicates per sample, one-way ANOVA with Tukey correction for multiple comparisons (* p ≤ 0.05, ** p ≤ 0.01, *** p ≤ 0.001, *** p ≤ 0.0001).

SPR measurements allow to determine binding kinetics. They, however, do not provide any information whether receptor:ligand binding induces receptor activation and downstream signaling. Downstream signaling, namely phosphorylation of CSF1R and extracellular signal-regulated kinases 1and 2 (ERK1/2), upon the addition of human and murine cytokines was examined *in vitro* utilizing monocultured iPSC-derived microglia. iMics were differentiated for 14 days and the growth factors in the cell culture medium were not replenished for 48 hours prior to the experiments to increase the availability of hCSF1R on the cell surface. Treating these "growth factor-starved" microglia with hCSF1 (100 ng/ml) or both human ligands for 5 minutes (100 ng/ml hCSF1 and 100 ng/ml hIL34) resulted in increased phosphorylation of CSF1R (hCSF1: 55.7 ± 3.44; both: 48.67 ± 6.27; mean ± SEM) and its downstream signaling targets ERK1 and ERK2 (hCSF1: 8.61 ± 0.5; both: 7.29 ± 2.1) (**Figure 19 G-I**). Remarkably, while stimulation with hIL34 alone did not induce strong activation signals (pCSF1R: 4.35 ± 2.29; pERK1/2: 2.82 ± 0.24), activating hCSF1R and ERK1/2 phosphorylation was observed upon treatment with mIL34 (100 ng/ml). Treatment with for mCSF1 (100 ng/ml) only resulted in low activating phosphorylation (pCSF1R: 0.78 ± 0.11; pERK1/2: 1.83 ± 0.57) (**Figure 19 G-I**), confirming the modeling and SPR data. Therefore, iMic differentiation in cBSCs was confirmed to be CSF1R-dependent and appears to be driven by binding of mIL34 to human CSF1R.

4.4.5 iMic differentiation in cBSCs is driven by mIL34

Considering these data and the reported tissue distribution of CSF1 and IL34 (Easley-Neal et al. 2019), iMic differentiation and survival in cBSCs is most likely driven by mIL34. To verify this, mIL34 was depleted in cBSCs by the addition of an α-mIL34 antibody (Biotechne) in addition to murine CSF1R-inihibtion. The idea is that the antibody scavenges mIL34 released by neurons, thus reducing the availability of the cytokine and consequently preventing hCSF1R activation and subsequent iMic integration, differentiation and survival. When mIL34 was blocked throughout the experiment, iMic integration was reduced to 8629.43 ± 308.43 iMics/mm^3 after 7 DIV compared to ca. 27,000 cells under control conditions (see **Figure 10 B**) with iMics predominantly located at the outer edges of cBSCs but not within the tissue in the center (**Figure 20**). Extended cultivation resulted in a further decrease of iMic survival in cBSCs after 14

(1589.01 ± 100.55 iMics/mm^3) and 35 DIV (524.3 ± 71.41 iMics/mm^3), respectively, with observable demise of iMics at the edges of cBSCs between 7 and 14 DIV (**Figure 20 A+B**). The iMics that engrafted and sustained for 7 or more days expressed very low levels of Iba1, were very small and showed no maturation as indicated by the presence of KU80$^+$ nuclei without surrounding Iba1 and short processes without arborization in Iba1-expressing cells. These observations were reminiscent of those for *CSF1R*-deficient iMics (**Figure 17**), underlining the necessity of functional hCSF1R signaling for iMic survival and maturation in cBSCs.

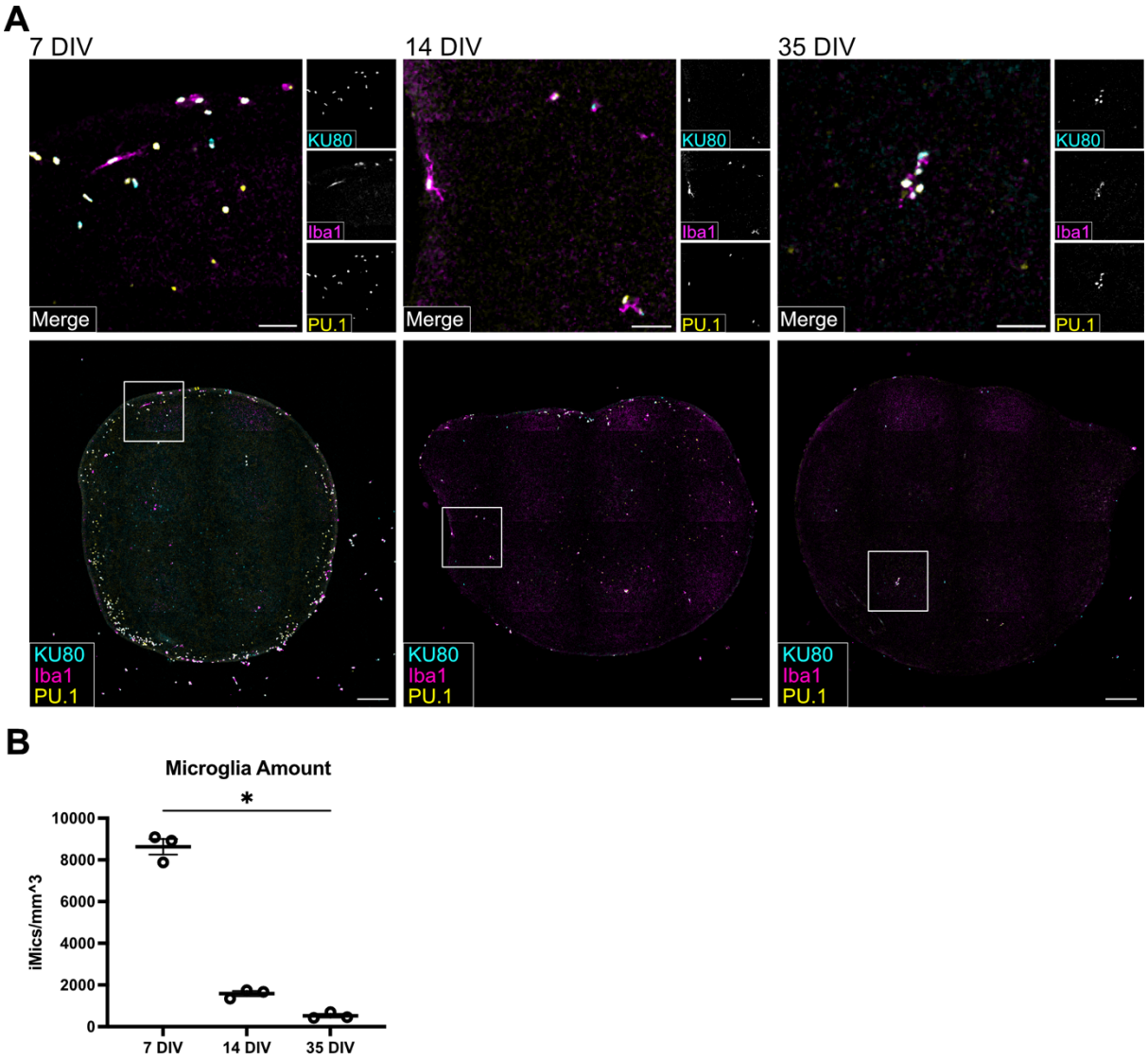

Figure 20 mIL34 is required for iMic differentiation in cBSCs

A) Representative images of cBSCs continuously treated with anti-mouse-IL34 antibody over the entire differentiation period. iMics (KU80$^+$, cyan) were located at the edge of slices at 7 DIV and demised over extended culture periods. iMics stained positive for microglial nuclear marker PU.1 (yellow) but showed little labelling by Iba1 (magenta) and did not adopt complex morphologies. Scale bars: 50 µm (close up), 200 µm (overview). DIV: days *in vitro*. **B)** Quantification of microglial numbers (PU.1$^+$ per volume) in conditions of (A). The presence of the anti-mIL34 antibody results in loss of iMics in cultures after 7 DIV. n (groups) = 3; number of independent experiments per group = 3; Kurskal-Wallis test with Dunn's multiple comparisons p = 0.0036. All values depicted are mean ± SEM.

Together with the data obtained from the *in silico* modeling and biochemical analyses, these results allow the conclusion that iMics survival and differentiation in cBSCs is primarily driven by mIL34 rather than mCSF1 and obligatorily depends on hCSF1R activation, as no iMic survival was observed in CSF1R-deficient iMics or upon blocking mIL34. Thus, cross-species interaction between the human receptor and its cognate murine ligands was demonstrated for the first time and shown to be biologically relevant for xenotransplantation approaches *in vitro*. It furthermore explains, why the supplementation of human cytokines to the model is not required for iMic survival and maturation. The findings validated that cBSC-iMics are biologically similar to microglia in their dependency on hCSF1R signaling.

4.5 Modeling neurodegenerative disease in cBSCs

After developing cBSCs as a model to study human iPSC-derived microglia homeostasis in a complex tissue environment, I aimed to investigate whether the system could be utilized to study microglial function in a neurodegenerative disease context. I adapted a model that had previously been established in the lab using BSCs (Barth et al. 2021) to cBSCs allowing me to study human microglial responses to proteinopathies.

4.5.1 iMics in cBSCs respond to tissue aging and alpha-synuclein pathology

To examine microglial responses to alpha-synuclein (αSyn), cBSCs were treated with pre-formed fibrils (pff) of synthetic αSyn to "seed" αSyn lesions as previously described by Barth et al. 2021 (**Figure 21 A**). Five weeks post-seeding, cBSCs had developed abundant neuritic αSyn lesions (**Figure 21 B**). Consistent with previous reports (Tanriöver et al. 2020; Barth et al. 2021), numerous intramicroglial inclusions that stained positive with the amyloid binding dye pentamer formyl thiopene acetic acid (pFTAA) were observed as well (**Figure 21C**). pFTAA does not selectively stain αSyn lesions, but the aggregation of αSyn is the most likely explanation for pFTAA-positivity within pff-seeded cBSCs compared to other amyloids like Aβ or tau.

Next, I was interested if microglia would show transcriptomic responses to the induced αSyn pathology. For this, I re-isolated iMics from pff-seeded cBSCs and compared them with age-matched untreated controls (11w control vs. 5w αSyn-treatment after 6 weeks of homeostatic maturation). After quality control, 9,400 Mics (4,938 control and 4462 αSyn, n = 2 independent differentiations of iMics) were retained for analysis. 11 unique clusters were revealed upon PCA,

UMAP and clustering analysis (**Figure 21 D**). While all clusters were present in both control and αSyn-treated cultures, their frequencies varied (**Figure 21 F+G**).

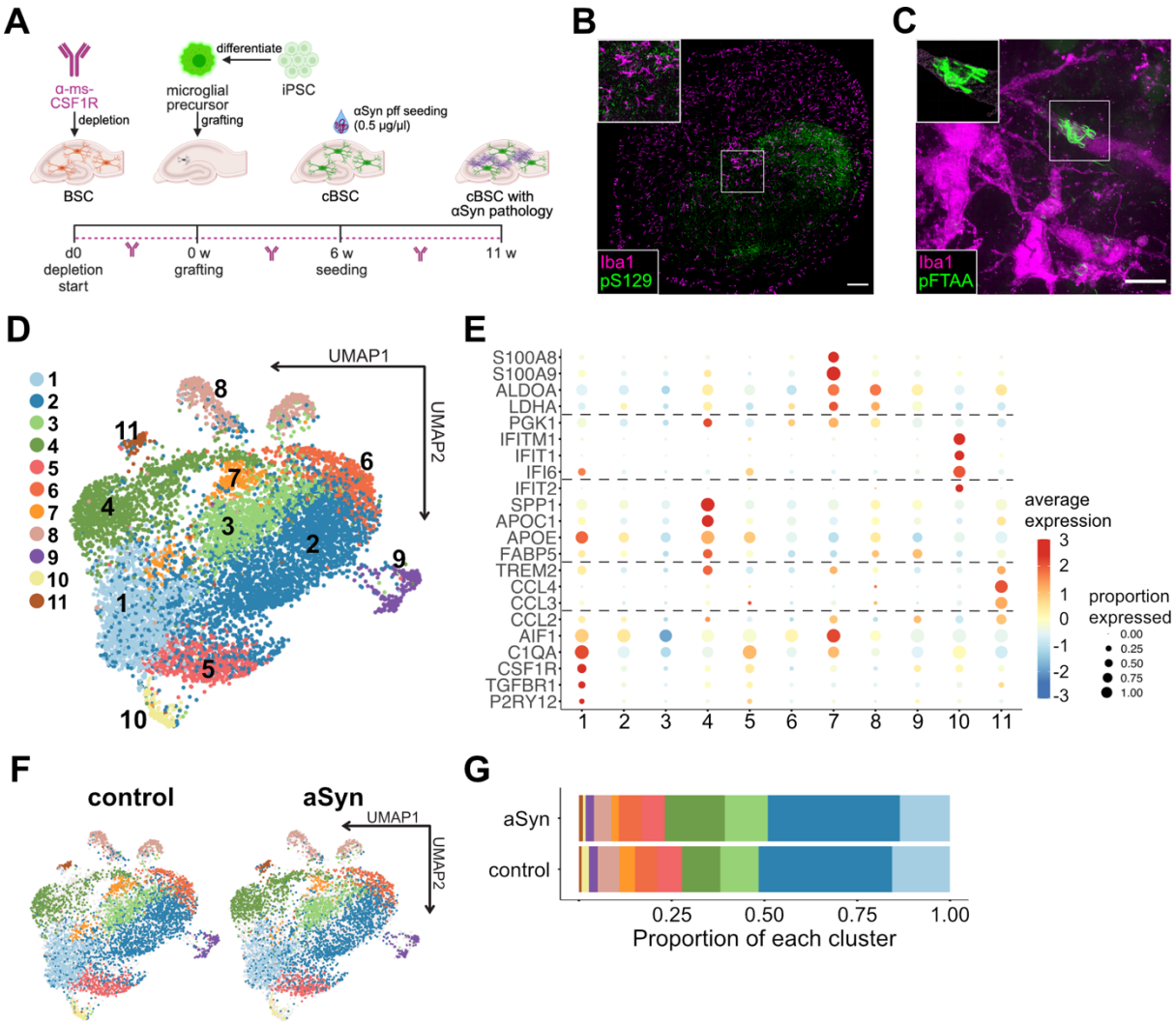

Figure 21 iMics in cBSCs respond to tissue aging and αSyn pathology

A) Scheme of experimental procedure: At 6 weeks post-grafting, cBSCs were treated with 0.5 µg/µl pre-formed fibrils (pff) of alpha-synuclein (αSyn) to induce the formation of αSyn lesions within cBSCs. After incubation for 5 weeks, αSyn-seeded and untreated control slices were subjected to single-cell RNA sequencing or analyzed using immunohistochemistry. Created in Biorender.com **B)** Representative images of αSyn-pathology throughout BSCs (neuritic lesions, stained positive for pS129, green). Scale bar: 200 µm. **C)** Some inclusions localized inside of microglia (Iba1, magenta) and stained positive for the amyloid-binding dye pFTAA (green). Scale bar: 10 µm. **D)** Scatterplot after principal component analysis and UMAP of microglia from αSyn pff-treated and control cBSCs at 11 weeks post-grafting, color-coded by cluster. In total 11 molecularly distinct subpopulations were identified. **E)** RNA expression levels of molecular markers enriched in different subsets of the scRNAseq dataset. The size of each circle depicts the percentage of cells per cluster in which the given transcript was detected, while the color coding represents the normalized z-scores. DAM genes were upregulated in cluster '4' whereas interferon-responsive genes were only found in cluster '10'. **F)** Scatterplot after principal component analysis and UMAP for control (left) or αSyn-seeded cBSCs (right) colored by cluster. All populations were present in both conditions. **G)** Analysis of proportional contribution of each cluster to total number of microglia. While most clusters remained stable in their proportion, cluster '10' was enriched in control slices, whereas cluster '4' was proportionally larger in αSyn-treated slices. n = 9,400 cells with n = 2 independent iMic differentiations per timepoint.

As seen in the previous scRNAseq timeline (**Figure 15**), homeostatic markers *P2RY12, CX3CR1, CSF1R* and *HEXB* were expressed after 11 weeks. Genes involved in complement activation (*C1QA,* C1QB), antigen presentation (*HLA-DRA, CD74)*, phagocytosis (*SPP1, CTSD*) and interferon response (*IFITM1, IFIT1, IFIT2, IFI6*) were expressed at higher levels, indicating a more age-related activation of microglia independent of αSyn pathology. In this dataset the expression of these aging-associated markers was higher than in the timeline experiment (see **4.3**). Interferon signaling-related genes (*IFITM1, IFIT1*) were upregulated in cells in 'cluster 10' (**Figure 21 E**), as observed in changing microglial interferon response signatures with aging (Sala Frigerio et al. 2019). Interestingly, the proportion of cells from αSyn-treated cBSCs in this cluster was reduced (ca. 25 % αSyn, 75 % control) (**Figure 21 G**), indicating a more pronounced interferon response with age rather than pathology. 'Cluster 7' microglia presented an upregulation of genes related to immunomodulation (*S100A8, S100A9*) and glycolysis (*ALDOA, LDHA, PGK1*) (**Figure 21 E**), suggesting an altered metabolic profile with age rather than pathology. On the other hand, iMics from αSyn-seeded cBSCs presented stronger upregulations of classical DAM-related signature genes like *APOE, TREM2, SPP1* ('cluster 4') and elevated levels of chemokine genes (*CCL2, CCL3, CCL4*) in 'cluster 11' (**Figure 21 E**). While DAM clusters have only been described for mice so far (Krasemann et al. 2017; Keren-Shaul et al. 2017; Srinivasan et al. 2020; Sun et al. 2023), the pre-activated 'chemokine-enriched' subset has previously only been observed in humans (Olah et al. 2018; Sala Frigerio et al. 2019).

Taken together, these data demonstrate that iMics in cBSCs not only transition to transcriptional profiles that have been reported to develop during aging ('IRM') but also respond to neuropathological changes induced by αSyn seeding ('DAM' and 'chemokine-enriched'). Given the time frame of this thesis, I was not able to discern whether these distinct transcriptional states correlate with functionally different subsets of microglia, cBSCs provide the required experimental accessibility to investigate microglial roles in aging and disease and dissect their various contributions to either.

All in all, I have presented the establishment of a novel *in vitro* model to study human iPSC-derived microglia in a complex tissue environment. The model recapitulates microglial maturation at morphological, functional and transcriptional levels to closely resemble adult human microglia. Furthermore, I was able to demonstrate cross-species activation of human CSF1R by its cognate murine ligand IL34 which I assume is the sole driver of iMic survival and differentiation in chimeric brain slice cultures. Lastly, I showed that cBSCs can be utilized to study iMics in

neurodegenerative disease conditions. In a proof-of-principle experiment, iMics in cBSCs with seeded synucleinopathy responded with microgliosis and the upregulation of DAM genes, highlighting that chimeric brain slice cultures offer a platform to study human microglia dynamics in health and disease conditions.

5 Discussion

5.1 Establishment of chimeric brain slice cultures

Microglia play an important role in the brain throughout life and previous studies have shown that significant differences between human and murine microglia exist (Mancuso et al. 2019; Hasselmann and Blurton-Jones 2020; Masuda et al. 2019; Geirsdottir et al. 2020). It is thus paramount to understand human microglia biology in a complex environment under homeostatic conditions, in order to investigate their role in neurodegenerative disease in subsequent studies. While murine microglia can be easily studied *in vivo* (Davalos et al. 2005; Nimmerjahn, Kirchhoff, and Helmchen 2005; Hefendehl et al. 2014; Füger et al. 2017), primary human microglia so far have only been studied *in vitro* which is known to alter their transcriptome and function significantly (Gosselin et al. 2017; F. C. Bennett et al. 2018). The advent of iPSC-derived microglia protocols and xenotransplantation models have significantly increased our knowledge about these intricate cells, by studying human microglia *in vivo* for the first time (Abud et al. 2017; Hasselmann et al. 2019; Mancuso et al. 2019; McQuade et al. 2020; Baligács et al. 2024). Xenotransplantation studies require the use of immunodeficient mice which complicates their use due to strict regulatory requirements (in Germany), a limited lifetime and more complicated housing conditions. My laboratory and I thus identified the need for an *in vitro* model system, that mimics the phenotypes of human *in vivo* microglia as closely as possible without the limitations imposed by immunodeficient mice. Similarly, Ogaki et al. generated chimeric hippocampal slice cultures by transplanting iPSC-derived microglia into BSCs but only showed data for 14 DIV (Ogaki, Ikegaya, and Koyama 2022), which is insufficient to study mature human microglia and function in homeostasis and disease.

As Ogaki et al., I utilized murine organotypic hippocampal slice cultures, which I depleted of their endogenous murine microglia to enable engraftment of iPSC-derived microglial precursor cells to generate chimeric brain slice cultures which I studied for up to three months. Below, I will discuss how I generated and characterized a novel model system to study human microglia in the most complex *in vitro* environment for extended culture periods and how to utilize the model to answer biological questions.

5.1.1 Generation of iPSC-derived microglia

In order to generate chimeric BSCs, iPSCs had to be differentiated to microglial precursor cells that could be transplanted into BSCs. Since iPSCs have been developed, several laboratories

have established protocols to differentiate the cells into microglia, taking their distinct ontogeny into account (Muffat et al. 2016; Abud et al. 2017; Haenseler et al. 2017; Takata et al. 2017). In this study, I utilized two different protocols that differ significantly in their approach. The protocol by (Haenseler et al. 2017) is based on the formation of embryoid bodies and the supplementation of mesoderm-inducing cytokines BMP4, VEGF and SCF followed by primitive hematopoietic fate induction using IL3 and CSF1. It relies on cell-cell interactions and paracrine release of growth factors within the embryoid bodies for differentiation. Most importantly, NOTCH signaling between adjacent cells prevents the differentiation towards definitive hematopoiesis and increases the proliferation of progenitor cells (Simon and Keith 2008; Gustafsson et al. 2005). On the other hand, Takata et al. provided a protocol that has more room for external control and manipulation, as cytokine concentrations and combinations are vigorously controlled in this monolayer-based approach. The monolayer approach needs to be subjected to hypoxic incubator conditions for the first 8 days of differentiation to mimic the environment of the yolk sac, that is known to be hypoxic, whereas reduced hypoxic tensions are expected to be generated within EBs due to their size. Consequently, both protocols closely simulate the microglial origin and activate important signaling cascades including NOTCH, which has been shown to work in tandem with hypoxia (Gustafsson et al. 2005), albeit by different methodology.

Independent of the approach, microglial precursor cells could be used after about three weeks of differentiation and matured into microglia-like cells in 2D within another two weeks (**Figure 5**). Precursor cells from both protocols were indiscernible by eye and resulted in similar morphology and engraftment rates and the expression of key microglial markers IBA1 and PU.1 when transplanted into BSCs (**Figure 9**) further underlining that both differentiations yield microglial (precursor) cells expressing adequate markers. Thus, the protocol used to differentiate microglia precursor cells from iPSCs does not affect the generation of cBSCs and makes this model easily adaptable to other laboratories as they can use the protocol they already have established. However, due to the higher and prolonged yield of pre-iMics, the lower costs and decreased work effort, the EB-based protocol was routinely used for all subsequent experiments

5.1.2 Generation and optimization of chimeric brain slice cultures

Next, a depletion paradigm was established to selectively remove murine microglia from BSCs to enable iPSC-microglia engraftment. Similar to some protocols established for xenotransplantation approaches (Mancuso et al. 2019; Fattorelli et al. 2021), the creation of a niche is required for high engraftment rates. Without previous depletion of endogenous microglia

grafting efficiencies were below 10 % but could be increased to 93 % in cBSCs subjected to continuous depletion (**Figure 7**). Although grafting efficiencies were above 90 %, ceasing the depletion of endogenous microglia after one week (or at any later timepoint during an experiment) resulted in the re-emergence of murine microglia and the loss of human microglia in the cultures (data not shown). While repopulation of microglia-depleted cultures is well-documented (Coleman Jr, Zou, and Crews 2020; Barth 2023), it is unknown why murine microglia are able to replace the human microglia after extended periods of depletion and stable human microglia integration (**Figure 10**). Since nobody has performed these experiments *in vitro* before, and xenotransplantation models usually do not use continuous depletion (Mancuso et al. 2019; Fattorelli et al. 2021), I can only speculate that murine microglia have a survival benefit in murine tissue compared to human cells due to stronger stimulation of surface receptors by endogenous growth factors compared to cross-species activation. This will be discussed in more detail below (see **5.5**).

Microglia depletion *in vitro* and *in vivo* is most commonly achieved by the administration of small molecule inhibitors of CSF1R including PLX3397 or PLX5622 (J. Han et al. 2022). Ogaki et al. used PLX3397 and Clodronate liposomes in their study to deplete murine microglia for the generation of chimeric BSCs. They showed that PLX3397 prevented human microglia engraftment completely while Clodronate-mediated depletion resulted in an 80 %-exchange of murine to human microglia (Ogaki, Ikegaya, and Koyama 2022). Their findings highlight the necessity for mouse-specific microglia depletion that does not affect human cells and therefore could mediate a near-complete exchange of microglia in cBSCs. To circumvent the unwanted effect on iMics, I used a species-specific antibody directed against murine CSF1R to continuously suppress murine microglia without affecting the grafted human cells. The anti-m-CSF1R antibody is highly specific for CSF1R and thus decreases the off-target effects on other surface receptors observed upon PLX3397 treatment (Hagemeyer et al. 2017). Consequently, other neural cell types are not directly affected by the depletion. Furthermore, working *in vitro* overcomes one of the major drawbacks faced when working with brain-targeting antibodies *in vivo*: the lacking penetration of the BBB by antibodies (David A. Hume and MacDonald 2012). Like small molecules, the CSF1R-antibody can be easily supplemented to the culture medium of BSCs and directly reaches the brain tissue, enabling fast and targeted microglia depletion by preventing CSF1R ligands from binding to the receptor. Using the anti-CSF1R antibody resulted in depletion rates of 85 % within one week, and more than 90 % after two weeks (**Figure 6**) which is comparable to efficiencies described for PLX3397 (Elmore et al. 2014; Green, Crapser, and Hohsfield 2020). Due to blocking

the same receptor and similar timing of depletion observed for antibody and small molecule treatments, one can assume that antibody treatment results in the induction of apoptosis of microglial cells due to cytokine deprivation (Elmore et al. 2014) rather than reduced proliferation which would have a significantly longer turnover time (Askew et al. 2017; Füger et al. 2017). Within one week, the withdrawal of the antibody from the culture medium results in a repopulation of the cultures from a small population of cells resistant to CSF1R inhibition (Huang et al. 2018; L. Zhan et al. 2020) as previously described for PLX3397 and PLX5622 (Elmore et al. 2014). These CSF1R-independent microglia, which highly express MAC2, are intriguing but investigating them in more detail was outside the scope of this thesis. Furthermore, the previously described 'overshoot' phenomenon during repopulation (Barth 2023) was not observed due to the limited number of timepoints observed in this study (**Figure 6**).

The number of microglial precursor cells grafted to each BSC was determined by titrating the graft size and evaluating graft survival, basic morphology, expression of Iba1 and network density and distribution to resemble endogenous parameters as closely as possible (**Figure 7**). Grafting excess numbers resulted in overpopulated niches, indicated by decreased morphological differentiation and a decreased expression of microglial markers PU.1 and Iba1. Conversely, grafting insufficient numbers resulted in higher variability between experiments and thus unreliable microglial densities, which would impair reproducibility. Even though graft sizes varied between 1k and 50k, the observed integration density did not vary 50-fold, but only 5-fold between the smallest and largest graft (ca. 4,000 and 23,000 iMics/mm^3, respectively), while the intermediate graft sizes of 5k and 10k resulted in a 1.2-fold increase density for doubled graft size (10,500 vs. 13,000 iMics/mm^3). These findings indicate that the tissue regulates the number of microglia to prevent severe overpopulation, even though the mechanism remains unknown (Nikodemova et al. 2015; Askew and Gomez-Nicola 2018). Consequently, the graft size was determined to be 10,000 cells per slice, which results in highly reproducible densities and highly mature morphologies while allowing the generation of several experiments in parallel because pre-iMic yields are not exhausted.

To demonstrate that the model overcomes major challenges faced by iPSC work, namely decreased reproducibility and increased variability between lines for more complex 3D models (Volpato and Webber 2020; Hedegaard et al. 2020), pre-iMics of three different lines and the two differentiation protocols were grafted to cBSCs (**Figure 9** and **Figure 17**). Independent of cell line and protocol, highly reproducible results were obtained, underlining the easy adaptation of the model by other labs.

5.2 Morphological characterization of iMics in cBSCs

The inaccessibility of human microglia for direct observation or manipulation *in vivo* requires the use of model systems that reflect key properties and features as closely as possible. For microglia model systems, a model's quality is evaluated on the cellular morphology and network organization of microglia, their functionality during homeostatic and disease-associated conditions as well as their transcriptional phenotypes. The comparison of morphological parameters between studies, however, is complicated by several factors and underline the importance of using appropriate controls within each experiment. 1) Microglia morphology is drastically influenced by activation status which is often determined by morphological readouts (Paolicelli et al. 2022). 2) Microglia present considerably different morphologies between species as well as between different brain regions within one species (Geirsdottir et al. 2020). 3) Sample preparation, analysis pipelines and software affect readouts independent of the tissue sources, while 4) post-mortal delay (PMD) is especially relevant for human tissue samples. Heng et al. showed that PMD induces transcriptional changes in both human and mouse samples suggesting that microglial morphology can also be altered upon increased PMD. Conversely, microglial yield decreases with increased PMD (Heng et al. 2021), indicating microglial cell death and/or changed expression of surface markers used for isolation. Human *ex vivo* experiments in this study were not affected by PMD, as the tissue was obtained during brain surgery and could be fixed immediately upon excision, resulting in the most *in vivo*-like reference possible. The limited availability of human brain tissue, however, only allowed for the inclusion of tissue from the prefrontal cortex which was compared to human and murine microglia in the hippocampus of (c)BSCs. Nevertheless, morphological analysis revealed no significant difference between human *ex vivo* microglia, murine microglia in BSCs and human iMics in cBSCs, demonstrating that iMics successfully differentiate and mature in cBSCs (**Figure 10**). Furthermore, increased expression of microglial marker IBA1 and increased ramification was observed over extended cultivation time, underlining morphological maturation (**Figure 10**). Interestingly, it was not possible to determine if iMics more closely resemble human microglia *ex vivo* or murine microglia in BSCs based on the analyses performed. While both the local brain environment and the species background have been implicated in determining microglial morphology (F. C. Bennett et al. 2018), the ultimate determinant remains unknown. Microglia in chimeric models might share characteristics with both species but this has to be analyzed in more detail in subsequent studies. iMics in cBSCs are less ramified than human or murine hippocampal microglia (Geirsdottir et al. 2020), indicative of a possible *in vitro* phenotype previously described (Ormel et al. 2018; Popova et al. 2021).

Compared to other 2D and 3D models, this activated/ decreased homeostatic phenotype is less pronounced in cBSC-iMics. While the study by Geirsdottir et al. was the most extensive on species differences, the values of their human cortical microglia deviated from the human *ex vivo* samples used in this thesis. This underlines that comparisons between studies are difficult and that observed differences might arise due to methodological differences. Thus, to determine if cBSC-iMics present an activated phenotype or are not fully mature, further investigations are required.

Microglial network organization was characterized by analyzing the microglial numbers per volume and the nearest-neighbor-distance. As for the morphological analyses, no differences between iMics and the other experimental groups were observed (**Figure 10**), indicating that engrafted iMics establish a homeostatic human microglial network within the mouse brain tissue *in vitro*. Nevertheless, observed NND values of 30-35 µm deviate from values reported in literature, that usually range between 40 and 50 µm (Hefendehl et al. 2014; Mancuso et al. 2019; Barry-Carroll et al. 2023). One factor might be the age difference between 1.5 month-old BSCs compared to three-week (Barry-Carroll et al. 2023) or three-month-old mice (Hefendehl et al. 2014). As a decrease of NND between embryonic stages and p21 as well as with age have been described, respectively (Nikodemova et al. 2015; Askew and Gomez-Nicola 2018). For murine microglia in BSCs, the generation of a glial scar might cause smaller NND values. However, the glial scar has been described to subside after two to three weeks in culture (Hailer, Jarhult, and Nitsch 1996; F. L. Heppner et al. 1998) and thus seems an unlikely explanation for sustained low NND values after 6 weeks. Furthermore, morphological analysis did not reveal an overly activated phenotype of murine microglia (**Figure 10**). A more logical explanation for the deviating values therefore might be found in methodology, as also human *ex vivo* samples showed the deviation from published values (Geirsdottir et al. 2020). While tissue sections from other studies were 25 to 80 µm thick, neither (c)BSCs nor human tissue slices were sectioned prior to staining and mounting, resulting in the analysis of 250-300 µm thick tissue sections. Compression of the tissue imposed by the coverslip most likely is higher for thicker tissue sections and thus results in an artificial reduction of NND in the sections analyzed in this thesis. Conversely, microglial density in (c)BSCs was increased compared to published results, which can be explained by increased compression as well as a possible primed microglial phenotype. Nevertheless, iMic density in cBSCs (7600 iMics/mm^3, **Figure 10**) is comparable to previously published values (5990 microglia/mm^3) (Keller, Erö, and Markram 2018) indicating that the tissue controls microglial numbers and results in a stabilization of iMic numbers after three weeks, as observed *in vivo* (Nikodemova et al. 2015; Askew and Gomez-Nicola 2018).

Overall, these data suggest that iMics in cBSC morphologically mature to reach the complexity and tissue distribution observed in human microglia *ex vivo*. This reminiscence of microglial networks validates the opportunities chimeric slice cultures offer to study human microglia biology *in vitro*.

5.3 Functional characterization of iMics in cBSCs

While morphological and network parameters indicate iMic maturation *in vitro*, they do not provide any information about functionality which is a prerequisite for the investigation of microglia biology. To assess functional characteristics of iMics three basic functions were investigated: process motility and lesion response, cytokine responses upon inflammatory stimulation and support of neuronal network activity.

2-Photon live cell imaging was performed to investigate microglial process movement during homeostatic conditions and upon focal laser lesion induction. These methods and readouts are commonly utilized to assess microglial function (Davalos et al. 2005; Nimmerjahn, Kirchhoff, and Helmchen 2005) but due to differences in analysis software and pipeline direct comparison to other studies is difficult. Endogenous murine microglia in Iba1-EGFP BSCs therefore were the comparison of choice and revealed no differences in human and murine microglia process motility (**Figure 11**). GFP^+ iMics have a stationary soma while actively monitoring their territory during homeostasis and within minutes move their processes towards the injury site upon focal laser lesion, as has been described *in vivo* (Davalos et al. 2005; Nimmerjahn, Kirchhoff, and Helmchen 2005; Hefendehl et al. 2014; Hasselmann et al. 2019). Comparison to human microglia in primary tissue is difficult, due to the limited availability of living tissue and problems in labeling primary microglia without causing inflammatory activation. Furthermore, the sectioning of tissue itself induces a pro-inflammatory environment and *in vitro* culture of primary tissue has activating effects on the cells and thus might affect their motility and lesion response. iMic responses, therefore, could only be compared to murine microglia while dynamics in humans could be different.

Next, cBSCs were subjected to chronic and acute stimulation with LPS to mimic a strong inflammatory activation and elicit microglial cytokine release (**Figure 12**). Although LPS is not a physiological stimulus of microglia as it is unable to cross the intact BBB, it is broadly applied for proof-of-principle experiments due to the strong effects elicited (Stöberl et al. 2023). iMics secreted IL1β, IL6, IL8 and TNFα as has been observed for primary microglia whereas immortalized microglia cell lines usually present impaired cytokine responses and release only

one or two cytokines (Nagai et al. 2001; Ahn et al. 2008; Timmerman, Burm, and Bajramovic 2018). Acute, 24 h stimulation with a high LPS dose elicited higher concentrations of all assessed cytokines compared to the low dose chronic treatment for seven days. Possibly, a lower dose for the acute treatment would have resulted in lower cytokine concentrations after 24 hours. On the other hand, the extended incubation in the chronic treatment might have induced tolerance mechanisms as described *in vivo* (Wendeln et al. 2018). Adjusting the applied concentrations, incubation periods and the panel of cytokines examined might lead to differential observations between groups but was outside the scope of this thesis, as the LPS response was only used as proof-of-principle for cytokine release.

Microglia play a key role in modulating neuronal circuits by synaptic pruning and it has been shown that the loss of microglia alters neuronal activity on post-synaptic and network levels (Paolicelli et al. 2011; Du et al. 2022). As endogenous microglia are depleted in cBSCs, I wondered whether iMics were able to take over their function and support neuronal activity over extended culture periods. Multi-electrode array analysis revealed no difference in spike counts between cBSCs with iMics and BSCs with endogenous microglia after six and twelve weeks in culture, respectively (**Figure 13**). Interestingly, baseline activity after twelve weeks was higher compared to six weeks for both iMics and endogenous microglia. While this increased activity might be due to technical reasons during data acquisition, it could also reflect a more mature neuronal network (Suresh et al. 2016). Regardless of the reason for the increased activity, this data shows that (c)BSCs are still viable after 12 weeks in culture and that the exchange of microglia from murine to human does not negatively affect neuronal function. Thus, cBSCs are a valid tool to study human microglia in intact, homeostatic neuronal networks for extended periods of time.

Taken together, iMics in cBSCs are able to fulfil three major microglial functions. However, microglia biology is complex, and the cells possess several other key functions not investigated in this thesis. These include phagocytosis of synapses and neuronal debris, antigen presentation and activation of the complement system. Additional investigation of these parameters would have exceeded the scope of this project. It would be interesting to examine those in later studies, as has been done for xenotransplantation mice, where initial reports did not investigate these features either but have been extended since (Mancuso et al. 2019; Hasselmann et al. 2019).

5.4 Transcriptional profile of iMics in cBSCs recapitulates *ex vivo* human microglia phenotypes

Microglia are highly complex cells which are strongly influenced by both their ontogeny and environment (Ginhoux et al. 2010; F. C. Bennett et al. 2018; Gosselin et al. 2017; Paolicelli et al. 2022). This intricate interplay results in a heterogenous cell population in homeostatic conditions that cannot be reflected by morphological analyses alone (Ransohoff 2016; Paolicelli et al. 2022). Single-cell RNA sequencing allows investigating changes in cellular gene expression upon experimental manipulation or to understand the maturation of a cell population in unprecedented detail. By now scRNAseq has become an essential tool to validate new model systems and defined many microglial transcriptional states.

In this study I utilized scRNAseq to investigate iMic maturation in monoculture and cBSCs and how well they reflect mature human microglia. For this, pre-iMics, mono iMics cultivated for 21 DIV and iMics re-isolated from cBSCs after 4, 8 and 12 weeks were subjected to RNA sequencing (**Figure 14**). After quality control and exclusion of contaminating neural cells, iMics clearly clustered according to developmental stage and culture condition. Independent of the time post-engraftment cBSC-iMics clustered away from precursors and mono iMics. Interestingly, while cBSC-iMics constituted only two clusters, a progression in transcriptional changes can be assumed as 8w cells cluster between 4w and 12w conditions. Cells from the 4w condition can be found in one cluster with mono iMics, whereas 12w cells clustered the furthest away from mono iMics (**Figure 14**). This would need to be analyzed in more detail using a refined clustering approach with higher resolution and or in a pseudotime analysis but was outside the temporal scope of this thesis.

cBSC-iMics constituted only two clusters, independent of isolation timepoint, whereas mono iMics and precursors could be subdivided into several sub-populations each (**Figure 14**). This does not necessarily reflect a higher homogeneity within the cBSC iMic populations but rather the limited number of cBSC-iMics in comparison to pre- and mono iMics which makes it more difficult to pick up subtle changes in that population. It would, thus, be interesting to analyze a larger cBSC iMic population to gain more information about a possible heterogeneity within slice cultures and whether this could be reflective of functional phenotypes. The microglial transcriptome differs between brain regions (Grabert et al. 2016; Lopes et al. 2022). By generating cBSCs from different brain regions like the cortex, striatum or cerebellum, one could analyze whether the regional heterogeneity could be recapitulated *ex vivo*. These different cBSCs might then be used to

decipher the effects of the microenvironment on microglial phenotypes and function and study microglial heterogeneity *in vitro*. Furthermore, disease region-specific cBSCs could be generated to allow more detailed studies.

Dolan et al. analyzed monocultured iPSC-microglia and the effect of brain substrates (neuronal debris, Aβ, synaptosomes) on their transcriptomes. They concluded that their iPSC-microglia reflect diverse transcriptional states observed in human brain microglia and can be considered mature and homeostatic (Dolan et al. 2023). Comparing this data with the dataset at hand, the transcriptomes observed in the *Dolan* microglia and my mono iMics share a high overlap in the top expressed genes (**Figure 15**). However, the lacking expression of key homeostatic markers like *P2RY12*, *CX3CR1*, the concurrent upregulation of senescence markers (*CDKN2A*), and of many DAM genes including *LPL*, *PICALM*, *GPNMB* indicate a primed/activated state in mono iMics. This activation was not observed in cBSC-iMics which had higher expression of functional markers including *HLA-DRA*, *CD74* and *SPP1*. Thus, cBSC-iMics seem to be more homeostatic than mono iMics which might be due to the influence of the tissue environment. As previously shown, co-culturing iPSC-microglia with other neural cell types enhances microglial maturation (Park et al. 2023) and the lack of input in monoculture might be a cause of cellular stress that results in the senescence observed in both datasets (Dolan et al. 2023).

Interestingly, the expression of key microglial markers *SALL1* and *TMEM119* was not detected in this study, whereas others have reported that more complex environments are able to induce the expression of those markers (Park et al. 2023). This might be caused by the relatively low sequencing depth of scRNAseq compared to bulk RNAseq approaches. It furthermore highlights that gene expression and protein expression are not linearly correlated, as I was able to stain for hTMEM119 protein in 4 week-old cBSCs (**Figure 10**). Additionally, the number of iMics re-isolated from cBSCs is a challenge due to the small size of the tissue and might not allow to dissect the entire heterogeneity of cBSC-iMic population as not all iMics are captured. Finally, the above-mentioned regional heterogeneity of microglia cannot be captured by using only hippocampal cBSCs which might explain why specific phenotypes were not detected in this data set.

Previous studies have shown, that the way microglia are handled prior to scRNAseq affects microglial transcriptomes and can induce an artificial activation phenotype (Marsh et al. 2022). However, no obvious confounding effect was observed in my data set which can be explained by a shortened processing time, less wash steps, no FACS and no labelling of human cells with antibodies/ antibody-coupled magnetic beads. All of these are known factors to cause microglial activation. As cBSCs did not present an overly activated phenotype, the applied approach seems

very well suited to analyze homeostatic microglia. The observed activated phenotype in mono iMics cannot be explained by too vigorous handling either. These cells were subjected to scRNAseq processing immediately after dissociation from the culture well without previous MACS or any other stressing procedures. Therefore, the observed activated phenotype is most likely a biological effect of the culture environment and underlines that cBSCs provide a more homeostatic environment for iMics to differentiate in.

In summary, cBSC-iMics adopt a homeostatic phenotype that highly reflects adult human microglia although the mapping to existing adult human data sets like the Olah et al. microglia atlas (Olah et al. 2020) was outside the scope of this thesis.

5.5 Cross-species CSF1R receptor:ligand interactions

The generation of cBSCs was adapted from published protocols for xenotransplantation and microglia replenishment studies in BSCs using similar methods for the generation of iPSC-microglia and engraftment (Masuch et al. 2016; Mancuso et al. 2019; Fattorelli et al. 2021; Hasselmann et al. 2019). However, cSBCs can be generated from WT Black-6 mice, whereas xenotransplantation requires animals to be immunodeficient (Rathinam et al. 2011; Hasselmann et al. 2019; Svoboda et al. 2019). Depending on the method and mouse model used, xenotransplantation experiments reach exchange rates from murine to human microglia of 20-80 % (Fattorelli et al. 2021; Hasselmann et al. 2019; Svoboda et al. 2019), whereas grafting efficiencies of 97 % were achieved in cBSCs and sustained for several weeks (**Figure 10**). There are two major difference between *in vivo* and *in vitro* xenotransplantation: 1) Murine microglia are constantly suppressed by anti-ms-CSF1R antibody in cBSCs whereas xenotransplantation models rely on depletion before engraftment using small molecules (Mancuso et al. 2019; Hasselmann et al. 2019). 2) According to a longstanding dogma in immunology human CSF1-receptors cannot be activated by their cognate murine ligands (Sieff 1987; Rathinam et al. 2011). Consequently, xenotransplantation models rely on the expression of human knock-in alleles of CSF1R ligands, hCSF1 in most cases, to allow iPSC-microglia integration, survival and maturation (Mancuso et al. 2019; Hasselmann et al. 2019; Svoboda et al. 2019; Fattorelli et al. 2021; Baligács et al. 2024; Serneels et al. 2025). cBSCs, however, were generated without the supplementation of human cytokines and showed reliable and consistent integration and differentiation of iMics for extended culture periods. Thus, the binding of murine ligands to human receptors and their effects on downstream signaling were investigated using *in vitro*, cell-free and *in silico*

approaches to understand how iMics in cBSCs maintain without the supplementation of human growth factors.

5.5.1 CSF1R dependency of iMics in 2D and 3D

First, to understand how iMics in cBSCs are able to survive and mature without supplementation of human CSF1R ligands, I investigated whether they depend on CSF1R signaling in 2D and 3D or if alternative pathways could compensate for CSF1R signaling. As expected, only iMics cultivated in hCSF1+hIL34 iMic medium differentiated into microglia-like cells, whereas slice culture medium did not even induce cell attachment in 2D (**Figure 16**), underlining the importance of CSF1R signaling for microglia differentiation. SCM is defined to sustain BSCs for as long as possible and thus contains horse serum. Exposure to serum, however, has been reported to induce microglial activation phenotypes (Hedegaard et al. 2020) and is highly artificial as homeostatic microglia *in vivo* are never exposed to it. iMic medium is therefore serum-free to reduce variability and promote a more *in vivo*-like homeostatic condition. Thus, exposure to serum in SCM is the most likely reason why pre-iMics do not attach to the cell culture vessel while cells in iMic medium without cytokines can survive and differentiate to some extent. It furthermore underlines, that differentiation of iMics in cBSCs does not occur because of SCM but rather despite of it and that the tissue environment plays an important role in driving differentiation. iMics also differentiated in BSCs cultivated in medium without serum (data not shown). However, BSCs did not sustain long enough in no-serum conditions to allow long-term studies.

Next, iPSCs harboring non-functional *CSF1R* alleles (loss of function mutation E633K or KO) were differentiated towards iMics and investigated in 2D and 3D for their capacity to fully mature. Early steps of differentiation occurred independent of CSF1R genotype, but homozygous loss of function resulted in morphologically aberrant pre-iMics, that were released in decreased numbers from $CSF1R^{E633K/E633K}$ and $CSF1R^{-/-}$ EBs and did not attach to the culture vessel to differentiate (**Figure 16**). These data are in line with previous reports that defined microglial fate induction to be CSF1R-dependent (Ginhoux et al. 2010; Erblich et al. 2011; Rocío Rojo et al. 2019) and underline, that CSF1R signaling is the sole driver of iMic differentiation in 2D. When the *CSF1R*-variant pre-iMics were engrafted to cBSCs, heterozygous $CSF1R^{+/E633K}$ cells initially integrated to a similar extent and with similar distribution and morphology as $CSF1R^{+/+}$ iMics but were lost during the subsequent three weeks of differentiation. Very few cells without functional CSF1R ($CSF1R^{E633K/E633K}$ and $CSF1R^{-/-}$) survived for more than seven days in the murine tissue and

those that did, showed no expression of microglial markers PU.1 or Iba1 (**Figure 17**) emphasizing the observation from 2D that pre-iMics without CSF1R are unable to give rise to iMics proper. Studies from human patients indicate a gene dosage effect of CSF1R on microglial survival. Heterozygous carriers of *CSF1R*^{E633K} are viable but present with reduced numbers of microglia and early-onset neurodegeneration defined as HDLS (Rademakers et al. 2011; Konno et al. 2018) whereas homozygous *CSF1R*^{E633K} carriers are very rare, present without microglia and with severe developmental brain abnormalities indicating an increased fetal lethality (L. Guo et al. 2019; Oosterhof et al. 2019). This gene dosage effect was reproduced in cBSCs using *CSF1R*-variant iMics by a gene dosage-dependent survival (WT> +/E633K > E633K/E633K = KO) and proves that CSF1R signaling in (pre-) iMics is required for engraftment and maturation of the cells. Additionally, these findings support the assumption that iMic maturation in cBSCs is purely driven by CSF1R without compensatory pathways being able to circumvent the loss of this pathway. This also allows the conclusion that the supplementation of human CSF1R ligands is dispensable for the generation of cBSCs. Murine ligands can activate the human CSF1-receptors sufficiently, as WT *CSF1R* iMics differentiate and sustain solely upon interaction with the murine tissue but loss-of-function mutants do not. However, to determine which ligand binds and activates the receptor more in-depth analyses of the human receptor and its cognate human and murine ligands were deployed.

5.5.2 Cross-species receptor:ligand interactions elicit human CSF1R activation

CSF1R and its ligands are highly conserved across evolution, and even though human and murine receptors and ligands share between 70 and 95 % sequence homology (Stanley et al. 1997; H. Lin et al. 2008; Otsuka, Wada, and Seino 2021), cross-species binding and receptor activation is highly debated. In this study *in silico* modelling of receptor and ligand interactions, however, revealed high overlap of predicted ternary complexes between human receptors and its cognate murine ligands (**Figure 18**). The data obtained for human-human receptor:ligand interactions are in line with published crystal structures (Ma et al. 2012; Felix et al. 2015), highlighting the reliability of the modelling approach. These analyses furthermore revealed subtle structural differences in the predicted interaction between human CSF1R and murine CSF1 compared to hCSF that could result in differential ligand-receptor kinetics. The kinetics would most likely be weaker due to a reduced number of hydrogen bonds and salt bridges at positions critical for receptor:ligand interaction (**Supplementary Figure 2**). On the other hand, no discrepancies between human and

murine IL34 complexes with hCSF1R were observed, allowing to expect very similar binding kinetics between both. Modelling was performed utilizing only the D_1-D_3 domains of hCSF1R as these are the critical domains for ligand binding. However, the D_4 and D_5 domains stabilize the interactions between receptors and ligands (H. Liu et al. 2012; Mun, Park, and Park-Min 2020). Differential binding of the ligands to the receptors might infer differential effects on the stabilization and conformation of the ternary complex that could not be predicted in this approach. Regardless of this limitation, this approach was chosen to increase the confidence of the prediction and because crystallization experiments, which served as reference, also focused on investigating D_{1-3}-ligand interactions (Felix et al. 2015).

The ColabFold predictions further increased my confidence that iMic differentiation in cBSCs is facilitated by cross-species interaction of CSF1R with its cognate murine ligands and indicated, that mIL34 might be the driving factor. Receptor:ligand interactions were assessed in a cell-free assay (surface plasmon resonance) that allows to examine binding kinetics between two potential interaction partners. The findings support the *in silico* prediction that mIL34 might act as the primary activator of hCSF1R in cBSCs: Murine IL34 bound the immobilized human receptor with high affinities at very low concentrations (< 1 nM), comparable to its binding to the murine receptor (40 pM) and to hIL34 binding hCSF1R (80 pM). On the other hand, mCSF1 showed fast-on and fast-off kinetics with much lower affinities for hCSF1R (20 mM) compared to its affinities to the murine receptor (12 pM) and that of hCSF1 to hCSF1R (25 pM) (**Figure 19**). To control for unspecific binding of ligands to receptors, the closely related hPDGFRβ was immobilized and no binding of either cytokine was observed (**Supplementary Figure 3**), which highlights the specificity and high sensitivity of the assay and that binding of murine ligands to human CSF1R does occur at biologically relevant concentrations.

Next, this presumed biological relevance was determined by a cytokine stimulation assay of starved 2D iMic monocultures. iMics had been matured for 14 days in 2D culture with complete iMic medium and starved for 48h prior to the assay by not changing the medium to increase receptor availability on the cell surface. Upon the addition of human or murine cytokines to the medium for five minutes, the cells were lysed and the phosphorylation of CSF1R and its downstream signaling effector hERK1/2 were assessed using Western Blot to determine which cytokine induces CSF1R pathway activation. The addition of hCSF1 alone or in combination with hIL34 induced the strongest phosphorylation of hCSF1R (up to 55-fold) and hERK1/2 (up to 9-fold), whereas hIL34 had little to no effect on phosphorylation levels (**Figure 19**). Interestingly, the effect of hCSF1 alone was stronger than the combination of both cytokines, even though not

significantly increased. Competition for the receptor can be an explanation as both cytokines were used at the same concentration and could have resulted in the saturation of the receptors or the formation of ligand-heterodimers that might not elicit activating phosphorylation. Furthermore, CSF1 and IL34 have slightly different binding sites within the same active center of the receptor (Garceau et al. 2010; Chihara et al. 2010) which might induce the phosphorylation of different tyrosine residues on the intracellular site of the receptors and consequently the activation of different downstream mediators. In this assay, however, only one phosphorylation site of hCSF1R and two residues in hERK1/2 were investigated. Thus, even though hIL34 did not result in strong phosphorylation of CSF1R and ERK1/2 at the investigated phosphorylation sites, this does not imply that the cytokine does not bind to or activate the receptor. It would require further, more detailed investigation using different cytokine concentrations, incubation periods, and detection antibodies for both phosphorylated CSF1R and ERK1/2 as well as other downstream signaling partners like PI3K or AKT to understand the complex signaling of CSF1R. Conversely, the addition of murine CSF1 did not induce the phosphorylation of hCSF1R nor hERK1/2 while mIL34 did induce a ca. 10-fold increase in hCSF1R phosphorylation and a phosphorylation of hERK1/2 similar to that of hCSF1 (**Figure 19**). These experimental data are in line with the predictions made by ColabFold and the SPR data, that indicated a weaker, yet existent, binding of mCSF1 to hCSF1R compared to mIL34. Together these findings support the assumption, that murine IL34 is indeed capable of binding human CSF1R and that this binding suffices to activate downstream signaling to support iMic integration, survival and maturation in cBSCs.

Finally, I aimed to prove experimentally that iMic differentiation in cBSCs is predominantly driven by mIL34 rather than mCSF1. In addition to blocking murine CSF1R using the anit-mouse-CSF1R antibody, I applied an antibody directed against murine IL34 directly onto the slice cultures with every medium change to scavenge the released cytokine in the tissue and prevent it from binding and activating the receptors on the engrafted human cells. As expected from the data obtained before, blocking mIL34 resulted in impaired iMic engraftment, survival and differentiation in cBSCs (**Figure 20**). Contrasting the uniform distribution throughout slices observed in all previous experiments, mIL34-blocking resulted in iMics to predominantly cluster around the edges of cBSCs after one week without migrating into the tissue and the loss of most of these cells over the subsequent cultivation period up to five weeks. This distribution pattern can be explained by the decreased thickness of BSCs at the edges that might enable easier adherence. Furthermore, the thinner tissue might have locally increased concentrations of mCSF1 released by neurons and

astrocytes and thus offers an initial induction of differentiation in iMics. This, however, is not sufficient for long-term differentiation and survival due to the decreased binding affinities and signal transduction explained above. Incomplete differentiation is furthermore underlined by the lack of Iba1 expression in human cells within mIL34-blocked cBSCs, which is reminiscent of the results obtained for CSF1R-deficient iMics (**Figure 17**) and highlights the importance of CSF1R activation by mIL34 for iMic differentiation in cBSCs.

Together, these results demonstrate for the first time that cross-species interaction between human CSF1R and its cognate murine ligands mCSF1 and mIL34 exists and that mIL34 is the primary interaction partner driving iMic differentiation. These findings are in line with data that described IL34 signaling to be dispensable for microglial fate induction but essential for their maintenance and differentiation later in life (Kana et al. 2019; Easley-Neal et al. 2019; Obst et al. 2020; Devlin et al. 2024). It, furthermore, opens the question, why xenotransplantation models rely on the expression of knock-in alleles of human *CSF1* rather than human *IL34*. In those models, iPSC-microglia are transplanted at a similar developmental stage as pre-iMics in the approach described here, leading to the assumption that their fate is already determined and that the expression of *hCSF1* might not be the right choice. It would be interesting to see, if the microglial phenotype changed upon the substitution of *hCSF1* to *hIL34* in xenotransplantation mice and whether microglial engraftment could be achieved in immunodeficient (and microglia-depleted), but non-humanized mice, similarly to the approach used in this study. The various approaches taken to confirm hCSF1R-mIL34 interaction furthermore demonstrate how important thorough investigation of possible mechanisms is for understanding how a model system works to further improve it in the future.

5.6 Modelling neurodegenerative disease in cBSCs

cBSCs offer the opportunity to study human microglia in complex tissue environment under homeostatic conditions. While this will be of high value to investigate human microglial function, a major interest of the lab and the research community is to understand microglial contribution to disease pathology. Brain slice culture models for neurodegenerative diseases including tauopathies, prion disease, AD and synucleinopathies exist (Falsig and Aguzzi 2008; Humpel 2015; Croft et al. 2019) and should be easily adaptable for cBSC studies by replacing murine microglia with human iMics as described in this thesis. Importantly, the replacement should be initiated before pathology onset/induction as Spangenberg et al. could show that plaque-associated microglia were less dependent on CSF1R and thus were not depleted with PLX5622

(E. Spangenberg et al. 2019). My laboratory has previously described the generation of BSC models with AD-like amyloid plaque formation and seeded αSyn aggregation which allow the investigation of microglia in disease context without the use of transgenic animal models (Novotny et al. 2016; Barth et al. 2021).

As a proof-of-principle experiment, I combined the previously established model for seeded αSyn pathology with the cBSC approach. Although PD most prominently affects the midbrain, the hippocampus has previously been shown to allow for modeling αSyn lesions and microglial responses (Tanriöver et al. 2020; Barth et al. 2021). Additionally, the hippocampus has two benefits compared to the midbrain when it comes to slice culture preparation: 1) The hippocampus forms axonal connections with only the entorhinal cortex, which minimizes axonal damage during BSC preparation and synaptic rearrangement (Gähwiler et al. 1997). 2) The intra-hippocampal axonal connections facilitate inter-neuronal spreading of protein aggregates along these axonal connection (Barth et al. 2021). A disadvantage is that the specific susceptibility of dopaminergic neurons in the *substantia nigra* cannot be studied using hippocampal slice cultures. As I was primarily interested in microglial responses to neuritic αSyn pathology, this was a limitation that I accepted although region-specific effects cannot be excluded.

5.6.1 iMics in cBSCs respond to tissue aging and alpha-synuclein pathology

To investigate iMic responses to αSyn pathology, iMics were allowed to differentiate under homeostatic conditions for 6 weeks, before αSyn pff was added to induce the formation of αSyn lesions. The lab has previously demonstrated, the formation of intra-microglial inclusions in pff-seeded BSCs (Tanriöver et al. 2020; Barth et al. 2021). As they had been described for both murine and human microglia, I was interested if iMics exposed to αSyn would show intra-microglial inclusions of αSyn at 5 weeks post-seeding. Indeed, cBSCs treated with αSyn pff had extensive neuritic lesions as previously described, and several iMics with the characteristic lesions were found (**Figure 21**) upon staining for amyloidogenic protein aggregations with the amyloid-binding dye pFTAA. pFTAA interacts with the beta-sheet structure of amyloid aggregates like Aβ, αSyn or tau (Klingstedt et al. 2013). While a staining using this LCO is not a definitive proof for αSyn aggregation in pff-treated cBSCs, it is the most logical protein to accumulate in this seeding approach, especially in combination with αSyn-specific antibody staining to confirm neuritic αSyn lesions. These intramicroglial inclusions have been described to range from almost undetectable to soma-sized and have a wool-like structure that can be observed using high-

resolution microscopes. This filamentous structure of inclusions (Tanriöver et al. 2020) was also observed in the intra-iMic lesions, underlining that iMics respond similarly to seeded αSyn pathology as murine microglia do. The most likely explanation for these intra-iMic aggregates is that microglia phagocytose αSyn but are unable to fully digest the (potentially aggregated and phosphorylated) protein which subsequently accumulates within the microglial cells. This hypothesis is supported by the lab's finding, that intra-microglial inclusions are truncated at the C-terminus and thus cannot be detected by pS129 antibody staining (Tanriöver et al. 2020). Since the C-terminus has been suggested to prevent αSyn fibrillization, the partial digest of αSyn by microglia could increase the aggregation propensities and thus lead to intra-microglial aggregation of αSyn (Gallardo, Escalona-Noguero, and Sot 2020). Since neuronal lesions are commonly detected using pS129-staining, the aggregates do not stem directly from phagocytosed αSyn aggregates from the extra-cellular space. It is more likely, that microglia phagocytose αSyn aggregates but fail to fully degrade the protein. Consequently, the C-terminally truncated αSyn accumulates within the microglial cells forming inclusions. This processing is also an explanation for the lag time between the onset of neuritic pS129^{+} lesions and the observation of intra-microglial inclusions (Barth et al. 2021). Scheiblich et al. suggest that microglia exchange αSyn aggregates via nanotubes to decrease the burden on each individual cell (Scheiblich et al. 2021). Besides that, the re-distribution might also contribute to increased microglial inclusions and potentially the spread of pathogenic aggregates to other brain regions as has been described for Aβ in AD (Joshi et al. 2014; Venegas et al. 2017). This and many other interesting questions regarding intra-microglial αSyn inclusions were outside of the scope of this study but are very intriguing and should be investigated in the future.

Finally, I investigated iMic transcriptional phenotypes in response to αSyn induction. cBSCs treated with αSyn pff from 6 weeks post-grafting onwards were compared to age-matched control slices not exposed to αSyn using scRNAseq analysis as described for the differentiation timeline. I found 11 distinct molecular clusters shared among both conditions (**Figure 21**), albeit with different frequencies. In general, iMics exposed to αSyn showed a downregulation of homeostatic markers and a concurrent upregulation of genes associated with lipid metabolism, phagocytosis, antigen presentation, complement system, inflammasome often associated with DAM phenotypes (Keren-Shaul et al. 2017; Krasemann et al. 2017). Control cBSCs were enriched for clusters '7' and '10' which are immune-mediating clusters often described for the '*interferon-response microglia*' phenotype (Olah et al. 2018; Sala Frigerio et al. 2019), which highlights that iMics show differential responses towards tissue aging and αSyn pathology (**Figure 21**).

Contrastingly, classical DAM markers including *APOE, TREM2* and *TYROBP* (cluster '4') were upregulated in αSyn treated iMics and I observed an enrichment of cells in that cluster (**Figure 21**). DAM have initially been described for AD (Keren-Shaul et al. 2017), but similar gene expression changes have by now been recorded for PD patients and model systems (Smajić et al. 2022). The gene expression changes described for PD patients were recapitulated in αSyn-treated cBSC-iMics and included the upregulation of *IL1B* and *SPP1*, genes involved in inflammation-response and phagocytosis. While I observed an expansion of the DAM phenotype in pff-seeded cBSCs, it was not a prominent, nor distinct novel cluster that emerged, contrasting reports from mouse models of neurodegeneration (Keren-Shaul et al. 2017; Krasemann et al. 2017). These differences between model systems and microglia species should be evaluated further.

These findings highlight, that cBSCs can be easily adopted to study human microglial responses to αSyn *in vitro*. Considering the flexibility of BSCs, an adaptation to other models and diseases should be very feasible and underlines the potential of cBSCs for the larger research community. As for the analysis of scRNAseq data under homeostatic conditions, a closer look at the distinct clusters and a possible progression from one state to the other should be taken. These analyses should include direct comparisons with human PD data sets and a more in-depth characterization of the clusters found. Furthermore, in the context of PD, using slice cultures from the midbrain, which is affected by the disease, should be considered but was not used in this study due to time constraints and for the sake of comparability between homeostasis and disease conditions.

5.7 Summary

cBSCs are a novel model for studying human iPSC-derived microglia *in vitro*. As all other model systems, they come with advantages and drawbacks. cBSCs have been adapted from *in vivo* xenotransplantation models to combine the benefits of a complex tissue environment in mice with the accessibility and scalability of *in vitro* models. Compared to 2D *in vitro* models, cBSCs extend the cultivation time of iMics from two or three weeks to three months, thereby resulting in advanced microglial maturity. Additionally, cBSCs adhere to the 3R principles, as multiple slices can be generated from a single mouse to compare various experimental conditions. This reduces the number of experimental animals used and enables the use of cBSCs for low-throughput screens. In contrast to *in vivo* xenotransplantation approaches, cBSCs do not rely on immunodeficient and/or humanized mice. This facilitates easier adaptation to existing mouse models of neurological diseases without the laborious and complex crossbreeding strategies. By utilizing patient-derived or gene-edited iPSCs, human-specific gene variants and their effects on microglial function under homeostatic and pathological conditions can be studied.

cBSCs demonstrate sustained neuronal network function and have a cellular complexity and organization as present in the postnatal brain, which allows for investigating processes beyond early development. The slice cultures are highly reproducible and allow for easy experimental manipulations like grafting of pre-iMics, seeding of pathological protein aggregates or viral transduction. Subsequent analyses including live-cell imaging and repeated sampling of medium for downstream analysis (eg. cytokine profiling, NFL measurements) can be easily performed.

Until recently, the brain was considered an *'immune-privileged'* site. By now this concept has been revised due to the observation of microglial interactions with peripheral immune cells *in vitro* and *in vivo* (Louveau, Harris, and Kipnis 2015; Castellani et al. 2023; Jorfi, Maaser-Hecker, and Tanzi 2023; X. Chen et al. 2023). Furthermore, peripheral immune reactions have been shown to modify microglia function and epigenetics (Wendeln et al. 2018). cBSCs as presented here are unable to model these reciprocal interactions between the brain and the periphery. This limitation might overcome by including peripheral components in on-chip models.

In summary, cBSCs are a valuable addition to the expanding methodological toolbox of microglia research. They combine human microglia with a cellularly complex *in vivo*-like environment while reducing the number of experimental animals needed and can be easily adopted to answer biological questions in the fields of basic neuroscience, neurodevelopment, and neurodegeneration.

5.8 Conclusion and Outlook

In this PhD thesis I presented the establishment and characterization of a chimeric brain slice culture model to study human microglia in an organotypic brain tissue environment.

Inspired by *in vivo* microglia xenotransplantation models, I engrafted human iPSC-derived microglia to murine BSCs and investigated their maturation and functionality. To this end, I established a paradigm to specifically deplete murine microglia while allowing the integration of human-derived microglia precursor cells. Subsequently, a near-complete and robust exchange of murine to human microglia within cBSCs was achieved. In this thesis I showed that iMics in cBSCs matured and differentiated, resulting in cells that morphologically, transcriptionally and functionally resemble human microglia *in vivo*.

Furthermore, I confirmed that iMic differentiation in 2D and in cBSCs was solely driven by CSF1R signaling by utilizing loss-of-function CSF1R-variant iPSC lines. In cBSCs, iMic survival and differentiation was facilitated by cross-species receptor:ligand interactions between human CSF1R and its cognate murine ligands. *In silico* modeling, SPR analyses, and cytokine stimulation assays revealed that murine IL34 binds and activates human CSF1R equivalent to its human counterpart. I thereby demonstrated for the first time human:mouse cross-species receptor:ligand interactions. Blocking mIL34 in cBSCs resulted in decreased survival and differentiation, underlining their dependency on mIL34:hCSF1R signaling. Finally, iMics adapted a transcriptional profile associated with neurodegeneration and aging in a seeded synucleinopathy model, highlighting the potential of cBSCs for disease research. Thus, cBSCs promise to be a valuable addition to the ever-growing methodological toolbox of microglia research.

This work has focused on the establishment and characterization of the model. Due to time constraints, I was unable to investigate how risk genes affect microglia function and whether cBSC-iMics can recapitulate observations made in human AD patients or other disease models. In a follow-up study it would be interesting to extent the work I have started by utilizing iMics with different APOE genotypes. I am curious to see whether the protective ε2 or *christchurch* variants or the disease-associated ε4 variant respond differently to seeded Aβ pathology compared to the neutral ε3 (**Figure 22**). These adaptations would benefit the entire neurodegenerative disease research community to better understand microglia-specific contributions to disease progression.

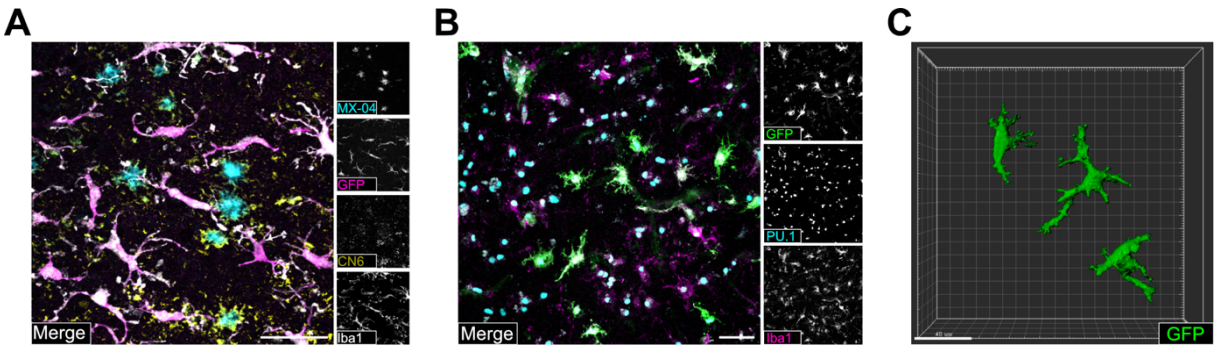

Figure 22 Future applications of chimeric brain slice cultures

A) Amyloid-beta aggregates were seeded in cBSCs following the protocol established by Novotny et al. 2016. At 6-weeks post-seeding, BIONi010C iMics (GFP$^+$, magenta; Iba1$^+$, white) interacted with Aβ deposits which stained positive for amyloid-binding dye Methoxy-X04 (cyan) and anti-Aβ antibody CN6 (yellow). Future research should compare the effect of microglial mutations in AD risk genes on interaction with depositions, iMic morphology and cytokine release. Scale bar: 50 µm. **B)** Human pre-iMics adapt ramified morphology after 7 DIV in human organotypic brain slice cultures of a 57-year-old tumor patient. iMics were identified by the expression of GFP (green) and shared the expression of PU.1 (cyan) and Iba1 (magenta) with endogenous microglia. Human BSCs were not depleted of endogenous microglia, creating microglial chimeras. Scale bar: 50 µm. **C)** Higher magnification of 3D-reconstructed iMics at 7 DIV in human BSC based on GFP expression. Scale bar: 40 µm. Human BSCs have the potential to study the effect of mature human brain environment on microglia differentiation and function. DIV: days *in vitro*.

Lastly, adapting cBSCs to a human-only system would overcome possible cross-species effects of the murine tissue on iMic differentiation and function. In the lab, we have transplanted pre-iMics to human organotypic brain slice cultures and have observed a rapid differentiation to highly ramified microglial cells within 7 days (**Figure 22**), indicating that mature human tissue may even be more specific in supporting iMic differentiation than murine tissue. Here the limiting factors are the availability of live human brain tissue, and the limited period human brain slice cultures can be maintained in culture. Until the limitations of human-only 3D systems have been overcome, cBSCs offer a valuable tool to study *in vivo*-like human microglia in one of the most complex *in vitro* models. The presented model bridges the gap between current *in vitro* models and chimeric xenotransplantation mice, and I anticipate that it will be of great value for the microglia research community.

6 References

Abud, Edsel M., Ricardo N. Ramirez, Eric S. Martinez, Luke M. Healy, Cecilia H. H. Nguyen, Sean A. Newman, Andriy V. Yeromin, et al. 2017. “iPSC-Derived Human Microglia-like Cells to Study Neurological Diseases.” *Neuron* 94 (2): 278-293.e9. https://doi.org/10.1016/j.neuron.2017.03.042.

Agalave, Nilesh M., Brandon T. Lane, Prapti H. Mody, Thomas A. Szabo-Pardi, and Michael D. Burton. 2020. “Isolation, Culture, and Downstream Characterization of Primary Microglia and Astrocytes from Adult Rodent Brain and Spinal Cord.” *Journal of Neuroscience Methods* 340 (July):108742. https://doi.org/10.1016/j.jneumeth.2020.108742.

Ahn, Sung-Min, Kyunghee Byun, Kun Cho, Jin Young Kim, Jong Shin Yoo, Deokhoon Kim, Sun Ha Paek, Seung U. Kim, Richard J. Simpson, and Bonghee Lee. 2008. “Human Microglial Cells Synthesize Albumin in Brain.” *PloS One* 3 (7): e2829. https://doi.org/10.1371/journal.pone.0002829.

Ajami, Bahareh, Jami L. Bennett, Charles Krieger, Wolfram Tetzlaff, and Fabio M. V. Rossi. 2007. “Local Self-Renewal Can Sustain CNS Microglia Maintenance and Function throughout Adult Life.” *Nature Neuroscience* 10 (12): 1538–43. https://doi.org/10.1038/nn2014.

Akiyama, H., and P. L. McGeer. 1990. “Brain Microglia Constitutively Express Beta-2 Integrins.” *Journal of Neuroimmunology* 30 (1): 81–93. https://doi.org/10.1016/0165-5728(90)90055-r.

Alliot, F., E. Lecain, B. Grima, and B. Pessac. 1991. “Microglial Progenitors with a High Proliferative Potential in the Embryonic and Adult Mouse Brain.” *Proceedings of the National Academy of Sciences of the United States of America* 88 (4): 1541–45. https://doi.org/10.1073/pnas.88.4.1541.

Alvarez, Veronica A., and Bernardo L. Sabatini. 2007. “Anatomical and Physiological Plasticity of Dendritic Spines.” *Annual Review of Neuroscience* 30:79–97. https://doi.org/10.1146/annurev.neuro.30.051606.094222.

Alzheimer, A., R. A. Stelzmann, H. N. Schnitzlein, and F. R. Murtagh. 1995. “An English Translation of Alzheimer’s 1907 Paper, ‘Uber Eine Eigenartige Erkankung Der Hirnrinde.’” *Clinical Anatomy (New York, N.Y.)* 8 (6): 429–31. https://doi.org/10.1002/ca.980080612.

Alzheimer, Alois. 1907. “Über Eine Eigenartige Erkrankung Der Hirnrinde.” *Allgemeine Zeitschrift Für Psychiatrie Und Psychisch-Gerichtliche Medizin*, no. 64 (January), 146–48.

Alzheimer’s Association. 2024. “2024 Alzheimer’s Disease Facts and Figures.” *Alzheimer’s & Dementia: The Journal of the Alzheimer’s Association* 20 (5): 3708–3821. https://doi.org/10.1002/alz.13809.

Alzheimer’s Disease International. 2024. “World Alzheimer Report 2024: Global Changes in Attitudes to Dementia,” September. https://www.alzint.org/resource/world-alzheimer-report-2024/.

Andrews, Shea J., Alan E. Renton, Brian Fulton-Howard, Anna Podlesny-Drabiniok, Edoardo Marcora, and Alison M. Goate. 2023. “The Complex Genetic Architecture of Alzheimer’s Disease: Novel Insights and Future Directions.” *eBioMedicine* 90 (April). https://doi.org/10.1016/j.ebiom.2023.104511.

Arnold, Tom, and Christer Betsholtz. 2013. “The Importance of Microglia in the Development of the Vasculature in the Central Nervous System.” *Vascular Cell* 5 (1): 4. https://doi.org/10.1186/2045-824X-5-4.

Ashwell, K. 1990. “Microglia and Cell Death in the Developing Mouse Cerebellum.” *Brain Research. Developmental Brain Research* 55 (2): 219–30. https://doi.org/10.1016/0165-3806(90)90203-b.

Ashwell, K. W., and P. M. Waite. 1991. “Cell Death in the Developing Trigeminal Nuclear Complex of the Rat.” *Brain Research. Developmental Brain Research* 63 (1–2): 291–95. https://doi.org/10.1016/0165-3806(91)90089-2.

Askew, Katharine, and Diego Gomez-Nicola. 2018. “A Story of Birth and Death: Insights into the Formation and Dynamics of the Microglial Population.” *Brain, Behavior, and Immunity* 69 (March):9–17. https://doi.org/10.1016/j.bbi.2017.03.009.

Askew, Katharine, Kaizhen Li, Adrian Olmos-Alonso, Fernando Garcia-Moreno, Yajie Liang, Philippa Richardson, Tom Tipton, et al. 2017. “Coupled Proliferation and Apoptosis Maintain the Rapid Turnover of Microglia in the Adult Brain.” *Cell Reports* 18 (2): 391–405. https://doi.org/10.1016/j.celrep.2016.12.041.

Axelsson, R., M. Röyttä, P. Sourander, H. O. Akesson, and O. Andersen. 1984. “Hereditary Diffuse Leucoencephalopathy with Spheroids.” *Acta Psychiatrica Scandinavica. Supplementum* 314:1–65.

Bachstetter, Adam D., Josh M. Morganti, Jennifer Jernberg, Andrea Schlunk, Staten H. Mitchell, Kaelin W. Brewster, Charles E. Hudson, et al. 2011. “Fractalkine and CX 3 CR1 Regulate Hippocampal Neurogenesis in Adult and Aged Rats.” *Neurobiology of Aging* 32 (11): 2030–44. https://doi.org/10.1016/j.neurobiolaging.2009.11.022.

Badimon, Ana, Hayley J. Strasburger, Pinar Ayata, Xinhong Chen, Aditya Nair, Ako Ikegami, Philip Hwang, et al. 2020. “Negative Feedback Control of Neuronal Activity by Microglia.” *Nature* 586 (7829): 417. https://doi.org/10.1038/s41586-020-2777-8.

Baligács, Nóra, Giulia Albertini, Sarah C. Borrie, Lutgarde Serneels, Clare Pridans, Sriram Balusu, and Bart De Strooper. 2024. “Homeostatic Microglia Initially Seed and Activated Microglia Later Reshape Amyloid Plaques in Alzheimer’s Disease.” *Nature Communications* 15 (1): 10634. https://doi.org/10.1038/s41467-024-54779-w.

Bandres-Ciga, S., S. Saez-Atienzar, J. J. Kim, M. B. Makarious, F. Faghri, M. Diez-Fairen, H. Iwaki, et al. 2020. “Large-Scale Pathway Specific Polygenic Risk and Transcriptomic Community Network Analysis Identifies Novel Functional Pathways in Parkinson Disease.” *Acta Neuropathologica* 140 (3): 341–58. https://doi.org/10.1007/s00401-020-02181-3.

Barry-Carroll, Liam, Philip Greulich, Abigail R. Marshall, Kristoffer Riecken, Boris Fehse, Katharine E. Askew, Kaizhen Li, Olga Garaschuk, David A. Menassa, and Diego Gomez-Nicola. 2023. “Microglia Colonize the Developing Brain by Clonal Expansion of Highly Proliferative Progenitors, Following Allometric Scaling.” *Cell Reports* 42 (5). https://doi.org/10.1016/j.celrep.2023.112425.

Barth, Melanie. 2023. “Organotypic Slice Culture Models for Induced Alpha-Synucleinopathy and Exploration of the Potential Role of Microglia in Pathogenesis,” June. https://doi.org/10.15496/publikation-58691.

Barth, Melanie, Mehtap Bacioglu, Niklas Schwarz, Renata Novotny, Janine Brandes, Marc Welzer, Sonia Mazzitelli, et al. 2021. “Microglial Inclusions and Neurofilament Light Chain Release Follow Neuronal α-Synuclein Lesions in Long-Term Brain Slice Cultures.” *Molecular Neurodegeneration* 16 (1): 54. https://doi.org/10.1186/s13024-021-00471-2.

Beers, David R., Jenny S. Henkel, Qin Xiao, Weihua Zhao, Jinghong Wang, Albert A. Yen, Laszlo Siklos, Scott R. McKercher, and Stanley H. Appel. 2006. “Wild-Type Microglia Extend Survival in PU.1 Knockout Mice with Familial Amyotrophic Lateral Sclerosis.” *Proceedings of the National Academy of Sciences of the United States of America* 103 (43): 16021–26. https://doi.org/10.1073/pnas.0607423103.

Bekris, Lynn M., Chang-En Yu, Thomas D. Bird, and Debby W. Tsuang. 2010. “Genetics of Alzheimer Disease.” *Journal of Geriatric Psychiatry and Neurology* 23 (4): 213–27. https://doi.org/10.1177/0891988710383571.

Bellenguez, Céline, Fahri Küçükali, Iris E. Jansen, Luca Kleineidam, Sonia Moreno-Grau, Najaf Amin, Adam C. Naj, et al. 2022. “New Insights into the Genetic Etiology of Alzheimer’s Disease and Related Dementias.” *Nature Genetics* 54 (4): 412–36. https://doi.org/10.1038/s41588-022-01024-z.

Benner, Brooke, Logan Good, Dionisia Quiroga, Thomas E. Schultz, Mahmoud Kassem, William E. Carson, Mathew A. Cherian, Sagar Sardesai, and Robert Wesolowski. 2020. “Pexidartinib, a Novel Small Molecule CSF-1R Inhibitor in Use for Tenosynovial Giant Cell Tumor: A Systematic Review of Pre-Clinical and Clinical Development.” *Drug Design, Development and Therapy* 14:1693–1704. https://doi.org/10.2147/DDDT.S253232.

Bennett, F. Chris, Mariko L. Bennett, Fazeela Yaqoob, Sara B. Mulinyawe, Gerald A. Grant, Melanie Hayden Gephart, Edward D. Plowey, and Ben A. Barres. 2018. “A Combination of Ontogeny and CNS Environment Establishes Microglial Identity.” *Neuron* 98 (6): 1170-1183.e8.

https://doi.org/10.1016/j.neuron.2018.05.014.

Bennett, Mariko L., F. Chris Bennett, Shane A. Liddelow, Bahareh Ajami, Jennifer L. Zamanian, Nathaniel B. Fernhoff, Sara B. Mulinyawe, et al. 2016. "New Tools for Studying Microglia in the Mouse and Human CNS." *Proceedings of the National Academy of Sciences of the United States of America* 113 (12): E1738-1746. https://doi.org/10.1073/pnas.1525528113.

Berki, Péter, Csaba Cserép, Zsuzsanna Környei, Balázs Pósfai, Eszter Szabadits, Andor Domonkos, Anna Kellermayer, et al. 2024. "Microglia Contribute to Neuronal Synchrony despite Endogenous ATP-Related Phenotypic Transformation in Acute Mouse Brain Slices." *Nature Communications* 15 (1): 5402. https://doi.org/10.1038/s41467-024-49773-1.

Bertrand, Julien Y., Abdelali Jalil, Michèle Klaine, Steffen Jung, Ana Cumano, and Isabelle Godin. 2005. "Three Pathways to Mature Macrophages in the Early Mouse Yolk Sac." *Blood* 106 (9): 3004–11. https://doi.org/10.1182/blood-2005-02-0461.

Bessis, Alain, Catherine Béchade, Delphine Bernard, and Anne Roumier. 2007. "Microglial Control of Neuronal Death and Synaptic Properties." *Glia* 55 (3): 233–38. https://doi.org/10.1002/glia.20459.

Bianchin, Marino Muxfeldt, and Zhezu Snow. 2022. "Primary Microglia Dysfunction or Microgliopathy: A Cause of Dementias and Other Neurological or Psychiatric Disorders." *Neuroscience* 497 (August):324–39. https://doi.org/10.1016/j.neuroscience.2022.06.032.

Blasi, E., R. Barluzzi, V. Bocchini, R. Mazzolla, and F. Bistoni. 1990. "Immortalization of Murine Microglial Cells by a V-Raf/v-Myc Carrying Retrovirus." *Journal of Neuroimmunology* 27 (2–3): 229–37. https://doi.org/10.1016/0165-5728(90)90073-v.

Bodnar, Brittany, Yongang Zhang, Jinbiao Liu, Yuan Lin, Peng Wang, Zhengyu Wei, Sami Saribas, et al. 2021. "Novel Scalable and Simplified System to Generate Microglia-Containing Cerebral Organoids From Human Induced Pluripotent Stem Cells." *Frontiers in Cellular Neuroscience* 15:682272. https://doi.org/10.3389/fncel.2021.682272.

Bohlen, Christopher J., F. Chris Bennett, Andrew F. Tucker, Hannah Y. Collins, Sara B. Mulinyawe, and Ben A. Barres. 2017. "Diverse Requirements for Microglial Survival, Specification, and Function Revealed by Defined-Medium Cultures." *Neuron* 94 (4): 759-773.e8. https://doi.org/10.1016/j.neuron.2017.04.043.

Braak, Heiko, Kelly Del Tredici, Udo Rüb, Rob A. I. de Vos, Ernst N. H. Jansen Steur, and Eva Braak. 2003. "Staging of Brain Pathology Related to Sporadic Parkinson's Disease." *Neurobiology of Aging* 24 (2): 197–211. https://doi.org/10.1016/s0197-4580(02)00065-9.

Brown, Guy C., and Jonas J. Neher. 2014. "Microglial Phagocytosis of Live Neurons." *Nature Reviews. Neuroscience* 15 (4): 209–16. https://doi.org/10.1038/nrn3710.

Brown, Guy C., and Anna Vilalta. 2015. "How Microglia Kill Neurons." *Brain Research*, Neuroprotection: Basic mechanisms and translational potential, 1628 (December):288–97. https://doi.org/10.1016/j.brainres.2015.08.031.

Brunialti, Electra, Alessandro Villa, Marianna Mekhaeil, Federica Mornata, Elisabetta Vegeto, Adriana Maggi, Donato A. Di Monte, and Paolo Ciana. 2021. "Inhibition of Microglial β-Glucocerebrosidase Hampers the Microglia-Mediated Antioxidant and Protective Response in Neurons." *Journal of Neuroinflammation* 18 (September):220. https://doi.org/10.1186/s12974-021-02272-2.

Bruttger, Julia, Khalad Karram, Simone Wörtge, Tommy Regen, Federico Marini, Nicola Hoppmann, Matthias Klein, et al. 2015. "Genetic Cell Ablation Reveals Clusters of Local Self-Renewing Microglia in the Mammalian Central Nervous System." *Immunity* 43 (1): 92–106. https://doi.org/10.1016/j.immuni.2015.06.012.

Burns, Mark P, Wendy J Noble, Vicki Olm, Kate Gaynor, Evelyn Casey, John LaFrancois, Lili Wang, and Karen Duff. 2003. "Co-Localization of Cholesterol, Apolipoprotein E and Fibrillar Aβ in Amyloid Plaques." *Molecular Brain Research* 110 (1): 119–25. https://doi.org/10.1016/S0169-328X(02)00647-2.

Butovsky, Oleg, Mark P. Jedrychowski, Ron Cialic, Susanne Krasemann, Gopal Murugaiyan, Zain Fanek, David J. Greco, et al. 2015. "Targeting miR-155 Restores Abnormal Microglia and Attenuates Disease in

SOD1 Mice." *Annals of Neurology* 77 (1): 75–99. https://doi.org/10.1002/ana.24304.

Butovsky, Oleg, Shafiuddin Siddiqui, Galina Gabriely, Amanda J. Lanser, Ben Dake, Gopal Murugaiyan, Camille E. Doykan, et al. 2012. "Modulating Inflammatory Monocytes with a Unique microRNA Gene Signature Ameliorates Murine ALS." *The Journal of Clinical Investigation* 122 (9): 3063–87. https://doi.org/10.1172/JCI62636.

Cadiz, Mika P., Tanner D. Jensen, Jonathon P. Sens, Kuixi Zhu, Won-Min Song, Bin Zhang, Mark Ebbert, Rui Chang, and John D. Fryer. 2022. "Culture Shock: Microglial Heterogeneity, Activation, and Disrupted Single-Cell Microglial Networks in Vitro." *Molecular Neurodegeneration* 17 (1): 26. https://doi.org/10.1186/s13024-022-00531-1.

Cakir, Bilal, Yoshiaki Tanaka, Ferdi Ridvan Kiral, Yangfei Xiang, Onur Dagliyan, Juan Wang, Maria Lee, et al. 2022. "Expression of the Transcription Factor PU.1 Induces the Generation of Microglia-like Cells in Human Cortical Organoids." *Nature Communications* 13 (1): 430. https://doi.org/10.1038/s41467-022-28043-y.

Capotondo, Alessia, Rita Milazzo, Letterio Salvatore Politi, Angelo Quattrini, Alessio Palini, Tiziana Plati, Stefania Merella, et al. 2012. "Brain Conditioning Is Instrumental for Successful Microglia Reconstitution Following Hematopoietic Stem Cell Transplantation." *Proceedings of the National Academy of Sciences of the United States of America* 109 (37): 15018–23. https://doi.org/10.1073/pnas.1205858109.

Castellani, Giulia, Tommaso Croese, Javier M. Peralta Ramos, and Michal Schwartz. 2023. "Transforming the Understanding of Brain Immunity." *Science* 380 (6640): eabo7649. https://doi.org/10.1126/science.abo7649.

Chadarevian, Jean Paul, Jonathan Hasselmann, Alina Lahian, Joia K. Capocchi, Adrian Escobar, Tau En Lim, Lauren Le, et al. 2024. "Therapeutic Potential of Human Microglia Transplantation in a Chimeric Model of CSF1R-Related Leukoencephalopathy." *Neuron* 112 (16): 2686-2707.e8. https://doi.org/10.1016/j.neuron.2024.05.023.

Chadarevian, Jean Paul, Sonia I. Lombroso, Graham C. Peet, Jonathan Hasselmann, Christina Tu, Dave E. Marzan, Joia Capocchi, et al. 2022. "Engineering an Inhibitor-Resistant Human CSF1R Variant for Microglia Replacement." *Journal of Experimental Medicine* 220 (3): e20220857. https://doi.org/10.1084/jem.20220857.

Chambers, Stuart M., Christopher A. Fasano, Eirini P. Papapetrou, Mark Tomishima, Michel Sadelain, and Lorenz Studer. 2009. "Highly Efficient Neural Conversion of Human ES and iPS Cells by Dual Inhibition of SMAD Signaling." *Nature Biotechnology* 27 (3): 275–80. https://doi.org/10.1038/nbt.1529.

Chan, W. Y., S. Kohsaka, and P. Rezaie. 2007. "The Origin and Cell Lineage of Microglia: New Concepts." *Brain Research Reviews* 53 (2): 344–54. https://doi.org/10.1016/j.brainresrev.2006.11.002.

Chen, Xiaoying, Maria Firulyova, Melissa Manis, Jasmin Herz, Igor Smirnov, Ekaterina Aladyeva, Chanung Wang, et al. 2023. "Microglia-Mediated T Cell Infiltration Drives Neurodegeneration in Tauopathy." *Nature* 615 (7953): 668–77. https://doi.org/10.1038/s41586-023-05788-0.

Chen, Yun, and Marco Colonna. 2021. "Microglia in Alzheimer's Disease at Single-Cell Level. Are There Common Patterns in Humans and Mice?" *The Journal of Experimental Medicine* 218 (9): e20202717. https://doi.org/10.1084/jem.20202717.

Chihara, T., S. Suzu, R. Hassan, N. Chutiwitoonchai, M. Hiyoshi, K. Motoyoshi, F. Kimura, and S. Okada. 2010. "IL-34 and M-CSF Share the Receptor Fms but Are Not Identical in Biological Activity and Signal Activation." *Cell Death and Differentiation* 17 (12): 1917–27. https://doi.org/10.1038/cdd.2010.60.

Chitu, Violeta, Solen Gokhan, Maria Gulinello, Craig A. Branch, Madhuvati Patil, Ranu Basu, Corrina Stoddart, Mark F. Mehler, and E. Richard Stanley. 2015. "Phenotypic Characterization of a Csf1r Haploinsufficient Mouse Model of Adult-Onset Leukodystrophy with Axonal Spheroids and Pigmented Glia (ALSP)." *Neurobiology of Disease* 74 (February):219–28. https://doi.org/10.1016/j.nbd.2014.12.001.

Chitu, Violeta, Şölen Gokhan, Sayan Nandi, Mark F. Mehler, and E. Richard Stanley. 2016. "Emerging Roles for CSF-1 Receptor and Its Ligands in the Nervous System." *Trends in Neurosciences* 39 (6): 378–93. https://doi.org/10.1016/j.tins.2016.03.005.

Choi, Insup, Yuanxi Zhang, Steven P. Seegobin, Mathilde Pruvost, Qian Wang, Kerry Purtell, Bin Zhang, and Zhenyu Yue. 2020. “Microglia Clear Neuron-Released α-Synuclein via Selective Autophagy and Prevent Neurodegeneration.” *Nature Communications* 11 (1): 1386. https://doi.org/10.1038/s41467-020-15119-w.

Claes, Christel, Emma Pascal Danhash, Jonathan Hasselmann, Jean Paul Chadarevian, Sepideh Kiani Shabestari, Whitney E. England, Tau En Lim, et al. 2021. “Plaque-Associated Human Microglia Accumulate Lipid Droplets in a Chimeric Model of Alzheimer’s Disease.” *Molecular Neurodegeneration* 16 (1): 50. https://doi.org/10.1186/s13024-021-00473-0.

Coleman, Colin, and Ian Martin. 2022. “Unraveling Parkinson’s Disease Neurodegeneration: Does Aging Hold the Clues?” *Journal of Parkinson’s Disease* 12 (8): 2321–38. https://doi.org/10.3233/JPD-223363.

Coleman Jr, Leon G, Jian Zou, and Fulton T. Crews. 2020. “Microglial Depletion and Repopulation in Brain Slice Culture Normalizes Sensitized Proinflammatory Signaling.” *Journal of Neuroinflammation* 17 (January):27. https://doi.org/10.1186/s12974-019-1678-y.

Colonna, Marco, and Oleg Butovsky. 2017. “Microglia Function in the Central Nervous System During Health and Neurodegeneration.” *Annual Review of Immunology* 35 (April):441–68. https://doi.org/10.1146/annurev-immunol-051116-052358.

Coniglio, Salvatore J., Eliseo Eugenin, Kostantin Dobrenis, E. Richard Stanley, Brian L. West, Marc H. Symons, and Jeffrey E. Segall. 2012. “Microglial Stimulation of Glioblastoma Invasion Involves Epidermal Growth Factor Receptor (EGFR) and Colony Stimulating Factor 1 Receptor (CSF-1R) Signaling.” *Molecular Medicine (Cambridge, Mass.)* 18 (1): 519–27. https://doi.org/10.2119/molmed.2011.00217.

Conway, James G., Brad McDonald, Janet Parham, Barry Keith, David W. Rusnak, Eva Shaw, Marilyn Jansen, et al. 2005. “Inhibition of Colony-Stimulating-Factor-1 Signaling in Vivo with the Orally Bioavailable cFMS Kinase Inhibitor GW2580.” *Proceedings of the National Academy of Sciences of the United States of America* 102 (44): 16078–83. https://doi.org/10.1073/pnas.0502000102.

Coussens, Lisa, Charles Van Beveren, Douglas Smith, Ellson Chen, Richard L. Mitchell, Clare M. Isacke, Inder M. Verma, and Axel Ullrich. 1986. “Structural Alteration of Viral Homologue of Receptor Proto-Oncogene Fms at Carboxyl Terminus.” *Nature* 320 (6059): 277–80. https://doi.org/10.1038/320277a0.

Croft, C. L., H. S. Futch, B. D. Moore, and T. E. Golde. 2019. “Organotypic Brain Slice Cultures to Model Neurodegenerative Proteinopathies.” *Molecular Neurodegeneration* 14 (1): 45. https://doi.org/10.1186/s13024-019-0346-0.

Cserép, Csaba, Balázs Pósfai, Nikolett Lénárt, Rebeka Fekete, Zsófia I. László, Zsolt Lele, Barbara Orsolits, et al. 2020. “Microglia Monitor and Protect Neuronal Function through Specialized Somatic Purinergic Junctions.” *Science (New York, N.Y.)* 367 (6477): 528–37. https://doi.org/10.1126/science.aax6752.

Czapiga, M., and C. A. Colton. 1999. “Function of Microglia in Organotypic Slice Cultures.” *Journal of Neuroscience Research* 56 (6): 644–51. https://doi.org/10.1002/(SICI)1097-4547(19990615)56:6<644::AID-JNR10>3.0.CO;2-9.

Damani, Mausam R., Lian Zhao, Aurora M. Fontainhas, Juan Amaral, Robert N. Fariss, and Wai T. Wong. 2011. “Age-Related Alterations in the Dynamic Behavior of Microglia.” *Aging Cell* 10 (2): 263–76. https://doi.org/10.1111/j.1474-9726.2010.00660.x.

Daneman, Richard, Lu Zhou, Amanuel A. Kebede, and Ben A. Barres. 2010. “Pericytes Are Required for Blood–Brain Barrier Integrity during Embryogenesis.” *Nature* 468 (7323): 562–66. https://doi.org/10.1038/nature09513.

Danzer, Karin M., Lisa R. Kranich, Wolfgang P. Ruf, Ozge Cagsal-Getkin, Ashley R. Winslow, Liya Zhu, Charles R. Vanderburg, and Pamela J. McLean. 2012. “Exosomal Cell-to-Cell Transmission of Alpha Synuclein Oligomers.” *Molecular Neurodegeneration* 7 (August):42. https://doi.org/10.1186/1750-1326-7-42.

Davalos, Dimitrios, Jaime Grutzendler, Guang Yang, Jiyun V. Kim, Yi Zuo, Steffen Jung, Dan R. Littman, Michael L. Dustin, and Wen-Biao Gan. 2005. “ATP Mediates Rapid Microglial Response to Local Brain Injury in Vivo.” *Nature Neuroscience* 8 (6): 752–58. https://doi.org/10.1038/nn1472.

De Miranda, Briana R., Samuel M. Goldman, Gary W. Miller, J. Timothy Greenamyre, and E. Ray Dorsey. 2022. “Preventing Parkinson’s Disease: An Environmental Agenda.” *Journal of Parkinson’s Disease* 12 (1): 45–68. https://doi.org/10.3233/JPD-212922.

Del Río-Hortega, Pio. 1932. “Micorglia.” In *Cytology of the Nervous System*, edited by Wilder Penfield, 482–534. Hafner Publishing.

Delbridge, Alex R. D., Dann Huh, Margot Brickelmaier, Jeremy C. Burns, Chris Roberts, Ravi Challa, Naideline Raymond, et al. 2020. “Organotypic Brain Slice Culture Microglia Exhibit Molecular Similarity to Acutely-Isolated Adult Microglia and Provide a Platform to Study Neuroinflammation.” *Frontiers in Cellular Neuroscience* 14:592005. https://doi.org/10.3389/fncel.2020.592005.

Dello Russo, Cinzia, Natalia Cappoli, Isabella Coletta, Daniele Mezzogori, Fabiola Paciello, Giacomo Pozzoli, Pierluigi Navarra, and Alessandra Battaglia. 2018. “The Human Microglial HMC3 Cell Line: Where Do We Stand? A Systematic Literature Review.” *Journal of Neuroinflammation* 15 (1): 259. https://doi.org/10.1186/s12974-018-1288-0.

Devlin, Benjamin A., Dang M. Nguyen, Gabriel Grullon, Madeline J. Clark, Alexis M. Ceasrine, Martha Deja, Ashka Shah, et al. 2024. “Neuron Derived Cytokine Interleukin-34 Controls Developmental Microglia Function.” *bioRxiv: The Preprint Server for Biology*, May, 2024.05.10.589920. https://doi.org/10.1101/2024.05.10.589920.

Dolan, Michael-John, Martine Therrien, Saša Jereb, Tushar Kamath, Vahid Gazestani, Trevor Atkeson, Samuel E. Marsh, et al. 2023. “Exposure of iPSC-Derived Human Microglia to Brain Substrates Enables the Generation and Manipulation of Diverse Transcriptional States in Vitro.” *Nature Immunology* 24 (8): 1382–90. https://doi.org/10.1038/s41590-023-01558-2.

Dolmetsch, Ricardo, and Daniel H. Geschwind. 2011. “The Human Brain in a Dish: The Promise of iPSC-Derived Neurons.” *Cell* 145 (6): 831–34. https://doi.org/10.1016/j.cell.2011.05.034.

Douvaras, Panagiotis, Bruce Sun, Minghui Wang, Ilya Kruglikov, Gregory Lallos, Matthew Zimmer, Cecile Terrenoire, et al. 2017. “Directed Differentiation of Human Pluripotent Stem Cells to Microglia.” *Stem Cell Reports* 8 (6): 1516–24. https://doi.org/10.1016/j.stemcr.2017.04.023.

Dräger, Nina M., Sydney M. Sattler, Cindy Tzu-Ling Huang, Olivia M. Teter, Kun Leng, Sayed Hadi Hashemi, Jason Hong, et al. 2022. “A CRISPRi/a Platform in Human iPSC-Derived Microglia Uncovers Regulators of Disease States.” *Nature Neuroscience*, August, 1–14. https://doi.org/10.1038/s41593-022-01131-4.

Du, Yixing, Faith H. Brennan, Phillip G. Popovich, and Min Zhou. 2022. “Microglia Maintain the Normal Structure and Function of the Hippocampal Astrocyte Network.” *Glia* 70 (7): 1359–79. https://doi.org/10.1002/glia.24179.

Dubbelaar, Marissa L., Laura Kracht, Bart J. L. Eggen, and Erik W. G. M. Boddeke. 2018. “The Kaleidoscope of Microglial Phenotypes.” *Frontiers in Immunology* 9:1753. https://doi.org/10.3389/fimmu.2018.01753.

Easley-Neal, Courtney, Oded Foreman, Neeraj Sharma, Ali A. Zarrin, and Robby M. Weimer. 2019. “CSF1R Ligands IL-34 and CSF1 Are Differentially Required for Microglia Development and Maintenance in White and Gray Matter Brain Regions.” *Frontiers in Immunology* 10:2199. https://doi.org/10.3389/fimmu.2019.02199.

Elfmann, Christoph, and Jörg Stülke. 2023. “PAE Viewer: A Webserver for the Interactive Visualization of the Predicted Aligned Error for Multimer Structure Predictions and Crosslinks.” *Nucleic Acids Research* 51 (W1): W404–10. https://doi.org/10.1093/nar/gkad350.

Elkabes, S., E. M. DiCicco-Bloom, and I. B. Black. 1996. “Brain Microglia/Macrophages Express Neurotrophins That Selectively Regulate Microglial Proliferation and Function.” *The Journal of Neuroscience: The Official Journal of the Society for Neuroscience* 16 (8): 2508–21. https://doi.org/10.1523/JNEUROSCI.16-08-02508.1996.

Elmore, Monica Renee Pittman, Allison Rachel Najafi, Maya Allegra Koike, Nabil Nazih Dagher, Elizabeth Erin Spangenberg, Rachel Anne Rice, Masashi Kitazawa, et al. 2014. “CSF1 Receptor Signaling Is Necessary for Microglia Viability, Which Unmasks a Cell That Rapidly Repopulates the Microglia-Depleted Adult

Brain." *Neuron* 82 (2): 380–97. https://doi.org/10.1016/j.neuron.2014.02.040.

Eme-Scolan, Elisa, and Samantha J. Dando. 2020. "Tools and Approaches for Studying Microglia In Vivo." *Frontiers in Immunology* 11 (October). https://doi.org/10.3389/fimmu.2020.583647.

Erblich, Bryna, Liyin Zhu, Anne M. Etgen, Kostantin Dobrenis, and Jeffrey W. Pollard. 2011. "Absence of Colony Stimulation Factor-1 Receptor Results in Loss of Microglia, Disrupted Brain Development and Olfactory Deficits." *PLOS ONE* 6 (10): e26317. https://doi.org/10.1371/journal.pone.0026317.

Esiri, M. M., M. S. al Izzi, and M. C. Reading. 1991. "Macrophages, Microglial Cells, and HLA-DR Antigens in Fetal and Infant Brain." *Journal of Clinical Pathology* 44 (2): 102–6. https://doi.org/10.1136/jcp.44.2.102.

Fagerlund, Ilkka, Antonios Dougalis, Anastasia Shakirzyanova, Mireia Gómez-Budia, Anssi Pelkonen, Henna Konttinen, Sohvi Ohtonen, et al. 2021. "Microglia-like Cells Promote Neuronal Functions in Cerebral Organoids." *Cells* 11 (1): 124. https://doi.org/10.3390/cells11010124.

Falsig, Jeppe, and Adriano Aguzzi. 2008. "The Prion Organotypic Slice Culture Assay--POSCA." *Nature Protocols* 3 (4): 555–62. https://doi.org/10.1038/nprot.2008.13.

Fantin, Alessandro, Joaquim M. Vieira, Gaia Gestri, Laura Denti, Quenten Schwarz, Sergey Prykhozhij, Francesca Peri, Stephen W. Wilson, and Christiana Ruhrberg. 2010. "Tissue Macrophages Act as Cellular Chaperones for Vascular Anastomosis Downstream of VEGF-Mediated Endothelial Tip Cell Induction." *Blood* 116 (5): 829–40. https://doi.org/10.1182/blood-2009-12-257832.

Fattorelli, Nicola, Anna Martinez-Muriana, Leen Wolfs, Ivana Geric, Bart De Strooper, and Renzo Mancuso. 2021. "Stem-Cell-Derived Human Microglia Transplanted into Mouse Brain to Study Human Disease." *Nature Protocols* 16 (2): 1013–33. https://doi.org/10.1038/s41596-020-00447-4.

Faust, Travis E., Philip A. Feinberg, Ciara O'Connor, Riki Kawaguchi, Andrew Chan, Haley Strasburger, Takahiro Masuda, et al. 2023. "A Comparative Analysis of Microglial Inducible Cre Lines." bioRxiv. https://doi.org/10.1101/2023.01.09.523268.

Felix, Jan, Steven De Munck, Kenneth Verstraete, Leander Meuris, Nico Callewaert, Jonathan Elegheert, and Savvas N. Savvides. 2015. "Structure and Assembly Mechanism of the Signaling Complex Mediated by Human CSF-1." *Structure (London, England: 1993)* 23 (9): 1621–31. https://doi.org/10.1016/j.str.2015.06.019.

Felix, Jan, Jonathan Elegheert, Irina Gutsche, Alexander V. Shkumatov, Yurong Wen, Nathalie Bracke, Erwin Pannecoucke, et al. 2013. "Human IL-34 and CSF-1 Establish Structurally Similar Extracellular Assemblies with Their Common Hematopoietic Receptor." *Structure* 21 (4): 528–39. https://doi.org/10.1016/j.str.2013.01.018.

Fellner, Lisa, Regina Irschick, Kathrin Schanda, Markus Reindl, Lars Klimaschewski, Werner Poewe, Gregor K. Wenning, and Nadia Stefanova. 2013. "Toll-like Receptor 4 Is Required for α-Synuclein Dependent Activation of Microglia and Astroglia." *Glia* 61 (3): 349–60. https://doi.org/10.1002/glia.22437.

Feng, Linjuan, Hsuan Lo, Zhaoxiang Hong, Jiahao Zheng, Yuhong Yan, Zucheng Ye, Xiaochun Chen, and Xiaodong Pan. 2023. "Microglial LRRK2-Mediated NFATc1 Attenuates α-Synuclein Immunotoxicity in Association with CX3CR1-Induced Migration and the Lysosome-Initiated Degradation." *Glia* 71 (9): 2266–84. https://doi.org/10.1002/glia.24422.

Feng, Yang, Chuyun Zheng, Yajun Zhang, Changyang Xing, Wenbin Cai, Ruru Li, Jianzong Chen, and Yunyou Duan. 2019. "Triptolide Inhibits Preformed Fibril-Induced Microglial Activation by Targeting the MicroRNA155-5p/SHIP1 Pathway." *Oxidative Medicine and Cellular Longevity* 2019:6527638. https://doi.org/10.1155/2019/6527638.

Fensterl, Volker, and Ganes C. Sen. 2014. "Interferon-Induced Ifit Proteins: Their Role in Viral Pathogenesis." *Journal of Virology* 89 (5): 2462–68. https://doi.org/10.1128/JVI.02744-14.

Filipello, Fabia, Raffaella Morini, Irene Corradini, Valerio Zerbi, Alice Canzi, Bernadeta Michalski, Marco Erreni, et al. 2018. "The Microglial Innate Immune Receptor TREM2 Is Required for Synapse Elimination and Normal Brain Connectivity." *Immunity* 48 (5): 979-991.e8. https://doi.org/10.1016/j.immuni.2018.04.016.

Flanary, Barry E., Nicole W. Sammons, Cuong Nguyen, Douglas Walker, and Wolfgang J. Streit. 2007. "Evidence That Aging and Amyloid Promote Microglial Cell Senescence." *Rejuvenation Research* 10 (1): 61–74. https://doi.org/10.1089/rej.2006.9096.

Fourgeaud, Lawrence, Paqui G. Través, Yusuf Tufail, Humberto Leal-Bailey, Erin D. Lew, Patrick G. Burrola, Perri Callaway, et al. 2016. "TAM Receptors Regulate Multiple Features of Microglial Physiology." *Nature* 532 (7598): 240–44. https://doi.org/10.1038/nature17630.

Freude, Kristine, Carlota Pires, Poul Hyttel, and Vanessa Jane Hall. 2014. "Induced Pluripotent Stem Cells Derived from Alzheimer's Disease Patients: The Promise, the Hope and the Path Ahead." *Journal of Clinical Medicine* 3 (4): 1402–36. https://doi.org/10.3390/jcm3041402.

Füger, Petra, Jasmin K. Hefendehl, Karthik Veeraraghavalu, Ann-Christin Wendeln, Christine Schlosser, Ulrike Obermüller, Bettina M. Wegenast-Braun, et al. 2017. "Microglia Turnover with Aging and in an Alzheimer's Model via Long-Term in Vivo Single-Cell Imaging." *Nature Neuroscience* 20 (10): 1371–76. https://doi.org/10.1038/nn.4631.

Gähwiler, B. H., M. Capogna, D. Debanne, R. A. McKinney, and S. M. Thompson. 1997. "Organotypic Slice Cultures: A Technique Has Come of Age." *Trends in Neurosciences* 20 (10): 471–77. https://doi.org/10.1016/s0166-2236(97)01122-3.

Galatro, Thais F., Inge R. Holtman, Antonio M. Lerario, Ilia D. Vainchtein, Nieske Brouwer, Paula R. Sola, Mariana M. Veras, et al. 2017. "Transcriptomic Analysis of Purified Human Cortical Microglia Reveals Age-Associated Changes." *Nature Neuroscience* 20 (8): 1162–71. https://doi.org/10.1038/nn.4597.

Gallardo, José, Carmen Escalona-Noguero, and Begoña Sot. 2020. "Role of α-Synuclein Regions in Nucleation and Elongation of Amyloid Fiber Assembly." *ACS Chemical Neuroscience* 11 (6): 872–79. https://doi.org/10.1021/acschemneuro.9b00527.

Garceau, Valerie, Jacqueline Smith, Ian R. Paton, Megan Davey, Mario A. Fares, David P. Sester, David W. Burt, and David A. Hume. 2010. "Pivotal Advance: Avian Colony-Stimulating Factor 1 (CSF-1), Interleukin-34 (IL-34), and CSF-1 Receptor Genes and Gene Products." *Journal of Leukocyte Biology* 87 (5): 753–64. https://doi.org/10.1189/jlb.0909624.

Geirsdottir, Laufey, Eyal David, Hadas Keren-Shaul, Assaf Weiner, Stefan Cornelius Bohlen, Jana Neuber, Adam Balic, et al. 2020. "Cross-Species Single-Cell Analysis Reveals Divergence of the Primate Microglia Program." *Cell* 181 (3): 746. https://doi.org/10.1016/j.cell.2020.04.002.

Ginhoux, Florent, Melanie Greter, Marylene Leboeuf, Sayan Nandi, Peter See, Solen Gokhan, Mark F. Mehler, et al. 2010. "Fate Mapping Analysis Reveals That Adult Microglia Derive from Primitive Macrophages." *Science (New York, N.Y.)* 330 (6005): 841–45. https://doi.org/10.1126/science.1194637.

Ginhoux, Florent, Shawn Lim, Guillaume Hoeffel, Donovan Low, and Tara Huber. 2013. "Origin and Differentiation of Microglia." *Frontiers in Cellular Neuroscience* 7 (April). https://doi.org/10.3389/fncel.2013.00045.

Glenner, G. G., and C. W. Wong. 1984. "Alzheimer's Disease and Down's Syndrome: Sharing of a Unique Cerebrovascular Amyloid Fibril Protein." *Biochemical and Biophysical Research Communications* 122 (3): 1131–35. https://doi.org/10.1016/0006-291x(84)91209-9.

Goddery, Emma N., Cori E. Fain, Chloe G. Lipovsky, Katayoun Ayasoufi, Lila T. Yokanovich, Courtney S. Malo, Roman H. Khadka, et al. 2021. "Microglia and Perivascular Macrophages Act as Antigen Presenting Cells to Promote CD8 T Cell Infiltration of the Brain." *Frontiers in Immunology* 12:726421. https://doi.org/10.3389/fimmu.2021.726421.

Godin, I. E., J. A. Garcia-Porrero, A. Coutinho, F. Dieterlen-Lièvre, and M. A. Marcos. 1993. "Para-Aortic Splanchnopleura from Early Mouse Embryos Contains B1a Cell Progenitors." *Nature* 364 (6432): 67–70. https://doi.org/10.1038/364067a0.

Gordon, Richard, Eduardo A. Albornoz, Daniel C. Christie, Monica R. Langley, Vinod Kumar, Susanna Mantovani, Avril A. B. Robertson, et al. 2018. "Inflammasome Inhibition Prevents α-Synuclein Pathology and Dopaminergic Neurodegeneration in Mice." *Science Translational Medicine* 10 (465): eaah4066.

https://doi.org/10.1126/scitranslmed.aah4066.

Gosselin, David, Dylan Skola, Nicole G. Coufal, Inge R. Holtman, Johannes C. M. Schlachetzki, Eniko Sajti, Baptiste N. Jaeger, et al. 2017. "An Environment-Dependent Transcriptional Network Specifies Human Microglia Identity." *Science (New York, N.Y.)* 356 (6344). https://doi.org/10.1126/science.aal3222.

Gow, Deborah J., Valerie Garceau, Ronan Kapetanovic, David P. Sester, Greg J. Fici, John A. Shelly, Thomas L. Wilson, and David A. Hume. 2012. "Cloning and Expression of Porcine Colony Stimulating Factor-1 (CSF-1) and Colony Stimulating Factor-1 Receptor (CSF-1R) and Analysis of the Species Specificity of Stimulation by CSF-1 and Interleukin 34." *Cytokine* 60 (3): 793–805. https://doi.org/10.1016/j.cyto.2012.08.008.

Gow, Deborah J., Valerie Garceau, Clare Pridans, Adam G. Gow, Kerry E. Simpson, Danielle Gunn-Moore, and David A. Hume. 2013. "Cloning and Expression of Feline Colony Stimulating Factor Receptor (CSF-1R) and Analysis of the Species Specificity of Stimulation by Colony Stimulating Factor-1 (CSF-1) and Interleukin-34 (IL-34)." *Cytokine* 61 (2): 630–38. https://doi.org/10.1016/j.cyto.2012.11.014.

Grabert, Kathleen, and Barry W. McColl. 2018. "Isolation and Phenotyping of Adult Mouse Microglial Cells." *Methods in Molecular Biology (Clifton, N.J.)* 1784:77–86. https://doi.org/10.1007/978-1-4939-7837-3_7.

Grabert, Kathleen, Tom Michoel, Michail H. Karavolos, Sara Clohisey, J. Kenneth Baillie, Mark P. Stevens, Tom C. Freeman, Kim M. Summers, and Barry W. McColl. 2016. "Microglial Brain Region-Dependent Diversity and Selective Regional Sensitivities to Aging." *Nature Neuroscience* 19 (3): 504–16. https://doi.org/10.1038/nn.4222.

Grabiec, Urszula, Tim Hohmann, Niels Hammer, and Faramarz Dehghani. 2017. "Organotypic Hippocampal Slice Cultures As a Model to Study Neuroprotection and Invasiveness of Tumor Cells." *Journal of Visualized Experiments: JoVE*, no. 126 (August), 55359. https://doi.org/10.3791/55359.

Green, Kim N., Joshua D. Crapser, and Lindsay A. Hohsfield. 2020. "To Kill a Microglia: A Case for CSF1R Inhibitors." *Trends in Immunology*, Special Issue: Microglia and Astrocytes, 41 (9): 771–84. https://doi.org/10.1016/j.it.2020.07.001.

Grozdanov, Veselin, and Karin M. Danzer. 2018. "Release and Uptake of Pathologic Alpha-Synuclein." *Cell and Tissue Research* 373 (1): 175–82. https://doi.org/10.1007/s00441-017-2775-9.

Guilbert, L. J., and E. R. Stanley. 1986. "The Interaction of 125I-Colony-Stimulating Factor-1 with Bone Marrow-Derived Macrophages." *The Journal of Biological Chemistry* 261 (9): 4024–32.

Guilliams, Martin, Ismé De Kleer, Sandrine Henri, Sijranke Post, Leen Vanhoutte, Sofie De Prijck, Kim Deswarte, Bernard Malissen, Hamida Hammad, and Bart N. Lambrecht. 2013. "Alveolar Macrophages Develop from Fetal Monocytes That Differentiate into Long-Lived Cells in the First Week of Life via GM-CSF." *The Journal of Experimental Medicine* 210 (10): 1977–92. https://doi.org/10.1084/jem.20131199.

Guo, Long, Débora Romeo Bertola, Asako Takanohashi, Asuka Saito, Yuko Segawa, Takanori Yokota, Satoru Ishibashi, et al. 2019. "Bi-Allelic CSF1R Mutations Cause Skeletal Dysplasia of Dysosteosclerosis-Pyle Disease Spectrum and Degenerative Encephalopathy with Brain Malformation." *American Journal of Human Genetics* 104 (5): 925–35. https://doi.org/10.1016/j.ajhg.2019.03.004.

Guo, Min, Jian Wang, Yanxin Zhao, Yiwei Feng, Sida Han, Qiang Dong, Mei Cui, and Kim Tieu. 2020. "Microglial Exosomes Facilitate α-Synuclein Transmission in Parkinson's Disease." *Brain: A Journal of Neurology* 143 (5): 1476–97. https://doi.org/10.1093/brain/awaa090.

Gustafsson, Maria V., Xiaowei Zheng, Teresa Pereira, Katarina Gradin, Shaobo Jin, Johan Lundkvist, Jorge L. Ruas, Lorenz Poellinger, Urban Lendahl, and Maria Bondesson. 2005. "Hypoxia Requires Notch Signaling to Maintain the Undifferentiated Cell State." *Developmental Cell* 9 (5): 617–28. https://doi.org/10.1016/j.devcel.2005.09.010.

Guvenek, Aysegul, Neelroop Parikshak, Daria Zamolodchikov, Sahar Gelfman, Arden Moscati, Lee Dobbyn, Eli Stahl, Alan Shuldiner, and Giovanni Coppola. 2024. "Transcriptional Profiling in Microglia across Physiological and Pathological States Identifies a Transcriptional Module Associated with Neurodegeneration." *Communications Biology* 7 (1): 1–11. https://doi.org/10.1038/s42003-024-06684-7.

Haass, C., and D. J. Selkoe. 1993. "Cellular Processing of Beta-Amyloid Precursor Protein and the Genesis

of Amyloid Beta-Peptide." *Cell* 75 (6): 1039–42. https://doi.org/10.1016/0092-8674(93)90312-e.

Haenseler, Walther, Stephen N. Sansom, Julian Buchrieser, Sarah E. Newey, Craig S. Moore, Francesca J. Nicholls, Satyan Chintawar, et al. 2017. "A Highly Efficient Human Pluripotent Stem Cell Microglia Model Displays a Neuronal-Co-Culture-Specific Expression Profile and Inflammatory Response." *Stem Cell Reports* 8 (6): 1727–42. https://doi.org/10.1016/j.stemcr.2017.05.017.

Hagemeyer, Nora, Klara-Maria Hanft, Maria-Anna Akriditou, Nicole Unger, Eun S. Park, E. Richard Stanley, Ori Staszewski, Leda Dimou, and Marco Prinz. 2017. "Microglia Contribute to Normal Myelinogenesis and to Oligodendrocyte Progenitor Maintenance during Adulthood." *Acta Neuropathologica* 134 (3): 441–58. https://doi.org/10.1007/s00401-017-1747-1.

Hailer, N. P., J. D. Jarhult, and R. Nitsch. 1996. "Resting Microglial Cells in Vitro: Analysis of Morphology and Adhesion Molecule Expression in Organotypic Hippocampal Slice Cultures." *Glia* 18 (4): 319–31. https://doi.org/10.1002/(sici)1098-1136(199612)18:4<319::aid-glia6>3.0.co;2-s.

Hammond, Timothy R., Connor Dufort, Lasse Dissing-Olesen, Stefanie Giera, Adam Young, Alec Wysoker, Alec J. Walker, et al. 2019. "Single-Cell RNA Sequencing of Microglia throughout the Mouse Lifespan and in the Injured Brain Reveals Complex Cell-State Changes." *Immunity* 50 (1): 253-271.e6. https://doi.org/10.1016/j.immuni.2018.11.004.

Hampe, A, B M Shamoon, M Gobet, C J Sherr, and F Galibert. 1989. "Nucleotide Sequence and Structural Organization of the Human FMS Proto-Oncogene." *Oncogene Research* 4 (1): 9–17.

Hampel, Harald, John Hardy, Kaj Blennow, Christopher Chen, George Perry, Seung Hyun Kim, Victor L. Villemagne, et al. 2021. "The Amyloid-β Pathway in Alzheimer's Disease." *Molecular Psychiatry* 26 (10): 5481–5503. https://doi.org/10.1038/s41380-021-01249-0.

Han, Dong, Hang Liu, and Yan Gao. 2020. "The Role of Peripheral Monocytes and Macrophages in Ischemic Stroke." *Neurological Sciences: Official Journal of the Italian Neurological Society and of the Italian Society of Clinical Neurophysiology* 41 (12): 3589–3607. https://doi.org/10.1007/s10072-020-04777-9.

Han, Jinming, Violeta Chitu, E. Richard Stanley, Zbigniew K. Wszolek, Virginija Danylaité Karrenbauer, and Robert A. Harris. 2022. "Inhibition of Colony Stimulating Factor-1 Receptor (CSF-1R) as a Potential Therapeutic Strategy for Neurodegenerative Diseases: Opportunities and Challenges." *Cellular and Molecular Life Sciences: CMLS* 79 (4): 219. https://doi.org/10.1007/s00018-022-04225-1.

Han, Jinming, Robert A. Harris, and Xing-Mei Zhang. 2017. "An Updated Assessment of Microglia Depletion: Current Concepts and Future Directions." *Molecular Brain* 10 (1): 25. https://doi.org/10.1186/s13041-017-0307-x.

Han, Xiaoning, Qian Li, Xi Lan, Leena EL-Mufti, Honglei Ren, and Jian Wang. 2019. "Microglial Depletion with Clodronate Liposomes Increases Proinflammatory Cytokine Levels, Induces Astrocyte Activation, and Damages Blood Vessel Integrity." *Molecular Neurobiology* 56 (9): 6184–96. https://doi.org/10.1007/s12035-019-1502-9.

Hardy, J. A., and G. A. Higgins. 1992. "Alzheimer's Disease: The Amyloid Cascade Hypothesis." *Science (New York, N.Y.)* 256 (5054): 184–85. https://doi.org/10.1126/science.1566067.

Haruwaka, Koichiro, Yanlu Ying, Yue Liang, Anthony D. Umpierre, Min-Hee Yi, Vaclav Kremen, Tingjun Chen, et al. 2024. "Microglia Enhance Post-Anesthesia Neuronal Activity by Shielding Inhibitory Synapses." *Nature Neuroscience* 27 (3): 449–61. https://doi.org/10.1038/s41593-023-01537-8.

Hason, Martina, Tereza Mikulasova, Olga Machonova, Antonio Pombinho, Tjakko J. van Ham, Uwe Irion, Christiane Nüsslein-Volhard, Petr Bartunek, and Ondrej Svoboda. 2022. "M-CSFR/CSF1R Signaling Regulates Myeloid Fates in Zebrafish via Distinct Action of Its Receptors and Ligands." *Blood Advances* 6 (5): 1474–88. https://doi.org/10.1182/bloodadvances.2021005459.

Hasselmann, Jonathan, and Mathew Blurton-Jones. 2020. "Human iPSC-Derived Microglia: A Growing Toolset to Study the Brain's Innate Immune Cells." *Glia* 68 (4): 721–39. https://doi.org/10.1002/glia.23781.

Hasselmann, Jonathan, Morgan A. Coburn, Whitney England, Dario X. Figueroa Velez, Sepideh Kiani Shabestari, Christina H. Tu, Amanda McQuade, et al. 2019. "Development of a Chimeric Model to Study

and Manipulate Human Microglia In Vivo." *Neuron* 103 (6): 1016-1033.e10. https://doi.org/10.1016/j.neuron.2019.07.002.

Hayes, G. M., M. N. Woodroofe, and M. L. Cuzner. 1987. "Microglia Are the Major Cell Type Expressing MHC Class II in Human White Matter." *Journal of the Neurological Sciences* 80 (1): 25–37. https://doi.org/10.1016/0022-510x(87)90218-8.

He, Yingbo, Natalie Taylor, Xiang Yao, and Anindya Bhattacharya. 2021. "Mouse Primary Microglia Respond Differently to LPS and Poly(I:C) in Vitro." *Scientific Reports* 11 (1): 10447. https://doi.org/10.1038/s41598-021-89777-1.

Hedegaard, Anne, Szymon Stodolak, William S. James, and Sally A. Cowley. 2020. "Honing the Double-Edged Sword: Improving Human iPSC-Microglia Models." *Frontiers in Immunology* 11:614972. https://doi.org/10.3389/fimmu.2020.614972.

Hefendehl, Jasmin K., Jonas J. Neher, Rafael B. Sühs, Shinichi Kohsaka, Angelos Skodras, and Mathias Jucker. 2014. "Homeostatic and Injury-Induced Microglia Behavior in the Aging Brain." *Aging Cell* 13 (1): 60–69. https://doi.org/10.1111/acel.12149.

Heneka, Michael T., Monica J. Carson, Joseph El Khoury, Gary E. Landreth, Frederic Brosseron, Douglas L. Feinstein, Andreas H. Jacobs, et al. 2015. "Neuroinflammation in Alzheimer's Disease." *The Lancet. Neurology* 14 (4): 388–405. https://doi.org/10.1016/S1474-4422(15)70016-5.

Heneka, Michael T., Wiesje M. van der Flier, Frank Jessen, Jeroen Hoozemanns, Dietmar Rudolf Thal, Delphine Boche, Frederic Brosseron, et al. 2024. "Neuroinflammation in Alzheimer Disease." *Nature Reviews Immunology*, December, 1–32. https://doi.org/10.1038/s41577-024-01104-7.

Heng, Yang, Marissa L. Dubbelaar, Suely K. N. Marie, Erik W. G. M. Boddeke, and Bart J. L. Eggen. 2021. "The Effects of Postmortem Delay on Mouse and Human Microglia Gene Expression." *Glia* 69 (4): 1053–60. https://doi.org/10.1002/glia.23948.

Henn, Anja, Søren Lund, Maj Hedtjärn, Andreé Schrattenholz, Peter Pörzgen, and Marcel Leist. 2009. "The Suitability of BV2 Cells as Alternative Model System for Primary Microglia Cultures or for Animal Experiments Examining Brain Inflammation." *ALTEX* 26 (2): 83–94. https://doi.org/10.14573/altex.2009.2.83.

Heppner, F. L., T. Skutella, N. P. Hailer, D. Haas, and R. Nitsch. 1998. "Activated Microglial Cells Migrate towards Sites of Excitotoxic Neuronal Injury inside Organotypic Hippocampal Slice Cultures." *The European Journal of Neuroscience* 10 (10): 3284–90. https://doi.org/10.1046/j.1460-9568.1998.00379.x.

Heppner, Frank L., Melanie Greter, Denis Marino, Jeppe Falsig, Gennadij Raivich, Nadine Hövelmeyer, Ari Waisman, et al. 2005. "Experimental Autoimmune Encephalomyelitis Repressed by Microglial Paralysis." *Nature Medicine* 11 (2): 146–52. https://doi.org/10.1038/nm1177.

Hickey, W. F., and H. Kimura. 1988. "Perivascular Microglial Cells of the CNS Are Bone Marrow-Derived and Present Antigen in Vivo." *Science (New York, N.Y.)* 239 (4837): 290–92. https://doi.org/10.1126/science.3276004.

Hickman, Suzanne E., Elizabeth K. Allison, and Joseph El Khoury. 2008. "Microglial Dysfunction and Defective β-Amyloid Clearance Pathways in Aging Alzheimer's Disease Mice." *The Journal of Neuroscience* 28 (33): 8354–60. https://doi.org/10.1523/JNEUROSCI.0616-08.2008.

Hickman, Suzanne E., Nathan D. Kingery, Toshiro K. Ohsumi, Mark L. Borowsky, Li-chong Wang, Terry K. Means, and Joseph El Khoury. 2013. "The Microglial Sensome Revealed by Direct RNA Sequencing." *Nature Neuroscience* 16 (12): 1896–1905. https://doi.org/10.1038/nn.3554.

Hickman, Suzanne, Saef Izzy, Pritha Sen, Liza Morsett, and Joseph El Khoury. 2018. "Microglia in Neurodegeneration." *Nature Neuroscience* 21 (10): 1359–69. https://doi.org/10.1038/s41593-018-0242-x.

Hirasawa, T., K. Ohsawa, Y. Imai, Y. Ondo, C. Akazawa, S. Uchino, and S. Kohsaka. 2005. "Visualization of Microglia in Living Tissues Using Iba1-EGFP Transgenic Mice." *Journal of Neuroscience Research* 81 (3): 357–62. https://doi.org/10.1002/jnr.20480.

Hoeffel, Guillaume, Jinmiao Chen, Yonit Lavin, Donovan Low, Francisca F. Almeida, Peter See, Anna E. Beaudin, et al. 2015. “C-Myb(+) Erythro-Myeloid Progenitor-Derived Fetal Monocytes Give Rise to Adult Tissue-Resident Macrophages.” *Immunity* 42 (4): 665–78. https://doi.org/10.1016/j.immuni.2015.03.011.

Hoeffel, Guillaume, Yilin Wang, Melanie Greter, Peter See, Pearline Teo, Benoit Malleret, Marylène Leboeuf, et al. 2012. “Adult Langerhans Cells Derive Predominantly from Embryonic Fetal Liver Monocytes with a Minor Contribution of Yolk Sac-Derived Macrophages.” *The Journal of Experimental Medicine* 209 (6): 1167–81. https://doi.org/10.1084/jem.20120340.

Holstege, Henne, Marc Hulsman, Camille Charbonnier, Benjamin Grenier-Boley, Olivier Quenez, Detelina Grozeva, Jeroen G. J. van Rooij, et al. 2022. “Exome Sequencing Identifies Rare Damaging Variants in ATP8B4 and ABCA1 as Risk Factors for Alzheimer’s Disease.” *Nature Genetics* 54 (12): 1786–94. https://doi.org/10.1038/s41588-022-01208-7.

Holtman, Inge R., Divya D. Raj, Jeremy A. Miller, Wandert Schaafsma, Zhuoran Yin, Nieske Brouwer, Paul D. Wes, et al. 2015. “Induction of a Common Microglia Gene Expression Signature by Aging and Neurodegenerative Conditions: A Co-Expression Meta-Analysis.” *Acta Neuropathologica Communications* 3 (May):31. https://doi.org/10.1186/s40478-015-0203-5.

Horvath, Ryan J., Nancy Nutile-McMenemy, Matthew S. Alkaitis, and Joyce A. Deleo. 2008. “Differential Migration, LPS-Induced Cytokine, Chemokine, and NO Expression in Immortalized BV-2 and HAPI Cell Lines and Primary Microglial Cultures.” *Journal of Neurochemistry* 107 (2): 557–69. https://doi.org/10.1111/j.1471-4159.2008.05633.x.

Hou, Jinchao, Yun Chen, Gary Grajales-Reyes, and Marco Colonna. 2022. “TREM2 Dependent and Independent Functions of Microglia in Alzheimer’s Disease.” *Molecular Neurodegeneration* 17 (1): 84. https://doi.org/10.1186/s13024-022-00588-y.

Huang, Yubin, Zhen Xu, Shanshan Xiong, Fangfang Sun, Guangrong Qin, Guanglei Hu, Jingjing Wang, et al. 2018. “Repopulated Microglia Are Solely Derived from the Proliferation of Residual Microglia after Acute Depletion.” *Nature Neuroscience* 21 (4): 530–40. https://doi.org/10.1038/s41593-018-0090-8.

Hugh Perry, V. 1998. “A Revised View of the Central Nervous System Microenvironment and Major Histocompatibility Complex Class II Antigen Presentation.” *Journal of Neuroimmunology* 90 (2): 113–21. https://doi.org/10.1016/S0165-5728(98)00145-3.

Hughes, Craig D., Minee L. Choi, Mina Ryten, Lee Hopkins, Anna Drews, Juan A. Botía, Maria Iljina, et al. 2019. “Picomolar Concentrations of Oligomeric Alpha-Synuclein Sensitizes TLR4 to Play an Initiating Role in Parkinson’s Disease Pathogenesis.” *Acta Neuropathologica* 137 (1): 103–20. https://doi.org/10.1007/s00401-018-1907-y.

Hume, D. A., P. Pavli, R. E. Donahue, and I. J. Fidler. 1988. “The Effect of Human Recombinant Macrophage Colony-Stimulating Factor (CSF-1) on the Murine Mononuclear Phagocyte System in Vivo.” *Journal of Immunology (Baltimore, Md.: 1950)* 141 (10): 3405–9.

Hume, David A., Maria W. Gutowska-Ding, Carla Garcia-Morales, Adebabay Kebede, Oladeji Bamidele, Adriana Vallejo Trujillo, Almas A. Gheyas, and Jacqueline Smith. 2020. “Functional Evolution of the Colony-Stimulating Factor 1 Receptor (CSF1R) and Its Ligands in Birds.” *Journal of Leukocyte Biology* 107 (2): 237–50. https://doi.org/10.1002/JLB.6MA0519-172R.

Hume, David A., and Kelli P. A. MacDonald. 2012. “Therapeutic Applications of Macrophage Colony-Stimulating Factor-1 (CSF-1) and Antagonists of CSF-1 Receptor (CSF-1R) Signaling.” *Blood* 119 (8): 1810–20. https://doi.org/10.1182/blood-2011-09-379214.

Humpel, C. 2015. “Organotypic Brain Slice Cultures: A Review.” *Neuroscience* 305 (October):86–98. https://doi.org/10.1016/j.neuroscience.2015.07.086.

Hutchins, K. D., D. W. Dickson, W. K. Rashbaum, and W. D. Lyman. 1990. “Localization of Morphologically Distinct Microglial Populations in the Developing Human Fetal Brain: Implications for Ontogeny.” *Brain Research. Developmental Brain Research* 55 (1): 95–102. https://doi.org/10.1016/0165-3806(90)90109-c.

Imamoto, K., and C. P. Leblond. 1978. “Radioautographic Investigation of Gliogenesis in the Corpus

Callosum of Young Rats. II. Origin of Microglial Cells." *The Journal of Comparative Neurology* 180 (1): 139–63. https://doi.org/10.1002/cne.901800109.

Ising, Christina, Carmen Venegas, Shuangshuang Zhang, Hannah Scheiblich, Susanne V. Schmidt, Ana Vieira-Saecker, Stephanie Schwartz, et al. 2019. "NLRP3 Inflammasome Activation Drives Tau Pathology." *Nature* 575 (7784): 669–73. https://doi.org/10.1038/s41586-019-1769-z.

Janabi, N., S. Peudenier, B. Héron, K. H. Ng, and M. Tardieu. 1995. "Establishment of Human Microglial Cell Lines after Transfection of Primary Cultures of Embryonic Microglial Cells with the SV40 Large T Antigen." *Neuroscience Letters* 195 (2): 105–8. https://doi.org/10.1016/0304-3940(94)11792-h.

Jin, Mengmeng, Ranjie Xu, Le Wang, Mahabub Maraj Alam, Ziyuan Ma, Sining Zhu, Alessandra C. Martini, et al. 2022. "Type-I-Interferon Signaling Drives Microglial Dysfunction and Senescence in Human iPSC Models of Down Syndrome and Alzheimer's Disease." *Cell Stem Cell* 29 (7): 1135-1153.e8. https://doi.org/10.1016/j.stem.2022.06.007.

Jo, Junghyun, Yixin Xiao, Alfred Xuyang Sun, Engin Cukuroglu, Hoang-Dai Tran, Jonathan Göke, Zi Ying Tan, et al. 2016. "Midbrain-like Organoids from Human Pluripotent Stem Cells Contain Functional Dopaminergic and Neuromelanin-Producing Neurons." *Cell Stem Cell* 19 (2): 248–57. https://doi.org/10.1016/j.stem.2016.07.005.

Joers, Valerie, Malú G. Tansey, Giovanna Mulas, and Anna R. Carta. 2017. "Microglial Phenotypes in Parkinson's Disease and Animal Models of the Disease." *Progress in Neurobiology* 155 (August):57–75. https://doi.org/10.1016/j.pneurobio.2016.04.006.

Jorfi, Mehdi, Anna Maaser-Hecker, and Rudolph E. Tanzi. 2023. "The Neuroimmune Axis of Alzheimer's Disease." *Genome Medicine* 15 (1): 6. https://doi.org/10.1186/s13073-023-01155-w.

Joshi, P., E. Turola, A. Ruiz, A. Bergami, D. D. Libera, L. Benussi, P. Giussani, et al. 2014. "Microglia Convert Aggregated Amyloid-β into Neurotoxic Forms through the Shedding of Microvesicles." *Cell Death and Differentiation* 21 (4): 582–93. https://doi.org/10.1038/cdd.2013.180.

Jucker, Mathias, and Lary C. Walker. 2013. "Self-Propagation of Pathogenic Protein Aggregates in Neurodegenerative Diseases." *Nature* 501 (7465): 45–51. https://doi.org/10.1038/nature12481.

Jucker, Mathias, and Lary C. Walker. 2018. "Propagation and Spread of Pathogenic Protein Assemblies in Neurodegenerative Diseases." *Nature Neuroscience* 21 (10): 1341–49. https://doi.org/10.1038/s41593-018-0238-6.

Jung, S., J. Aliberti, P. Graemmel, M. J. Sunshine, G. W. Kreutzberg, A. Sher, and D. R. Littman. 2000. "Analysis of Fractalkine Receptor CX(3)CR1 Function by Targeted Deletion and Green Fluorescent Protein Reporter Gene Insertion." *Molecular and Cellular Biology* 20 (11): 4106–14. https://doi.org/10.1128/MCB.20.11.4106-4114.2000.

Kaji, Seiji, Stefan A. Berghoff, Lena Spieth, Lennart Schlaphoff, Andrew O. Sasmita, Simona Vitale, Luca Büschgens, et al. 2024. "Apolipoprotein E Aggregation in Microglia Initiates Alzheimer's Disease Pathology by Seeding β-Amyloidosis." *Immunity* 57 (11): 2651-2668.e12. https://doi.org/10.1016/j.immuni.2024.09.014.

Kalia, Lorraine V., and Anthony E. Lang. 2015. "Parkinson's Disease." *Lancet (London, England)* 386 (9996): 896–912. https://doi.org/10.1016/S0140-6736(14)61393-3.

Kamphuis, Willem, Lieneke Kooijman, Sjoerd Schetters, Marie Orre, and Elly M. Hol. 2016. "Transcriptional Profiling of CD11c-Positive Microglia Accumulating around Amyloid Plaques in a Mouse Model for Alzheimer's Disease." *Biochimica Et Biophysica Acta* 1862 (10): 1847–60. https://doi.org/10.1016/j.bbadis.2016.07.007.

Kana, Veronika, Fiona A. Desland, Maria Casanova-Acebes, Pinar Ayata, Ana Badimon, Elisa Nabel, Kazuhiko Yamamuro, et al. 2019. "CSF-1 Controls Cerebellar Microglia and Is Required for Motor Function and Social Interaction." *The Journal of Experimental Medicine* 216 (10): 2265–81. https://doi.org/10.1084/jem.20182037.

Karch, Celeste M., and Alison M. Goate. 2015. "Alzheimer's Disease Risk Genes and Mechanisms of

Disease Pathogenesis." *Biological Psychiatry* 77 (1): 43–51. https://doi.org/10.1016/j.biopsych.2014.05.006.

Keller, Daniel, Csaba Erö, and Henry Markram. 2018. "Cell Densities in the Mouse Brain: A Systematic Review." *Frontiers in Neuroanatomy* 12. https://www.frontiersin.org/article/10.3389/fnana.2018.00083.

Keren-Shaul, Hadas, Amit Spinrad, Assaf Weiner, Orit Matcovitch-Natan, Raz Dvir-Szternfeld, Tyler K. Ulland, Eyal David, et al. 2017. "A Unique Microglia Type Associated with Restricting Development of Alzheimer's Disease." *Cell* 169 (7): 1276-1290.e17. https://doi.org/10.1016/j.cell.2017.05.018.

Kettenmann, Helmut, Frank Kirchhoff, and Alexei Verkhratsky. 2013. "Microglia: New Roles for the Synaptic Stripper." *Neuron* 77 (1): 10–18. https://doi.org/10.1016/j.neuron.2012.12.023.

Kierdorf, Katrin, Daniel Erny, Tobias Goldmann, Victor Sander, Christian Schulz, Elisa Gomez Perdiguero, Peter Wieghofer, et al. 2013. "Microglia Emerge from Erythromyeloid Precursors via Pu.1- and Irf8-Dependent Pathways." *Nature Neuroscience* 16 (3): 273–80. https://doi.org/10.1038/nn.3318.

Kim, Jonggeol Jeffrey, Dan Vitale, Diego Véliz Otani, Michelle Mulan Lian, Karl Heilbron, Hirotaka Iwaki, Julie Lake, et al. 2024. "Multi-Ancestry Genome-Wide Association Meta-Analysis of Parkinson's Disease." *Nature Genetics* 56 (1): 27–36. https://doi.org/10.1038/s41588-023-01584-8.

Klingstedt, Therése, Hamid Shirani, K O Andreas Åslund, Nigel J Cairns, Christina J Sigurdson, Michel Goedert, and K Peter R Nilsson*. 2013. "The Structural Basis for Optimal Performance of Oligothiophene-Based Fluorescent Amyloid Ligands: Conformational Flexibility Is Essential for Spectral Assignment of a Diversity of Protein Aggregates." *Chemistry (Weinheim an Der Bergstrasse, Germany)* 19 (31): 10179–92. https://doi.org/10.1002/chem.201301463.

Konishi, Hiroyuki, Schuichi Koizumi, and Hiroshi Kiyama. 2022. "Phagocytic Astrocytes: Emerging from the Shadows of Microglia." *Glia* 70 (6): 1009–26. https://doi.org/10.1002/glia.24145.

Konno, Takuya, Koji Kasanuki, Takeshi Ikeuchi, Dennis W. Dickson, and Zbigniew K. Wszolek. 2018. "CSF1R-Related Leukoencephalopathy: A Major Player in Primary Microgliopathies." *Neurology* 91 (24): 1092. https://doi.org/10.1212/WNL.0000000000006642.

Krasemann, Susanne, Charlotte Madore, Ron Cialic, Caroline Baufeld, Narghes Calcagno, Rachid El Fatimy, Lien Beckers, et al. 2017. "The TREM2-APOE Pathway Drives the Transcriptional Phenotype of Dysfunctional Microglia in Neurodegenerative Diseases." *Immunity* 47 (3): 566-581.e9. https://doi.org/10.1016/j.immuni.2017.08.008.

Krauser, Joel A., Yi Jin, Markus Walles, Ulrike Pfaar, James Sutton, Marion Wiesmann, Daniel Graf, et al. 2015. "Phenotypic and Metabolic Investigation of a CSF-1R Kinase Receptor Inhibitor (BLZ945) and Its Pharmacologically Active Metabolite." *Xenobiotica; the Fate of Foreign Compounds in Biological Systems* 45 (2): 107–23. https://doi.org/10.3109/00498254.2014.945988.

Krissinel, Evgeny, and Kim Henrick. 2007. "Inference of Macromolecular Assemblies from Crystalline State." *Journal of Molecular Biology* 372 (3): 774–97. https://doi.org/10.1016/j.jmb.2007.05.022.

Kumaravelu, Parasakthy, Lilian Hook, Aline M. Morrison, Jan Ure, Suling Zhao, Sergei Zuyev, John Ansell, and Alexander Medvinsky. 2002. "Quantitative Developmental Anatomy of Definitive Haematopoietic Stem Cells/Long-Term Repopulating Units (HSC/RUs): Role of the Aorta-Gonad-Mesonephros (AGM) Region and the Yolk Sac in Colonisation of the Mouse Embryonic Liver." *Development (Cambridge, England)* 129 (21): 4891–99. https://doi.org/10.1242/dev.129.21.4891.

Lancaster, Madeline A., and Juergen A. Knoblich. 2014. "Organogenesis in a Dish: Modeling Development and Disease Using Organoid Technologies." *Science* 345 (6194): 1247125. https://doi.org/10.1126/science.1247125.

Lancaster, Madeline A., Magdalena Renner, Carol-Anne Martin, Daniel Wenzel, Louise S. Bicknell, Matthew E. Hurles, Tessa Homfray, Josef M. Penninger, Andrew P. Jackson, and Juergen A. Knoblich. 2013. "Cerebral Organoids Model Human Brain Development and Microcephaly." *Nature* 501 (7467): 373–79. https://doi.org/10.1038/nature12517.

Lassmann, H., M. Schmied, K. Vass, and W. F. Hickey. 1993. "Bone Marrow Derived Elements and Resident

Microglia in Brain Inflammation." *Glia* 7 (1): 19–24. https://doi.org/10.1002/glia.440070106.

Lawson, L. J., V. H. Perry, P. Dri, and S. Gordon. 1990. "Heterogeneity in the Distribution and Morphology of Microglia in the Normal Adult Mouse Brain." *Neuroscience* 39 (1): 151–70. https://doi.org/10.1016/0306-4522(90)90229-w.

Lawson, L. J., V. H. Perry, and S. Gordon. 1992. "Turnover of Resident Microglia in the Normal Adult Mouse Brain." *Neuroscience* 48 (2): 405–15. https://doi.org/10.1016/0306-4522(92)90500-2.

Le, L. H. D., M. K. O'Banion, and A. K. Majewska. 2024. "Partial Microglial Depletion and Repopulation Exert Subtle but Differential Effects on Amyloid Pathology at Different Disease Stages." *Scientific Reports* 14 (1): 30912. https://doi.org/10.1038/s41598-024-81910-0.

Lee, Christopher Z. W., Tatsuya Kozaki, and Florent Ginhoux. 2018. "Studying Tissue Macrophages in Vitro: Are iPSC-Derived Cells the Answer?" *Nature Reviews. Immunology* 18 (11): 716–25. https://doi.org/10.1038/s41577-018-0054-y.

Lee, Moonhee, Claudia Schwab, and Patrick L. McGeer. 2011. "Astrocytes Are GABAergic Cells That Modulate Microglial Activity." *Glia* 59 (1): 152–65. https://doi.org/10.1002/glia.21087.

Lee, P. S., Y. Wang, M. G. Dominguez, Y. G. Yeung, M. A. Murphy, D. D. Bowtell, and E. R. Stanley. 1999. "The Cbl Protooncoprotein Stimulates CSF-1 Receptor Multiubiquitination and Endocytosis, and Attenuates Macrophage Proliferation." *The EMBO Journal* 18 (13): 3616–28. https://doi.org/10.1093/emboj/18.13.3616.

Leong, S. K., and E. A. Ling. 1992. "Amoeboid and Ramified Microglia: Their Interrelationship and Response to Brain Injury." *Glia* 6 (1): 39–47. https://doi.org/10.1002/glia.440060106.

Li, Jie-Qiong, Lan Tan, and Jin-Tai Yu. 2014. "The Role of the LRRK2 Gene in Parkinsonism." *Molecular Neurodegeneration* 9 (November):47. https://doi.org/10.1186/1750-1326-9-47.

Li, Na, Tessandra Stewart, Lifu Sheng, Min Shi, Eugene M. Cilento, Yufeng Wu, Jau-Syong Hong, and Jing Zhang. 2020. "Immunoregulation of Microglial Polarization: An Unrecognized Physiological Function of α-Synuclein." *Journal of Neuroinflammation* 17 (1): 272. https://doi.org/10.1186/s12974-020-01940-z.

Li, Qingyun, Zuolin Cheng, Lu Zhou, Spyros Darmanis, Norma F. Neff, Jennifer Okamoto, Gunsagar Gulati, et al. 2019. "Developmental Heterogeneity of Microglia and Brain Myeloid Cells Revealed by Deep Single-Cell RNA Sequencing." *Neuron* 101 (2): 207-223.e10. https://doi.org/10.1016/j.neuron.2018.12.006.

Li, Xiaoyu, Yuxin Li, Yuxiao Jin, Yuheng Zhang, Jingchuan Wu, Zhen Xu, Yubin Huang, et al. 2023. "Transcriptional and Epigenetic Decoding of the Microglial Aging Process." *Nature Aging*, September, 1–24. https://doi.org/10.1038/s43587-023-00479-x.

Li, Yanxin, Zhongqiu Li, Min Yang, Feiyang Wang, Yuehong Zhang, Rong Li, Qian Li, et al. 2022. "Decoding the Temporal and Regional Specification of Microglia in the Developing Human Brain." *Cell Stem Cell* 29 (4): 620-634.e6. https://doi.org/10.1016/j.stem.2022.02.004.

Lichanska, A. M., and D. A. Hume. 2000. "Origins and Functions of Phagocytes in the Embryo." *Experimental Hematology* 28 (6): 601–11. https://doi.org/10.1016/s0301-472x(00)00157-0.

Liddelow, Shane A., Kevin A. Guttenplan, Laura E. Clarke, Frederick C. Bennett, Christopher J. Bohlen, Lucas Schirmer, Mariko L. Bennett, et al. 2017. "Neurotoxic Reactive Astrocytes Are Induced by Activated Microglia." *Nature* 541 (7638): 481–87. https://doi.org/10.1038/nature21029.

Lin, Haishan, Ernestine Lee, Kevin Hestir, Cindy Leo, Minmei Huang, Elizabeth Bosch, Robert Halenbeck, et al. 2008. "Discovery of a Cytokine and Its Receptor by Functional Screening of the Extracellular Proteome." *Science* 320 (5877): 807–11. https://doi.org/10.1126/science.1154370.

Lin, Rui, Youtong Zhou, Ting Yan, Ruiyu Wang, Heng Li, Zhaofa Wu, Xinshuang Zhang, et al. 2022. "Directed Evolution of Adeno-Associated Virus for Efficient Gene Delivery to Microglia." *Nature Methods* 19 (8): 976–85. https://doi.org/10.1038/s41592-022-01547-7.

Ling, E. A. 1976. "Some Aspects of Amoeboid Microglia in the Corpus Callosum and Neighbouring Regions of Neonatal Rats." *Journal of Anatomy* 121 (Pt 1): 29–45.

Ling, E. A. 1979. “Transformation of Monocytes into Amoeboid Microglia in the Corpus Callosum of Postnatal Rats, as Shown by Labelling Monocytes by Carbon Particles.” *Journal of Anatomy* 128 (Pt 4): 847–58.

Ling, E. A., D. Penney, and C. P. Leblond. 1980. “Use of Carbon Labeling to Demonstrate the Role of Blood Monocytes as Precursors of the ‘ameboid Cells’ Present in the Corpus Callosum of Postnatal Rats.” *The Journal of Comparative Neurology* 193 (3): 631–57. https://doi.org/10.1002/cne.901930304.

Liu, Heli, Cindy Leo, Xiaoyan Chen, Brian R. Wong, Lewis T. Williams, Haishan Lin, and Xiaolin He. 2012. “The Mechanism of Shared but Distinct CSF-1R Signaling by the Non-Homologous Cytokines IL-34 and CSF-1.” *Biochimica Et Biophysica Acta* 1824 (7): 938–45. https://doi.org/10.1016/j.bbapap.2012.04.012.

Liu, Yong U., Yanlu Ying, Yujiao Li, Ukpong B. Eyo, Tingjun Chen, Jiaying Zheng, Anthony D. Umpierre, et al. 2019. “Neuronal Network Activity Controls Microglial Process Surveillance in Awake Mice via Norepinephrine Signaling.” *Nature Neuroscience* 22 (11): 1771–81. https://doi.org/10.1038/s41593-019-0511-3.

Long, Justin M., and David M. Holtzman. 2019. “Alzheimer Disease: An Update on Pathobiology and Treatment Strategies.” *Cell* 179 (2): 312–39. https://doi.org/10.1016/j.cell.2019.09.001.

Lopes, Katia de Paiva, Gijsje J. L. Snijders, Jack Humphrey, Amanda Allan, Marjolein A. M. Sneeboer, Elisa Navarro, Brian M. Schilder, et al. 2022. “Genetic Analysis of the Human Microglial Transcriptome across Brain Regions, Aging and Disease Pathologies.” *Nature Genetics* 54 (1): 4–17. https://doi.org/10.1038/s41588-021-00976-y.

Louveau, Antoine, Tajie H. Harris, and Jonathan Kipnis. 2015. “Revisiting the Mechanisms of CNS Immune Privilege.” *Trends in Immunology*, Special Issue: Neuroimmunology, 36 (10): 569–77. https://doi.org/10.1016/j.it.2015.08.006.

Luo, Cong, Ryuta Koyama, and Yuji Ikegaya. 2016. “Microglia Engulf Viable Newborn Cells in the Epileptic Dentate Gyrus.” *Glia* 64 (9): 1508–17. https://doi.org/10.1002/glia.23018.

Lynch, Marina A. 2015. “Neuroinflammatory Changes Negatively Impact on LTP: A Focus on IL-1β.” *Brain Research* 1621 (September):197–204. https://doi.org/10.1016/j.brainres.2014.08.040.

Ma, Xiaolei, Wei Yu Lin, Yongmei Chen, Scott Stawicki, Kiran Mukhyala, Yan Wu, Flavius Martin, J. Fernando Bazan, and Melissa A. Starovasnik. 2012. “Structural Basis for the Dual Recognition of Helical Cytokines IL-34 and CSF-1 by CSF-1R.” *Structure (London, England: 1993)* 20 (4): 676–87. https://doi.org/10.1016/j.str.2012.02.010.

Mancuso, Renzo, Johanna Van Den Daele, Nicola Fattorelli, Leen Wolfs, Sriram Balusu, Oliver Burton, Adrian Liston, et al. 2019. “Stem-Cell-Derived Human Microglia Transplanted in Mouse Brain to Study Human Disease.” *Nature Neuroscience* 22 (12): 2111–16. https://doi.org/10.1038/s41593-019-0525-x.

Marotti, Jonathan D., Sharon Tobias, Jonathan D. Fratkin, James M. Powers, and C. Harker Rhodes. 2004. “Adult Onset Leukodystrophy with Neuroaxonal Spheroids and Pigmented Glia: Report of a Family, Historical Perspective, and Review of the Literature.” *Acta Neuropathologica* 107 (6): 481–88. https://doi.org/10.1007/s00401-004-0847-x.

Marschallinger, Julia, Tal Iram, Macy Zardeneta, Song E. Lee, Benoit Lehallier, Michael S. Haney, John V. Pluvinage, et al. 2020. “Lipid-Droplet-Accumulating Microglia Represent a Dysfunctional and Proinflammatory State in the Aging Brain.” *Nature Neuroscience* 23 (2): 194–208. https://doi.org/10.1038/s41593-019-0566-1.

Marsh, Samuel E., Alec J. Walker, Tushar Kamath, Lasse Dissing-Olesen, Timothy R. Hammond, T. Yvanka de Soysa, Adam M. H. Young, et al. 2022. “Dissection of Artifactual and Confounding Glial Signatures by Single-Cell Sequencing of Mouse and Human Brain.” *Nature Neuroscience* 25 (3): 306–16. https://doi.org/10.1038/s41593-022-01022-8.

Marshall, Eleanor M., Ahmad S. Rashidi, Michiel van Gent, Barry Rockx, and Georges M. G. M. Verjans. 2024. “Neurovirulence of Usutu Virus in Human Fetal Organotypic Brain Slice Cultures Partially Resembles Zika and West Nile Virus.” *Scientific Reports* 14 (1): 20095. https://doi.org/10.1038/s41598-024-71050-w.

Masuch, Annette, Rianne van der Pijl, Lisa Füner, Yochai Wolf, Bart Eggen, Erik Boddeke, and Knut Biber. 2016. “Microglia Replenished OHSC: A Culture System to Study in Vivo like Adult Microglia.” *Glia* 64 (8): 1285–97. https://doi.org/10.1002/glia.23002.

Masuda, Takahiro, Lukas Amann, Roman Sankowski, Ori Staszewski, Maximilian Lenz, Paolo D Errico, Nicolas Snaidero, et al. 2020. “Novel Hexb-Based Tools for Studying Microglia in the CNS.” *Nature Immunology* 21 (7): 802–15. https://doi.org/10.1038/s41590-020-0707-4.

Masuda, Takahiro, Roman Sankowski, Ori Staszewski, Chotima Böttcher, Lukas Amann, Sagar, Christian Scheiwe, et al. 2019. “Spatial and Temporal Heterogeneity of Mouse and Human Microglia at Single-Cell Resolution.” *Nature* 566 (7744): 388–92. https://doi.org/10.1038/s41586-019-0924-x.

Mathews, Saumi, Amanda Branch Woods, Ikumi Katano, Edward Makarov, Midhun B. Thomas, Howard E. Gendelman, Larisa Y. Poluektova, Mamoru Ito, and Santhi Gorantla. 2019. “Human Interleukin-34 Facilitates Microglia-like Cell Differentiation and Persistent HIV-1 Infection in Humanized Mice.” *Molecular Neurodegeneration* 14 (1): 12. https://doi.org/10.1186/s13024-019-0311-y.

Mathys, Hansruedi, Chinnakkaruppan Adaikkan, Fan Gao, Jennie Z. Young, Elodie Manet, Martin Hemberg, Philip L. De Jager, Richard M. Ransohoff, Aviv Regev, and Li-Huei Tsai. 2017. “Temporal Tracking of Microglia Activation in Neurodegeneration at Single-Cell Resolution.” *Cell Reports* 21 (2): 366–80. https://doi.org/10.1016/j.celrep.2017.09.039.

Mayer, Meredith G., and Tracy Fischer. 2024. “Microglia at the Blood Brain Barrier in Health and Disease.” *Frontiers in Cellular Neuroscience* 18:1360195. https://doi.org/10.3389/fncel.2024.1360195.

Mazaheri, Fargol, Nicolas Snaidero, Gernot Kleinberger, Charlotte Madore, Anna Daria, Georg Werner, Susanne Krasemann, et al. 2017. “TREM2 Deficiency Impairs Chemotaxis and Microglial Responses to Neuronal Injury.” *EMBO Reports* 18 (7): 1186–98. https://doi.org/10.15252/embr.201743922.

McGrath, Kathleen E., Anne D. Koniski, Jeffrey Malik, and James Palis. 2003. “Circulation Is Established in a Stepwise Pattern in the Mammalian Embryo.” *Blood* 101 (5): 1669–76. https://doi.org/10.1182/blood-2002-08-2531.

McLellan, Micheal A., Nadia A. Rosenthal, and Alexander R. Pinto. 2017. “Cre-loxP-Mediated Recombination: General Principles and Experimental Considerations.” *Current Protocols in Mouse Biology* 7 (1): 1–12. https://doi.org/10.1002/cpmo.22.

McLeod, Faye, Anna Dimtsi, Amy C Marshall, David Lewis-Smith, Rhys Thomas, Gavin J Clowry, and Andrew J Trevelyan. 2023. “Altered Synaptic Connectivity in an in Vitro Human Model of STXBP1 Encephalopathy.” *Brain* 146 (3): 850–57. https://doi.org/10.1093/brain/awac396.

McQuade, Amanda, and Mathew Blurton-Jones. 2019. “Microglia in Alzheimer’s Disease: Exploring How Genetics and Phenotype Influence Risk.” *Journal of Molecular Biology* 431 (9): 1805–17. https://doi.org/10.1016/j.jmb.2019.01.045.

McQuade, Amanda, Morgan Coburn, Christina H. Tu, Jonathan Hasselmann, Hayk Davtyan, and Mathew Blurton-Jones. 2018. “Development and Validation of a Simplified Method to Generate Human Microglia from Pluripotent Stem Cells.” *Molecular Neurodegeneration* 13 (1): 67. https://doi.org/10.1186/s13024-018-0297-x.

McQuade, Amanda, You Jung Kang, Jonathan Hasselmann, Amit Jairaman, Alexandra Sotelo, Morgan Coburn, Sepideh Kiani Shabestari, et al. 2020. “Gene Expression and Functional Deficits Underlie TREM2-Knockout Microglia Responses in Human Models of Alzheimer’s Disease.” *Nature Communications* 11 (1): 5370. https://doi.org/10.1038/s41467-020-19227-5.

Medvinsky, A. L., N. L. Samoylina, A. M. Müller, and E. A. Dzierzak. 1993. “An Early Pre-Liver Intraembryonic Source of CFU-S in the Developing Mouse.” *Nature* 364 (6432): 64–67. https://doi.org/10.1038/364064a0.

Melief, J., M. a. M. Sneeboer, M. Litjens, P. R. Ormel, S. J. M. C. Palmen, I. Huitinga, R. S. Kahn, E. M. Hol, and L. D. de Witte. 2016. “Characterizing Primary Human Microglia: A Comparative Study with Myeloid Subsets and Culture Models.” *Glia* 64 (11): 1857–68. https://doi.org/10.1002/glia.23023.

Mildner, Alexander, Hauke Schmidt, Mirko Nitsche, Doron Merkler, Uwe-Karsten Hanisch, Matthias Mack,

Mathias Heikenwalder, Wolfgang Brück, Josef Priller, and Marco Prinz. 2007. “Microglia in the Adult Brain Arise from Ly-6ChiCCR2+ Monocytes Only under Defined Host Conditions.” *Nature Neuroscience* 10 (12): 1544–53. https://doi.org/10.1038/nn2015.

Mirdita, Milot, Konstantin Schütze, Yoshitaka Moriwaki, Lim Heo, Sergey Ovchinnikov, and Martin Steinegger. 2022. “ColabFold: Making Protein Folding Accessible to All.” *Nature Methods* 19 (6): 679–82. https://doi.org/10.1038/s41592-022-01488-1.

Mizutani, Makiko, Paula A. Pino, Noah Saederup, Israel F. Charo, Richard M. Ransohoff, and Astrid E. Cardona. 2012. “The Fractalkine Receptor but Not CCR2 Is Present on Microglia from Embryonic Development throughout Adulthood.” *Journal of Immunology (Baltimore, Md.: 1950)* 188 (1): 29–36. https://doi.org/10.4049/jimmunol.1100421.

Moore, Craig S., Ariel R. Ase, Angham Kinsara, Vijayaraghava T. S. Rao, Mackenzie Michell-Robinson, Soo Yuen Leong, Oleg Butovsky, et al. 2015. “P2Y12 Expression and Function in Alternatively Activated Human Microglia.” *Neurology(R) Neuroimmunology & Neuroinflammation* 2 (2): e80. https://doi.org/10.1212/NXI.0000000000000080.

Moore, Malcolm A. S., and Donald Metcalf. 1970. “Ontogeny of the Haemopoietic System: Yolk Sac Origin of In Vivo and In Vitro Colony Forming Cells in the Developing Mouse Embryo.” *British Journal of Haematology* 18 (3): 279–96. https://doi.org/10.1111/j.1365-2141.1970.tb01443.x.

Morris, C. S., and M. M. Esiri. 1991. “Immunocytochemical Study of Macrophages and Microglial Cells and Extracellular Matrix Components in Human CNS Disease. 1. Gliomas.” *Journal of the Neurological Sciences* 101 (1): 47–58. https://doi.org/10.1016/0022-510x(91)90017-2.

Morris, Huw R., Maria Grazia Spillantini, Carolyn M. Sue, and Caroline H. Williams-Gray. 2024. “The Pathogenesis of Parkinson’s Disease.” *Lancet (London, England)* 403 (10423): 293–304. https://doi.org/10.1016/S0140-6736(23)01478-2.

Morris, John C., Paul S. Aisen, Randall J. Bateman, Tammie L.S. Benzinger, Nigel J. Cairns, Anne M. Fagan, Bernardino Ghetti, et al. 2012. “Developing an International Network for Alzheimer Research: The Dominantly Inherited Alzheimer Network.” *Clinical Investigation* 2 (10): 975–84. https://doi.org/10.4155/cli.12.93.

Muffat, Julien, Yun Li, Attya Omer, Ann Durbin, Irene Bosch, Grisilda Bakiasi, Edward Richards, Aaron Meyer, Lee Gehrke, and Rudolf Jaenisch. 2018. “Human Induced Pluripotent Stem Cell-Derived Glial Cells and Neural Progenitors Display Divergent Responses to Zika and Dengue Infections.” *Proceedings of the National Academy of Sciences of the United States of America* 115 (27): 7117–22. https://doi.org/10.1073/pnas.1719266115.

Muffat, Julien, Yun Li, Bingbing Yuan, Maisam Mitalipova, Attya Omer, Sean Corcoran, Grisilda Bakiasi, et al. 2016. “Efficient Derivation of Microglia-like Cells from Human Pluripotent Stem Cells.” *Nature Medicine* 22 (11): 1358–67. https://doi.org/10.1038/nm.4189.

Mukherjee, Sumit, Laura Heath, Christoph Preuss, Suman Jayadev, Gwenn A. Garden, Anna K. Greenwood, Solveig K. Sieberts, et al. 2020. “Molecular Estimation of Neurodegeneration Pseudotime in Older Brains.” *Nature Communications* 11 (1): 5781. https://doi.org/10.1038/s41467-020-19622-y.

Mun, Se Hwan, Peter Sang Uk Park, and Kyung-Hyun Park-Min. 2020. “The M-CSF Receptor in Osteoclasts and Beyond.” *Experimental & Molecular Medicine* 52 (8): 1239–54. https://doi.org/10.1038/s12276-020-0484-z.

Munro, David A. D., Nadine Bestard-Cuche, Conor McQuaid, Audrey Chagnot, Sepideh Kiani Shabestari, Jean Paul Chadarevian, Upasana Maheshwari, et al. 2024. “Microglia Protect against Age-Associated Brain Pathologies.” *Neuron* 112 (16): 2732-2748.e8. https://doi.org/10.1016/j.neuron.2024.05.018.

Nagai, A., E. Nakagawa, K. Hatori, H. B. Choi, J. G. McLarnon, M. A. Lee, and S. U. Kim. 2001. “Generation and Characterization of Immortalized Human Microglial Cell Lines: Expression of Cytokines and Chemokines.” *Neurobiology of Disease* 8 (6): 1057–68. https://doi.org/10.1006/nbdi.2001.0437.

Naito, M., K. Takahashi, and S. Nishikawa. 1990. “Development, Differentiation, and Maturation of

Macrophages in the Fetal Mouse Liver." *Journal of Leukocyte Biology* 48 (1): 27–37. https://doi.org/10.1002/jlb.48.1.27.

Naj, Adam C., Gyungah Jun, Christiane Reitz, Brian W. Kunkle, William Perry, Yo Son Park, Gary W. Beecham, et al. 2014. "Effects of Multiple Genetic Loci on Age at Onset in Late-Onset Alzheimer Disease: A Genome-Wide Association Study." *JAMA Neurology* 71 (11): 1394–1404. https://doi.org/10.1001/jamaneurol.2014.1491.

Namba, Y., M. Tomonaga, H. Kawasaki, E. Otomo, and K. Ikeda. 1991. "Apolipoprotein E Immunoreactivity in Cerebral Amyloid Deposits and Neurofibrillary Tangles in Alzheimer's Disease and Kuru Plaque Amyloid in Creutzfeldt-Jakob Disease." *Brain Research* 541 (1): 163–66. https://doi.org/10.1016/0006-8993(91)91092-f.

Nikodemova, Maria, Rebecca S. Kimyon, Ishani De, Alissa L. Small, Lara S. Collier, and Jyoti J. Watters. 2015. "Microglial Numbers Attain Adult Levels after Undergoing a Rapid Decrease in Cell Number in the Third Postnatal Week." *Journal of Neuroimmunology* 0 (January):280–88. https://doi.org/10.1016/j.jneuroim.2014.11.018.

Nimmerjahn, Axel, Frank Kirchhoff, and Fritjof Helmchen. 2005. "Resting Microglial Cells Are Highly Dynamic Surveillants of Brain Parenchyma in Vivo." *Science (New York, N.Y.)* 308 (5726): 1314–18. https://doi.org/10.1126/science.1110647.

Novotny, Renata, Franziska Langer, Jasmin Mahler, Angelos Skodras, Andreas Vlachos, Bettina M. Wegenast-Braun, Stephan A. Kaeser, et al. 2016. "Conversion of Synthetic Aβ to In Vivo Active Seeds and Amyloid Plaque Formation in a Hippocampal Slice Culture Model." *The Journal of Neuroscience: The Official Journal of the Society for Neuroscience* 36 (18): 5084–93. https://doi.org/10.1523/JNEUROSCI.0258-16.2016.

O'Brien, Richard J., and Philip C. Wong. 2011. "Amyloid Precursor Protein Processing and Alzheimer's Disease." *Annual Review of Neuroscience* 34:185–204. https://doi.org/10.1146/annurev-neuro-061010-113613.

Obst, Juliane, Emilie Simon, Maria Martin-Estebane, Elena Pipi, Liana M. Barkwill, Ivette Gonzalez-Rivera, Fergus Buchanan, et al. 2020. "Inhibition of IL-34 Unveils Tissue-Selectivity and Is Sufficient to Reduce Microglial Proliferation in a Model of Chronic Neurodegeneration." *Frontiers in Immunology* 11:579000. https://doi.org/10.3389/fimmu.2020.579000.

Ogaki, Ari, Yuji Ikegaya, and Ryuta Koyama. 2022. "Replacement of Mouse Microglia With Human Induced Pluripotent Stem Cell (hiPSC)-Derived Microglia in Mouse Organotypic Slice Cultures." *Frontiers in Cellular Neuroscience* 16. https://www.frontiersin.org/articles/10.3389/fncel.2022.918442.

Ohgidani, Masahiro, Takahiro A. Kato, and Shigenobu Kanba. 2015. "Introducing Directly Induced Microglia-like (iMG) Cells from Fresh Human Monocytes: A Novel Translational Research Tool for Psychiatric Disorders." *Frontiers in Cellular Neuroscience* 9:184. https://doi.org/10.3389/fncel.2015.00184.

Olah, Marta, Vilas Menon, Naomi Habib, Mariko F. Taga, Yiyi Ma, Christina J. Yung, Maria Cimpean, et al. 2020. "Single Cell RNA Sequencing of Human Microglia Uncovers a Subset Associated with Alzheimer's Disease." *Nature Communications* 11 (1): 6129. https://doi.org/10.1038/s41467-020-19737-2.

Olah, Marta, Ellis Patrick, Alexandra-Chloe Villani, Jishu Xu, Charles C. White, Katie J. Ryan, Paul Piehowski, et al. 2018. "A Transcriptomic Atlas of Aged Human Microglia." *Nature Communications* 9 (1): 539. https://doi.org/10.1038/s41467-018-02926-5.

Oosterhof, Nynke, Irene J. Chang, Ehsan Ghayoor Karimiani, Laura E. Kuil, Dana M. Jensen, Ray Daza, Erica Young, et al. 2019. "Homozygous Mutations in CSF1R Cause a Pediatric-Onset Leukoencephalopathy and Can Result in Congenital Absence of Microglia." *American Journal of Human Genetics* 104 (5): 936–47. https://doi.org/10.1016/j.ajhg.2019.03.010.

Orkin, Stuart H., and Leonard I. Zon. 2008. "Hematopoiesis: An Evolving Paradigm for Stem Cell Biology." *Cell* 132 (4): 631–44. https://doi.org/10.1016/j.cell.2008.01.025.

Ormel, Paul R., Renata Vieira de Sá, Emma J. van Bodegraven, Henk Karst, Oliver Harschnitz, Marjolein A. M. Sneeboer, Lill Eva Johansen, et al. 2018. “Microglia Innately Develop within Cerebral Organoids.” *Nature Communications* 9 (1): 4167. https://doi.org/10.1038/s41467-018-06684-2.

Otsuka, Ryo, Haruka Wada, and Ken-ichiro Seino. 2021. “IL-34, the Rationale for Its Expression in Physiological and Pathological Conditions.” *Seminars in Immunology*, The regulation of the immune system by CSFs in the steady state and pathology, 54 (April):101517. https://doi.org/10.1016/j.smim.2021.101517.

Palis, J., S. Robertson, M. Kennedy, C. Wall, and G. Keller. 1999. “Development of Erythroid and Myeloid Progenitors in the Yolk Sac and Embryo Proper of the Mouse.” *Development (Cambridge, England)* 126 (22): 5073–84. https://doi.org/10.1242/dev.126.22.5073.

Paloneva, Juha, Tuula Manninen, Grant Christman, Karine Hovanes, Jami Mandelin, Rolf Adolfsson, Marino Bianchin, et al. 2002. “Mutations in Two Genes Encoding Different Subunits of a Receptor Signaling Complex Result in an Identical Disease Phenotype.” *American Journal of Human Genetics* 71 (3): 656–62. https://doi.org/10.1086/342259.

Pandya, Hetal, Michael J. Shen, David M. Ichikawa, Andrea B. Sedlock, Yong Choi, Kory R. Johnson, Gloria Kim, et al. 2017. “Differentiation of Human and Murine Induced Pluripotent Stem Cells to Microglia-like Cells.” *Nature Neuroscience* 20 (5): 753–59. https://doi.org/10.1038/nn.4534.

Paolicelli, Rosa C., Giulia Bolasco, Francesca Pagani, Laura Maggi, Maria Scianni, Patrizia Panzanelli, Maurizio Giustetto, et al. 2011. “Synaptic Pruning by Microglia Is Necessary for Normal Brain Development.” *Science (New York, N.Y.)* 333 (6048): 1456–58. https://doi.org/10.1126/science.1202529.

Paolicelli, Rosa C., Amanda Sierra, Beth Stevens, Marie-Eve Tremblay, Adriano Aguzzi, Bahareh Ajami, Ido Amit, et al. 2022. “Microglia States and Nomenclature: A Field at Its Crossroads.” *Neuron* 110 (21): 3458–83. https://doi.org/10.1016/j.neuron.2022.10.020.

Parhizkar, Samira, Thomas Arzberger, Matthias Brendel, Gernot Kleinberger, Maximilian Deussing, Carola Focke, Brigitte Nuscher, et al. 2019. “Loss of TREM2 Function Increases Amyloid Seeding but Reduces Plaque-Associated ApoE.” *Nature Neuroscience* 22 (2): 191–204. https://doi.org/10.1038/s41593-018-0296-9.

Park, Dong Shin, Tatsuya Kozaki, Satish Kumar Tiwari, Marco Moreira, Ahad Khalilnezhad, Federico Torta, Nicolas Olivié, et al. 2023. “iPS-Cell-Derived Microglia Promote Brain Organoid Maturation via Cholesterol Transfer.” *Nature* 623 (7986): 397–405. https://doi.org/10.1038/s41586-023-06713-1.

Parkhurst, Christopher N., Guang Yang, Ipe Ninan, Jeffrey N. Savas, John R. Yates, Juan J. Lafaille, Barbara L. Hempstead, Dan R. Littman, and Wen-Biao Gan. 2013. “Microglia Promote Learning-Dependent Synapse Formation through Brain-Derived Neurotrophic Factor.” *Cell* 155 (7): 1596–1609. https://doi.org/10.1016/j.cell.2013.11.030.

Paşca, Anca M., Steven A. Sloan, Laura E. Clarke, Yuan Tian, Christopher D. Makinson, Nina Huber, Chul Hoon Kim, et al. 2015. “Functional Cortical Neurons and Astrocytes from Human Pluripotent Stem Cells in 3D Culture.” *Nature Methods* 12 (7): 671–78. https://doi.org/10.1038/nmeth.3415.

Patel, Anita R, Rodney Ritzel, Louise D McCullough, and Fudong Liu. 2013. “Microglia and Ischemic Stroke: A Double-Edged Sword.” *International Journal of Physiology, Pathophysiology and Pharmacology* 5 (2): 73–90.

Pérez, María José, Dina Ivanyuk, Vasiliki Panagiotakopoulou, Gabriele Di Napoli, Stefanie Kalb, Dario Brunetti, Rawaa Al-Shaana, et al. 2021. “Loss of Function of the Mitochondrial Peptidase PITRM1 Induces Proteotoxic Stress and Alzheimer’s Disease-like Pathology in Human Cerebral Organoids.” *Molecular Psychiatry* 26 (10): 5733–50. https://doi.org/10.1038/s41380-020-0807-4.

Perry, V. H., D. A. Hume, and S. Gordon. 1985. “Immunohistochemical Localization of Macrophages and Microglia in the Adult and Developing Mouse Brain.” *Neuroscience* 15 (2): 313–26. https://doi.org/10.1016/0306-4522(85)90215-5.

Perry, V. Hugh, Colm Cunningham, and Clive Holmes. 2007. “Systemic Infections and Inflammation Affect

Chronic Neurodegeneration." *Nature Reviews. Immunology* 7 (2): 161–67. https://doi.org/10.1038/nri2015.

Petrelli, Francesco, Luca Pucci, and Paola Bezzi. 2016. "Astrocytes and Microglia and Their Potential Link with Autism Spectrum Disorders." *Frontiers in Cellular Neuroscience* 10:21. https://doi.org/10.3389/fncel.2016.00021.

Pettersen, Eric F., Thomas D. Goddard, Conrad C. Huang, Elaine C. Meng, Gregory S. Couch, Tristan I. Croll, John H. Morris, and Thomas E. Ferrin. 2021. "UCSF ChimeraX: Structure Visualization for Researchers, Educators, and Developers." *Protein Science: A Publication of the Protein Society* 30 (1): 70–82. https://doi.org/10.1002/pro.3943.

Pocock, Jennifer M., and Helmut Kettenmann. 2007. "Neurotransmitter Receptors on Microglia." *Trends in Neurosciences* 30 (10): 527–35. https://doi.org/10.1016/j.tins.2007.07.007.

Poewe, Werner, Klaus Seppi, Caroline M. Tanner, Glenda M. Halliday, Patrik Brundin, Jens Volkmann, Anette-Eleonore Schrag, and Anthony E. Lang. 2017. "Parkinson Disease." *Nature Reviews Disease Primers* 3 (1): 1–21. https://doi.org/10.1038/nrdp.2017.13.

Polymeropoulos, M. H., C. Lavedan, E. Leroy, S. E. Ide, A. Dehejia, A. Dutra, B. Pike, et al. 1997. "Mutation in the Alpha-Synuclein Gene Identified in Families with Parkinson's Disease." *Science (New York, N.Y.)* 276 (5321): 2045–47. https://doi.org/10.1126/science.276.5321.2045.

Popova, Galina, Sarah S. Soliman, Chang N. Kim, Matthew G. Keefe, Kelsey M. Hennick, Samhita Jain, Tao Li, et al. 2021. "Human Microglia States Are Conserved across Experimental Models and Regulate Neural Stem Cell Responses in Chimeric Organoids." *Cell Stem Cell* 0 (0). https://doi.org/10.1016/j.stem.2021.08.015.

Priller, J., A. Flügel, T. Wehner, M. Boentert, C. A. Haas, M. Prinz, F. Fernández-Klett, et al. 2001. "Targeting Gene-Modified Hematopoietic Cells to the Central Nervous System: Use of Green Fluorescent Protein Uncovers Microglial Engraftment." *Nature Medicine* 7 (12): 1356–61. https://doi.org/10.1038/nm1201-1356.

Prusiner, Stanley B. 1991. "Molecular Biology of Prion Diseases." *Science* 252 (5012): 1515–22. https://doi.org/10.1126/science.1675487.

Prusiner, Stanley B. 2013. "Biology and Genetics of Prions Causing Neurodegeneration." *Annual Review of Genetics* 47:601–23. https://doi.org/10.1146/annurev-genet-110711-155524.

Qian, Xuyu, Hongjun Song, and Guo-Li Ming. 2019. "Brain Organoids: Advances, Applications and Challenges." *Development (Cambridge, England)* 146 (8): dev166074. https://doi.org/10.1242/dev.166074.

Quadrato, Giorgia, Tuan Nguyen, Evan Z. Macosko, John L. Sherwood, Sung Min Yang, Daniel R. Berger, Natalie Maria, et al. 2017. "Cell Diversity and Network Dynamics in Photosensitive Human Brain Organoids." *Nature* 545 (7652): 48–53. https://doi.org/10.1038/nature22047.

Rademakers, Rosa, Matt Baker, Alexandra M. Nicholson, Nicola J. Rutherford, NiCole Finch, Alexandra Soto-Ortolaza, Jennifer Lash, et al. 2011. "Mutations in the Colony Stimulating Factor 1 Receptor (CSF1R) Cause Hereditary Diffuse Leukoencephalopathy with Spheroids." *Nature Genetics* 44 (2): 200–205. https://doi.org/10.1038/ng.1027.

Rai, Mohammad A., Jason Hammonds, Mario Pujato, Christopher Mayhew, Krishna Roskin, and Paul Spearman. 2020. "Comparative Analysis of Human Microglial Models for Studies of HIV Replication and Pathogenesis." *Retrovirology* 17 (1): 35. https://doi.org/10.1186/s12977-020-00544-y.

Ransohoff, Richard M. 2016. "A Polarizing Question: Do M1 and M2 Microglia Exist?" *Nature Neuroscience* 19 (8): 987–91. https://doi.org/10.1038/nn.4338.

Rathinam, Chozhavendan, William T. Poueymirou, Jose Rojas, Andrew J. Murphy, David M. Valenzuela, George D. Yancopoulos, Anthony Rongvaux, Elizabeth E. Eynon, Markus G. Manz, and Richard A. Flavell. 2011. "Efficient Differentiation and Function of Human Macrophages in Humanized CSF-1 Mice." *Blood* 118 (11): 3119–28. https://doi.org/10.1182/blood-2010-12-326926.

Reitz, Christiane, Margaret A. Pericak-Vance, Tatiana Foroud, and Richard Mayeux. 2023. “A Global View of the Genetic Basis of Alzheimer Disease.” *Nature Reviews. Neurology* 19 (5): 261–77. https://doi.org/10.1038/s41582-023-00789-z.

Rojas, Itziar de, Sonia Moreno-Grau, Niccolo Tesi, Benjamin Grenier-Boley, Victor Andrade, Iris E. Jansen, Nancy L. Pedersen, et al. 2021. “Common Variants in Alzheimer’s Disease and Risk Stratification by Polygenic Risk Scores.” *Nature Communications* 12 (1): 3417. https://doi.org/10.1038/s41467-021-22491-8.

Rojo, Leonel E., Jorge A. Fernández, Andrea A. Maccioni, José M. Jimenez, and Ricardo B. Maccioni. 2008. “Neuroinflammation: Implications for the Pathogenesis and Molecular Diagnosis of Alzheimer’s Disease.” *Archives of Medical Research* 39 (1): 1–16. https://doi.org/10.1016/j.arcmed.2007.10.001.

Rojo, Rocio, Clare Pridans, David Langlais, and David A. Hume. 2017. “Transcriptional Mechanisms That Control Expression of the Macrophage Colony-Stimulating Factor Receptor Locus.” *Clinical Science (London, England: 1979)* 131 (16): 2161–82. https://doi.org/10.1042/CS20170238.

Rojo, Rocío, Anna Raper, Derya D. Ozdemir, Lucas Lefevre, Kathleen Grabert, Evi Wollscheid-Lengeling, Barry Bradford, et al. 2019. “Deletion of a Csf1r Enhancer Selectively Impacts CSF1R Expression and Development of Tissue Macrophage Populations.” *Nature Communications* 10 (1): 3215. https://doi.org/10.1038/s41467-019-11053-8.

Ronaldson, Patrick T., and Thomas P. Davis. 2020. “Regulation of Blood-Brain Barrier Integrity by Microglia in Health and Disease: A Therapeutic Opportunity.” *Journal of Cerebral Blood Flow and Metabolism: Official Journal of the International Society of Cerebral Blood Flow and Metabolism* 40 (1_suppl): S6–24. https://doi.org/10.1177/0271678X20951995.

Rothwell, V M, and L R Rohrschneider. 1987. “Murine C-Fms cDNA: Cloning, Sequence Analysis and Retroviral Expression.” *Oncogene Research* 1 (4): 311–24.

Roussel, Martine F., James R. Downing, Carl W. Rettenmier, and Charles J. Sherr. 1988. “A Point Mutation in the Extracellular Domain of the Human CSF-1 Receptor (c-Fms Proto-Oncogene Product) Activates Its Transforming Potential.” *Cell* 55 (6): 979–88. https://doi.org/10.1016/0092-8674(88)90243-7.

Ryan, Katie J., Charles C. White, Kruti Patel, Jishu Xu, Marta Olah, Joseph M. Replogle, Michael Frangieh, et al. 2017. “A Human Microglia-like Cellular Model for Assessing the Effects of Neurodegenerative Disease Gene Variants.” *Science Translational Medicine* 9 (421): eaai7635. https://doi.org/10.1126/scitranslmed.aai7635.

Sabate-Soler, Sonia, Sarah Louise Nickels, Cláudia Saraiva, Emanuel Berger, Ugne Dubonyte, Kyriaki Barmpa, Yan Jun Lan, et al. 2022. “Microglia Integration into Human Midbrain Organoids Leads to Increased Neuronal Maturation and Functionality.” *Glia* 70 (7): 1267–88. https://doi.org/10.1002/glia.24167.

Sabogal-Guaqueta, Angelica Maria, Teresa Mitchell-Garcia, Jasmijn Hunneman, Daniëlle Voshart, Arun Thiruvalluvan, Floris Foijer, Frank Kruyt, et al. 2024. “Brain Organoid Models for Studying the Function of iPSC-Derived Microglia in Neurodegeneration and Brain Tumours.” *Neurobiology of Disease* 203 (December):106742. https://doi.org/10.1016/j.nbd.2024.106742.

Safaiyan, Shima, Simon Besson-Girard, Tuğberk Kaya, Ludovico Cantuti-Castelvetri, Lu Liu, Hao Ji, Martina Schifferer, et al. 2021. “White Matter Aging Drives Microglial Diversity.” *Neuron* 109 (7): 1100-1117.e10. https://doi.org/10.1016/j.neuron.2021.01.027.

Sakaguchi, Hideya, Taisuke Kadoshima, Mika Soen, Nobuhiro Narii, Yoshihito Ishida, Masatoshi Ohgushi, Jun Takahashi, Mototsugu Eiraku, and Yoshiki Sasai. 2015. “Generation of Functional Hippocampal Neurons from Self-Organizing Human Embryonic Stem Cell-Derived Dorsomedial Telencephalic Tissue.” *Nature Communications* 6 (November):8896. https://doi.org/10.1038/ncomms9896.

Sala Frigerio, Carlo, Leen Wolfs, Nicola Fattorelli, Nicola Thrupp, Iryna Voytyuk, Inga Schmidt, Renzo Mancuso, et al. 2019. “The Major Risk Factors for Alzheimer’s Disease: Age, Sex, and Genes Modulate the Microglia Response to Aβ Plaques.” *Cell Reports* 27 (4): 1293-1306.e6. https://doi.org/10.1016/j.celrep.2019.03.099.

Salles, P., J. M. Tirapegui, and P. Chaná-Cuevas. 2024. “Genetics of Parkinson’s Disease: Dominant Forms and *GBA*.” *Neurology Perspectives* 4 (3): 100153. https://doi.org/10.1016/j.neurop.2024.100153.

Sargeant, Timothy J., and Célia Fourrier. 2023. “Human Monocyte-Derived Microglia-like Cell Models: A Review of the Benefits, Limitations and Recommendations.” *Brain, Behavior, and Immunity* 107 (January):98–109. https://doi.org/10.1016/j.bbi.2022.09.015.

Sauer, B. 1998. “Inducible Gene Targeting in Mice Using the Cre/Lox System.” *Methods (San Diego, Calif.)* 14 (4): 381–92. https://doi.org/10.1006/meth.1998.0593.

Sauer, B., and N. Henderson. 1989. “Cre-Stimulated Recombination at loxP-Containing DNA Sequences Placed into the Mammalian Genome.” *Nucleic Acids Research* 17 (1): 147–61. https://doi.org/10.1093/nar/17.1.147.

Schafer, Dorothy P., Emily K. Lehrman, Amanda G. Kautzman, Ryuta Koyama, Alan R. Mardinly, Ryo Yamasaki, Richard M. Ransohoff, Michael E. Greenberg, Ben A. Barres, and Beth Stevens. 2012. “Microglia Sculpt Postnatal Neural Circuits in an Activity and Complement-Dependent Manner.” *Neuron* 74 (4): 691–705. https://doi.org/10.1016/j.neuron.2012.03.026.

Schafer, Dorothy P., and Beth Stevens. 2010. “Synapse Elimination during Development and Disease: Immune Molecules Take Centre Stage.” *Biochemical Society Transactions* 38 (2): 476–81. https://doi.org/10.1042/BST0380476.

Schafer, Dorothy P., and Beth Stevens. 2013. “Phagocytic Glial Cells: Sculpting Synaptic Circuits in the Developing Nervous System.” *Current Opinion in Neurobiology* 23 (6): 1034–40. https://doi.org/10.1016/j.conb.2013.09.012.

Schafer, Simon T., Abed AlFatah Mansour, Johannes C. M. Schlachetzki, Monique Pena, Saeed Ghassemzadeh, Lisa Mitchell, Amanda Mar, et al. 2023. “An in Vivo Neuroimmune Organoid Model to Study Human Microglia Phenotypes.” *Cell* 186 (10): 2111-2126.e20. https://doi.org/10.1016/j.cell.2023.04.022.

Scheiblich, Hannah, Cira Dansokho, Dilek Mercan, Susanne V. Schmidt, Luc Bousset, Lena Wischhof, Frederik Eikens, et al. 2021. “Microglia Jointly Degrade Fibrillar Alpha-Synuclein Cargo by Distribution through Tunneling Nanotubes.” *Cell* 184 (20): 5089-5106.e21. https://doi.org/10.1016/j.cell.2021.09.007.

Schindelin, Johannes, Ignacio Arganda-Carreras, Erwin Frise, Verena Kaynig, Mark Longair, Tobias Pietzsch, Stephan Preibisch, et al. 2012. “Fiji: An Open-Source Platform for Biological-Image Analysis.” *Nature Methods* 9 (7): 676–82. https://doi.org/10.1038/nmeth.2019.

Schulz, Christian, Elisa Gomez Perdiguero, Laurent Chorro, Heather Szabo-Rogers, Nicolas Cagnard, Katrin Kierdorf, Marco Prinz, et al. 2012. “A Lineage of Myeloid Cells Independent of Myb and Hematopoietic Stem Cells.” *Science (New York, N.Y.)* 336 (6077): 86–90. https://doi.org/10.1126/science.1219179.

Schwarz, Niklas, Ulrike B. S. Hedrich, Hannah Schwarz, Harshad P A, Nele Dammeier, Eva Auffenberg, Francesco Bedogni, et al. 2017. “Human Cerebrospinal Fluid Promotes Long-Term Neuronal Viability and Network Function in Human Neocortical Organotypic Brain Slice Cultures.” *Scientific Reports* 7 (1): 12249. https://doi.org/10.1038/s41598-017-12527-9.

Schwarz, Niklas, Betül Uysal, Marc Welzer, Jacqueline C. Bahr, Nikolas Layer, Heidi Löffler, Kornelijus Stanaitis, et al. 2019. “Long-Term Adult Human Brain Slice Cultures as a Model System to Study Human CNS Circuitry and Disease.” *eLife* 8 (September). https://doi.org/10.7554/eLife.48417.

Selkoe, D. J. 1991. “The Molecular Pathology of Alzheimer’s Disease.” *Neuron* 6 (4): 487–98. https://doi.org/10.1016/0896-6273(91)90052-2.

Selkoe, Dennis J., and John Hardy. 2016. “The Amyloid Hypothesis of Alzheimer’s Disease at 25 Years.” *EMBO Molecular Medicine* 8 (6): 595–608. https://doi.org/10.15252/emmm.201606210.

Sellgren, C. M., S. D. Sheridan, J. Gracias, D. Xuan, T. Fu, and R. H. Perlis. 2017. “Patient-Specific Models of Microglia-Mediated Engulfment of Synapses and Neural Progenitors.” *Molecular Psychiatry* 22 (2): 170–77. https://doi.org/10.1038/mp.2016.220.

Sellgren, Carl M., Jessica Gracias, Bradley Watmuff, Jonathan D. Biag, Jessica M. Thanos, Paul B.

Whittredge, Ting Fu, et al. 2019. “Increased Synapse Elimination by Microglia in Schizophrenia Patient-Derived Models of Synaptic Pruning.” *Nature Neuroscience* 22 (3): 374–85. https://doi.org/10.1038/s41593-018-0334-7.

Serneels, Lutgarde, Annerieke Sierksma, Emanuela Pasciuto, Ivana Geric, Arya Nair, Anna Martinez-Muriana, An Snellinx, and Bart De Strooper. 2025. “A Versatile Mouse Model to Advance Human Microglia Transplantation Research in Neurodegenerative Diseases.” *Molecular Neurodegeneration* 20 (March):29. https://doi.org/10.1186/s13024-025-00823-2.

Shaker, Mohammed R., Julio Aguado, Harman Kaur Chaggar, and Ernst J. Wolvetang. 2021. “Klotho Inhibits Neuronal Senescence in Human Brain Organoids.” *NPJ Aging and Mechanisms of Disease* 7 (August):18. https://doi.org/10.1038/s41514-021-00070-x.

Sharma, Kaushik, Kanchan Bisht, and Ukpong B. Eyo. 2021. “A Comparative Biology of Microglia Across Species.” *Frontiers in Cell and Developmental Biology* 9:652748. https://doi.org/10.3389/fcell.2021.652748.

Shi, Ju, Jenny Johansson, Nathaniel S. Woodling, Qian Wang, Thomas J. Montine, and Katrin Andreasson. 2010. “The Prostaglandin E2 E-Prostanoid 4 Receptor Exerts Anti-Inflammatory Effects in Brain Innate Immunity.” *The Journal of Immunology* 184 (12): 7207–18. https://doi.org/10.4049/jimmunol.0903487.

Shi, Yanhong, Haruhisa Inoue, Joseph C. Wu, and Shinya Yamanaka. 2017. “Induced Pluripotent Stem Cell Technology: A Decade of Progress.” *Nature Reviews. Drug Discovery* 16 (2): 115–30. https://doi.org/10.1038/nrd.2016.245.

Shigemoto-Mogami, Yukari, Kazue Hoshikawa, James E. Goldman, Yuko Sekino, and Kaoru Sato. 2014. “Microglia Enhance Neurogenesis and Oligodendrogenesis in the Early Postnatal Subventricular Zone.” *The Journal of Neuroscience: The Official Journal of the Society for Neuroscience* 34 (6): 2231–43. https://doi.org/10.1523/JNEUROSCI.1619-13.2014.

Sieff, C. A. 1987. “Hematopoietic Growth Factors.” *The Journal of Clinical Investigation* 79 (6): 1549–57. https://doi.org/10.1172/JCI112988.

Sierra, Amanda, Fernando de Castro, Juan Del Río-Hortega, José Rafael Iglesias-Rozas, Manuel Garrosa, and Helmut Kettenmann. 2016. “The ‘Big-Bang’ for Modern Glial Biology: Translation and Comments on Pío Del Río-Hortega 1919 Series of Papers on Microglia.” *Glia* 64 (11): 1801–40. https://doi.org/10.1002/glia.23046.

Sierra, Amanda, Juan M. Encinas, Juan J. P. Deudero, Jessica H. Chancey, Grigori Enikolopov, Linda S. Overstreet-Wadiche, Stella E. Tsirka, and Mirjana Maletic-Savatic. 2010. “Microglia Shape Adult Hippocampal Neurogenesis through Apoptosis-Coupled Phagocytosis.” *Cell Stem Cell* 7 (4): 483–95. https://doi.org/10.1016/j.stem.2010.08.014.

Sierra, Amanda, Andres C. Gottfried-Blackmore, Bruce S. McEwen, and Karen Bulloch. 2007. “Microglia Derived from Aging Mice Exhibit an Altered Inflammatory Profile.” *Glia* 55 (4): 412–24. https://doi.org/10.1002/glia.20468.

Sierra, Amanda, Rosa C. Paolicelli, and Helmut Kettenmann. 2019. “Cien Años de Microglía: Milestones in a Century of Microglial Research.” *Trends in Neurosciences* 42 (11): 778–92. https://doi.org/10.1016/j.tins.2019.09.004.

Simon, M. Celeste, and Brian Keith. 2008. “The Role of Oxygen Availability in Embryonic Development and Stem Cell Function.” *Nature Reviews. Molecular Cell Biology* 9 (4): 285–96. https://doi.org/10.1038/nrm2354.

Singleton, Andrew B., and Thomas Gasser. 2020. “The Discovery of LRRK2 Mutations as a Cause of Parkinson’s Disease.” *Movement Disorders: Official Journal of the Movement Disorder Society* 35 (4): 551–54. https://doi.org/10.1002/mds.27999.

Smajić, Semra, Cesar A. Prada-Medina, Zied Landoulsi, Jenny Ghelfi, Sylvie Delcambre, Carola Dietrich, Javier Jarazo, et al. 2022. “Single-Cell Sequencing of Human Midbrain Reveals Glial Activation and a Parkinson-Specific Neuronal State.” *Brain: A Journal of Neurology* 145 (3): 964–78.

https://doi.org/10.1093/brain/awab446.

Smith, Amy M., and Mike Dragunow. 2014. “The Human Side of Microglia.” *Trends in Neurosciences* 37 (3): 125–35. https://doi.org/10.1016/j.tins.2013.12.001.

Song, Liqing, Xuegang Yuan, Zachary Jones, Cynthia Vied, Yu Miao, Mark Marzano, Thien Hua, et al. 2019. “Functionalization of Brain Region-Specific Spheroids with Isogenic Microglia-like Cells.” *Scientific Reports* 9 (1): 11055. https://doi.org/10.1038/s41598-019-47444-6.

Sosna, Justyna, Stephan Philipp, Ricardo Albay, Jorge Mauricio Reyes-Ruiz, David Baglietto-Vargas, Frank M. LaFerla, and Charles G. Glabe. 2018. “Early Long-Term Administration of the CSF1R Inhibitor PLX3397 Ablates Microglia and Reduces Accumulation of Intraneuronal Amyloid, Neuritic Plaque Deposition and Pre-Fibrillar Oligomers in 5XFAD Mouse Model of Alzheimer’s Disease.” *Molecular Neurodegeneration* 13 (1): 11. https://doi.org/10.1186/s13024-018-0244-x.

Soysa, Yvanka T. de, Martine Therrien, Alicia C. Walker, and Beth Stevens. 2022. “Redefining Microglia States: Lessons and Limits of Human and Mouse Models to Study Microglia States in Neurodegenerative Diseases.” *Seminars in Immunology* 60 (March):101651. https://doi.org/10.1016/j.smim.2022.101651.

Spangenberg, Elizabeth E., Rafael J. Lee, Allison R. Najafi, Rachel A. Rice, Monica R. P. Elmore, Mathew Blurton-Jones, Brian L. West, and Kim N. Green. 2016. “Eliminating Microglia in Alzheimer’s Mice Prevents Neuronal Loss without Modulating Amyloid-β Pathology.” *Brain: A Journal of Neurology* 139 (Pt 4): 1265–81. https://doi.org/10.1093/brain/aww016.

Spangenberg, Elizabeth, Paul L. Severson, Lindsay A. Hohsfield, Joshua Crapser, Jiazhong Zhang, Elizabeth A. Burton, Ying Zhang, et al. 2019. “Sustained Microglial Depletion with CSF1R Inhibitor Impairs Parenchymal Plaque Development in an Alzheimer’s Disease Model.” *Nature Communications* 10 (1): 3758. https://doi.org/10.1038/s41467-019-11674-z.

Speicher, Anna M., Heinz Wiendl, Sven G. Meuth, and Matthias Pawlowski. 2019. “Generating Microglia from Human Pluripotent Stem Cells: Novel in Vitro Models for the Study of Neurodegeneration.” *Molecular Neurodegeneration* 14 (1): 46. https://doi.org/10.1186/s13024-019-0347-z.

Spillantini, M. G., M. L. Schmidt, V. M. Lee, J. Q. Trojanowski, R. Jakes, and M. Goedert. 1997. “Alpha-Synuclein in Lewy Bodies.” *Nature* 388 (6645): 839–40. https://doi.org/10.1038/42166.

Squarzoni, Paola, Morgane S. Thion, and Sonia Garel. 2015. “Neuronal and Microglial Regulators of Cortical Wiring: Usual and Novel Guideposts.” *Frontiers in Neuroscience* 9:248. https://doi.org/10.3389/fnins.2015.00248.

Srinivasan, Karpagam, Brad A. Friedman, Ainhoa Etxeberria, Melanie A. Huntley, Marcel P. van der Brug, Oded Foreman, Jonathan S. Paw, et al. 2020. “Alzheimer’s Patient Microglia Exhibit Enhanced Aging and Unique Transcriptional Activation.” *Cell Reports* 31 (13): 107843. https://doi.org/10.1016/j.celrep.2020.107843.

Srinivasan, Karpagam, Brad A. Friedman, Jessica L. Larson, Benjamin E. Lauffer, Leonard D. Goldstein, Laurie L. Appling, Jovencio Borneo, et al. 2016. “Untangling the Brain’s Neuroinflammatory and Neurodegenerative Transcriptional Responses.” *Nature Communications* 7 (April):11295. https://doi.org/10.1038/ncomms11295.

Stanley, E. Richard, Karen L. Berg, Douglas B. Einstein, Pierre S.W. Lee, Fiona J. Pixley, Yun Wang, and Yee-Guide Yeung. 1997. “Biology and Action of Colony-Stimulating Factor-1.” *Molecular Reproduction and Development* 46 (1): 4–10. https://doi.org/10.1002/(SICI)1098-2795(199701)46:1<4::AID-MRD2>3.0.CO;2-V.

Stanley, E. Richard, and Violeta Chitu. 2014. “CSF-1 Receptor Signaling in Myeloid Cells.” *Cold Spring Harbor Perspectives in Biology* 6 (6): a021857. https://doi.org/10.1101/cshperspect.a021857.

Stansley, Branden, Jan Post, and Kenneth Hensley. 2012. “A Comparative Review of Cell Culture Systems for the Study of Microglial Biology in Alzheimer’s Disease.” *Journal of Neuroinflammation* 9 (May):115. https://doi.org/10.1186/1742-2094-9-115.

Steiner, Katharina, and Christian Humpel. 2022. “Effects of Ischemia on the Migratory Capacity of Microglia

Along Collagen Microcontact Prints on Organotypic Mouse Cortex Brain Slices." *Frontiers in Cellular Neuroscience* 16 (June). https://doi.org/10.3389/fncel.2022.858802.

Stevens, Beth, Nicola J. Allen, Luis E. Vazquez, Gareth R. Howell, Karen S. Christopherson, Navid Nouri, Kristina D. Micheva, et al. 2007. "The Classical Complement Cascade Mediates CNS Synapse Elimination." *Cell* 131 (6): 1164–78. https://doi.org/10.1016/j.cell.2007.10.036.

Stifter, Sebastian A., and Melanie Greter. 2020. "STOP Floxing around: Specificity and Leakiness of Inducible Cre/loxP Systems." *European Journal of Immunology* 50 (3): 338–41. https://doi.org/10.1002/eji.202048546.

Stöberl, Nina, Emily Maguire, Elisa Salis, Bethany Shaw, and Hazel Hall-Roberts. 2023. "Human iPSC-Derived Glia Models for the Study of Neuroinflammation." *Journal of Neuroinflammation* 20 (1): 231. https://doi.org/10.1186/s12974-023-02919-2.

Stoppini, L., P. A. Buchs, and D. Muller. 1991. "A Simple Method for Organotypic Cultures of Nervous Tissue." *Journal of Neuroscience Methods* 37 (2): 173–82. https://doi.org/10.1016/0165-0270(91)90128-m.

Streit, Wolfgang J. 2006. "Microglial Senescence: Does the Brain's Immune System Have an Expiration Date?" *Trends in Neurosciences* 29 (9): 506–10. https://doi.org/10.1016/j.tins.2006.07.001.

Streit, Wolfgang J., Nicole W. Sammons, Amanda J. Kuhns, and D. Larry Sparks. 2004. "Dystrophic Microglia in the Aging Human Brain." *Glia* 45 (2): 208–12. https://doi.org/10.1002/glia.10319.

Streit, Wolfgang J., Qing-Shan Xue, Jasmin Tischer, and Ingo Bechmann. 2014. "Microglial Pathology." *Acta Neuropathologica Communications* 2 (1): 142. https://doi.org/10.1186/s40478-014-0142-6.

Sturchler-Pierrat, C., D. Abramowski, M. Duke, K. H. Wiederhold, C. Mistl, S. Rothacher, B. Ledermann, et al. 1997. "Two Amyloid Precursor Protein Transgenic Mouse Models with Alzheimer Disease-like Pathology." *Proceedings of the National Academy of Sciences of the United States of America* 94 (24): 13287–92. https://doi.org/10.1073/pnas.94.24.13287.

Sun, Na, Matheus B. Victor, Yongjin P. Park, Xushen Xiong, Aine Ni Scannail, Noelle Leary, Shaniah Prosper, et al. 2023. "Human Microglial State Dynamics in Alzheimer's Disease Progression." *Cell* 186 (20): 4386-4403.e29. https://doi.org/10.1016/j.cell.2023.08.037.

Suresh, Jyothsna, Mihailo Radojicic, Lorenzo L. Pesce, Anita Bhansali, Janice Wang, Andrew K. Tryba, Jeremy D. Marks, and Wim van Drongelen. 2016. "Network Burst Activity in Hippocampal Neuronal Cultures: The Role of Synaptic and Intrinsic Currents." *Journal of Neurophysiology* 115 (6): 3073–89. https://doi.org/10.1152/jn.00995.2015.

Svoboda, Devon S., M. Inmaculada Barrasa, Jian Shu, Rosalie Rietjens, Shupei Zhang, Maya Mitalipova, Peter Berube, et al. 2019. "Human iPSC-Derived Microglia Assume a Primary Microglia-like State after Transplantation into the Neonatal Mouse Brain." *Proceedings of the National Academy of Sciences of the United States of America* 116 (50): 25293–303. https://doi.org/10.1073/pnas.1913541116.

Swinnen, Nina, Sophie Smolders, Ariel Avila, Kristof Notelaers, Rik Paesen, Marcel Ameloot, Bert Brône, Pascal Legendre, and Jean-Michel Rigo. 2013. "Complex Invasion Pattern of the Cerebral Cortex Bymicroglial Cells during Development of the Mouse Embryo." *Glia* 61 (2): 150–63. https://doi.org/10.1002/glia.22421.

Szalay, Gergely, Bernadett Martinecz, Nikolett Lénárt, Zsuzsanna Környei, Barbara Orsolits, Linda Judák, Eszter Császár, et al. 2016. "Microglia Protect against Brain Injury and Their Selective Elimination Dysregulates Neuronal Network Activity after Stroke." *Nature Communications* 7 (1): 11499. https://doi.org/10.1038/ncomms11499.

Tada, Mari, Takuya Konno, Masayoshi Tada, Toshiyuki Tezuka, Takeshi Miura, Naomi Mezaki, Ken-Ichi Okazaki, et al. 2016. "Characteristic Microglial Features in Patients with Hereditary Diffuse Leukoencephalopathy with Spheroids." *Annals of Neurology* 80 (4): 554–65. https://doi.org/10.1002/ana.24754.

Takahashi, K., F. Yamamura, and M. Naito. 1989. "Differentiation, Maturation, and Proliferation of Macrophages in the Mouse Yolk Sac: A Light-Microscopic, Enzyme-Cytochemical, Immunohistochemical,

and Ultrastructural Study." *Journal of Leukocyte Biology* 45 (2): 87–96. https://doi.org/10.1002/jlb.45.2.87.

Takahashi, Kazutoshi, Koji Tanabe, Mari Ohnuki, Megumi Narita, Tomoko Ichisaka, Kiichiro Tomoda, and Shinya Yamanaka. 2007. "Induction of Pluripotent Stem Cells from Adult Human Fibroblasts by Defined Factors." *Cell* 131 (5): 861–72. https://doi.org/10.1016/j.cell.2007.11.019.

Takahashi, Kazutoshi, and Shinya Yamanaka. 2006. "Induction of Pluripotent Stem Cells from Mouse Embryonic and Adult Fibroblast Cultures by Defined Factors." *Cell* 126 (4): 663–76. https://doi.org/10.1016/j.cell.2006.07.024.

Takata, Kazuyuki, Yoshihisa Kitamura, Mana Saeki, Maki Terada, Sachiko Kagitani, Risa Kitamura, Yasuhiro Fujikawa, et al. 2010. "Galantamine-Induced Amyloid-{beta} Clearance Mediated via Stimulation of Microglial Nicotinic Acetylcholine Receptors." *The Journal of Biological Chemistry* 285 (51): 40180–91. https://doi.org/10.1074/jbc.M110.142356.

Takata, Kazuyuki, Tatsuya Kozaki, Christopher Zhe Wei Lee, Morgane Sonia Thion, Masayuki Otsuka, Shawn Lim, Kagistia Hana Utami, et al. 2017. "Induced-Pluripotent-Stem-Cell-Derived Primitive Macrophages Provide a Platform for Modeling Tissue-Resident Macrophage Differentiation and Function." *Immunity* 47 (1): 183-198.e6. https://doi.org/10.1016/j.immuni.2017.06.017.

Tanaka, Yoshiaki, Bilal Cakir, Yangfei Xiang, Gareth J. Sullivan, and In-Hyun Park. 2020. "Synthetic Analyses of Single-Cell Transcriptomes from Multiple Brain Organoids and Fetal Brain." *Cell Reports* 30 (6): 1682-1689.e3. https://doi.org/10.1016/j.celrep.2020.01.038.

Tanriöver, Gaye, Mehtap Bacioglu, Manuel Schweighauser, Jasmin Mahler, Bettina M. Wegenast-Braun, Angelos Skodras, Ulrike Obermüller, et al. 2020. "Prominent Microglial Inclusions in Transgenic Mouse Models of α-Synucleinopathy That Are Distinct from Neuronal Lesions." *Acta Neuropathologica Communications* 8 (1): 133. https://doi.org/10.1186/s40478-020-00993-8.

Tay, Tuan Leng, Dominic Mai, Jana Dautzenberg, Francisco Fernández-Klett, Gen Lin, null Sagar, Moumita Datta, et al. 2017. "A New Fate Mapping System Reveals Context-Dependent Random or Clonal Expansion of Microglia." *Nature Neuroscience* 20 (6): 793–803. https://doi.org/10.1038/nn.4547.

Taylor, Deanna L., Fleur Jones, Eva S. F. Chen Seho Kubota, and Jennifer M. Pocock. 2005. "Stimulation of Microglial Metabotropic Glutamate Receptor mGlu2 Triggers Tumor Necrosis Factor Alpha-Induced Neurotoxicity in Concert with Microglial-Derived Fas Ligand." *The Journal of Neuroscience: The Official Journal of the Society for Neuroscience* 25 (11): 2952–64. https://doi.org/10.1523/JNEUROSCI.4456-04.2005.

Taylor, Lewis W., Elizabeth M. Simzer, Claire Pimblett, Oscar T. T. Lacey-Solymar, Robert I. McGeachan, Soraya Meftah, Jamie L. Rose, et al. 2024. "P-Tau Ser356 Is Associated with Alzheimer's Disease Pathology and Is Lowered in Brain Slice Cultures Using the NUAK Inhibitor WZ4003." *Acta Neuropathologica* 147 (1): 7. https://doi.org/10.1007/s00401-023-02667-w.

Timmerman, Raissa, Saskia M. Burm, and Jeffrey J. Bajramovic. 2018. "An Overview of in Vitro Methods to Study Microglia." *Frontiers in Cellular Neuroscience* 12:242. https://doi.org/10.3389/fncel.2018.00242.

Tong, Liqi, G. Aleph Prieto, Enikö A. Kramár, Erica D. Smith, David H. Cribbs, Gary Lynch, and Carl W. Cotman. 2012. "Brain-Derived Neurotrophic Factor-Dependent Synaptic Plasticity Is Suppressed by Interleukin-1β via P38 Mitogen-Activated Protein Kinase." *The Journal of Neuroscience: The Official Journal of the Society for Neuroscience* 32 (49): 17714–24. https://doi.org/10.1523/JNEUROSCI.1253-12.2012.

Tremblay, Marie-Ève, Rebecca L. Lowery, and Ania K. Majewska. 2010. "Microglial Interactions with Synapses Are Modulated by Visual Experience." *PLoS Biology* 8 (11): e1000527. https://doi.org/10.1371/journal.pbio.1000527.

Unger, E. R., J. H. Sung, J. C. Manivel, M. L. Chenggis, B. R. Blazar, and W. Krivit. 1993. "Male Donor-Derived Cells in the Brains of Female Sex-Mismatched Bone Marrow Transplant Recipients: A Y-Chromosome Specific in Situ Hybridization Study." *Journal of Neuropathology and Experimental Neurology* 52 (5): 460–70. https://doi.org/10.1097/00005072-199309000-00004.

Vahsen, Björn F., Elizabeth Gray, Ana Candalija, Kaitlyn M. L. Cramb, Jakub Scaber, Ruxandra Dafinca,

Antigoni Katsikoudi, et al. 2022. “Human iPSC Co-Culture Model to Investigate the Interaction between Microglia and Motor Neurons.” *Scientific Reports* 12 (1): 12606. https://doi.org/10.1038/s41598-022-16896-8.

Vainchtein, I. D., J. Vinet, N. Brouwer, S. Brendecke, G. Biagini, K. Biber, H. W. G. M. Boddeke, and B. J. L. Eggen. 2014. “In Acute Experimental Autoimmune Encephalomyelitis, Infiltrating Macrophages Are Immune Activated, Whereas Microglia Remain Immune Suppressed.” *Glia* 62 (10): 1724–35. https://doi.org/10.1002/glia.22711.

Vallières, Luc, and Paul E. Sawchenko. 2003. “Bone Marrow-Derived Cells That Populate the Adult Mouse Brain Preserve Their Hematopoietic Identity.” *The Journal of Neuroscience: The Official Journal of the Society for Neuroscience* 23 (12): 5197–5207. https://doi.org/10.1523/JNEUROSCI.23-12-05197.2003.

Van Rooijen, N., and A. Sanders. 1994. “Liposome Mediated Depletion of Macrophages: Mechanism of Action, Preparation of Liposomes and Applications.” *Journal of Immunological Methods* 174 (1–2): 83–93. https://doi.org/10.1016/0022-1759(94)90012-4.

Varvel, Nicholas H., Stefan A. Grathwohl, Frank Baumann, Christian Liebig, Andrea Bosch, Bianca Brawek, Dietmar R. Thal, et al. 2012. “Microglial Repopulation Model Reveals a Robust Homeostatic Process for Replacing CNS Myeloid Cells.” *Proceedings of the National Academy of Sciences of the United States of America* 109 (44): 18150–55. https://doi.org/10.1073/pnas.1210150109.

Velasco, Silvia, Amanda J. Kedaigle, Sean K. Simmons, Allison Nash, Marina Rocha, Giorgia Quadrato, Bruna Paulsen, et al. 2019. “Individual Brain Organoids Reproducibly Form Cell Diversity of the Human Cerebral Cortex.” *Nature* 570 (7762): 523–27. https://doi.org/10.1038/s41586-019-1289-x.

Venegas, Carmen, Sathish Kumar, Bernardo S. Franklin, Tobias Dierkes, Rebecca Brinkschulte, Dario Tejera, Ana Vieira-Saecker, et al. 2017. “Microglia-Derived ASC Specks Cross-Seed Amyloid-β in Alzheimer’s Disease.” *Nature* 552 (7685): 355–61. https://doi.org/10.1038/nature25158.

Verney, Catherine, Anne Monier, Catherine Fallet-Bianco, and Pierre Gressens. 2010. “Early Microglial Colonization of the Human Forebrain and Possible Involvement in Periventricular White-Matter Injury of Preterm Infants.” *Journal of Anatomy* 217 (4): 436–48. https://doi.org/10.1111/j.1469-7580.2010.01245.x.

Volpato, Viola, and Caleb Webber. 2020. “Addressing Variability in iPSC-Derived Models of Human Disease: Guidelines to Promote Reproducibility.” *Disease Models & Mechanisms* 13 (1): dmm042317. https://doi.org/10.1242/dmm.042317.

Wake, Hiroaki, Andrew J. Moorhouse, Shozo Jinno, Shinichi Kohsaka, and Junichi Nabekura. 2009. “Resting Microglia Directly Monitor the Functional State of Synapses in Vivo and Determine the Fate of Ischemic Terminals.” *The Journal of Neuroscience: The Official Journal of the Society for Neuroscience* 29 (13): 3974–80. https://doi.org/10.1523/JNEUROSCI.4363-08.2009.

Warden, Anna S., Claudia Han, Emily Hansen, Samantha Trescott, Celina Nguyen, Roy Kim, Danielle Schafer, et al. 2023. “Tools for Studying Human Microglia: In Vitro and In Vivo Strategies.” *Brain, Behavior, and Immunity* 107 (January):369–82. https://doi.org/10.1016/j.bbi.2022.10.008.

Wendeln, Ann-Christin, Karoline Degenhardt, Lalit Kaurani, Michael Gertig, Thomas Ulas, Gaurav Jain, Jessica Wagner, et al. 2018. “Innate Immune Memory in the Brain Shapes Neurological Disease Hallmarks.” *Nature* 556 (7701): 332–38. https://doi.org/10.1038/s41586-018-0023-4.

Wickham, Jenny, Andrea Corna, Niklas Schwarz, Betül Uysal, Nikolas Layer, Jürgen B. Honegger, Thomas V. Wuttke, Henner Koch, and Günther Zeck. 2020. “Human Cerebrospinal Fluid Induces Neuronal Excitability Changes in Resected Human Neocortical and Hippocampal Brain Slices.” *Frontiers in Neuroscience* 14:283. https://doi.org/10.3389/fnins.2020.00283.

Wilgenburg, Bonnie van, Cathy Browne, Jane Vowles, and Sally A. Cowley. 2013. “Efficient, Long Term Production of Monocyte-Derived Macrophages from Human Pluripotent Stem Cells under Partly-Defined and Fully-Defined Conditions.” *PloS One* 8 (8): e71098. https://doi.org/10.1371/journal.pone.0071098.

Wilson, David M., Mark R. Cookson, Ludo Van Den Bosch, Henrik Zetterberg, David M. Holtzman, and Ilse Dewachter. 2023. “Hallmarks of Neurodegenerative Diseases.” *Cell* 186 (4): 693–714.

https://doi.org/10.1016/j.cell.2022.12.032.

Xia, Yun, Guoxin Zhang, Chao Han, Kai Ma, Xingfang Guo, Fang Wan, Liang Kou, et al. 2019. "Microglia as Modulators of Exosomal Alpha-Synuclein Transmission." *Cell Death & Disease* 10 (3): 174. https://doi.org/10.1038/s41419-019-1404-9.

Ximerakis, Methodios, Scott L. Lipnick, Brendan T. Innes, Sean K. Simmons, Xian Adiconis, Danielle Dionne, Brittany A. Mayweather, et al. 2019. "Single-Cell Transcriptomic Profiling of the Aging Mouse Brain." *Nature Neuroscience* 22 (10): 1696–1708. https://doi.org/10.1038/s41593-019-0491-3.

Xiong, Ying, Da Song, Yunfei Cai, Wenfeng Yu, Yee-Guide Yeung, and E. Richard Stanley. 2011. "A CSF-1 Receptor Phosphotyrosine 559 Signaling Pathway Regulates Receptor Ubiquitination and Tyrosine Phosphorylation." *The Journal of Biological Chemistry* 286 (2): 952–60. https://doi.org/10.1074/jbc.M110.166702.

Xu, Ranjie, Xiaoxi Li, Andrew J. Boreland, Anthony Posyton, Kelvin Kwan, Ronald P. Hart, and Peng Jiang. 2020. "Human iPSC-Derived Mature Microglia Retain Their Identity and Functionally Integrate in the Chimeric Mouse Brain." *Nature Communications* 11 (1): 1577. https://doi.org/10.1038/s41467-020-15411-9.

Yan, Ping, Ki-Wook Kim, Qingli Xiao, Xiucui Ma, Leah R. Czerniewski, Haiyan Liu, David R. Rawnsley, et al. 2022. "Peripheral Monocyte–Derived Cells Counter Amyloid Plaque Pathogenesis in a Mouse Model of Alzheimer's Disease." *The Journal of Clinical Investigation* 132 (11): e152565. https://doi.org/10.1172/JCI152565.

Yeung, Y G, P T Jubinsky, A Sengupta, D C Yeung, and E R Stanley. 1987. "Purification of the Colony-Stimulating Factor 1 Receptor and Demonstration of Its Tyrosine Kinase Activity." *Proceedings of the National Academy of Sciences* 84 (5): 1268–71. https://doi.org/10.1073/pnas.84.5.1268.

Yger, Pierre, Giulia LB Spampinato, Elric Esposito, Baptiste Lefebvre, Stéphane Deny, Christophe Gardella, Marcel Stimberg, et al. 2018. "A Spike Sorting Toolbox for up to Thousands of Electrodes Validated with Ground Truth Recordings in Vitro and in Vivo." Edited by David Kleinfeld. *eLife* 7 (March):e34518. https://doi.org/10.7554/eLife.34518.

Yu, Wenfeng, Jian Chen, Ying Xiong, Fiona J. Pixley, Yee-Guide Yeung, and E. Richard Stanley. 2012. "Macrophage Proliferation Is Regulated through CSF-1 Receptor Tyrosines 544, 559, and 807." *The Journal of Biological Chemistry* 287 (17): 13694–704. https://doi.org/10.1074/jbc.M112.355610.

Yuan, Peng, Carlo Condello, C. Dirk Keene, Yaming Wang, Thomas D. Bird, Steven M. Paul, Wenjie Luo, Marco Colonna, David Baddeley, and Jaime Grutzendler. 2016. "TREM2 Haplodeficiency in Mice and Humans Impairs the Microglia Barrier Function Leading to Decreased Amyloid Compaction and Severe Axonal Dystrophy." *Neuron* 90 (4): 724–39. https://doi.org/10.1016/j.neuron.2016.05.003.

Zhan, Lihong, Li Fan, Lay Kodama, Peter Dongmin Sohn, Man Ying Wong, Gergey Alzaem Mousa, Yungui Zhou, Yaqiao Li, and Li Gan. 2020. "A MAC2-Positive Progenitor-like Microglial Population Is Resistant to CSF1R Inhibition in Adult Mouse Brain." *eLife* 9 (October):e51796. https://doi.org/10.7554/eLife.51796.

Zhan, Yang, Rosa C. Paolicelli, Francesco Sforazzini, Laetitia Weinhard, Giulia Bolasco, Francesca Pagani, Alexei L. Vyssotski, et al. 2014. "Deficient Neuron-Microglia Signaling Results in Impaired Functional Brain Connectivity and Social Behavior." *Nature Neuroscience* 17 (3): 400–406. https://doi.org/10.1038/nn.3641.

Zhang, Jingfei, Aqsa Malik, Hyun B. Choi, Rebecca W. Y. Ko, Lasse Dissing-Olesen, and Brian A. MacVicar. 2014. "Microglial CR3 Activation Triggers Long-Term Synaptic Depression in the Hippocampus via NADPH Oxidase." *Neuron* 82 (1): 195–207. https://doi.org/10.1016/j.neuron.2014.01.043.

Zhang, Wendiao, Jiamei Jiang, Zhenhong Xu, Hongye Yan, Beisha Tang, Chunyu Liu, Chao Chen, and Qingtuan Meng. 2023. "Microglia-Containing Human Brain Organoids for the Study of Brain Development and Pathology." *Molecular Psychiatry* 28 (1): 96–107. https://doi.org/10.1038/s41380-022-01892-1.

Zhang, Ye, Kenian Chen, Steven A. Sloan, Mariko L. Bennett, Anja R. Scholze, Sean O'Keeffe, Hemali P. Phatnani, et al. 2014. "An RNA-Sequencing Transcriptome and Splicing Database of Glia, Neurons, and Vascular Cells of the Cerebral Cortex." *The Journal of Neuroscience: The Official Journal of the Society for*

Neuroscience 34 (36): 11929–47. https://doi.org/10.1523/JNEUROSCI.1860-14.2014.

Zhang, Ye, Steven A. Sloan, Laura E. Clarke, Christine Caneda, Colton A. Plaza, Paul D. Blumenthal, Hannes Vogel, et al. 2016. "Purification and Characterization of Progenitor and Mature Human Astrocytes Reveals Transcriptional and Functional Differences with Mouse." *Neuron* 89 (1): 37–53. https://doi.org/10.1016/j.neuron.2015.11.013.

Zrzavy, Tobias, Simon Hametner, Isabella Wimmer, Oleg Butovsky, Howard L. Weiner, and Hans Lassmann. 2017. "Loss of 'homeostatic' Microglia and Patterns of Their Activation in Active Multiple Sclerosis." *Brain: A Journal of Neurology* 140 (7): 1900–1913. https://doi.org/10.1093/brain/awx113.

7 Statement of Contributions

A novel brain slice culture model to investigate human microglia in homeostasis and disease

Lena Erlebach, Marc Welzer, Teresa Bartling, Jun-Hoe Lee, Daniela Miely, Anika Bühler, Gamze Özata, Vasiliki Pangiotakopoulou, Marius Lambert, Katleen Wild, Katrin Patzer, Ulrike Hedrich-Klimosch, Henner Koch, Jonas Neher, Mathias Jucker, Deborah Kronenberg-Versteeg

Personal contribution: Experimental design and planning of the study (together with MW, JN, MJ, DKV); iPSC culture and microglia differentiation (assisted by MW, GÖ, VP, AB, KW); iMic precursor harvesting and grafting (assisted by MW, GÖ); preparation of hippocampal slice cultures (together with MW); maintenance of hippocampal slice cultures incl. microglia depletion (together with MW, AB, VP, KP, KW); slice culture fixation (together with MW, AB, VP, KP, KW); seeding of slice cultures with pre-formed fibrils of αSyn and Aβ (together with MW); LPS treatment of slice cultures (**Figure 12**); collection of culture media for MSD analysis (**Figure 12**; together with MW, AB) differentiation of 2D iMic monocultures (**Figures 5, 15, 16, 19**); microglia isolation for scRNAseq (together with MW); scRNAseq sample processing and library generation (**Figures 14, 15, 21**); scRNAseq data visualization (**Figures 14, 15, 21**; together with DKV); immunofluorescent and LCO staining (together with MW); confocal imaging (**Figures 5-10,17, 20, 21**; together with MW); quantification of microglia (**Figures 6, 7, 9, 10, 17, 20**; together with MW); morphological and network analysis of microglia (**Figure 10**; together with MW); 2-Photon live cell imaging and analysis of microglia dynamics (**Figure 11**; mostly by MW); analysis of MSD measurements (**Figure 12**; together with MW, DKV); experiments with amyloid-beta (**Figure 22**), human slice engraftment (**Figure 22**), statistical analysis (together with MW, DKV); figure design and preparation (together with MW, MJ, DKV).

Others: Vera Pichler and Carina Leibssle performed earmarking; AB and Carina Leibssle performed mouse genotyping; MW performed microglial inclusion analyses; AB, KP and KW collected culture medium for cytokine measurements; Marta Vilademunt-Alcaide established LPS treatment paradigm in cBSC; GÖ generated one replicate of CSF1R mutant iMics engrafted slice cultures; TB performed cytokine stimulation assay, Western Blot and SPR experiments and analyses; Natalie Beschorner provided brain homogenate to serve as Aβ seed; Single-cell RNA sequencing was performed by the NGS competence center Tübingen; DKV and JHL performed

scRNAseq analysis; DKV performed ColabFold modeling; John Weir supported SPR experiments and ColabFold modeling; ML performed MSD measurements; DM and UKH performed and analyzed MEA recordings; Henner Koch obtained and provided human brain tissue for *ex vivo* analysis; Thomas Wuttke and Nikals Schwarz obtained and supported culture of human brain tissue slice cultures; Angelos Skodras supported imaging and analysis; Ulrike Obermüller established and advised immunohistochemical staining procedures

Since initial submission of the thesis the results have been published on ResearchSquare and are publicly available at https://doi.org/10.21203/rs.3.rs-8176878/v1 under a CC BY 4.0 License.

8 Abbreviations

αSyn	alpha-synuclein
°C	degrees Celsius
1wd / 2wd	1/2 week(s) depletion
AAV	adeno-associated virus
AB	antibody
AD	Alzheimer's disease
AGM	aorta, gonads and mesonephros
AIF1/Iba1	allograft inflammatory factor 1/ ionized calcium-binding adapter molecule 1
ALS	amyotrophic lateral sclerosis
ALSP	adult-onset leukodystrophy with neuroaxonal spheroids and pigmented glia
APOE	apolipoprotein E
APP	amyloid precursor protein
ARM	activated response microglia
ATP	adenosine triphosphate
Aβ	amyloid-beta
BBB	blood-brain barrier
BDNF	brain-derived neurotrophic factor
BM	bone marrow
BMP4	bone morphogenetic factor 4
BSA	bovine serum albumin
BSC	organotypic brain slice cultures
cBSC	chimeric organotypic brain slice cultures
CD	cluster of differentiation
CJD	Creutzfeldt-Jacob disease
CNS	central nervous system
CSF1	colony stimulating factor 1
CSF1R	colony stimulating factor 1 receptor
CX3CR1	fractalkine receptor
DAM	disease-associated microglia
DAPI	4',6-diamidino-2-phenylindole
DEG	differentially expressed genes

DIV	days in vitro
DKK1	dickkopf-1
DMEM	Dulbecco’s modified essential medium
DNA	deoxyribonucleic acid
E	embryonic day
EB	embryoid body
EBiSC	European Bank for induced Pluripotent Stem Cells
EDTA	ethylenediaminetetraacetic acid
ERK1/2	extracellular signal-regulated kinase 1/2
ESC	embryonic stem cells
FIRE	*fms*-intronic regulatory element
FTLD	frontotemporal lobar degeneration
g = rcf	relative centrifugal force
GABA	gamma-aminobutyric acid
GDNF	glia-derived neurotrophic factor
GEM	gel bead in emulsion
GWAS	genome-wide association studies
h	human
HBSS	Hank’s Buffered Salt Solution
HDLS	Hereditary diffuse leukoencephalopathy with spheroids
HEPES	4-(2-hydroxyethyl)-1-piperazineethanesulfonic acid
(E)GFP	(enhanced) green fluorescent protein
IFIT	interferon-induced protein with tetratricopeptide repeats
Ig	immunoglobulin
IL	interleukin
IMDM	Iscove's Modified Dulbecco's Medium
iMic	iPSC-derived microglia
iMicros	iPSC-derived microglia-like cells
iPSC	induced pluripotent stem cells
IRF	interferon regulatory factor
IRM	interferon-responsive microglia
Jax	The Jackson Laboratories

KO	knock-out
LCO	luminescent conjugated oligothiophene
LPS	lipopolysaccharide
m	murine
MACS	magnetic advanced cell sorting
MEA	multielectrode array
MEM	minimal essential medium
MGnD	microglial neurodegenerative phenotype
MHC-II	major histocompatibility complex class II
min	minute
mono iMic	monocultured iMic
MS	multiple sclerosis
MSD	mesoscale discovery
NDS	normal donkey serum
NND	nearest neighbor distance
nod	no depletion
OASL2	2'-5' oligoadenylate synthetase-like 2
p	post-natal day
P2RY12	purinergic receptor P2Y12
PBS	phosphate-buffered saline
PCA	principal component analysis
PCR	polymerase chain reaction
PD	Parkinson’s disease
PDGFRβ	platelet-derived growth factor receptor beta
PFA	paraformaldehyde
pff	pre-formed fibrils
PMD	post-mortem delay
pre-iMic	iMic precursor cell
PSEN1/2	presenilin1/2
PU.1 = SPI1	transcription factor PU.1
qFTAA	quatroformylthiophene acetic acid
RMSD	root-mean-square deviation

RNA	ribonucleic acid
ROS	reactive oxygen species
rt	room temperature
RUNX	runt-related transcription factor 1
s	second
SALL1	sal-like 1
SCF	stem cell factor
SCM	slice culture medium
scRNAseq	single-cell RNA sequencing
SEM	standard error of the mean
SIGLEC	sialic acid-binding immunoglobulin-type lectin
SPR	surface plasmon resonance
TBS-T	tris buffered saline with Tween
TGFβ1	transforming growth factor 1 beta
TMEM119	transmembrane protein 119
TNFa	tumor necrosis factor alpha
TREM2	triggering receptor expressed on myeloid cells 2
TYROBP	TYRO protein tyrosine kinase-binding protein
UMAP	uniform Manifold Approximation and Projection for Dimension Reduction
VEGF	vascular endothelial growth factor
w	week
WT	wildtype
YS	yolk sac

9 Acknowledgment

First of all, I would like to thank my PhD advisor Prof. Dr. Mathias Jucker for taking me on in his lab during master studies and allowing me to stay for my PhD work. Thank you for your continued support, confidence in my work, your advice and great mentorship.

Furthermore, I would like to express my gratitude to Prof. Dr. Katja Schenke-Layland and Prof. Dr. Jonas Neher for their support as members on my scientific advisory board. I highly appreciate the time you took for me and the thoughtful and constructive input and criticism during our meetings. Additionally, I would like to thank Prof. Dr. Stefan Liebau for serving on my thesis board.

I am beyond grateful to Dr. Deborah Kronenberg-Versteeg for her extraordinary support in every imaginable situation, and her understanding that sometimes science is not all that matters in life. Thank you so much for taking me on for my lab rotation, seeing and supporting my potential and interest at every step along the way to where I stand today. I could not have done this without you and our regular chats that started with science and often ended in gardening, baking and hiking recommendations – thank you for always having your door open and your great scientific guidance! I would also like to thank Dr. Marc Welzer for being a fantastic lab partner and teacher and for the fun moments we shared not only in but also outside the lab.

Next, I would like to express my deepest gratitude to all current and former members of the Department of Cellular Neurology and the Hertie Institute and DZNE Tübingen for their support and the great time! Special thanks go to our technicians Anika Bühler, Katleen Wild, Katrin Patzer, Ulrike Obermüller and Marius Lambert for keeping the lab running and taking so much work off my shoulders. Jörg Odenthal and Vera Pichler helped with animal work. Lisa Häsler, Stefan Käser and Dr. Angelos Skodras gave great technical support. Thank you! Special thanks to my fellow PhD students for all the fun we had in the PhD office, during lunch and in private: Dr. Christine Rother, Dr. Carina Bergmann, Dr. Marc Welzer, Ying Xu, Antonia Keller, Sinja Buchner, Teresa Bartling and Hariharan Menon. I would like to thank Dr. Jessica Wagner, Dr. Vasiliki Panagiotakopoulou and Dr. Marc Oudart for the great conversations and fantastic support.

This work would not have been possible without the great collaborations within the Tübingen NeuroCampus (especially Daniela Miely, Dr. Ulrike Klimosch-Hedrich, Dr. Thomas Wuttke, Dr. Niklas Schwarz at the Department of Epileptology) and outside (Dr. Henner Koch and colleagues at the RWTH Aachen; Dr. Nicolas Casadei and colleagues at the NCCT and Qbic in Tübingen).

My PhD was supported by PhD scholarships from the *Studienstiftung des Deutschen Volkes* and by the International Max Planck Research School for the Mechanisms of Mental Function and Dysfunction (IMPRS-MMFD). I thank both organizations for their trust in my abilities and project, the financial support and all the amazing events I was able to attend because of these scholarships. This work has furthermore received support from the Chan Zuckerberg Initiative DAF (#2020-221779 and #2022-250474), the Hertie Foundation (#P1230003), and the Alzheimer Forschung Initiative e.V. (#20019p).

Finally, I would like to thank my family and friends for their constant support throughout my academic journey. Thank you for your patience, unconditional love and the joy you give me. Thank you to my mother Kerstin for always believing in me. I send much love and gratitude to heaven to my father Dirk and my grandmother Roswitha, who were unable to see me complete this work – you are dearly missed. Thank you, Eike, for your love and always having my back. Dr. Victoria Schmidt-Heuschele and Amina Kremić were the best flat mates I could have asked for. Special thanks go to Johanna Dürrwald and Mara John for going this journey with me since our Bachelor studies and being the best travel buddies – I am proud of my soon-to-be doctor friends and grateful to have you by my side!

10 Supplementary Material

10.1 Iba1-EGFP PCR

10.1.1 Primer sequences:

EGFP Fwd: 5′AAG TTC ATC TGC ACC ACC G 3′

EGFP Rev: 5′CGG CCA TGA TAT AGA CGT TG 3′

KO2F: 5′CCA CGC AGG ATC ACG ATG 3′

KO1R: 5′TCT GCG TTC AAG GCT CGT CC 3′

10.1.2 Protocol PCR Iba1-EGFP:

H_2O	5.3 µl
EGFP fwd	0.25 µl
EGFP rev	0.25 µl
K02F	0.1 µl
K02R	0.1 µl
Mastermix (Sigma-Aldrich)	10 µl
	16 µl
Tissue Extract	4 µl
	20 µl

1. Incubate at 95 °C for 5´
2. Incubate at 95 °C for 45 s
3. Incubate at 60 °C for 45 s
4. Incubate at 72 °C for 45 s

Repeat steps 2 – 4 35x

5. Incubate at 72 °C for 10´
6. Incubate at 4 °C forever

Products: Transgenic: 375 bp

WT control: 400 bp

10.2 Human CSF1R PCR

10.2.1 Primer sequences:

CSF1R Fwd: 5′ACA TTT CAA CCT GTT GAA GCC TGG G 3′

CSF1R Rev: 5′CAG TGA AGA GGA TGT GGG GCA CTT G 3′

10.2.2 Protocol PCR CSF1R:

H_2O	5.8 µl
EGFP fwd	0.1 µl
EGFP rev	0.1 µl
Mastermix (Sigma-Aldrich)	10 µl
	16 µl
Isolated DNA Extract	4 µl
	20 µl

1. Incubate at 95 °C for 5´
2. Incubate at 95 °C for 45 s
3. Incubate at 63 °C for 45 s
4. Incubate at 72 °C for 45 s

Repeat steps 2 – 4 30x

5. Incubate at 72 °C for 5´
6. Incubate at 4 °C forever

mutation causes G>A

10.3 Supplementary Figures

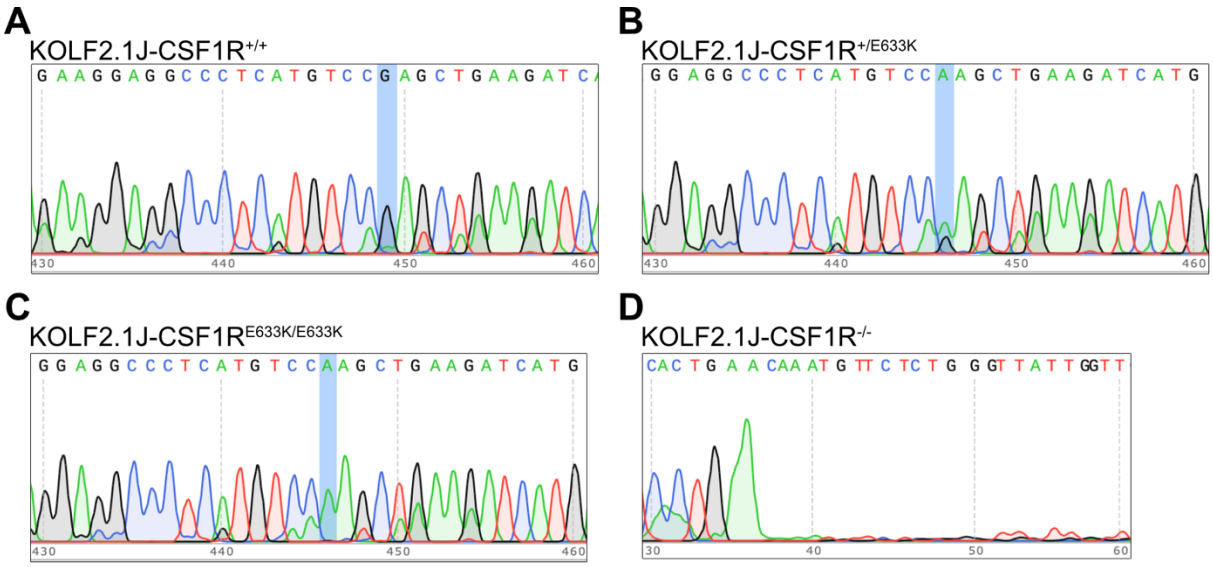

Supplementary Figure 1 Sanger Sequencing of CSF1R variant KOLF2.1J iPSCs

A) At dbSNP rs281860269 wildtype cells have the codon GAG. **B)** This is mutated to exchange the first guanine to adenosine [G→A] on one allele in heterozygous cells resulting in the genotype [G/A]AG and an amino acid substitution from glutamic acid [E] to lysine [K] at amino acid position 633. **C)** Homozygous cells express adenosine on both alleles, resulting in the genotype AAG. **D)** In knockout cells, no amplification of DNA was detected in the region of interest, supporting the deletion of this gene section.

A

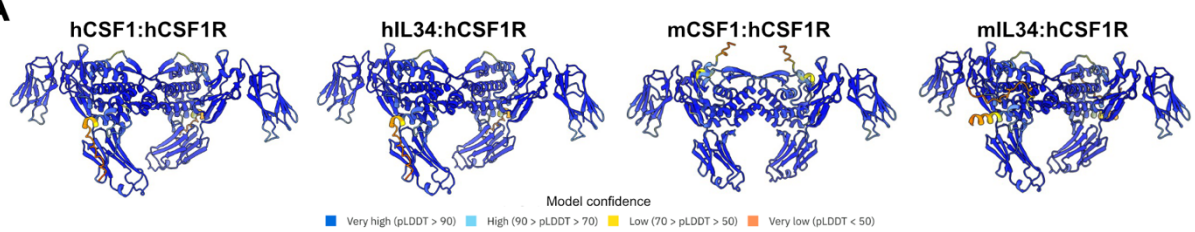

B

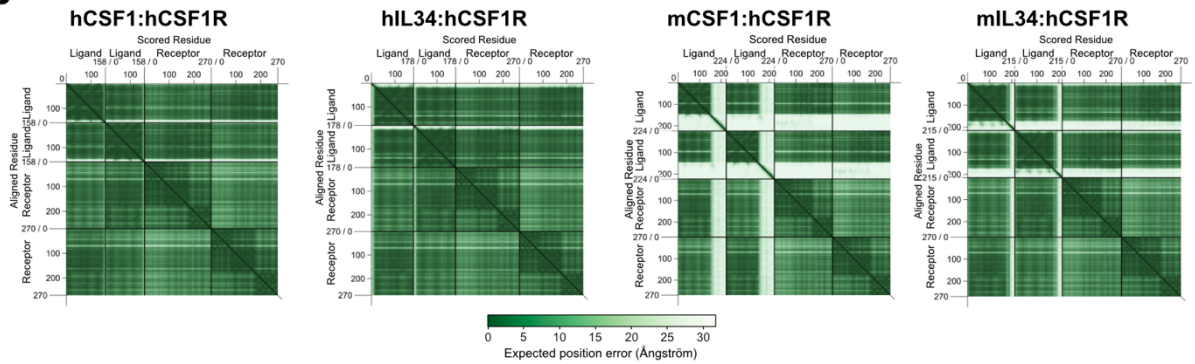

C

hCSF1:hCSF1R

Hydrogen Bonds

	hCSF1	hCSF1R	Dist. [Å]
1	TYR 6[HH]	ASP 234[OD2]	2.04
2	SER 13[H]	ASP 251[OD1]	2.35
3	GLY 14[H]	ASP 251[OD1]	1.81
4	GLN 79[HE22]	ASN 255[OD1]	2.11
5	GLU 62[OE2]	ARG 142[HH22]	1.71
6	ASP 59[OD2]	ARG 144[HH12]	1.86
7	ASP 59[OD1]	ARG 144[HH21]	1.83
8	ASP 63[OD2]	ARG 146[HH11]	1.67
9	ASP 63[OD1]	ARG 146[HH21]	1.83
10	GLU 62[OE2]	ARG 146[HH22]	1.83
11	ASP 69[OD2]	ARG 150[HE]	2.35
12	ASP 69[OD2]	ARG 150[HH22]	1.95
13	GLU 1[OE1]	LYS 194[HZ3]	1.78
14	GLU 82[OE1]	LYS 197[HZ3]	1.78
15	MET 10[O]	TYR 257[HH]	1.99
16			
17			

Salt Bridges

	hCSF1	hCSF1R	Dist. [Å]
1	GLU 62[OE2]	ARG 142[NH1]	3.50
2	GLU 62[OE1]	ARG 142[NH2]	2.66
3	GLU 62[OE2]	ARG 142[NH2]	2.71
4	ASP 59[OD2]	ARG 144[NH1]	2.84
5	ASP 59[OD1]	ARG 144[NH1]	3.95
6	ASP 59[OD2]	ARG 144[NH2]	3.09
7	ASP 59[OD1]	ARG 144[NH2]	2.76
8	ASP 59[OD1]	ARG 146[NE]	3.58
9	GLU 62[OE2]	ARG 146[NE]	3.76
10	ASP 59[OD1]	ARG 146[NH1]	3.91
11	ASP 63[OD1]	ARG 146[NH1]	3.32
12	ASP 63[OD2]	ARG 146[NH1]	2.68
13	ASP 59[OD1]	ARG 146[NH2]	3.75
14	ASP 63[OD1]	ARG 146[NH2]	2.76
15	ASP 63[OD2]	ARG 146[NH2]	3.31
16	GLU 62[OE2]	ARG 146[NH2]	2.82
17	ASP 69[OD1]	ARG 150[NE]	2.94
18	ASP 69[OD2]	ARG 150[NE]	3.10
19	ASP 69[OD1]	ARG 150[NH2]	3.66
20	ASP 69[OD2]	ARG 150[NH2]	2.83
21	ASP 69[OD1]	HIS 151[NE2]	2.97
22	ASP 69[OD2]	HIS 151[NE2]	3.02
23	GLU 1[OE1]	LYS 194[NZ]	2.77
24	GLU 82[OE1]	LYS 197[NZ]	2.78
25	GLU 82[OE2]	LYS 197[NZ]	3.47

hIL34:hCSF1R

Hydrogen Bonds

	hIL34	hCSF1R	Dist. [Å]
1	LEU 186[H]	GLN 248[O]	2.07
2	ASN 187[HD21]	SER 250[O]	1.92
3	LYS 44[HZ1]	PHE 252[O]	1.77
4	LYS 117[HZ2]	ASN 254[OD1]	1.70
5	GLU 103[OE1]	ARG 142[HH11]	1.89
6	GLU 103[OE2]	ARG 142[HH22]	1.79
7	GLU 143[OE1]	ARG 144[HE]	1.89
8	TYR 92[OH]	ARG 144[HH22]	2.21
9	GLU 143[OE2]	ARG 144[HH21]	2.09
10	GLU 103[OE1]	ARG 146[HH22]	1.90
11	GLU 103[OE2]	ARG 146[HH21]	1.95
12	ASP 107[O]	ARG 150[HH12]	1.97
13	SER 184[O]	GLN 248[H]	2.30
14	ASN 187[OD1]	SER 250[H]	1.86
15	GLU 121[OE1]	ASN 254[H]	2.00
16			
17			

Salt Bridges

	hIL34	hCSF1R	Dist. [Å]
1	GLU 103[OE1]	ARG 142[NH1]	2.88
2	GLU 103[OE2]	ARG 142[NH1]	3.85
3	GLU 103[OE1]	ARG 142[NH2]	3.24
4	GLU 103[OE2]	ARG 142[NH2]	2.76
5	GLU 143[OE2]	ARG 144[NE]	3.53
6	GLU 143[OE1]	ARG 144[NE]	2.89
7	GLU 143[OE2]	ARG 144[NH2]	3.07
8	GLU 143[OE1]	ARG 144[NH2]	3.78
9	GLU 103[OE1]	ARG 146[NH1]	3.58
10	GLU 103[OE1]	ARG 146[NH2]	2.70
11	GLU 103[OE2]	ARG 146[NH2]	2.66
12	ASP 107[OD1]	ARG 150[NH1]	3.59
13	GLU 111[OE1]	HIS 151[NE2]	3.43

mCSF1:hCSF1R

Hydrogen Bonds

	mCSF1	hCSF1R	Dist. [Å]
1	ASN 85[HD21]	PHE 169[O]	2.30
2	ASN 85[HD22]	ILE 170[O]	2.05
3	ASN 13[H]	ASP 251[OD1]	2.29
4	GLY 14[H]	ASP 251[OD1]	1.85
5	ASN 13[HD22]	ASP 251[OD2]	2.40
6	GLN 58[O]	ARG 146[HH11]	2.47
7	ASP 59[OD1]	ARG 144[HH22]	1.78
8	ASP 59[OD1]	ARG 146[HH12]	1.79
9	ASP 59[OD2]	ARG 144[HH12]	1.71
10	ASP 62[OD2]	ARG 142[HH12]	1.71
11	ASP 62[OD2]	ARG 142[HH21]	1.82
12	ASP 69[OD1]	ARG 150[HE]	1.97
13	ASP 69[OD2]	ARG 150[HH22]	1.76

Salt Bridges

	mCSF1	hCSF1R	Dist. [Å]
1	ASP 59[OD1]	ARG 144[NH1]	3.68
2	ASP 59[OD1]	ARG 144[NH2]	2.72
3	ASP 59[OD1]	ARG 146[NE]	3.51
4	ASP 59[OD1]	ARG 146[NH1]	2.67
5	ASP 59[OD2]	ARG 144[NH1]	2.71
6	ASP 59[OD2]	ARG 144[NH2]	3.06
7	ASP 62[OD1]	ARG 142[NH2]	3.53
8	ASP 62[OD2]	ARG 146[NH1]	3.24
9	ASP 62[OD2]	ARG 146[NH2]	3.96
10	ASP 62[OD2]	ARG 142[NH1]	2.67
11	ASP 62[OD2]	ARG 142[NH2]	2.73
12	ASP 69[OD1]	ARG 150[NE]	2.83
13	ASP 69[OD1]	ARG 150[NH2]	3.49
14	ASP 69[OD1]	HIS 151[NE2]	2.72
15	ASP 69[OD2]	ARG 150[NE]	3.31
16	ASP 69[OD2]	ARG 10[NH2]	2.75
17	ASP 69[OD2]	HIS 151[NE2]	3.53
18	GLU 82[OE1]	LYS 197[NZ]	2.73
19	GLU 82[OE2]	LYS 197[NZ]	2.73

mIL34:hCSF1R

Hydrogen Bonds

	mIL34	hCSF1R	Dist. [Å]
1	ARG 131[HH22]	SER 172[OG]	2.16
2	ARG 131[HH21]	VAL 195[O]	1.95
3	LYS 187[HZ3]	SER 250[O]	1.83
4	LYS 187[HZ2]	ASP 251[OD1]	1.96
5	LYS 44[HZ2]	PHE 252[O]	1.82
6	LYS 107[HZ2]	ASN 254[OD1]	1.70
7	ASN 128[HD21]	TYR 257[OH]	1.92
8	GLU 103[OE1]	ARG 142[HH11]	2.03
9	GLU 103[OE2]	ARG 142[HH21]	1.77
10	GLU 143[OE1]	ARG 144[HE]	1.92
11	GLU 143[OE2]	ARG 144[HH21]	1.87
12	GLU 103[OE2]	ARG 146[HH22]	2.01
13	GLU 103[OE1]	ARG 146[HH21]	1.96
14	ASP 107[O]	ARG 150[HH11]	2.17
15	LEU 109[O]	ARG 150[HH21]	2.46
16	GLU 121[OE1]	ASN 254[H]	2.13
17	GLU 121[OE1]	ASN 255[H]	2.13

Salt Bridges

	mIL34	hCSF1R	Dist. [Å]
1	LYS 187[NZ]	ASP 251[OD1]	2.88
2	GLU 103[OE2]	ARG 142[NH1]	3.73
3	GLU 103[OE1]	ARG 142[NH1]	3.03
4	GLU 103[OE2]	ARG 142[NH2]	2.76
5	GLU 103[OE1]	ARG 142[NH2]	3.52
6	GLU 143[OE1]	ARG 144[NE]	2.89
7	GLU 143[OE2]	ARG 144[NE]	3.15
8	GLU 143[OE1]	ARG 144[NH2]	3.95
9	GLU 143[OE2]	ARG 144[NH2]	2.83
10	GLU 103[OE1]	ARG 146[NH1]	3.90
11	GLU 103[OE2]	ARG 146[NH2]	2.70
12	GLU 103[OE1]	ARG 146[NH2]	2.78

Supplementary Figure 2 ColabFold predictions of the ternary complexes of hCSF1R with its cognate human or respective murine ligands

A) The ColabFold model of the ternary complex of two $hCSF1R_{D1-D3}$ molecules with their cognate dimerized ligands human CSF1 or IL34, or the dimerized murine counterpart mCSF1 or mIL34. The prediction is color-coded by the pLDDT values indicating the confidence level of the prediction. Dark blue – very high confidence (pLDDT > 90), light blue – confident (90 > pLDDT > 70), yellow – low (70 > pLDDT > 50), orange – very low (pLDDT <50). **B)** Predicted aligned error of the predicted ternary complexes. Dark green – low prediction error (0 Å), white – high prediction error (30 Å). **C)** Predicted interactions at the $hCSF1R_{D1-D3}$:ligand interface in the ColabFold model predictions divided into salt bridges and hydrogen bonds between receptors and respective ligand. mCSF1 has fewer interactions with hCSF1R than hCSFm while mIL34 and hIL34 barely differ.

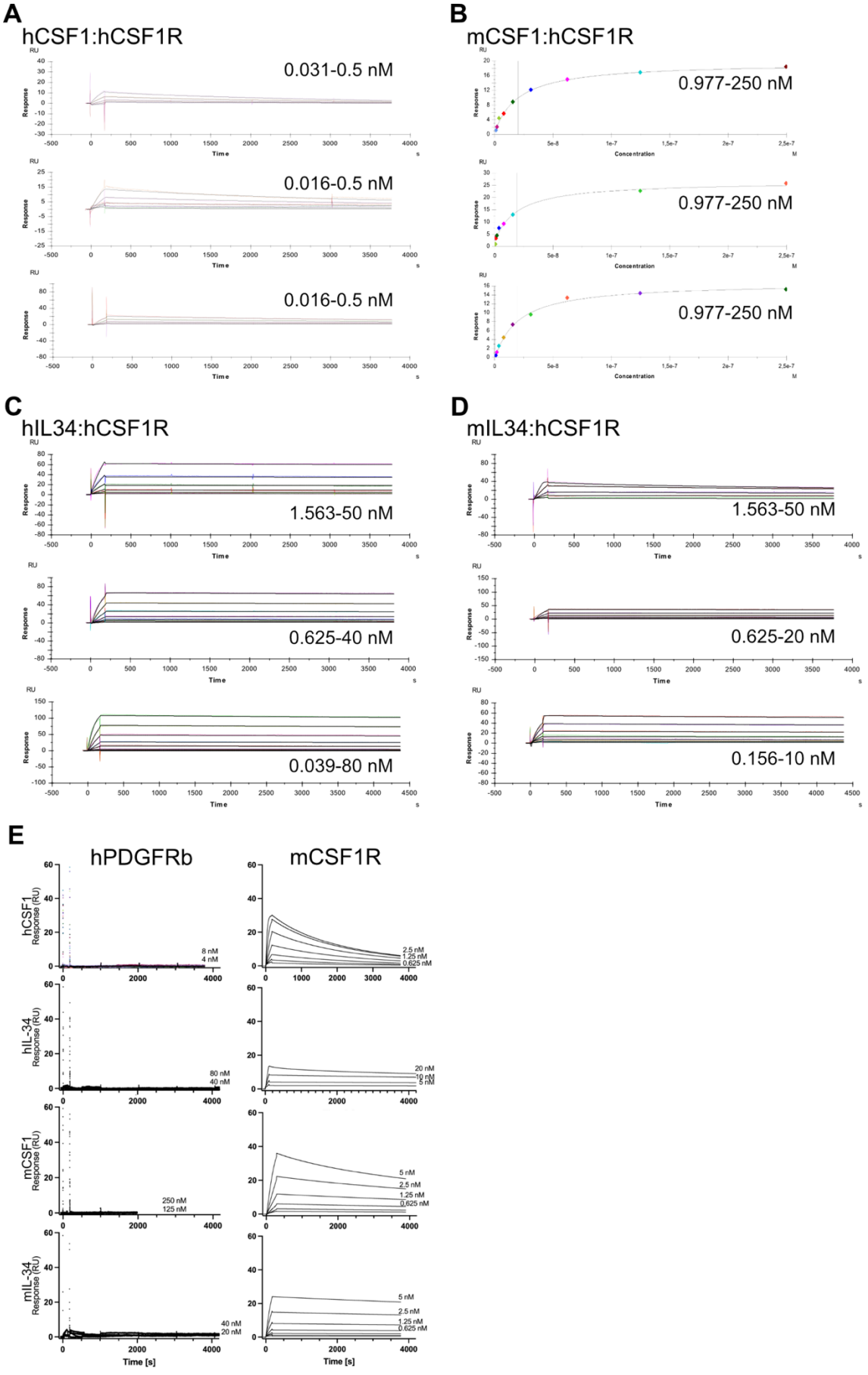
A
hCSF1:hCSF1R
0.031-0.5 nM
0.016-0.5 nM
0.016-0.5 nM
B
mCSF1:hCSF1R
0.977-250 nM
0.977-250 nM
0.977-250 nM
C
hIL34:hCSF1R
1.563-50 nM
0.625-40 nM
0.039-80 nM
D
mIL34:hCSF1R
1.563-50 nM
0.625-20 nM
0.156-10 nM
E
hPDGFRb
mCSF1R
hCSF1
hIL-34
mCSF1
mIL-34
Response (RU)
Time [s]

Supplementary Figure 3 Ligand binding to CSF1R as assessed by surface plasma resonance
Kinetic binding parameters were determined by Biacore-SPR. **A-D)** Sensogram plots generated by SPR kinetic analysis demonstrate the association and dissociation characteristics between immobilized ligand (hCSF1R) and analytes (hCSF1, mCSF1, hIL34, and mIL34). Shown are the three technical replicates for each analyte and the fitted curves. **E)** hPDGFRb, like CSF1R a member of the receptor tyrosine kinase type II subfamily, was used as a negative control to exclude unspecific binding of analytes to the receptor surface. No binding of any analyte was detected. Murine CSF1R was used to demonstrate binding of murine analytes to the murine receptor while little binding of human analytes to the murine receptor was observed.

11 Scripts and Macros

11.1 Laser Injury

Normalization

```
%%select folder with xls-files containing scatter plot coordinates
filename= input ('Name of output-file? ','s');
folder=uigetdir;
cd(folder);

%%Find all excel files in folder
matfiles = dir(fullfile(folder, '*.xls*'));
nfiles = length(matfiles);

%%summarize all excel files of one image in one variable
for i = 1 : nfiles
   data=readtable(matfiles(i).name);
   x=[];
   y=[];
   for j = 2: height(data)
       xvalue=str2double(cell2mat(data{j,1}));
       yvalue=str2double(cell2mat(data{j,3}));
       x=[x xvalue];
       y=[y yvalue];
   end
   alldata.x(i)={x};
   alldata.y(i)={y};
end

%Search min & max for each timepoint
for i= 1 : nfiles
   alldata.max(i)=max(alldata.y{i});
```

```
   alldata.min(i)=min(alldata.y{i});
end

%Normalize all timepoints to global max and min
globalmax=max(alldata.max);
globalmin=min(alldata.min);
for i= 1: nfiles
       alldata.y{i}=(alldata.y{i}-globalmin)/(globalmax-globalmin)*100;
end
save(strcat(filename,'.mat'),'alldata');
```

Summary

```
%%select folder with mat-files containing normalized scatter plot
coordinates
filename= input ('Name of output-file? ','s');
folder=uigetdir;
cd(folder);
timepoints=16;

%%Find all mat files in folder
matfiles = dir(fullfile(folder, '*.mat*'));
nfiles = length(matfiles);
for timepoint= 0:timepoints
%%summarize all mat files of one analysis in one variable
   for i = 1 : nfiles
       data=open(matfiles(i).name);
       if i==1
            summary.x=data.alldata.x{i}';
            leng=length(data.alldata.x{i});
       else
            if length(data.alldata.x{i})<leng
            leng=length(data.alldata.x{i});
```

```
            summary.x=data.alldata.x{i}';
            end
        end
        summary.y{i}=data.alldata.y{timepoint+1}';
    end

    output=zeros(leng,nfiles+1);
    output(:,1)=summary.x;
    for i = 1: nfiles
        y=summary.y{i};
        output(:,i+1)=y(1:leng);
    end

    output=array2table(output);
    output.Properties.VariableNames{1}='x';
    for i = 1 : nfiles
        output.Properties.VariableNames{i+1}=char(matfiles(i).name);
    end
    fulloutput.timepoint{timepoint+1}=output;
end

save(strcat(filename,'.mat'),'fulloutput');
```

12 List of Figures

13 List of Tables